CONDUCTING POLYANILINE AND POLYPYRROLE: STUDIES OF THEIR CATALYTIC PROPERTIES

A Thesis submitted to the

UNIVERSITY OF PUNE

For the degree of

DOCTOR OF PHILOSOPHY

IN

CHEMISTRY

BY

ARINDAM ADHIKARI

Polymer Science and Engineering Group

Chemical Engineering Division

National Chemical Laboratory (NCL)

Pune-411008 (INDIA)

MAY 2004

CERTIFICATE

Certified that the work incorporated in the Thesis entited "CONDUCTING POLYANILINE AND POLYPYRROLE: STUDIES OF THEIR CATALYTIC PROPERTIES" submitted by Mr Arindam Adhikari, was carried out by him under my supervision/guidance at the Chemical Engineering Division, National Chemical Laboratory, Pune-8. Such material as has been obtained from other sources has been duly acknowledged in the thesis.

May 2004 Dr. S. Radhakrishnan

ACKNOWLEDGEMENT

I express my deep gratitude and respects to my guide Dr. S. Radhakrishnan for his keen interest and valuable guidance, strong motivation and constant encouragement during the course of the work. I thank him from the bottom of my heart for introducing me to the science of electrically conducting polymer. I thank him for his great patience, constructive criticism and myriad useful suggestions apart from invaluable guidance to me.

I am grateful to the Director, National Chemical Laboratory, Pune for permitting me to carry out this research work in the NCL.

My special thanks to Dr. A. B. Mandale, Dr.(Mrs.)A. Mitra, Dr.(Ms) N. R Pavaskar of Center for Material Characterization, NCL and Dr. A. Kelkar, Dr. S. P. Gupte, Mr. Nandu M. Patil of Homogeneous Catalysis Division, NCL for their help in doing different characterizations.

I wish my sincere thanks to my entire lab colleague and wish to thank specially to Dr. S. D. Deshpande, Mr. Shivkalyan Kanhegaokar, Sreejith, Swarnendu, Pradip, Shalaka, Narendra, Francis, Subramaniyam, Santhosh, VVR and Mr. M. P. Raut for their co-operation during entire work period.

I would like to thank my friends Manash, Jadab, Selvakannan, Mahesh, Arun, Prerna, Suresha, Santosh, Aarti, Gahininath, and ever smiling Shubhangi for their help during different phases.

I owe sincere thanks to the entire family of Dr. Anand Y. Lele for their love, moral support and encouragement.

Last but not the least, I would like to thank Anirban, Dulal and my parents for their moral support that kept my spirit up during the endeavor.

Arindam Adhikari

Dedicated To My Parents

LIST OF ACRONYMS

B.E.	binding energy
CV	cyclic voltammetry
CuPc	copper phthalocyanine
DRS	diffused reflectance spectroscopy
DMFC	direct methanol fuel cell
ESCA	electron spectroscopy for chemical analysis
ESR	electron spin resonance
GC	gas chromatography
FWHM	full width half maxima
HOMO	highest occupied molecular orbital
IR	infra red
LED	light emitting diode
LUMO	lowest unoccupied molecular orbital
MO	molecular orbital
NMP	N,N′- dimethyl pyrrolidone
PET	polyethylene terephthalate
PAni	polyaniline
PPy	polypyrrole
SCE	saturated calomel electrode
SEM	scanning electron microscopy
UV	ultra violet
XPS	x-ray photoelectron spectroscopy
XRD	x-ray diffraction

LIST OF SYMBOLS

A	ampere
c	concentration (molar)
C	Coulomb
d	interplanner distance
eV	electron volt
ΔE	activation energy
I	current
K	Kelvin
k	Boltzmann constant
K	rate parameter
nm	nanometer
mV	milli volt
ml	milli liter
mA	milli ampere
μ	mobility
μA	micro ampere
Ω	ohm
R	resistance
ρ	resistivity
Q	charge
S	second
σ	conductivity
t	time
T	temperature
V	applied voltage

Chapter I

INTRODUCTION

1.1. INTRODUCTION

Discovery of polymers has given a new dimension to the present era. The strength to weight, processibility, resistance to corrosion, has given polymer advantage over metal. Polymers are generally known for their insulating property. In the mid 1970s, the first polymer capable of conducting electricity, polyacetylene, was reportedly prepared by accident by Shirakawa. The subsequent discovery by Heeger and MacDiarmid that the polymer would undergo an increase in conductivity of 12 orders of magnitude by oxidative doping quickly reverberated around the polymer and electrochemistry communities, and an intensive search for other conducting polymers soon followed. In 1976, Alan MacDiarmid, Hideki Shirakawa, and Alan Heeger, along with a group of young students started research in the field of conducting polymers and the ability to dope these polymers over the full range from insulator to metal. This was particularly exciting because it created a new field of research and a number of opportunities on the boundary between chemistry and condensed-matter physics.[1-3]

As the commonly known polymers in general are saturated and so insulators, these were viewed as uninteresting from the point of view of electronic materials. In conjugated polymers the electronic configuration is fundamentally different, where, the chemical bonding leads to one unpaired electron (the □ electron) per carbon atom. Moreover, □ bonding, in which the carbon orbitals are in the sp^2p_z configuration and in which the orbitals of successive carbon atoms along the backbone overlap, leads to electron delocalization along the backbone of the polymer. This electronic delocalization provides the highway for charge mobility along the backbone of the polymer chain. Therefore, the electronic structure in conducting polymers is determined by the chain symmetry, i.e. the number and kind of atoms within the repeat unit, with the result that such polymers can exhibit semiconducting or even metallic properties. Professor Bengt Ranby, in his lecture at the Nobel Symposium in the year 1991, designated electrically conducting polymers as the fourth generation of polymeric materials.[1]

Electronically conducting polymers are extensively conjugated in nature and therefore it is believed that they possess a spatially delocalized band-like electronic structure. These bands stem from the splitting of interacting molecular orbitals of the constituent monomer units in a manner reminiscent of the band structure of solid-state

semiconductors. It is generally agreed that the mechanism of conductivity in these polymers is based on the motion of charged defects within the conjugated framework. The charge carriers, either positive p-type or negative n-type, are the products of oxidizing or reducing the polymer respectively. The simplest possible form of conducting polymer is of course the arche type polyacetylene $(CH)_x$. Polyacetylene itself is too unstable to be of any practical value, its structure constitutes the core of all conjugated polymers. Because of its structural and electronic simplicity, polyacetylene is well suited to ab-initio and semi-empirical calculations and has therefore played a critical role in the elucidation of the theoretical aspects of conducting polymers. Little et al had proposed that properly substituted polyacetylene molecule would exhibit superconductivity at room temperature.[4] Hatano et al are the first to report the electrical conductivity of the order of 10^{-5} S/cm for trans polyacetylene sample.[5]

Since late seventies, a large number of polymers have been added to the list of conducting polymers such as polypyrrole[6], polythiophene[7], polyparaphenylene[8], polyphenylene sulphide[9], polyaniline[10], polyphenylene vinylene[11] etc.

1.2. TYPES OF CONDUCTING POLYMERS

Conducting polymers can be classified in to different types on the basis of conduction mechanism that renders electrical conductivity to polymers.

1.2.1. Conducting polymer composites

1.2.2. Organometallic polymeric conductors

1.2.3. Polymeric charge transfer complexes

1.2.4. Inherently conducting polymers.

Brief description of the conducting materials have been given here but as present study deals with the inherently conducting polymers, detail discussion have been done for this type of conducting material.

1.2.1.Conducting Polymer Composites

Conducting polymer composites are mixture or blends of conductive particles and polymers. Various conductors have been used in different forms together with large number of conducting and engineering plastic. These can be injection molded in to

desired shapes. Various conductive fillers have been tried such as carbon blacks, graphite flakes, fibers, metal powders etc. The electrical conductivity of the compound is decided by the volume fraction of the filler. A transition from insulating to non-insulating behavior is generally observed when volume fraction of conductive filler in the mixture reaches a threshold of about 25%. The various polymers, which have been used as major matrix, are typically ABS, PC, PET, PP, Nylon, PVC, HDPE etc.

1.2.2. Organometallic Polymeric Conductors

This type of conducting materials are obtained by adding organometallic groups to polymer molecules. In this type of materials the d- orbital of metal may overlap □-orbitals of the organic structure and thereby increases the electron delocalization. The d-orbital may also bridge adjacent layers in crystalline polymers to give conducting property to it.

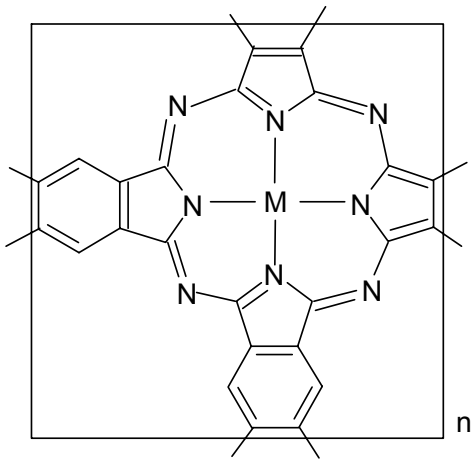

Figure 1.1: Polyphthalocyanines

Metallophthalocyanines and their polymers fall in this class of polymeric material. These polymers have extensively conjugated structures. The bridge transition metal complexes form one of the stable systems exhibiting intrinsic electrical conductivities, without external oxidative doping. Polyferrocenylene is also an example of this type of polymer. These materials possess strong potential for future applications such as molecular wires, antistatic foils, fibers and in xerography.

1.2.3. Polymeric Charge Transfer Complexes

Polymeric charge transfer complexes (CTC) are formed when acceptor like molecules are added to the insulating polymers. There are many charge transfer complexes reported in the literature, e.g. CTC of tetrathaifulvalene (TTF) with bromine, chlorine etc is a good conductor. CTC's of TTF with organic □-acceptors, such as 7,7/, 8,8/-tetracyanoquinodimethane (TCNQ) or metal 1,2-dichalcogenolenes, such as $Ni(mnt)_2$ where 'mnt' is malenonitriledithiolate were found to be good room temperature conductors. The reason for high conductivity in polymeric charge transfer complexes and radical ion salts are still somewhat obscure. It is likely that in polymeric materials, the donor – acceptor interaction promotes orbital overlap, which contributes to alter molecular arrangements and enhanced electron delocalization.

1.2.4. Inherently Conducting Polymers

Research in the field of inherently conducting polymer started nearly three decades ago when Shirakawa and his group found drastic increase in the electrical conductivity of polyacetylene films when exposed to iodine vapor. Leading on from this breakthrough, many small conjugated molecules were found to polymerize, producing conjugated polymers, which were either insulating or semiconducting in the oxidized or doped state. The conjugated polymers are studied as the intrinsically conductive polymers. The electronic properties of conjugated polymers are due to the presence of □-electrons, the wave functions of which are delocalized over long portions of polymer chain when the molecular structure of the backbone is planar.[12, 13] Hence it is necessary that there are no torsion angles at the bonds, which would decrease the delocalization of the □-electron system. Some of the examples of conjugated polymers are shown in the **figure 1.2** below**.**

Features, which differentiate, conjugated polymers from conventional polymers are as follows:

- Band gap Eg (electronic □ –band gap) is small (~ 1 to 3.5 eV) with corresponding low excitations and semiconducting behavior.
- Can be oxidized or reduced through charge transfer reactions with atomic or molecular dopant species.

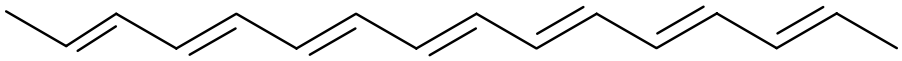

Polyacetylene

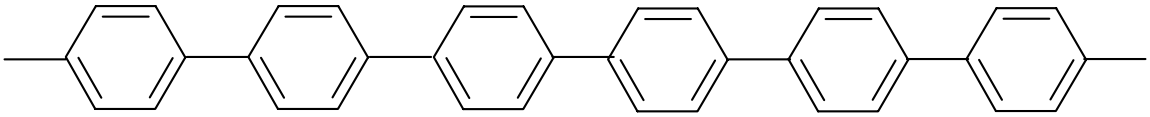

Polyphenylene

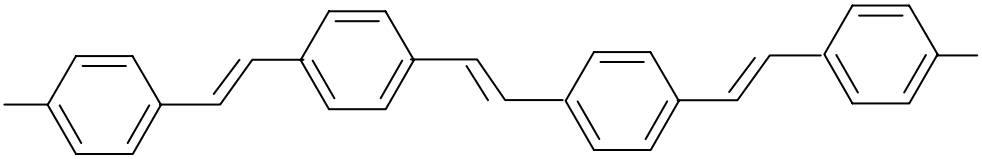

Poly(phenylene vinylene)

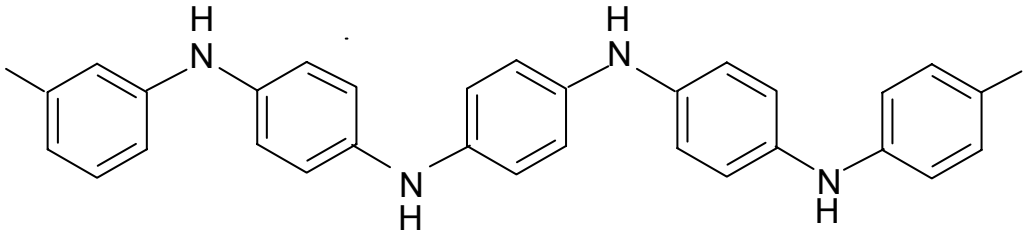

Polyaniline

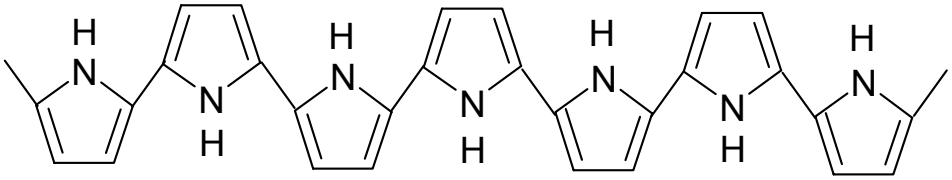

Polypyrrole

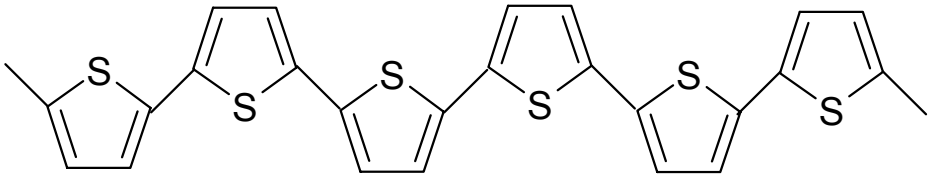

Polythiophene

Figure 1.2: Schematic representation of Conjugated Polymers

- Net charge carrier mobilities in the conducting state are large enough and because of this high electrical conductivity is observed.
- Quasiparticle, which under certain conditions, may move relatively freely through the material.

The electrical and optical properties of these kinds of materials depend on the electronic structure and on the chemical nature of the repeated units. The electronic conductivity is proportional to both density and the drift mobility of the charged carriers. The carrier drift mobility is defined as the ratio of the drift velocity to the electric field and reflects the ease with which carriers are propagated. To enhance the electrical conductivity of polymers, an increase in the carrier mobility and the density of the charge carriers is required.[14]

As the present work deals with conducting materials polypyrrole and polyaniline, a brief history of these materials is given here.

1.2.4 (A) Polypyrrole (PPy)

Among known conducting polymers polypyrrole is most frequently used in the commercial applications due to the high conductivity, long term stability of its conductivity and the possibility of forming homopolymers or composites with optimal mechanical properties. It is know for its stability in the oxidized state and interesting redox properties. Conducting polypyrrole can be prepared by various methods such as chemical, electrochemical, vapor phase etc. The different two oxidation states of PPy are shown in the **Figure 1.3** below.

Chemical Synthesis

Chemical polymerization of pyrrole was first reported in the year 1916 by Angeli and his group.[15] They synthesized polypyrrole by the oxidation of pyrrole with H_2O_2. PPy powder as obtained was amorphous in nature and was known as pyrrole black. Generally, pyrrole black have been prepared in presence of various oxidizing agents like H_2O_2,

PbO_2, Quinones or O_3. The materials thus obtained by this method are mainly insulating in nature with room temperature conductivity 10^{-10} to 10^{-11} Scm^{-1}, but

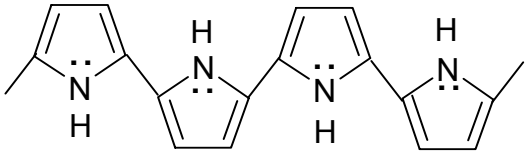

Aromatic Structure

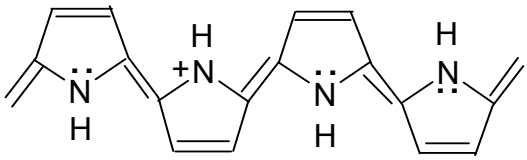

Quinoid Structure

Figure 1.3: Various oxidation states of polypyrrole

after subjecting to doping with halogenic electron acceptor, the conductivity rises to 10^{-5} Scm^{-1}.[16] The low conductivity of polypyrroles prepared from acid or peroxide initiators is associated with the high degree of saturation of the pyrrole rings in the polymer. One of the great advantages of PPy from synthetic point of view is its low oxidation potential of the pyrrole monomer. Pyrrole is one of the most easily oxidized monomer and hence a variety of oxidizing agents are available for preparing polypyrrole. Commonly used oxidants for pyrrole polymerization are oxidative transition metal ions. Various metallic salts such as $FeCl_3$, $Fe(NO_3)_3$, $Fe(SO_4)_3$, $K_3Fe(CN)_6$, $CuCl_2$ etc have been employed to polymerize pyrrole with conductivity between 10^{-5} to $200Scm^{-1}$. Ferric salts are the most commonly used oxidizing agents for the synthesis of highly conducting PPy, scheme for which is given below.

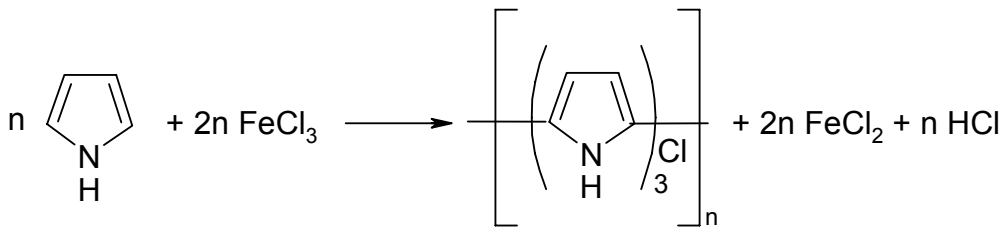

Figure 1.4: Reaction scheme for PPy chemical synthesis

The mechanism is similar to the mechanism proposed by Hsing et al.[17] The reaction would be initiated by the cationic radical $C_4H_5\cdot^+$, which coordinates with the other pyrrole units. The transition metal ion being the electron acceptor, probably forms a donor acceptor complex with the □-system of pyrrole at the chain initiation step as well as the polymer intermediate at the final rearomatization step.

Electrochemical Synthesis

The electrochemical synthesis of PPy was first carried out by Dall'Ollio in aqueous sulphuric acid on Pt electrode.[18] According to Diaz and Kanazawa the electrochemical synthesis of PPy film proceeds via the oxidation of pyrrole at the platinum electrode to produce an unstable □-radical cation which then reacts with the neighboring pyrrole species.[19] Cyclic voltammograms of this solution shows an irreversible peak for the oxidation of pyrrole at +1.2V versus SCE. The mechanism of the overall reaction for the formation of fully aromatized product is very complicated and involves series of oxidation and deprotonation steps.

Generally PPy films are prepared by the electro-oxidation of pyrrole in one compartment cell equipped with platinum working electrode, gold wire counter electrode and SCE as the reference electrode. A wide variety of solvents and electrolytes can be used as the electrical resistance of the solution is high and the nucleophilicity does not interfere with the polymerization reaction. The reaction mechanism for the electrochemical synthesis of PPy is given in the **figure 1.5**.

These conditions can be accomplished by selecting solution where the electrolyte is highly dissociative and slightly acidic. Films of various thicknesses can be prepared by changing the current density. As the electrical potential needed to oxidize the monomer is

higher than the charging (or doping) of the formed polymer, the polymer is directly obtained in the conducting state.

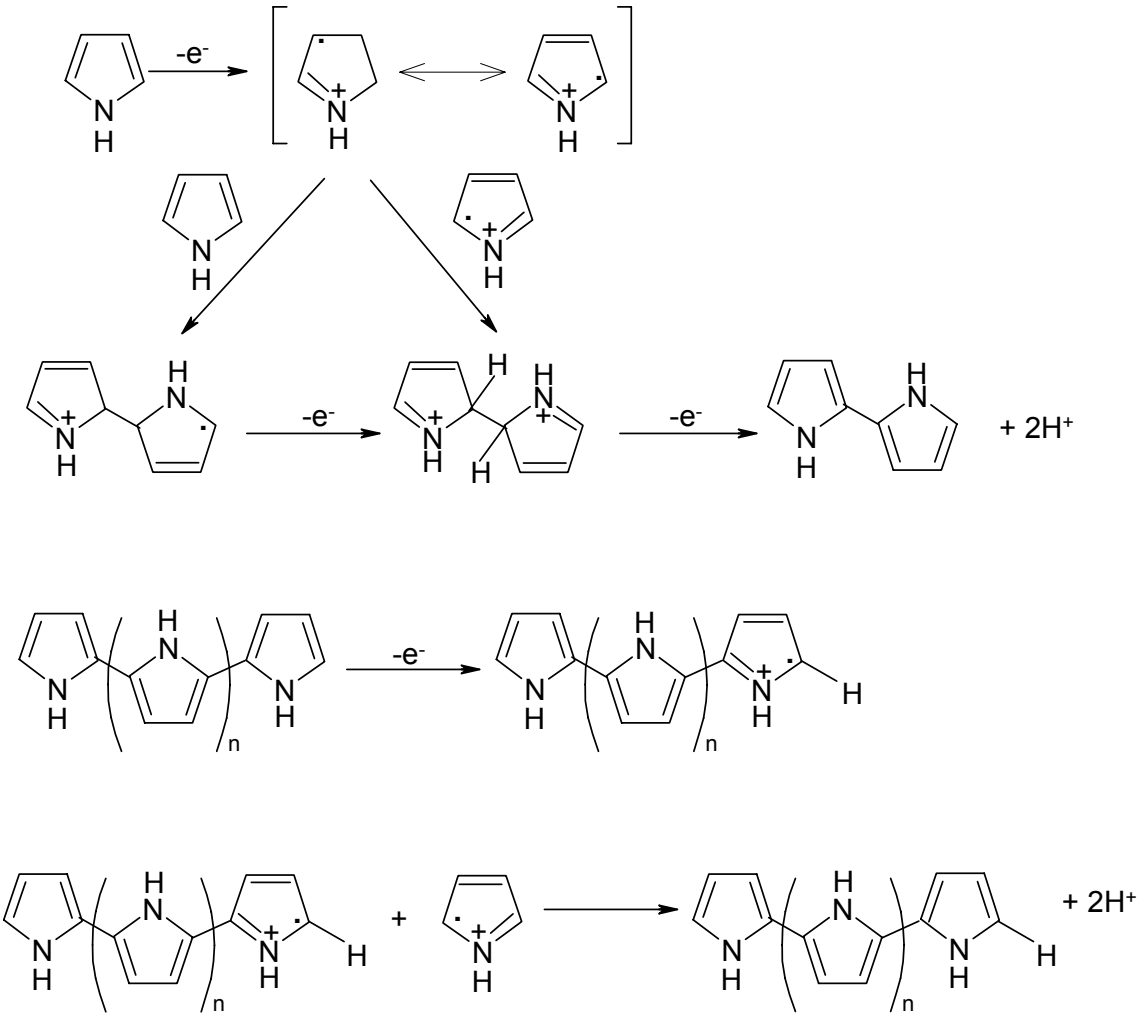

Figure 1.5: Mechanism for the electropolymerisation of pyrrole

1.2.4 (B)Polyaniline (PANI)

The continuously growing interest in the study of PANI over the years is mainly because of it's diverse, but unique properties of PANI, allowing its potential applications in

various fields. Among all the conducting polymers, polyaniline is known for it's (i) ease of synthesis (ii) environmental stability and (iii) easy to dope by protonic acids.

Polyaniline is a typical phenylene based polymer having a chemically flexible –NH- group in a polymer chain flanked either side by a phenylene ring. It can also be defined as the simple 1,4- coupling product of monomeric aniline molecule. The protonation and deprotonation and various other physico-chemical properties of polyaniline is due to the presence of the –NH- group. Polyaniline is the oxidative polymeric product of aniline under acidic conditions and has been known since 1862 as an aniline black.[20] There are several reports of polyaniline found in the literature over the decades about the structure and constitutional aspect of aniline polymerization.[21] In the year 1968, Surville et al reported the proton exchange and redox properties with the influence of water on the conductivity of polyaniline.[22] However, interest in polyaniline was generated only after the fundamental discovery in 1977 that iodine doped polyacetylene gives metallic conductivity which triggered research interest in new organic conducting materials.[23] Polyaniline can be synthesized by both chemical and electrochemical oxidative polymerization.[24,25] Polyaniline exists in four main oxidation states viz.

(i) Leucoemeraldine base,
(ii) Emeraldine base
(iii) Emeraldine salt and
(iv) Pernigraniline,

Schematic representations for which are shown in the **figure 1.6**.

Chemical Synthesis

Synthesis of polyaniline by chemical oxidative route involves the use of either hydrochloric or sulfuric acid in the presence of ammonium peroxo-di-sulfate as the oxidizing agent in the aqueous medium.[26-29]

The principal function of the oxidant is to withdraw a proton from an aniline molecule, without forming a strong co-ordination bond either with the substrate / intermediate or with the final product. However smaller quantity of oxidant is used to avoid oxidative degradation of the polymer formed. In the review article by Gospodinova et al [24], they

had reported that the propagation of polymer chains proceeds by a redox process between the growing chain (as an oxidant) and aniline (as a reducer) with addition of monomer to

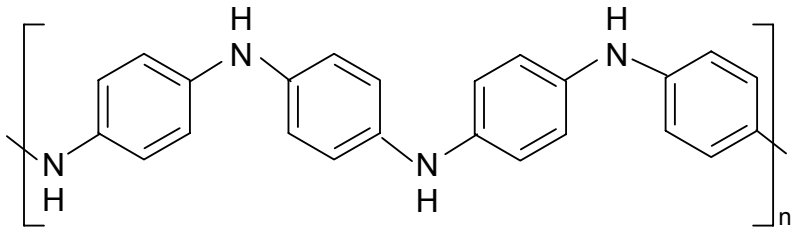

Leucoemeraldine

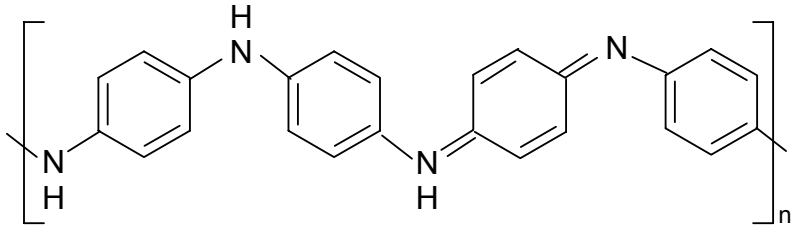

Emeraldine base

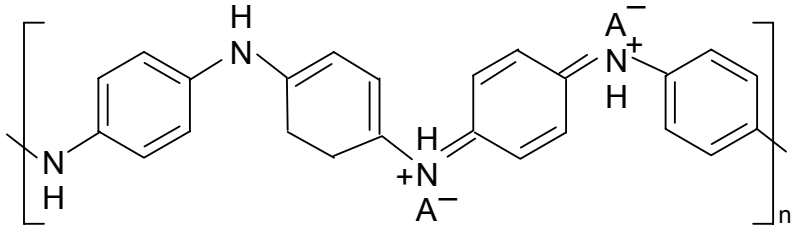

Emeraldine salt

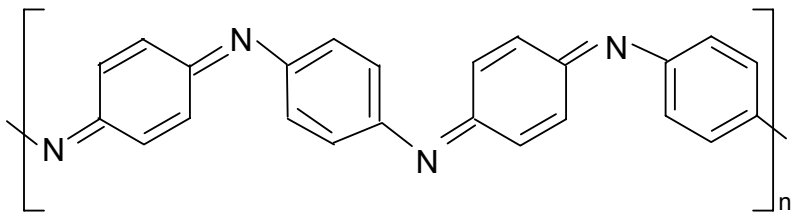

Pernigraniline

Figure 1.6: Various oxidation states of Polyaniline

the chain end. The high concentration of a strong oxidant, $(NH_4)_2S_2O_8$, at the initial stage of the polymerization enables the fast oxidation of oligo- and polyaniline, as well as their existence in the oxidized form. They reported the presence of oxidized oligomers and

$$Ar\text{-}NH_2 \xrightarrow{Ar\text{-}NH_2} Ar\text{-}NH\text{-}Ar\text{-}NH_2$$

$$Ar\text{-}NH\text{-}Ar\text{-}NH_2 \xrightarrow[2e,\ -2H^+]{Ar\text{-}NH_2} Ar\text{-}NH\text{-}Ar\text{-}NH\text{-}Ar\text{-}NH_2$$

$$Ar\text{-}NH\text{-}Ar\text{-}NH\text{-}Ar\text{-}NH_2 \xrightarrow[Coupling]{Further\ Oxidative} Polyaniline$$

pernigraniline at the initial stage of polymerization. Armes et al had reported the polymerization of aniline at 20°C using ammonium per-oxo- disulfate as oxidant, where they reported the effect of the oxidant / monomer initial mole ratio. Conclusion they derived is that the conductivity, yield, elemental composition and degree of oxidation of the resulting polymer are independent of the oxidant/ monomer ratio when its value is below 1.15. They also concluded that over oxidation of polyaniline occurs at higher oxidant : monomer mole ratios. Asturias et al studied the influence of the atmosphere (viz air and argon) on the degree of oxidation of polyaniline, using $(NH_4)_2S_2O_8$ as the initiator. Cao et al reported the commonly employed procedure for protonation of polyemeraldine salt ie. stirring of polyaniline powder with concentrated aqueous HCl solution, leading to the significant degradation of polyaniline. Pron et al had synthesized polyaniline with four different oxidizing agents and at different aniline: oxidant ratios and compared the electrical conductivity and the reaction yield. They reported that the redox potential of the oxidant is not a dominant parameter in the chemical oxidative polymerization of aniline.[27-33]

Electrochemical Synthesis

Electrochemical synthesis of polyaniline is a radical combination reaction and is diffusion controlled. Electropolymerization is generally carried out in aqueous protonic acid medium and this can be achieved by any one of the methods given here

i) Galvenostatic: constant current in the range of 1-10mA.

ii) Potentiostatic: at constant potentials- 0.7 to 1.1V versus SCE. and

iii) Sweeping the potential: between two potential limits -0.2V to +1.0V vs. SCE.

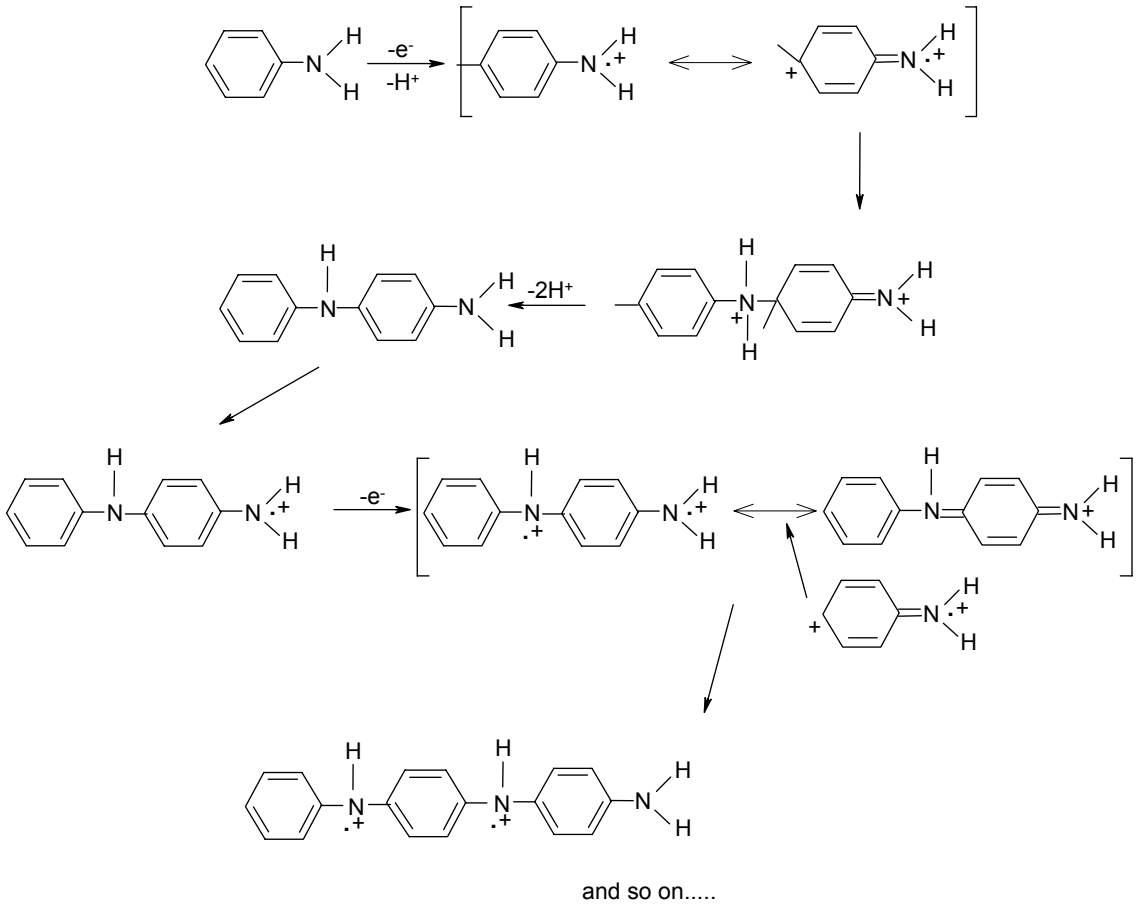

Figure 1.7: Electrochemical synthesis of Polyaniline

The first electrochemical synthesis of polyemeraldine salt was reported by Letheby in the year 1862.[20] In the year 1962 Mohilner et al reported the mechanistic aspects of aniline

oxidation.[29] Major interest in the electrochemistry of polyaniline was generated only after the discovery that aromatic amine, pyrrole, thiophene, furan, indole and benzene can be polymerized anodically to conducting film.[36,37] Electrochemically prepared polyaniline is the preferred method to obtain a clean and better ordered polymer thin film. Diaz et al [35,37] and others [34],[38] have reported the preparation of polyaniline in an aqueous solution using a platinum electrode by cycling the potential between –0.2 to 0.8V versus SCE. The physicochemical properties of polyaniline films cast from organic solvent like NMP are reported by Kang et al.[39] Shaolin et. al[40] had reported that the conductivity of Pani films synthesized in presence of NaCl salt is about 30 times higher than that the Pani films prepared without NaCl. Chan and Lee investigated the structure and doping behavior Pani films plasticized with NMP.[41]Lux had reported the various properties of conducting polyaniline in his review article.[33]

1.3. CHARGE TRANSPORT IN CONDUCTING POLYMER

It is well known that polymers with conjugate bonding system, running through the whole molecule are usually electrically conducting. The electrical properties of conducting polymers depend on the electronic band structure. When the bands are filled or empty, no conduction occurs. If the band gap is small compared with thermal excitation energies, electrons are excited to the conduction band and thus conductivity increases. When the band gap is too wide, thermal excitation is insufficient to excite electrons to the conduction band and the material is an insulator.

The conductive polymers carry current without having partially empty or partially filled bands. The most important characteristics, however, is that when the polymers are highly oxidized the charge carriers are spinless. To explain the conduction phenomena, it is proposed that when an electron is removed from the top of the valence band by oxidation a vacancy (hole or radical cation) is created, but it does not delocalize completely. Partial delocalization occurs over several monomer units, and the units deform structurally. The energy level associated with the radical cation represents a destabilized bonding orbital and thus has a higher energy than that of the valence band. A radical cation that is partially delocalized over some polymer segment is called a ‘polaron’. A dication or ‘ bipolaron’ has two charges associated with the localized polymer segment. Thus, low

oxidation levels yield polarons and higher oxidation levels give the bipolarons. Both polarons and bipolarons are mobile and can move along the polymeric chain by the rearrangement of the double and single bonds in the conjugated system that occurs in an electric field. Conduction by polarons and bipolarons is the dominant mechanism of charge transport in polymers with non-degenerate ground states.

There are several models for electrical conduction. The most widely used is the one-electron band model. This is based on extending the simple model of a bond between two atoms over whole crystalline solid.

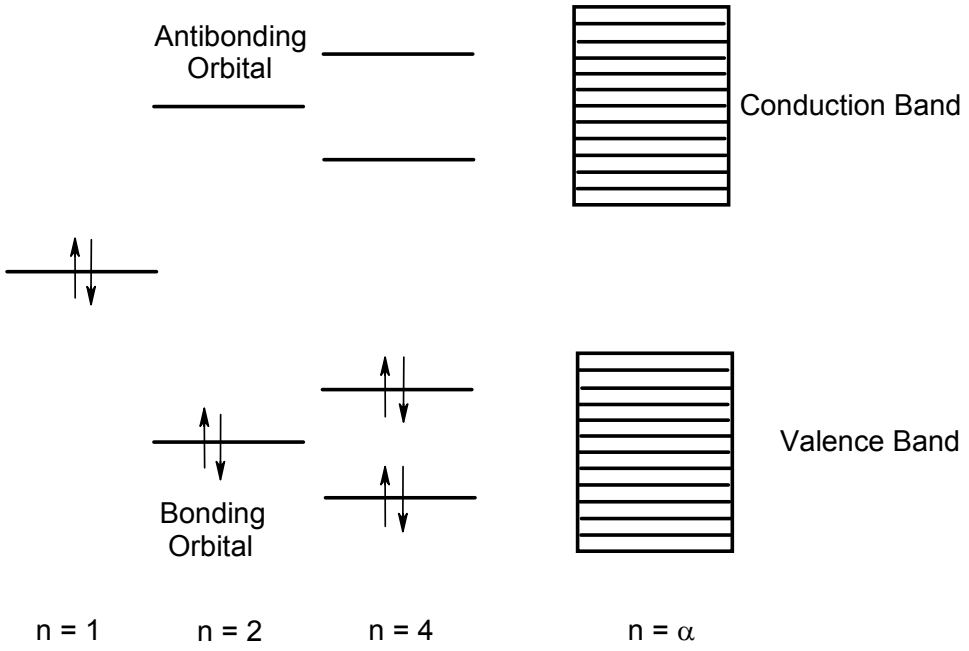

Figure 1.8: One Electron Band model for electrical conduction

When two identical atoms each having a half filled orbital are brought together closely enough for their orbitals to overlap, the two orbitals interact to produce two new orbitals, one of lower energy and one of higher energy. The magnitude of this energy difference is determined by the extent of orbital overlap. The two electrons go in to the lower energy orbital. The (now filled) lower energy orbital is a bonding orbital and the high energy(empty) orbital is an antibonding orbital. The magnitude of the conductivity is determined by the number of charge carriers available for conduction and the rate at

which they move. In order to consider the effect of temperature on the electrical conductivity of the three main classes of materials (metals, semiconductors and insulators), it is therefore necessary to consider its effect on both charge carrier concentration and mobility. In a metal all the electrons are available for conduction, so the conductivity is determined by the mobility. As the temperature of a crystal lattice is increased, the atoms vibrate and interact with the electrons to scatter them. Thus in a metal the conductivity decreases with increasing temperature. In a semiconductor the same is true, but also the charge carrier concentration increases with increasing temperature. Since the charge carrier concentration is much more temperature dependent than the mobility, this is the dominant factor and conductivity increases with increase in temperature. In an insulator the band gap is so large that it is very difficult to thermally excite electrons across it to provide charge carriers, and thus at reasonable temperatures the conductivity remains low.

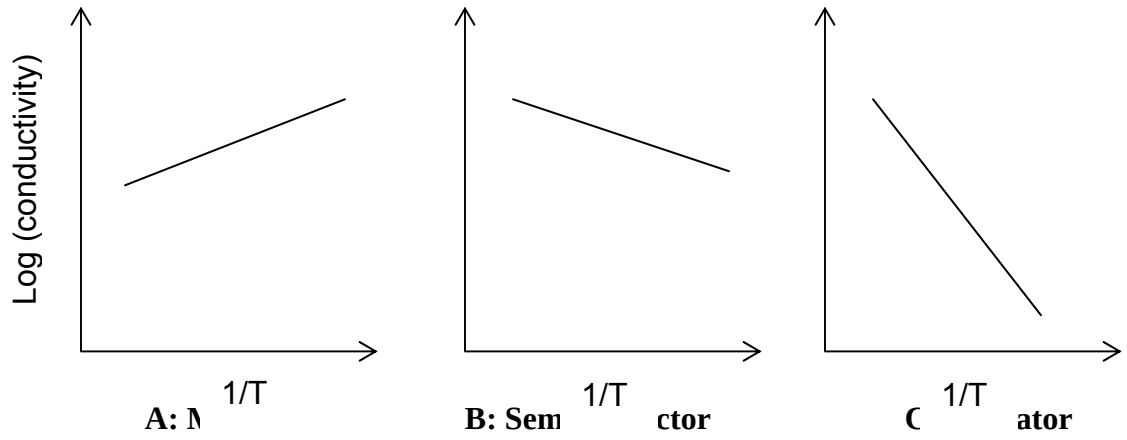

Figure 1.9: Conductivity behavior of metal, semiconductor and insulator as a function of reciprocal of temperature.

Conducting polymers are amorphous in nature with short conjugation lengths. Therefore it has been suggested that electrical conduction take place by charge hopping between polymeric chains.

The electrical conductivity in homogeneous systems can be well explained by quasi-particles such as polaron, bipolaron and solitons. In heterogeneous systems the structure is not uniform but rather a more disordered or branched one. In this type of system the charge transport along the polymer chains take place by hopping or tunneling process.

1.4. DOPING OF POLYMERS

Conjugated organic polymers are either electrical insulators or semiconductors. These polymers can become highly electrically conductive after carrying out a structural modification process called “doping”. Doping can be simply regarded as the insertion or ejection of electrons. Doping process results in dramatic changes in the electronic, electrical, magnetic, optical, and structural properties of the polymer. Doping of polymeric semiconductors is different from that in inorganic or conventional semiconductors. Inorganic semiconductors have three dimensional crystal lattice and on incorporation of specific dopant, n-type or p-type in ppm level, the lattice becomes only highly distorted. The dopant is distributed along specific crystal orientations in specific sites on a repetitive basis. Whereas, doping of conducting polymer involves random dispersion or aggregation of dopants in molar concentrations in the disordered structure of entangled chains and fibrils. The dopant concentration may be as high as 50%. Also incorporation of the dopant molecules in the quasi one dimensional polymer systems considerably disturbs the chain order leading to reorganization of the polymer. Doping process is reversible, and it produces the original polymer with little or no degradation of the polymer backbone. Both doping and undoping processes, involving dopant counterions which stabilize the doped state, may be carried out chemically or electrochemically

Doping of inorganic semiconductors generates either holes in the valence band or electrons in the conduction band. On the other hand, doping of polymer leads to the formation of conjugation defects, viz. solitons, polarons or bipolarons in the polymer chain. The ultimate conductivity in polymeric semiconductors depends on many factors, viz. nature and concentration of dopants, homogeneity of doping, carrier mobility, crystallinity and morphology of polymers. By controllably adjusting the doping level,

conductivity anywhere between that of the non-doped (insulating or semiconducting) and that of the fully doped (highly conducting) form of the polymer can be easily obtained.

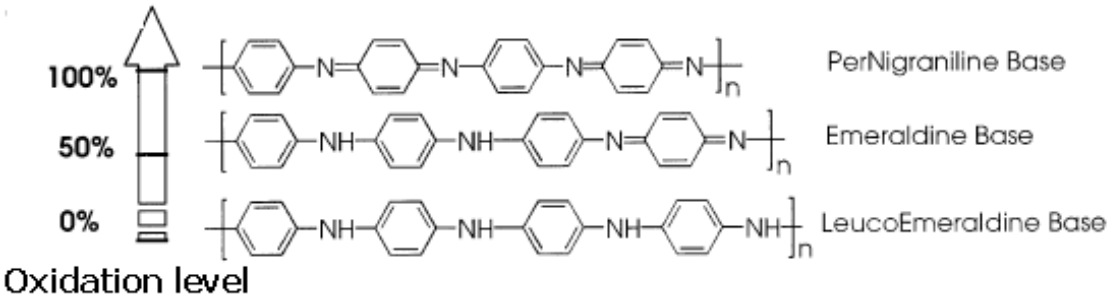

Figure 1.10: Different percentage of oxidation level obtained in Pani by *p-doping*

The various oxidation states of Pani obtained by different doping is given in the **Figure 1.10.** Generally in conducting polymers p-type doping is conducted with an electron acceptor, such as I_2 and n-type doping is conducted with donor specie, such as Li.

In the doped state, the backbone of a conducting polymer consists of a delocalized □ -system. In the undoped state, the polymer may have a conjugated backbone such as in trans- $(CH)_x$ which is retained in a modified form after doping, or it may have a nonconjugated backbone, as in polyaniline (leucoemeraldine base form), which becomes truly conjugated only after p-doping, or a nonconjugated structure as in the emeraldine base form of polyaniline which becomes conjugated only after protonic acid doping which is shown in the **Figure 1.10** above.

1.4.1. Different types of Doping

Redox doping

All conducting polymers e.g., PPy, PT, Pani etc undergo p- and/ or n- redox doping by chemical and/ or electrochemical processes during which the number of electrons associated with the polymer backbone changes. p-doping is accompanied by partial oxidation of the □-backbone of the polymer. It was first discovered by treating trans-$(CH)_x$ with an oxidizing agents such as iodine. p-doping can also be done by electrochemical anodic oxidation by immersing a trans-$(CH)_x$ film in a solution of $LiClO_4$

and attaching it to the positive terminal of a DC power source, the negative terminal being attached to an electrode also immersed in the solution.

n-doping, ie partial reduction of the backbone □-system of an organic polymer, was also discovered using trans-$(CH)_x$ by treating it with a reducing agents such as sodium naphthalide.

Photo doping

When trans$(CH)_x$ is exposed to radiation of energy greater than its band gap, electrons are promoted across the gap and polymer undergoes "photo-doping".

Charge injection doping

Charge injection doping is most conveniently carried out using a metal/insulator/semiconductor (MIS) configuration involving a metal and a conducting polymer separated by a thin layer of a high dielectric strength insulator. Application of an appropriate potential across the structure can give rise to a surface charge layer. The resulting charges in the polymer, for example, $(CH)_x$ or poly (3-hexylthiophene) are present without any associated dopant ion.

Non redox doping

This type of doping differs from redox doping is that the number of electrons associated with the polymer backbone does not change during the doping process. The energy levels are rearranged during doping. The emeraldine base form of Pani was the first example of the doping of an organic polymer to a highly conductive regime by non-redox type doping.

1.4.2. Types of Doping Agents

Dopants may be classified as (a) Neutral dopants, (b) Ionic dopants, (c) Organic dopants, and (d) Polymeric dopants.

(a) Neutral dopants: I_2, Br_2, AsF_2, Na, K, H_2SO_4, $FeCl_3$ etc.
(b) Ionic dopants: $LiClO_4$, $FeClO_4$, CF_3SO_3Na, $BuNClO_4$ etc.
(c) Organic dopants: CF_3COOH, CF_3SO_3Na, p-$CH_3C_6H_4SO_3H$
(d) Polymeric dopants: PVS, PPS, PS-co-MA

Neutral dopants are converted into negative or positive ions with or without chemical modifications during the process of doping. Ionic dopants are either oxidized or reduced by an electron transfer with the polymer and the counter ion remains with the polymer to make the system neutral. Organic dopants are anionic dopants, generally incorporated into polymers from aqueous electrolytes during anodic deposition of the polymer. Polymer dopants are functionalized polymer electrolytes containing amphiphilic anions.

1.4.3. Doping Techniques

Doping in polymers can be done by following ways,

- Gaseous doping
- Solution doping
- Electrochemical doping
- Self doping
- Radiation induced doping
- Ion exchange doping

Gaseous, solution and electrochemical doping methods are widely used because of the convenience in carrying out and of low cost. In gaseous doping process, the polymers are exposed to the vapor of the dopant under vacuum. The level of dopant concentrations in polymers may be easily controlled by temperature, vacuum and time of exposure.

Solution doping involves the use of a solvent in which all the products of doping are soluble. Polar solvents such as acrylonitrile, tetrahydrofuran, nitro methane are used as solvents. The polymer is treated with dopant solutions.

In the electrochemical doping technique simultaneous polymerization and doping generally occurs. But sometimes this method is used for doping for polymers obtained by other methods also. In this process only ionic type dopants are used as the electrolyte in polar solvents.

1.4.4. Effect of Doping on Conductivity.

The doping process involves transfer of the charge to or from the □-bonding system of the conjugated polymer, leaving the □-system essentially intact and hence the structural

identity of an individual chain preserved. However, vibrational, electronic and other properties of the polymer are strongly altered upon doping as well as it's supramolecular structure. The most spectacular result of the doping is the increase of the polymer conductivity over several orders of magnitude. In some cases conjugated polymers reach the conductivity of metals with a negative temperature coefficient which is characteristic of metallic behavior.[42-46]

Doping with acceptor or donor molecules causes a partial oxidation (p-doping) or reduction (n-doping) of the polymer molecule. As a result positively or negatively charged quasi-particles are created presumably polarons in the first step of doping. When doping proceeds, reactions among polarons take place, leading to energetically more favorable quasi-particles, ie a pair of charged solitons (bipolarons) in materials with a degenerate ground state. Thus due to the changes in the environment of the chains disorders are created from doping.

At low dopant concentration, the dopant molecules occupy random positions between the chains. The effect the electronic properties by their coulomb potential and by hybridization with the polymer p-orbitals. As polarons produced has long lifetime, they are treated as quasi-particles. Polarons have low mobility, which results in obtaining moderate conductivity at low doping concentration. As the doping level is increased, the concentration of polarons goes up and they become crowded together, close enough to form bipolaron. At this point in the doping process, conductivity undergoes a marked increase. Once the radical components of the polarons have combined to form □-bonds, the remaining charges achieve high mobility along the chain. Example showing formation of polarons –bipolarons in polypyrrole chain is given in the **figure 1.11** below.

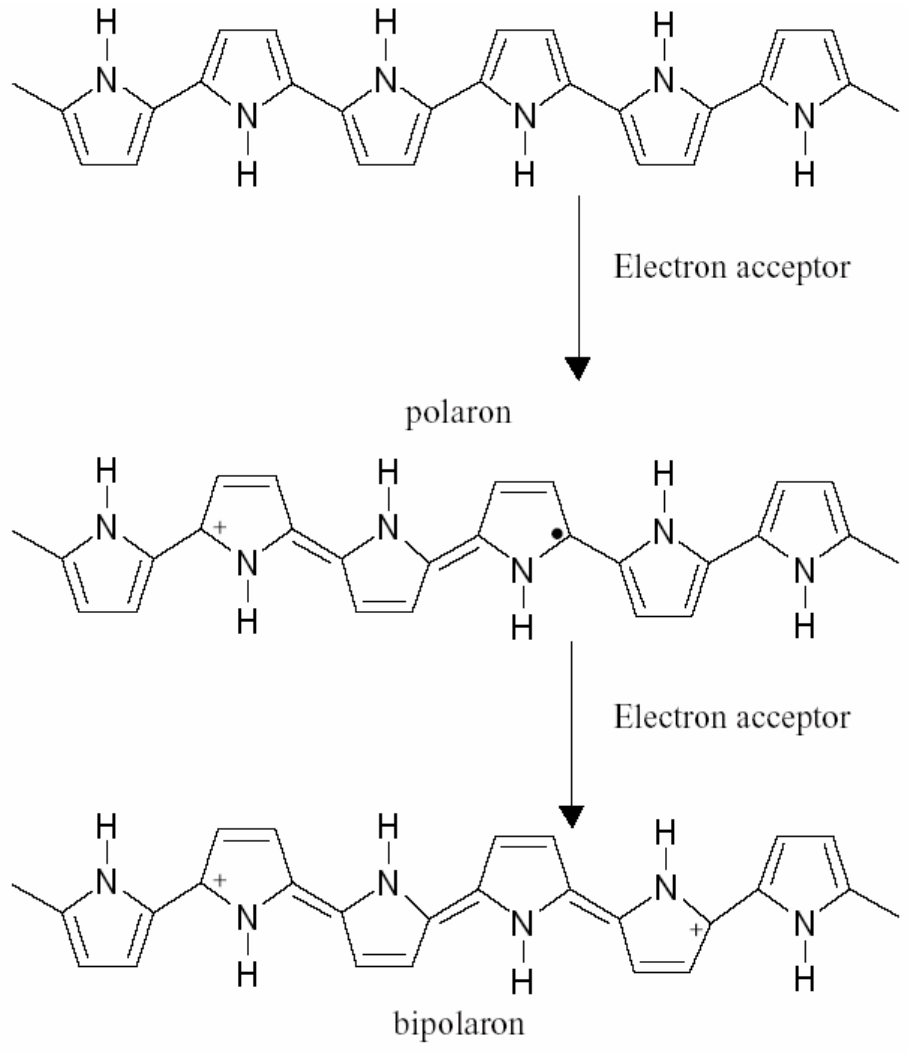

Figure 1.11: Formation of polaron-bipolaron in the PPy chain

1.5. APPLICATION OF CONDUCTING POLYMERS.

Research shows that conducting polymers exhibit conductivity from the semiconducting range (~10^{-5} S/cm) right up to metallic conductivity (~10^{4} S/cm). With this range of electrical conductivity and low density coupled with low cost polymeric conductor pose a serious challenge to the established inorganic semiconductor technology. There are mainly two groups of applications for organic conducting polymers which is briefly described below:

Group I: These applications just use the conductivity of the polymers. The polymers are used because of either their lightweight, biological compatibility for ease of manufacturing or cost. Electrostatic materials, Conducting adhesives, Electromagnetic shielding, Printed circuit boards, Artificial nerves, Antistatic clothing, Piezoceramics, Active electronics (diodes, transistors), Aircraft structures

Electrostatic materials: By coating an insulator with a very thin layer of conducting polymer it is possible to prevent the buildup of static electricity. This is particularly important where such a discharge is undesirable. Such a discharge can be dangerous in an environment with flammable gasses and liquids and also in the explosives industry. Bayer uses polythiophene as an anti-static layer in film products.

Conducting adhesives: By placing monomer between two conducting surfaces and allowing it to polymerize it is possible to stick them together. This is a conductive adhesive and is used to stick conducting objects together and allow an electric current to pass through them

Electromagnetic shielding: Many electrical devices, particularly computers, generate electromagnetic radiation, often radio and microwave frequencies. This can cause malfunctions in nearby electrical devices. By coating the inside of the plastic casing with a conductive surface this radiation can be absorbed.

Printed circuit boards: Many electrical appliances use printed circuit boards. These are copper coated epoxy-resins. The copper is selectively etched to produce conducting lines used to connect various devices. These devices are placed in holes cut into the resin. In order to get a good connection the holes need to be lined with a conductor. Copper has been used but the coating method, electroless copper plating, has several problems. This process is being replaced by the polymerization of a conducting plastic. If the board is etched with potassium permanganate solution a thin layer of manganese dioxide is produced only on the surface of the resin. This will then initiate polymerisation of a suitable monomer to produce a layer of conducting polymer.

Artificial nerves: Due to the biocompatibility of some conducting polymers they may be used to transport small electrical signals through the body, i.e. act as artificial nerves.

Aircraft structures: Modern planes and spacecraft are often made with lightweight composites. This makes them vulnerable to damage from lightning bolts. By coating aircraft with a conducting polymer the electricity can be directed away from the vulnerable internals of the aircraft.

Group II: This group utilizes the electroactivity character property of the materials. Molecular electronics, Electrical displays, Chemical, biochemical and thermal sensors, Rechargeable batteries and solid electrolytes, Drug release systems, Optical computers, Ion exchange membranes, Electromechanical actuators, 'Smart' structures, Switches

Rechargeable batteries: Batteries were one of the first areas where conducting polymers promised to have a commercial impact. Conducting polymer batteries were investigated by leading companies like BASF/VARTA and Allied Signal.[47] A number of conducting polymers such as polyacetylene, polyaniline and other polyheterocycles have been used as electrode materials for rechargeable batteries. Bridgestone has already marketed a button sized battery using polyaniline and lithium. Trivedi et al had studied extensively on rechargeable batteries using conducting polymers.[48]

Sensors: Since electrical conductivity of conducting polymers varies in the presence of different substances, these are widely used as chemical sensors or as gas sensors. In its simplest form, a sensor consists of a planar interdigital electrode coated with conducting polymer thin film. If a particular vapor is absorbed by the film and affects the conductivity, its presence may be detected as a conductivity change. Interdigited electrodes covered by a PPy layer have been tested by Miasik et al[49]. Yoneyama et. al. showed that electropolymerized PPy films exhibit gas sensitivities to electron acceptor gases such as PCl_3, SO_2 and NO_2 at room temperature. The same group investigated the gas sensing behavior of polythiophene film also.[50-51] Radhakrishnan et al had used phthalocyanine incorporated conducting polymers viz. Pani, PPy and PT as sensor materials for detecting NO_2 gas.[52] Dhawan and coworker devised ammonia sensors with

polyaniline.[53] Contractor et al had reported the use of electrochemically prepared polyaniline film for urea sensors.[54] The same group is working on biosensors based on conducting polymer also.[55]

*Electrochromic devices***:** The phenomenon of electrochromism can be defined as the change of the optical properties of a material due to the action of an electric field. The field reversal allows the return to the original state. Conjugated polymers that can be repeatedly driven from insulating to conductive state electrochemically with high contrast in color are promising materials for electrochromic device technology. Conjugated polymers have an electronic band structure. The energy gap between the valence band and the conduction band determines the intrinsic optical properties of the polymers. The color changes elicited by doping are due to the modification of the polymer band electronic structure. The electrochromic materials first drew interest in large area display panels. In architecture electrochromic devices are used to control the sun energy crossing a window. In automotive industry rearview mirrors are a good application for electrochromic system. With oxidation, polypyrrole turns from yellow to black whereas polythiophene turns from red to blue.[56]

Electromechanical Actuators: Conducting polymers also change volume depending on their oxidation state. Therefore it is possible for conducting polymers to convert electrical energy into mechanical work. Conducting polymer actuators were proposed by Baughmann and coworkers.[57] Oxidation induced strain of polyaniline[58] and polypyrrole based actuators has been reported.[59] The first self contained actuators were reported by MacDiarmid et al.[60]

*Drug release systems***:** Another application for conducting polymers is controlled release devices. Ions[61-63] can be selectively released, as well as biologically active ions such as adenosine 5- triphosphate(ATP) [64,65]and Heparin. Principle used in this application is potential dependence ion transport. This potential dependence ion transport is an interesting way to deliver ionic drugs to certain biological systems. One can deliver selective ions depending on the requirement.

Catalyst: Conducting polymers show redox property, therefore these are expected to behave as redox catalyst. Several reports have been found in the literature on modification of conducting polymers and their use as catalyst for small organic molecules. Conducting polymers in their various oxidation states interconvert each other, which permits to construct redox cycle for catalytic reactions. The catalytic activity has been revealed to be controlled by doping. Coordination of transition metals to the nitrogen atoms (in case of Pani and PPy) affords the complexes, in which transition metals are considered to interact through a □-conjugated chain. The characteristics of □-conjugated polymers are reflected on the complexes, which are expected to provide a novel catalytic system. The complex catalyst consisting of Pd(II) acetate and Pani or PPy is capable of inducing the Wacker oxidation also. As the present work deals with studies of the catalytic properties of conducting polymers, details about the catalytic properties have been discussed in the following sections.

1.6. CATALYST MATERIALS

Role of catalyst is to accelerate a chemical reaction, without affecting the position of the chemical equilibrium. Catalyst offers reactants, an alternative lower energy path way to products. It makes it easier for a system to go from initial to final state. A catalyst sets out to make the free energy of activation as small as possible or at least less than that found in the uncatalyzed reaction. Catalyst involved in chemical bonding with the reactants are bound to one form of the catalyst, and the products are released from another form, regenerating the initial state. The intermediate catalyst complexes are in most cases highly reactive and difficult to detect.

In theory, an ideal catalyst would not be consumed, but this is not the case in practice. The catalyst undergoes chemical changes, and it's activity becomes lower (deactivation).

Apart from accelerating reactions, catalysts have another important property, they can influence the selectivity of chemical reactions. Catalysts can be solids, liquids or gases. The suitability of a catalyst for an industrial process depends on-

- Activity
- Selectivity
- Stability

Activity is a measure of how fast one or more reactions proceed in the presence of a catalyst. Activity can be defined in terms of kinetics. In formal kinetic treatment, it is appropriate to measure reaction rates in the temperature and concentration ranges that will be present in the reactor. Catalyst activity can be expressed in the form of Turn Over Number (TON) also which is defined as

for heterogeneous catalyst,

- No of reactant molecules reacted per active center per second.

and for homogeneous catalyst,

- Moles of reactant consumed per mole catalyst per second.

The *selectivity* of a reaction is the fraction of the starting material that is converted to the desired product. It is expressed by the ratio of the amount of desired product formed to the reactant quantity of a reaction partner and therefore gives information about the course of the reaction. In addition to the desired reaction, parallel and sequential reactions can also occur.

The chemical, thermal and mechanical *stability* of a catalyst determines it's lifetime in reactors. Catalyst deactivation can be followed by measuring activity or selectivity as a function of time. The total catalyst lifetime is of crucial importance for the economics of a process.

Catalysis are classified according to the state of aggregation in which they act. There are two large groups,

- Heterogeneous Catalysts (solid state catalysts)
- Homogeneous Catalyst.

Catalytic processes that take place in a uniform gas or liquid phase are classified as *homogeneous* catalysis. Homogeneous catalysts are generally well defined chemical compounds or co-ordination complexes, which together with the reactants, are molecularly dispersed in the reaction medium. Examples of homogeneous catalysts include mineral acids and transition metal compounds.

Heterogeneous catalytic process takes place between several phases. Generally the catalyst is solid and the reactants are gases or liquids, e.g., Pt/Rh nets for the oxidation of ammonia to nitrous gases and supported catalysts such as Ni on Kieselguhr fat hardening.

Comparison of homogeneous and heterogeneous catalyst

For heterogeneous catalysts, phase boundaries are always present between the catalyst and the reactants. In homogeneous catalysis, catalyst, starting materials and products are present in the same phase. Homogeneous catalysts have a higher degree of dispersion and each individual atom can be catalytically active and therefore exhibits a higher activity per unit mass of metal, then heterogeneous catalysts, where only surface atoms are active. The most prominent feature of homogeneous transition metal catalysts are that high selectivities can be achieved.

Homogeneously catalyzed reactions are controlled mainly by the kinetics and less by material support, because diffusion of the reactants to the catalyst can occur more readily. Due to the well defined reaction site, the mechanism of homogeneous catalysis is relatively well understood. In contrast, processes occurring in heterogeneous catalysis are often obscure. The major disadvantages of homogeneous catalysts is the difficulty of separation of catalyst from product.

There are various reports available of using polymer supported catalyst also[66-70]. These catalysts, which may be considered as heterogeneous, mainly consist of fine particles of metals/ metal oxides incorporated in conventional insulating polymers. These provide better catalytic activity than the heterogeneous ones due to better surface area and these can be removed from the final products easily. However, due to the insulating nature of the polymer, charge transfer process is considerably hindered

1.7. CHEMICAL OXIDATION OF ALKENE

In the conventional industrial method for the oxidation of olefin palladium based catalyst (Pd^{+2} salts) are used.[71-77] In this process Pd^{+2} is reduced to Pd^{0}, and in the presence of some reoxidant(e.g. $CuCl_2$, $MnCl_2$, $FeCl_3$ etc.) Pd^{0} is converted back to Pd^{+2}, which is also known as the Wacker oxidation. A simple example of industrial oxidation of ethylene to acetaldehyde is given below.

$$H_2C=CH_2 + H_2O + PdCl_2 \longrightarrow H_3C-CH=O + Pd(0) + 2HCl$$

$$Pd(0) + 2CuCl_2 \longrightarrow PdCl_2 + 2CuCl$$

$$2CuCl + 2HCl + \frac{1}{2}O_2 \longrightarrow 2CuCl_2 + H_2O$$

$$H_2C=CH_2 + \frac{1}{2}O_2 \longrightarrow H_3C-CH=O$$

These sequential oxidation and reduction reactions constitute a catalytic cycle. In general, in the Wacker oxidation terminal olefins are converted to methyl ketones.

In the industrial Wacker process, the reaction is carried out in aqueous HCl using palladium (II) chloride/ copper (II) chloride as the catalyst under oxygen pressure. The oxidation of higher terminal olefins under the same conditions is slow and sometimes accompanied by undesired by-products formed by the chlorination of carbonyl compounds by copper (II)chloride, and isomerization of double bonds. The low rate of the reaction was partly solved by the addition of suitable organic solvents which can mix olefins with water. The oxidation and double bond isomerization are competitive reactions and the extents of the reactions are influenced by solvents. DMF is good for the oxidation, whereas use of acetic acid facilitates the isomerization. But according to some group acetonitrile and dimethyl sulphoxide retard oxidation by complex formation with the catalyst.[78,80] Migration of double bond also take place at high temperature.

The use of reoxidant is essential in the Wacker processes. Copper (II) salts are good re-oxidants, but chlorination of carbonyl compounds takes place with copper (II) chloride.[79] For example chloroacetaldehyde is one of the by products of the Wacker process.

H_2O_2 can also be used to re-oxidize Pd(0) in the ethylene oxidation, which was reported by Tsuji et al. H_2O_2 was used for the styrene oxidation also with disodium tetrachloro chloro-palladate in NMP. Compared with Pd(II) chloride , the rate of the oxidation was very high.[80] However extensive double bond migration of terminal olefins occurred in the presence of H_2O_2.

The higher molecular weight □-olefine(1-hexene and larger) donot readily react with an entirely aqueous solution of $PdCl_2$ as do the lower homologues. In addition to low yields, the product obtained is often highly contaminated with the more internal ketone isomers

which are difficult to separate.[81] Higher □-olefins are subject to both oxidation and isomerization in the presence of Pd(II) salts.[82-84] Many processes have been described in the literature in which an olefin is induced to undergo reaction in presence of catalytic amount of transition metal complex. In many of these reactions the mediation of a transition metal –olefin complex has been postulated.[85-88] Whereas in some other cases palladium complex with the solvent (e.g. acetonitrile, DMF) was said to form. But the exact nature of the reaction is not understood till today.

Four principal types of reaction are encountered in these systems namely, polymerization, molecular addition to a multiple bond, multiple bond migrations and group substitutions in the vicinity of multiple bonds. Usually one of these reactions will predominate, but, frequently several may be observed to occur simultaneously.[89] Metal catalyzed oxidation of organic compounds is an expanding area of organic chemistry with many applications in industrial processes.[91] Today there is an increasing need for mild aerobic catalytic processes due to energy saving and environmental reasons. Most of the known oxidation processes based on molecular oxygen, however required elevated temperature and pressure. Recently, macro-cyclic metal complexes, in particular metalloporphyrins, have attracted attention as catalysts in oxidation reactions. There are very few reports available regarding the use of conducting polymers as catalyst. Higuchi et al and Sobczak et al had used conducting polymers for the chemical oxidation-reduction reaction.[91,92]

Here in the current study conducting polyaniline incorporated with copper phthalocyanine have been used as catalyst for the oxidation of alkenes viz. decene.

1.8. ELECTROCATALYSIS

Electrocatalysis is the science of modifying the overall rates of electrochemical reactions so that selectivity, yield and efficiency are maximized. In the electrocatalysis process electron transport takes place at the electrode/electrolyte interface. Electrode potential is used as the driving force for reaction rather than temperature and/or pressure.

Electrochemical Reactions

Electrochemical oxidation-reduction process takes place when potential is applied in the working electrode with respect to the reference electrode and this process is equivalent to

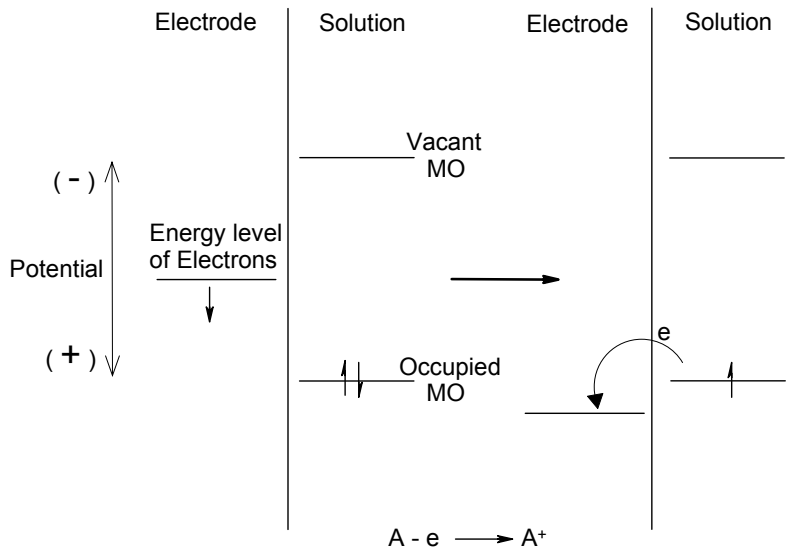

Oxidation Process

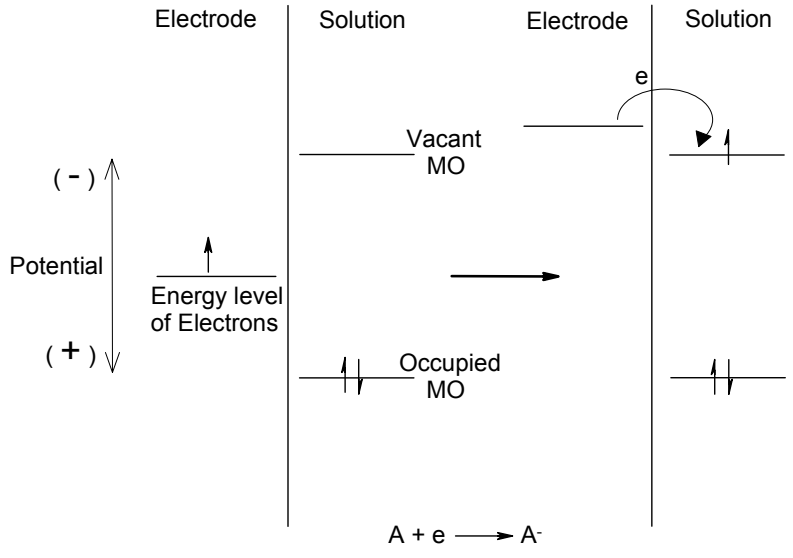

Reduction Process

Figure 1.12: Mechanism of electrochemical (a) oxidation and (b) reduction reaction

controlling the energy of the electrons within the working electrode. By driving the electrode to more negative potentials the energy of the electrons is raised, and they will eventually reach a level high enough to occupy vacant states on species in the electrolyte. In this case, a flow of electrons from the electrode to the solution (ie. reduction current) occurs. In the same manner, the energy of the electrons can be lowered by imposing more positive potential, and at some point electrons on solutes in the electrolyte will find enough energy on the electrode and will transfer there. This flow from solution to the electrode is an oxidation current. The critical potential at which these processes occur is related to the standard potentials, E^0 for the specific chemical substances in the system. Therefore it is seen that the position of the electrode and the position of the reactant in the energy level representation is the most crucial factor in determining the reaction process.

There are two basic different types of electrocatalysis: Heterogeneous, and Homogeneous,

Heterogeneous electrocatalysts

Heterogeneous electrocatalysis involves three different steps:

- Transfer of electroactive species from bulk solution to the electrode surface or within the double layer
- Exchange of electrons between the electrode and the electroactive species.
- Removal of the products from the electrode, this may involve desorption.

In heterogeneous electrocatalysis, direct charge transfer from electrode to substrate takes place to produce the product.

Homogeneous electrocatalysts

In the case of homogeneous electrocatalysis the substrate does not exchange electrons with electrode directly, but with some intermediate. Electron transfers and chemical reactions can then take place in the bulk. This process usually occurs for redox system. Two processes can occur, in one the mediator and reactant are both present in the same solution and in the other process the substrate is present in a secondary phase, and it is necessary to introduce a transfer catalyst into the system.

1.9. FACTORS INFLUENCING ELECTROCHEMICAL CATALYSIS

1. Pre-requisites for rational development of catalysts

The principle characteristic of electrocatalysis is its potential dependence. The rate does not increase with potential in the same way for all mechanisms for a given overall reaction. Hence, catalyst A will be faster than B, for a given reaction, at an overpotential, η_1, but the situation will be reverse at overpotential η_2. Thus one must decide upon some potential at which the current density per true unit area is a rational measure of the catalytic power of the given electrode. The most reasonable potential is that of zero charge. Reaction rate at the potential of zero charge on a series of electrocatalysts represents a fundamental way of comparing catalytic power; it compares the thermal part of the electrochemical catalysis, i.e., k_0 in the equation:

$$k = k_0 \exp [\pm (V - V_{p,z,e})F/RT]$$

Where $V_{p,z,e}$ is the potential zero charge. Hence a knowledge and an interpretation of k_0, although important to the understanding of catalytic power, is insufficient to predict the polarization at given potential.

It is important to note the necessity of avoiding competing reactions, when discussing the potential dependence of k. For example, for a given oxidation reaction, the thermodynamic reversible potential must be at least 0.5V more negative than the reversible potential of the nest anodic reaction possible in the system concerned.

An important pre-requisite is the knowledge of adsorption of the reactant and its dependence on potential. Substances react on electrodes only if the potential for the region in which adsorption is appreciable coincides with a potential region (for oxidation) positive to the reversible redox potential for the indicated reaction.

2. Factors which may increase rate constant:

(a)Electronic factors : In all reactions involved in electrochemical processes, charge transport plays a very important role. Hence, the electrode material should be able to

transport the charge easily. This depends on the electronic factors such as carrier mobility, number of free charges available, impurity levels, etc. in the electrode material.

(b) Surface configuration : If the necessary mechanism determination has shown that the breaking of bond is the rate determining step, the geometric factors will have effect parallel to those in chemical catalysis. An increase in the defect concentration is important in increasing catalysis in some electrode reactions. For example, in the oxidation of H_2, it is suggested that if 0.1% of 'C' is introduced in to zone refined Fe, the rate constant for the charge transfer to protons is increased about ten times.

(c) Alloys: Alloys change d-character. Introduction of a second component may increase the number of surface defects; if the less noble components (eg Mo in Pt) is an atom undergoing easy redox potential changes in solution, it may set up a redox system in the double layer, which allows a change of path of the overall reaction to one having a lower heat of activation. Several binary and ternary alloys containing Pt, or of other noble metals exhibit higher catalytic activity than does platinized Pt. It was seen that in the methanol oxidation, binary catalyst like Pt-Ru gives improved catalytic activity than the platinized Pt. The enhanced catalysis alloys in methanol oxidation cannot be explained by physical properties such as surface area, since it is same for both the catalyst. However it is difficult to relate the catalysis to merely electronic factors, since a number of metals in ternary alloys with widely varying electronic characteristics perform equally well as in binary compositions. Activation energies for oxidation on Pt and Pt-Ru alloys are also similar. It is thus possible that increase in the concentrations of surface defects on the alloyed catalyst, compared with the pure metal, gives the origin of the catalysis.

(d) *Semiconductor surfaces:* Electrode kinetics on semi-conductors has already been reported in the literature. The use of boride and carbide electrodes in oxidation reactions was first reported in 1963. Ni_2B proved to be a good catalyst in hydrazine oxidation (0.1V less polarization than Pd). The catalytic activity of Ni_2B seems to be connected primarily with its chemisorptive properties. Control of the electron energy levels in a

semi-conductor by the choice of suitable donor and acceptor species makes it possible a particular well controlled model system for work in electrocatalysis. [93]

(e)Imposed pulse of potential: Suitable pulses(say an anodic pulse to cover the electrode with O and a cathodic pulse to remove this layer, with a pulse time of 10^{-3}sec) should clean the surface from inhibiting impurity layers which may build up there, and hence maintain catalysts of constant activity. There is possibility that grain growth can also be controlled because the size of grains which nucleate is potential dependent. In principle, the momentary dissolution of surface atoms, i.e., the creation of defects, should be attainable.

3. Use of redox systems to change the path of the overall reaction.

Let us consider, the oxidation of methanol to CO_2, where the rate determining step of the reaction is charge transfer from CH_3OH to the substrate, catalytic effect should be observed if a redox couple is present which has (a) a standard potential in the neighborhood of the reversible potential, (b) i_0 values for charge transfer much greater than those exhibited by the direct transfer from the organic; (c) a sufficiently high rate constant for the subsequent homogeneous phase oxidation. Then

$$M^{2+} \longrightarrow M^{3+} + e \text{ (at electrode)}$$
$$2M^{3+} + CH_3OH \longrightarrow HCHO + 2M^{2+} + 2H^{+} \text{ (in solution)} \quad \text{etc...}$$

4. Photo-, sono-, radioactive and radio-galvenic effects.

The basic theory of photo-, sono- effect has been known for some time. Large photo-effects (decrease in over voltage by 0.5V) have been observed upon uv irradiation of Si. Significant acceleration of the oxygen reduction reaction by a-emitters dissolved in the substrate has been established.

1.10. ELECTROCATALYTIC REACTIONS USING CONDUCTING POLYMER

As mentioned earlier that conducting polymers show redox behavior. Because of this property these were expected to show some catalytic activity and extensive research have been going on in this field. Some advantages of polymer modified electrodes are:

a) Control of the reaction rate by the applied potential or current.
b) Close proximity of electrocatalytic sites to the electrode.
c) High concentration of active centers despite low amount of material required.
d) Cooperative effects stemming from the proximity of other catalyst sites.
e) Easy removal of the catalyst from the substrate

A few studies have been reported in the catalytic properties of conducting polymers such as PPy, Pani for electro-oxidation of small molecules like formic acid, formaldehyde, methanol, hydrocarbons etc and electro-reduction of CO_2, O_2, etc. Current study deals with the oxidation of methanol and alkene and the reduction of nitroaromatic compounds, so brief discussion about these reactions are given below.

1.10.1. Methanol Electrocatalytic Oxidation

Electrooxidation of methanol is an important process from the point of view that it can be used as a fuel in the methanol fuel cells.[94-103] A fuel cell is a device that converts the chemical energy of a fuel (H_2, natural gas, alcohol, gasoline) and an oxidant (air or O_2) in to electrical energy / electricity. Fuel cell consisted of two electrodes, the cathode and the anode. The reactions that produce electricity take place at the electrodes. Fuel cells create electricity chemically, rather than by combustion, they are not subjected to the thermodynamic laws that limit a conventional power plant (Carnot Limit). Therefore, fuel cells are more efficient in extracting energy from a fuel. Methanol is now a days considered to be the most promising fuel for fuel cell because of it's low molecular weight, can be easily handled, stored and transported using present liquid fuel infrastructure. It's energy density is about 10kWh kg^{-1} which is comparable to the other liquid fuel.

The thermodynamic potential of methanol oxidation to carbon-di-oxide lies very close to the equilibrium potential of hydrogen

$$`CH_3OH + H_2O \longrightarrow CO_2 + 6H^+ + 6e^-$$

But this reaction is slower in several magnitude compared to hydrogen oxidation, because total oxidation process consists of some parallel reactions which is shown below

$$CH_3OH \rightarrow (\text{Adsorbed intermediate}) \rightarrow CO_{ad} \rightarrow CO_2$$
$$\downarrow$$
$$HCHO, HCOOH \rightarrow CO_2$$

Both the pathways require catalyst, which should be able to (a) dissociated the C-H bond and (b) facilitate the reaction of the resulting residue with some O-containing species to form CO_2 (or HCOOH). Pt catalyst which was considered to be the best catalyst so far for methanol oxidation. The overall complete oxidation of methanol on Pt anode can be shown in the following steps. The first step in the reaction is the adsorption of the methanol molecule immediately followed by its dissociation in to several adsorbed species. These different species are themselves transformed through several further reactions in to more strongly adsorbed species, responsible for poisoning.

$$Pt + (CH_3OH)_{sol} \rightarrow Pt\text{-}(CH_3OH)_{ads} \text{ ----------(1)}$$

$$Pt\text{-}(CH_3OH)_{ads} \rightarrow Pt\text{-}(\bullet CH_2OH)_{ads} + H^+_{aq} + e^- \text{ -----(2)}$$

or

$$Pt\text{-}(CH_3OH)_{ads} \rightarrow Pt\text{-}(CH_3O\bullet)_{ads} + H^+_{aq} + e^- \text{ -------(2')}$$

$$Pt\text{–}(CH_2OH)_{ads} \rightarrow Pt\text{–}(\bullet CHOH)_{ads} + H^+_{aq} + e^- \text{ ----------(3)}$$

or

$$Pt\text{-}(CH_3O\bullet)_{ads} \rightarrow Pt\text{-}(CH_2O\bullet)_{ads} + H^+_{aq} + e^- \text{ ----------(3')}$$

$$Pt-(\bullet CHOH)_{ads} \rightarrow Pt-(\bullet CHO)_{ads} + H^{+}_{aq} + e^{-} \text{----------(4)}$$

or

$$Pt-(CH_2O\bullet)_{ads} \rightarrow Pt-(\bullet CHO)_{ads} + H^{+}_{aq} + e^{-} \text{----------(4')}$$

The formyl like species (•CHO)ads is spontaneously dissociated on pure Pt according to the following reaction,

$$Pt-(\bullet CHO)_{ads} \rightarrow Pt-(\bullet CO)_{ads} + H^{+}_{aq} + e^{-} \text{----------(5)}$$

The strongly adsorbed CO-species formed during this step is the main poisoning species blocking the electrode active sites. The step(5) is the fast and is the main reason for the rapid poisoning phenomena observed on pure Pt.

Thus, a crucial step in the reaction mechanism is the formation of the intermediate (CHO)ads, which can be considered either as an active intermediate, leading directly to the final oxidation product, or as the precursor to the poisoning species requires the presence of OH species arising from the dissociation of water according to the reaction,

$$Pt + H_2O \rightarrow Pt-(OH)_{ads} + H^{+}_{aq} + e^{-} \text{----------(6)}$$

leading to the surface reaction responsible for the formation of CO_2

$$Pt-(\bullet CHO)_{ads} + Pt-(OH)_{ads} \rightarrow 2Pt + CO_2 + 2H^{+}_{aq} + 2e^{-} \text{----------(7)}$$

One other reaction has also been observed

$$Pt-(\bullet CHO)_{ads} + Pt-(OH)_{ads} \rightarrow Pt + Pt-(\bullet COOH)_{ads} + H^{+}_{aq} + e^{-} \text{----------(8)}$$

then leading also to the formation of CO_2 through the reaction

$$Pt-(\bullet COOH)_{ads} \rightarrow Pt + CO_2 + H^{+}_{aq} + e^{-} \text{----------(9)}$$

On the other hand, at more '+'ve potentials, the poisoning species (adsorbed CO) can be oxidized through the reaction

$$Pt-(\bullet CO)_{ads} + Pt-(OH)_{ads} \rightarrow 2Pt + CO_2 + H^{+}_{aq} + e^{-} \text{----------(10)}$$

or

$$Pt-(CO)_{ads} + Pt-(OH)_{ads} \leftrightarrow Pt + Pt-(COOH)_{ads} \text{----------(11)}$$

followed by equation (9)

There are several report found in the literature on Pt electrode and it's modified version.[104-112] However drawbacks in using Pt electrode is the formation of strongly adsorbed CO leading to the decrease in the catalytic activity.

In order to improve the catalytic activity and to minimize the CO adsorption on the surface tremendous amount of research have been going on in this field. Research of reports on bimetallic Pt-Ru alloy electrodes are also available where CO adsorption is found to be less.[113-116] As conducting polymers can be used as redox catalyst, modified forms of these are also being used for the electrooxidation of methanol. Mainly various transition metals like Pt, Ru, Ni etc dispersed on the conducting polymer are used as electrodes.[117-132] Metal microparticles entrapped in polymer films can act as catalytic sites for multielectron-transfer processes. The reason for incorporating metallic particles into porous matrices is to increase the specific surface area of these materials and thus, improve catalytic efficiency. Conductive polymers are sufficiently conductive to avoid any ohmic drop in its bulk and are sufficiently porous so that there will be no mass transfer limitations for the electroactive to reach the catalytic sites. It was shown by Tourillon and Garnier[133] that the presence of metallic aggregates in the conducting polymer not only improve the stability of the polymers films but also enhance its electrocatalytic activity.

Andreev et al [134] had synthesized polyaniline film on glassy carbon substrate and deposited platinum particles of various sizes on the film and studied the electrocatalytic activity of these films towards methanol electrooxidation. They observed that with the increase in the size of the metallic micro particles in the polymer film catalytic activity towards methanol oxidation decreases. Whereas Arico et al studied the electrooxidation of methanol on commercially available carbon supported and unsupported Pt-Ru catalyst. They have studied it in the solid polymer electrolyte direct methanol fuel cells at 90°C and 130°C with varying amounts of Nafion ionomer in the catalytic layer. It was found that unsupported Pt-Ru anode catalyst and 15% Nafion gives superior performance which might be due to the formation of homogeneous distribution of unsupported Pt-Ru catalyst composite in presence of Nafion as argued by them.[135]

Lefebvre et al had prepared supported catalyst of Pt and Pt-Ru particles by chemical deposition on chemically prepared poly(3,4-ethylenedioxythipohene)/poly(styrene-4-

sulphonate) (PEDOT/PSS) and PEDOT/polyvinylsulfate (PVS)composites. They reasoned high electron and proton conductivities for these catalysts which facilitates rapid electrochemical reaction rates.[136] In some other study Hammache and his group had used PPy/Au electrodes, prepared by electrochemical method for the inclusion of metallic gold species in the electropolymerized polypyrrole film. They argued that the increased electrocatalytic activity for Au dispersed on PPy film as compared to the bare Au electrode is due to the increased surface area. The catalytic activity of the Au microparticles is further enhanced when the Au nuclei are relatively small and well separated. However, with increasing gold coverage, the electrocatalytic activity of the modified electrode decreases. This is due to the size variation of the deposited gold particles. When the deposition time is longer, the gold microparticles coalesced and formed clusters which lead to an effective reduction in surface area.[137]

Laborde et al studied oxidation of methanol on platinum dispersed on polyaniline electrode. They suggested that the greater electrocatalytic on dispersed platinum particles might come from a smaller amount of adsorbed CO formed during methanol oxidation than on the bulk platinum.[138] Xue et al had carried out methanol oxidation with different loading of platinum particle on PPy of varying thickness. They observed that thickness of conducting polymer film is not sensitive but higher loading of Pt produces greater electrocatalysis[139] which is in agreement with the results obtained by other groups [140,141]

Becerik et al had studied the oxidation at Pt dispersed on ClO_4^- doped PPy film. They suggested that the counter-ion effects the PPy film morphology and conductivity. The higher activity obtained with these electrodes compared to Pt dispersed PPy film might be due to the protective effect against the poisoning reactions of methanol oxidation and which in turn is because of the increase in the conductivity and change in morphology.[142]

1.10.2. Electrochemical Oxidation of Alkenes

Electrochemical oxidation of simple alkenes was first observed in an aprotic solvent at smooth platinum electrode in the year 1968 by Fleischmann and coworker. By the use of cyclic voltammetry they showed that the reactions are highly irreversible.[143] Barnes et al had also shown that the reactions are highly irreversible.[144]

For aliphatic alkenes no standard value potentials is mentioned in the literature. Olefins react at the electrodes according to one of the following methods:

a) Direct one electron transfer, creating a short lived cation radical which reacts with a nucleophile

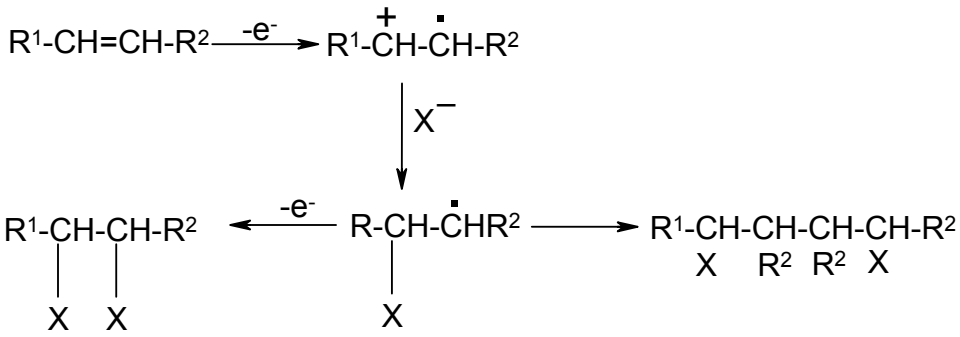

The intermediate then undergoes a second one –electron oxidation or dimerizes.

b) Two successive one electron steps leading to the formation of a proton and an allylic carbenium ion which reacts with the nucleophile S^-,

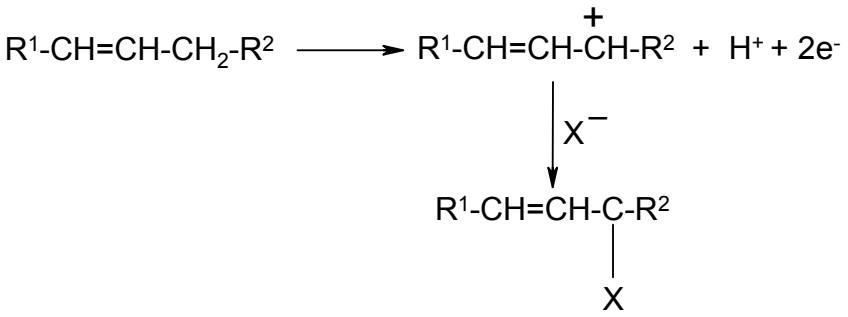

c) Electrooxidation of the solvent or the supporting electrolyte giving radicals which can add to the C=C bond or abstract a hydrogen atom from the allylic position leading to the formation of an allylic radical which is further oxidized and the reacts with S^-.

d) Indirect electrode reactions eg. Chlorination.

$$CH_2=CH-R \longrightarrow \dot{C}H_2-\overset{+}{C}H-R + e^-$$

$$Cl^- \longrightarrow Cl\cdot + e^-$$

$$Cl\cdot + CH_2=CH-R \longrightarrow \dot{C}H_2-\overset{+}{C}H-R + Cl^-$$

f) Via complex intermediates, for example, the well known Wacker type process for oxidation of ethylene in aqueous solution at a palladium electrode.

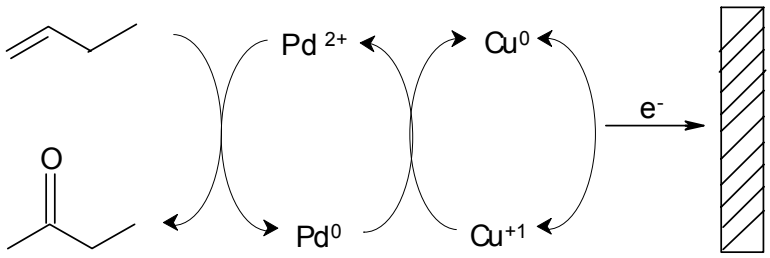

Figure 1.13 : Electrochemical Wacker oxidation process

The electrocatalytic oxidation of olefines has been studied intensively by Bockris et al. They had studied the oxidation of unsaturated hydrocarbon in 0.1M H_2SO_4 at elevated temperature(80ºC) on a platinized Pt electrode. They observed small decrease of reaction rate at constant potential with increasing size and polarizability of the organic. They have attributed this decrease to differences in coverage and to an effect of the organic on the stability of the –OH radicals formed on the surface in the water discharge step, which is assumed to be the rate determining step.[145,146] They determined the charge passed through the circuit per mole of CO_2 produced during complete oxidation of a hydrocarbon to CO_2 in acid medium was found to form the general equation to be

$$C_xH_y + 2x\,H_2O \longrightarrow xCO_2 + (4x + y)\,H^+ + (4x + y)\,e_m$$

$$(4x + y) / x = 4 + y / x \quad \text{Faradays}$$

The results obtained and conclusions deduced are similar to those in gas phase catalytic oxidation of the same compounds. In gas phase catalytic oxidation as well as in electrocatalytic oxidation, the coverage by olefins on platinum is intensive and rate

determining step on this metal involves the oxidation species only. Thus for electrocatalytic oxidation of olefins with catalyst like Pt and Pd, the oxidative adsorption of water from the electrolyte to give OH(ads) is suggested to be rate determining step. The noble metal electrocatalysts are not covered by oxygen at the potential where most of the hydrocarbon oxidation occurs. That means hydrocarbons are oxidized on the anode by adsorbed oxidized water species OH(ads).

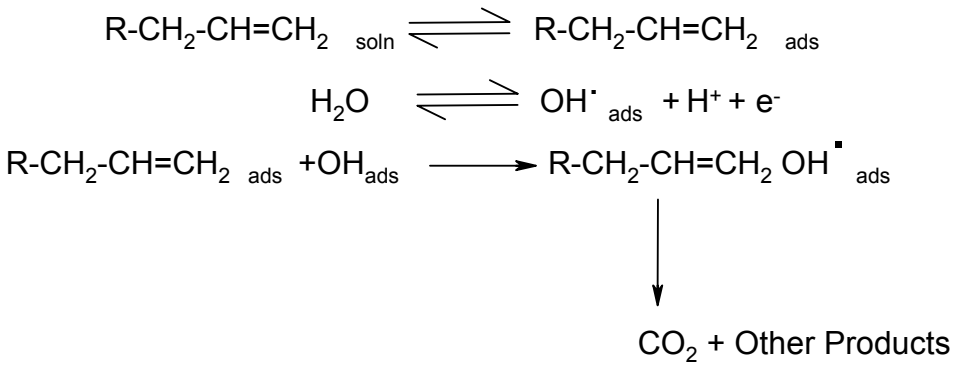

According to the authors Pt is minimally selective and promotes the complete oxidation. Rh and Ir are quite unselective in the C_2H_4 electrooxidation, while Au and Pd show selectivity in the electrooxidation of ethylene. Whereas electrooxidation of C_2H_4 with Au electrodes in presence of water leads to the formation of acetaldehyde, acetic acid and small quantities of glycol, glycoaldehyde, oxalic acid and CO_2.

There are very few reports available in the literature about the electrooxidation of alkene at different modified electrodes. Chen et al in their study used modified ruthenium porphyrin electrode to study the electrooxidation of styrene. They found the major product to be phenylacetaldehyde along with minor quantity of benzaldehyde. They suggested that styrene was first oxidized electrochemically by the catalyst to styrene oxide, which then reacts rapidly with the electrocatalyst to yield phenylacetaldehyde and benzaldehyde.[147] Madurro et al had used polypyridyl complexes of Ru for the oxidation of cyclohexene and found cyclohexanone to be the main product.[148] Liu et al had studied the electrooxidation of alkene at oxo-ferryl porphyrin. The advantage of using metalloporphyrin in aqueous solutions is that the oxygen atom which is the coordination atom of the central metal ion is readily available in water and the oxo-metal porphyrin can be obtained cleanly by controlling the exact electrode potential.[149] But there is

hardly any reference found in the literature about the oxidation of alkene using conducting polymer electrodes. Present work regarding the oxidation of alkene, viz decene and hexene, using different modified conducting polymer electrodes have been given in the chapter IV.

1.10.3. Electrochemical Reduction of Organic Compounds

There are various reports available on the electroreduction process of small organic molecules at conventional electrocatalyst. But very few reports are available in the literature on conducting polymer and modified conducting polymer electrodes. Mainly reports about the electrochemical reduction of O_2 reduction[150-158], small olefines[159], CO_2 [160], nitroaromatic compounds[161-166] and some other compounds[167,168] have been found in the literature. In most of the cases Cu, Ni, Fe Pt dispersed on the conducting polymer like PPy or Pani, or Nafion have been used. As present work deals mainly with the reduction of nitroaromatic compound, a brief discussion is given here in this part of the chapter.

F. Haber, in the year 1898 was the first to study the electrochemical reduction of nitrobenzene. Haber used platinized platinum electrode for the electrochemical reduction of nitrobenzene. The reduction of nitro aromatic compounds is of considerable interest because these are common groundwater contaminants and reduction reactions can play a central role in their environmental fate or cleanup. Sources of nitro aromatic contaminants include activities associated with the production or utilization of explosives, dyes, agrichemicals and pesticides.

Reduction products of nitrobenzene are nitrosobenzene, phenylhydroxylamine, aniline and coupled products such as azoxy-, azo- and hydrazobenzene. The course of reactions were varied depending on the choice of electrode material, electrode potential and electrolyte solutions. The mechanism of the electrochemical reduction of nitrobenzene to phenylhydroxylamine and aniline has received a considerable attention over the past 30 years.

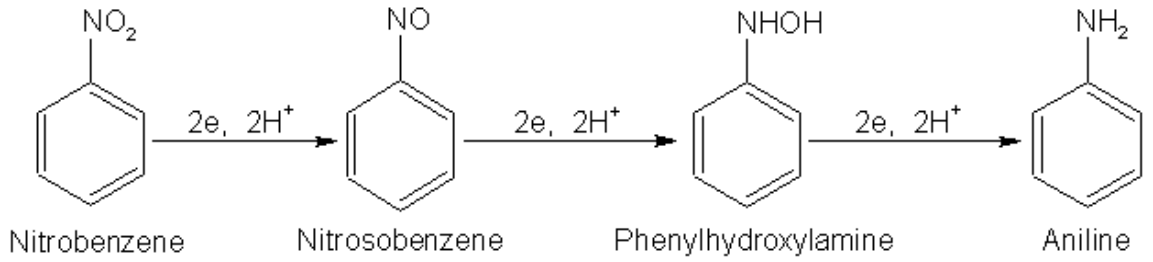

Figure 1.14: Electrochemical reduction reaction of Nitrobenzene

In aqueous solution nitrobenzene is reduced to phenylhydroxylamine in a single four electron reduction step at all pH value. At lower pH (<5), nitrobenzene is assumed to be preprotonated giving the species $C_6H_5NO_2H_2^+$. Analysis shows that the rate determining step involves the addition of two electrons and a single proton. The reduction mechanism is given as,

$$C_6H_5NO_2H_2^{2+} + 2e^- + H^+ \longrightarrow C_6H_5NOH^+ + H_2O \quad \text{(slow)}$$

$$C_6H_5NOH^+ + 2e^- + 2H^+ \longrightarrow C_6H_5NH_2OH^+ \quad \text{(fast)}$$

The reduction of the rate determining step ($C_6H_5NOH^+$) is reducible at a less negative potential than the starting compound $C_6H_5NO_2H_2^{+2}$, which explains why this intermediate has never been detected during the course of an experiment.

In acidic solution, at more negative potential, a second wave is seen, which corresponds to the reduction of protonated phenylhydroxylamine species $C_6H_5NH_2OH^+$, to yield aniline in a single two-electron transfer step.

$$C_6H_5NH_2OH^+ + 2H^+ + 2e^- \longrightarrow C_6H_5NH_3^+ + H_2O$$

In neutral and alkaline medium, there is no evidence for protonation of the parent molecule. Analysis also shows that the rate determining step consisting of the addition of two electrons and a single proton. The mechanism is given as

$$C_6H_5NO_2 + 2e^- + H_2O \longrightarrow C_6H_5NO_2H^- + OH^- \quad \text{(slow)}$$

$$C_6H_5NO_2H^- + 2e^- + H_2O \longrightarrow C_6H_5NHOH + 3OH^- \quad \text{(fast)}$$

At pH value greater than 5, no wave corresponding to the reduction of phenylhydroxylamine is observed. In aqueous alkaline solution(pH greater than 10) presence of a short lived intermediate corresponding to nitrobenzene radical anion is observed in the ESR studies.

In the nonaqueous solvents like acetonitrile and dimethylformamide, the nitrobenzene radical anion is stable, and the reduction of phenylhydroxylamine occurs in two steps:

A single electron addition to form the radical anion followed by a three electron addition and protonation to form phenylhydroxylamine.

The intermediate nitrosobenzene also undergoes reduction during the course of the reaction. In aqueous alkaline solution, nitrosobenzene undergoes a base catalyzed self condensation reaction to from azoxybenzene. In neutral and acidic aqueous solution, the compound is reduced to phenyl hydroxylamine in a single two electron transfer step. Bulk electrolysis gives an overall electron addition of somewhere between one and two with the formation of azoxybenzene which was attributed to the reaction of the reduction product phenylhydroxylamine with parent compound

$$C_6H_5NO + 2e^- + 2H^+ \longrightarrow C_6H_5NHOH$$

$$C_6H_5NO + C_6H_5NHOH \longrightarrow C_6H_5 - N{=}N(\downarrow O) - C_6H_5 + H_2O$$

In anhydrous dimethylformamide, nitrosobenzene is reduced in a single one electron transfer step to yield an unstable radical anion. In all solvent medium reported, nitrosobenzene is reduced at a less negative potential than nitrobenzene and as a result, it has never been detected as an intermediate in the reduction of nitrobenzene to phenylhydroxylamine.[169]

Sheshadri et al had studied the electrochemical reduction of nitrobenzene at Mo electrodes over a wide range of pH from 4.4 to 13. They found the final reduction product to be phenyl hydroxylamine, which is a four-electron process. Under alkaline conditions,

aniline has been observed to form at various electrodes along with azoxybenzene, azobenzene and hydrazobenzene.[170]

Marquez et al had studied the electrochemical reduction of O-halonitrobenzene in acidic 1 : 1 n-propanol : H_2O at Hg and compared with that of nitrobenzene. They observed that on increasing acidity of the medium, nitrosobenzene product was not observed and the yield aniline increases. They have observed the product aniline in acidic electrolyte and at slow potential scan rates. They have also observed that stirring causes the intermediate product to be convected away from the electrode surface preventing it from further reduction. They have reported to obtain high yield of aniline from nitrobenzene, careful selection of acid concentration, cathode material, potential and stirring condition is necessary.[171]

Gard et al studied the electrochemical reduction of nitrobenzene to nitrosobenzene with Pt electrode in THF medium. They have suggested that nitrobenzene radical anion is first formed, which further reduced to dianion. This strong base is immediately protonated to $PhNO_2H^-$ which eliminates an hydroxide ion to give PhNO. The latter is then reduced further. There is some amount of azoxybenzene also formed in the reduction of PhNO.[172]

Chizuko Nishahara had also reported the formation of nitrobenzene radical anion in the electroreduction of nitrobenzene in aqueous alkaline solution at an Au electrode. But along with nitrobenzene radical, nitrosobenzene radical also reported to form.[173] Barbara Kwiatek et al had studied the effect of seven carboxylic acid in the reduction of para substituted nitrobenzene in N,N-dimethyl formamide. They concluded that reduction proceeds via a hydrogen bonded complex of 1:1 type formed between the nitro and compound and the acid in the double layer.[174]

In the present work, electrochemical reduction of nitrobenzene is done using modified conducting polypyrrole

1.11. AIM AND SCOPE OF THE WORK

Conducting polymers are known to show excellent redox behavior and therefore these are expected to be potentially useful for their application as catalysts. Polymer supported catalysts have been investigated in the past. However, conducting polymers offer great advantages due to sufficient current flow between the solution substrate, the

electrocatalyst and the current collector, stable under experimental conditions employed, sufficiently permeable to electroactive species, fibrillar nature which can be exploited to provide a large surface area for depositing micro/nano particulate catalysts

Present research was undertaken to carry out detailed investigations on the synthesis and modification of conducting polymers, and their catalytic activity towards oxidation and reduction processes. Characterization of the modified conducting polymers prepared was done to bring out the changes occurring due to modification. Different characterization techniques employed were XPS, FT-IR, XRD, ESR etc. Studies on electrical properties, cyclic voltammetry, chronoamperometry etc. also were done for these conducting polymers. Using these polymers as electrodes, the methanol electro-oxidation process was mainly studied because of its application in the Direct Methanol Fuel Cell (DMFC) where conventional electrodes containing platinum are not only expensive but also become inactive after few cycles due to the CO adsorption on the electrode surface. Other oxidation processes, typically Wacker type, were also studied such as oxidation of alkenes, viz. decene and hexene. The chemical oxidation of alkenes was also performed employing chemically prepared and modified conducting polymer powders. Reduction of nitrobenzene was also carried out which is of considerable interest because these are common groundwater contaminants and reduction reactions can play a central role in their environmental cleanup. The characterization of the products was done by running GC, FTIR, UV-Vis.

In order to understand the various factors which may affect the electro-catalytic activity of the conducting polymers, systematic investigations were undertaken on variation of doping agent, surface roughness, degree of complex formation, activation energy, kinetics of reaction etc. All these studies are expected to lead to optimizing the conducting polymer for best performance as catalyst. Proper modification of the conducting polymers may lead to the catalyst with higher conversion and better selectivity. If these targets are achieved, the conducting polymers can be used as alternate to the precious metal based conventional catalysts bringing about cost effective alternative processes for the chemical industry.

1.12. REFERENCES

1. A. J. Heeger, Angew. Chem. Int. Ed. *40 (2001) 2591*.
2. H. Shirakawa, E. J. Louis, A. G. MacDiarmid, C. K. Chiang, A. J. Heeger, Chem. Commun. *(1977) 578.*
3. C. K. Chiang, C. R. Fincher, Jr., Y. W. Park, A. J. Heeger, H. Shirakawa, E. J. Louis, Phys. Rev. Lett.*39(1977)1098.*
4. W. A. Little; Phys. Rev.*134A (1964) 1416.*
5. M. Hatano, S. Kambara and S. Dkamoto; J. Polym. Sci.; *51 (1961) S26.*
6. 'Polypyrrole: An electrochemical approach to conducting polymers' by A. F. Diaz and K. K. Kanazawa. in ' Extended Linear Chain Compounds" vol.3, Ed. J. S. Miller; Plenum Publishing Corporation.
7. G. Tourillon and F. Garnier; J. Electroanal. Chem. *135(1982)173.*
8. D. M. Ivory, G. G. Miller, J. M. Sowa, L. W. Shacklette, R. R. Chance and R. H. Baughman; J. Chem. Phys, *71(1979) 1506.*
9. J. F. Rabolt, T. C. Clarke, K. K. Kanazawa, J. R. Reynolds, G. B. Street; J. Chem. Soc., Chem. Commun.*(1980)347.*
10. A. F. Diaz and J. A. Logan; J.Electroanal.Chem,*111(1980)111*
11. J. D. Capistran, D. R. Gagnon, S. Antoun, R. W. Lenz and F. E. Karasz. Polym. Prepr. (Am. Chem. Soc. Div. Polym. Chem.) *25 (1984) 282.*
12. J. L. Bredas and R. Silbey, " Conjugated Polymers"(Kluwer Dordrecht,1991)
13. W. R. Salaneck, S. Stafstrom and J. L. Bredas; " Conjugated Polymer surfaces and interfaces." Chapter 4, Cambridge University Press (1996)
14. W. R. Salaneck and J. L. Bredas; Solid State Communications, Special issue on " Highlights in condensed Matter Physics and Material Science" *92(1994) 31*
15. A. Angeli and L. Alessandri; Gazz.Chim.Ital*. 46 (1916) 283.*
16. H. S. Nalawa, L. R. Dalton and W. F. Schmidt and J. G. Rebe; Polym. Commun. *27 (1985) 240.*
17. C. F. Hsing, P. Kovacic and I. A. Khoury; J. Polym. Sci., Polym. Chem. Ed., *21 (1983) 457*
18. A. Dall'Ollio, Y. Dascola, V. Varacca and V. Vocchi; Comptes Rendus *267C (1968) 433.*

19. A. F. Diaz, K. K. Kanazawa and G. P. Gardini; J. Chem. Soc.; Chem. Commun.*(1979) 635*
20. H. Letheby, J. Am. Chem. Soc. *15 (1862) 161.*
21. A. G. Green and A. E. Woodhead; J. Chem. Soc*. 97(1910)2388.*
22. R. Surville, M. Josefowicz, L. T. Yu, J. Perichon and R. Buvet; Electrochim. Acta. *13(1968)1451.*
23. H. Shirakawa, E. J. Louis, A G. MacDiarmid, C. K. Chiang and A. J. Heeger; J. Chem. Soc., Chem. Commun. *578(1977)*
24. N. Gospodinova and L. Terlemezyan; Prog. Polym. Sci., *23(1998)1443.*
25. Y. Cao, P. Smith and A. J. Heeger; Synthetic Metals *48(1992)91.*
26. J. C. Chiang and A. G. MacDiarmid; Synthetic Metals. *13(1986)193.*
27. S. P. Armes and J. F. Miller; Synth. Metals *22(1988)385.*
28. Y. Cao, A. Andreatta, A. J. Heeger and P. Smith; Polymer *30(1989)2305.*
29. D. C. Trivedi, Handbook of Organic Conductive Molecules and Polymers; Vol.2, Ch. 12; Ed H. S. Nalwa, John Wiley & Sons.
30. G. E. Asturias, A. G. MacDiarmid and A. J. Epstein; Synth. Metals *29(1989) E157*
31. Y. Cao, A. Andreatta, A. J. Heeger and P. Smith; Polymer *30 (1989) 2305.*
32. A. Pron, F. Genoud, C. Menardo and M. Nechtscein; Synth. Metals *24(1988) 193.*
33. F. Lux; Polymer *35(1994)2915.*
34. R. Noufi, A. J. Nozik,J. White and L. Watte, J.Electrochem.Soc.*129(1982)2261*
35. A. F. Diaz, J. I. Castillo, J. A. Logan and W. Ylee; J. Electroanal. Chem*.129(1981)115.*
36. D. C. Trivedi; Electrochem Soc. *35 (1986) 243.*
37. A. F. Diaz and J. A. Logan; J. Electroanal. Chem*.111(1980)111.*
38. R. Noufi, A. J. Nozik, J. White and L. Watten; J. Electrochem. Soc *129(1982) 2261*.
39. E. T. Kang, K. G. Neoh, Y. L. Woo, K. L. Tan, C. H. A. Huan and A. T. S. Wee; Synth. Metals. *53(1993)333.*
40. Mu. Shaolin and K Jinqing; Synth. Metals *92(1998)149.*
41. S. Chen and H.T. Lee; Macromolecules *26(1993)3254*

42. P. Rannou, A. Gawlicka, D. Berner, A. Pron, M. Nechtschein, D. Djurado; Macromolecules; *31(9) (1998)3007*

43. M. Reghu, Y. Cao, D. Moses, A. J. Heeger; Phys.Rev. B; *47(4)(1993)1758*

44. H. Naarmann, N. Theophilou; Synth. Metal *22(1987)1*

45. T. Hagiwara, M. Hirasaka, K. Sato, M. Yamamura; Synth. Metal *36(1990)241*

46. C. O. Yoon, M. Reghu, D. Moses, A. J. Heeger; Phys. Rev. B *49(16)(1994) 10851*

47. L. W. Shacklette, T. R. Jow, M. Maxfield and R. Hatami; Synth. Met.*28(1989) C655*

48. S. K. Dhawan, D. C. Trivedi, N. Muniyandi, A. Sivashanmugam, G. Kumar; Synth. Metal *80 (1996) 279.*

49. J. Miasik, A. Hopper and B. Tofield; "Conducting Polymer Gas Sensors". J. Chem. Soc., Faraday Trans. I, *82(1986)1117*

50. H. Yoneyama and T. Hanawa; Synth. Met *30(1989)341.*

51. H. Yoneyama, T. Hanawa, S. Huwabata and H. Hashimoto; Synth. Met *30(1989)173*

52. S. Radhakrishnan and S. D. Deshpande; Sensors, *2(2002)185*

53. S. K. Dhawan, D. C. Trivedi, D. Kumar, M. K. Ram, S. Chandra; Sensors & Actuators B*: 40 (1997) 99.*

54. A. Q. Contractor, A. Kumar, M. Kanungo; J. Electroanal. Chem. *528(2002)46*

55. A. Q. Contractor, T. N. Sureshkumar, R. Narayanan, S. Sukeerthi, R. Lal, R. S. Srinivasa; Electrochim. Acta. *39(1994)1321.*

56. A. Q. Contractor, K. Krishnamoorthy, M. Kanungo, A. Kumar; Synth. Metal. *124(2001)471.*

57. R. H. Baughmann; Synth. Met. *78(1996)339*

58. J. B. Schlenoff and T. E. Herod; Chem. Mater. *5(7) (1993) 951.*

59. T. F. Otero, E. Angulo, J. Rodriguez and J. C. Santamaria; J. Electroanal. Chem. *341(1992)369.*

60. A. G. MacDiarmid, K. Kaneto, H. Saito and Y. Mm; Am. Chem. Soc. PMSE Prepr. *71(1994) 713*

61. S. Demoustier-Champagne, J. R. Reynolds and M. Pomerantz; Chem. Mater *7(2)(1995)277*
62. M. Pyo, Y.-J. Qui and J. R. Reynolds; Synth. Met. *55-57(1993)1388*
63. M. Pyo and J. R. Reynolds; J. Chem Soc. Chem.Commun. *3(1993)258*
64. M. Pyo and J. R. Reynolds; Synth. Met. *71(1993)2233*
65. M. Pyo, G. Maeder, R.T. Kennedy and J. R. Reynolds; J. Electroanal. Chem.*368(1994)329*
66. S. Dengi, C. Wilen and R.Leino; Tett.Asym. *15(2004)231*
67. B. Tamani and K.P.Borujeny; Tett.Lett. *45(2004)715*
68. B. Basu, Md. M. H. Bhuiyan, P. Das and I. Hossain; Tett.Lett. *44(2003)893.*
69. M. L. Kantam, B. Kavita, V. Neeraja, Y. Haritha, M. K. Choudhari, S. K. Dehury; Tett. Lett. *44(2003)9029*
70. F. Li, L. Xu and C. Xia; Appl. Catal.A *253(2003)509*
71. W. H. Clement, C. M. Selwitz, J. Org. Chem.*29(1964)241.*
72. W. G. Lloyd, B. J. Luberoff, J. Org. Chem *34(1969)3949*
73. D. R. Fahey, E. A. Zuech, J. Org. Chem. *39(1974)3276*
74. J. Tsuji, H. Nagashima and H. Nemoto; Org. Synthesis. *62(1984)9*
75. J. Tsuji; New J. Chem., *24(2004)127*
76. T. Nishimura, N. Kakiuchi, T. Onoue, K. Ohe and S. Uemura; J. Chem. Soc., Perkin Trans. *1(2000)1915.*
77. J. Tsuji; Synthesis, *(1984)369*
78. A. Kaszonyi, J. Vojyko, M. Hrusovsky, Collect. Czech. Chem. Commun. *47(1982)2128*
79. D. R. Fahey, E. A. Zuech, J. Org. Chem. *39(1974)3276*
80. J. Tsuji, H. Nagashima, K. Hori, Chem. Lett.*(1980)257*
81. W. H. Clement, C. M. Selwitz, J. Org. Chem. *29(1964) 241*
82. N. R. Davies, Nature, *201(1964)490*
83. J. F. Harrod and A. J. Chalk, J. Amer. Chem. Soc., *86(1964)1776*
84. G. C. Bond and M. Hillier, J. Catal. *4(1965)1.*
85. Chem. Eng. News *39(1961)43*
86. M. Orchin and G. L. Karapinka, J. Org. Chem. *26(1961)4187*

87. C. S. Marvel and J. R. Roger, J. Polymer Sci. *49(1961)335*

88. W. L. Carrick, J. Am. Chem. Soc. *80(1958)6455*

89. J. F. Harrod and A. J. Chalk, J. Amer. Chem. Soc.*86(1964)1776*

90. G. W. Parshall, Homogeneous Catalysis, Wiley-Intersciences, NewYork 1980.

91. M. Higuchi, I. Ikeda and T. Hirao; J.Org.Chem.*62(1997)1072*

92. J. W. Sobczak, B. Lesiak, A. Jablonski, A. Kosinski and W. Palczewska; Polish J. Chem. *69(1995)1732.*

93. F. Mazza and S. Trassatti, J. Electrochem.Soc.*110(1963)847*

94. A. S. Arico, A. K. Shukla, K. M. El-Khatib, P. Creti, V. Antonucci; J. Appl. Electrochem. *29(1999)671*

95. A. Hamnett, Catalysis Today; *38(1997)445*

96. G. T. Burstein, C. J. Barnett, A. R. Kucernak, K. R. Williams; Catalysis Today; *38(1997)425*

97. S. Wasmus, A. Kuver; J. Electroanal. Chem, *461(1999)14*

98. P. V. Samant, J. B. Fernandes; J. Power Sources; *79(1999)114*

99. W. H. Lizcano-Valbuena, V. A. Paganin, E. R. Gonzalez; Electrochim Acta *47(2002)3715*

100. K. Ramya, K. S. Dhathathreyan; J. Electroanal. Chem.; *542(2003)109.*

101. J. Yu, P. Cheng, Z. Ma, B. Yi Electrochim. Acta. *48(2003)1537*

102. S. S. Sandhu, R. O. Crowther, S. C. Krishnan, J. P. Fellner, Electrochim. Acta. *554-555(2003)25*

103. C. Lamy, E. M. Belsir, J-M. Leger; J. Appl. Electrochem, *31(2001)799.*

104. E. A. Batista, G. R. P. Malpass, A. J. Motheo and T. Iwasita; Electrochem. Comm., *5 (2003) 843*

105. S. Blais, G. Jerkiewicz, E. Herrero and J. M. Feliu; Langmuir *17(2001)3030*

106. V. S. Bagotzky and Yu. B. Vassilyev; Electrochim. Acta. *12(1967)1323*

107. A. Stoyanova, V. Naidenov, K. Petrov, I. Nikolov, T. Vitanov and E. Budevski; J. App. Electrochem. *29(1999)1197.*

108. P. J. Kulesza, B. Grzybowska, M. A. Malik, M. Chojak, K. Miecznikowski; J. Electroanal. Chem. *512(2001)110.*

109. L. Gao, H. Huang, C. Korzeniewski; Electrochim. Acta. *49(2004)1281*

110. T. Iwasita; Electrochim. Acta *47(2002)3663*

111. E. Herrero, K. Franaszczuk and A. Wieckowski; J. Phys. Chem.*898(1994)5074*

112. S.-C. Chang, L. –W. H. Leung and M. J. Weaver; J. Phys. Chem. *94(1990) 6013*

113. J. Choi, K. Park, B. Kwon and Y. Sung; J. Electrochem. Soc. *150(2003)A973*

114. S. L. Gojkovic, T. R. Vidakovic, D. R. Durovic; Electrochim. Acta *48(2003)3607*

115. J. Choi, K. Park, B. Kwon, H. Lee, Y. Kim, J. Lee and Y. Sung; Electrochim. Acta *48(2003)2781*.

116. W. H. Lizcano-Valbuena, V. A. Paganin, E. R. Gonzalez; Electrochim Acta *47 (2002) 3715*

117. P. O. Esteban, J. -M. Leger, C. Lamy and E. Genies; J. Appl. Electrochem. *19(1989)462.*

118. M. Hepel; J. Electrochem. Soc.*145(1998)124.*

119. F. Gloaguen, J. -M. Leger, C. Lamy; J.App.Electrochem. *27(1997)1052*

120. K. Bouzek, K. -M. Mangold and K. Juttner; J. App. Electrochem. *31(2001)501*

121. Yu. M. Maksimov, O. V. Afanas'eva and B. I. Podlovchenko; Russian J. Electrochem. *31 (1995) 133.*

122. A. A. Mikhaylova, O. A. Khazova and V. S. Bagotzky; J. Electroanal. Chem. *480 (2000) 225.*

123. C. T. Hable and M. S. Wrighton, Langmuir *7(1991)1305*

124. T. Kessler, A. M. Castro Luna; J. Solid State Electrochem.*7(2003)593*

125. P. J. Kulesza, M. Matczak, A. Wolkiewicz, B. Grzybowska, M. Galkowski, M. A. Malik, A. Wieckowski, Electrochim Acta, *44(1999)2131*

126. A. M. Castro Luna; J. App. Electrochem. *30(2000)1137*

127. L. Makhloufi, H. Hammache, B. Saidani, N. Akilal and Y. Maloum J. App. Electrochem. *30(2000)1143*

128. H. Laborde, J. -M. Leger, C. Lamy, F. Garnier, A. Yassar J. App. Electrochem. *20 (1990) 524.*

129. M. A. Del Valle, F. R. Diaz, M. E. Bodini, T. Pizarro, R. Cordova, H. Gomez, R. Schrebler; J. App. Electrochem.*28 (1998) 943*

130. H. Laborde, J.-M. Leger and C. Lamy; J. App. Electrochem.*24(1994)1019*

131. A. S. Arico, A. K. Shukla, K. M. El-Khatib, P. Creti, V. Antonucci; J. Appl Electrochem. *29(1999)671.*

132. I. Becerik, S. Suzer, F. Kadirgan; J. Electroanal. Chem *502(2001)118*

133. G. Tourillon; F. Garnier, J. Phys. Chem*. 88(1984)5281.*

134. V. N. Andreev, M. A. Spitsyn and V. E. Kazarinov; Russian J. Electrochem *32(1996)1307.*

135. A. S. Arico, A. K. Shukla, K. M. El-Khatib, P. Creti, V. Antonucci; J. Appl. Electrochem. *29(1999)671*

136. M. C. Lefebvre, Z. Qi and P. G. Pickup; J. Electrochem. Soc. *146(1999)2054.*

137. H. Hammache, L. Makhloufi, B. Saidani, Synth. Metal, *123(2001)515*

138. H. Laborde, J.-M. Leger and C. Lamy; J.App.Electrochem.*24(1994)219*

139. K. H. Xue, C .X . Lai, H. Yang, Y. M. Zhou, S. G. Sun, S. P. Chen, G. Xu, J. Power Sources *75 (1998) 207*

140. K. M. Kost and J. E. Bartak, Anal. Chem. *60 (1988) 2379*

141. A. A. Mikhaylova, E. B. Molodkina, O. A. Khazova and V. S. Bagotzky; J. Electroanal. Chem. *509(2001)119*

142. İ. Becerik, Ş. Süzer and F. Kadirgan; J. Electroanal. Chem. *502(2001)118*

143. M. Fleischmann and D. Pletcher, Tetrahdron Letter, *60(1968)6255.*

144. K. K. Barnes and C. K. Mann, J. Org. Chem; *32(1967)1474.*

145. A. T. Kuhn, H. Wroblowa and J. O'M. Bockris, Trans. Faraday Soc., *63(1967)1458.*

146. J. O'M. Bockris, H. Wroblowa, E. Gileadi and B. Piersma; Trans. Faraday Soc.,*61(1965)2531.*

147. C. Chen, S. Cheng, Y. O. Su; J. Electroanal. Chem. *478(2000)51*

148. J. M. Madurro and G. Chiericato Jr; Tetrahedron Lett. *29(1988)765*

149. M. Liu and Y. O. Su; Electroanal. Chem. *452(1998)113*

150. E. K.W. Lai, P. D. Beattie, F. P. Orfino, E. Simon, S. Holdcroft; Electrochim. Acta. *44(1999) 2559*

151. M. T. Giacomini, E. A. Ticianelli, J. McBreen and M. Balasubramanian; J. Electrochem. Soc. *148(2001)323*

152. F. T. Avork and E. Barendrecht; Electrochim. Acta. *35(1990)135*

153. O. Antoine, Y. Bultel, R. Durand; J. Electroanal. Chem., *499(2001)85.*

154. C. C. Chen, C. S. C. Bose and K. Rajeshwar; J. Electroanal. Chem. *350(1993)161*

155. G. Bidan, M. Lapkowski and J. P. Travers; Synth. Metal. *28(1989)C113*

156. L. Doubova, G. Mengoli, M. M. Musiani and S. Valcher; Electrochim. Acta. *34(1989)337*

157. M. S. El-Deab, T. Ohsaka; Electrochem. Commun. *4(2002)288*

158. N. Phougat and P. Vasudevan; J. Power Sources. *69(1997)161*

159. P. S. Fedkiw, J. M. Potente and W. H. Her; J. Electrochem. Soc.*137(1990)1451*

160. K. Ogura, N. Endo and M. Nakayama; J. Electrochem. Soc.*145(1998) 3801*

161. A. Zouaoui, O. Stephan, M. Carrier and J -C. Moutet; J. Electroanal. Chem. *474(1999)113.*

162. G. Kokkinidis and K. Juttner Electrochim. Acta. *26(1981)971.*

163. C. Ravichandran, S. Chellammal and P. N. Anantharaman; J. Appl. Electrochem. *19(1989)465*

164. M. Inaba, Z. Ogumi and Z. Takehara; J. Electrochem. Soc. *140(1993)19*

165. P. J. Kulesza and L. R. Faulkner; Colloids and Surfaces. *41(1989)123*

166. P. Giannoccaro and E. Pannacciulli; Inorg. Chim. Acta; *117(1986)69.*

167. F. V. Agado, S. G. Granados, S. Sucar-Succar, C. B. Cherreton, F. Bedioui; New J. Chem *21(1997)1009*

168. B. Fabre and G. Bidan; Electrochim Acta *42(1997)2587*

169. W. H. Smith and A. J. Bard, J. Amer. Chem. Soc. *97(1975)5203*

170. G. Sheshadri and J. A. Kelber; J. Electrochem. Soc. *146(1999)3762.*

171. J. Marquez and D. Pletcher; Electrochim. Acta. *26(1981)1751.*

172. J. C. Gard, J. Lessard and Y. Mugnier; Electrochim. Acta *38(1993)677.*

173. C. Nishahara and H. Shindo J. Electroanal. Chem.*221(1987)245.*

174. B. Kwiatek and M. K. Kalinowski; J.Electroanal. Chem *226(1987)61*

Chapter II

EXPERIMENTAL

2.1.INTRODUCTION

Present investigation deals with the synthesis and modification of conducting polymers, their characterization, their catalytic activity towards oxidation and reduction of organic molecules and identification of the products. The conducting polymers chosen were polypyrrole and polyaniline. Synthesis and modification of these polymers were done by chemical and electrochemical methods.

2.2. CHEMICALS USED

The various chemicals used along with the sources are presented in the *table 2.1*. The chemicals used were of AR grade.

2.3. SYNTHESIS AND MODIFICATION OF CONDUCTING POLYMER

2.3.1. Chemical Synthesis of Conducting Polymers

Synthesis of conducting polymer involves the oxidation of the monomer viz. aniline and pyrrole with oxidizing agents such as APS or $FeCl_3$ in acidic medium. Solvents used for the polymerization reaction is distilled water or NMP-water (1:1) mixture. Detailed procedure for the synthesis is given below.

i) Synthesis of polypyrrole:

In the chemical polymerization of pyrrole, $FeCl_3$ was used as oxidizing agent. Reaction was carried out in the aqueous medium. Monomer to oxidizing agent ratio was 1:1. The reaction was carried out at room temperature for 24 hours. In the polymerization reaction of pyrrole, it was observed that as soon as the $FeCl_3$ was added to the reaction mixture, the color changed almost instantaneously. There was increase in temperature after the reaction was started, which was the indication of an auto acceleration reaction and exothermic system. The color of polypyrrole obtained was dark green/black. The yield for the polymerization reaction was 50-60% in every case. Polypyrrole obtained by this method was Cl^- doped.

Chemicals	**Acronym**	**Source**
Pyrrole	Py	E-Merck
Aniline	Ani	Merck, India
Ammonium persulfate	$(NH_4)_2S_2O_8$	Merck, S. D. Fine, India
Lithium perchlorate	$LiClO_4$	Aldrich Chemical Co.
Copper phthalocyanine	CuPc	Color Chem. / Hoechst (India)
Ferric Chloride, Nickel Chloride, Copper Chloride, Manganese Chloride, Cobalt Chloride, Potassium Chloride	$FeCl_3$, $NiCl_2$, $CuCl_2$, $MnCl_2$, $CoCl_2$, KCl	Merck, India
Palladium Chloride	$PdCl_2$	S. D. Fine, India
Zirconium Chloride	$ZrCl_4$	Lancaster
Agar agar		Loba Chemie
Decene, Hexene		Aldrich Chemical Co.
Perchloric Acid	$HClO_4$	Merck, India
Acetonitrile, Methanol	CH_3CN, CH_3OH	Merck
Nitrobenzene,	$C_6H_5NO_2$	Merck, India
Sulphuric Acid, Hydrochloric Acid	H_2SO_4, HCl	Merck, India
Styrene butadiene styrene, Polyvinylbutyral	SBS, PVB	
Acetophenone, Benzaldehyde		Merck, India

Table : 2.1 Table of chemicals used with their formulae and origin

ii) Polyaniline synthesis:

Chemical synthesis of polyaniline was done at aqueous medium in presence of HCl. The reaction was carried out at room temperature for 24 hours. Polyaniline thus obtained was dark green in color. Ammonium peroxodisulphate was used as the oxidizing agent. Monomer to oxidizing agent ratio was 1:1.1

Polyaniline incorporated with copper phthalocyanine was synthesized in the NMP**:**H_2O (1:1) medium instead of distilled water. Copper phthalocyanine green was used for incorporating phthalocyanine in the polyaniline. Concentration of copper phthalocyanine was varied from 0 - 10% weight with respect to monomer.

Purification of the polymers

After the reaction was over, the reaction mixture was poured in to beaker containing 500ml distilled water, stirred for half an hour and the precipitated polymer was filtered by conventional method. The polymer was washed with distilled water several times till the filtrate obtained was colorless and neutral in nature. The polymer samples obtained in powder form were dried first at room temperature for few hours and then finally dried in the oven kept at 60ºC for 4-5 hours. The dried polymer powder was then preserved in dessicator.

Doping of conducting polymers

Conducting polymer powder thus obtained was doped with different transition metal doping agents viz., $PdCl_2$, $NiCl_2$, $ZrCl_4$, $FeCl_3$, $MnCl_2$, $CuCl_2$ and $CoCl_2$. Prior to doping these powders were undoped completely by dumping into 2M NH_3 solution for 4 hours. These were then washed thoroughly with distilled water to remove ammonia. The brown colored powder was then dried in ambient followed by vacuum drying. Redoping of these powders were done with dopants mentioned above with concentrations 0.003M, 0.006M, 0.009M, 0.012M, and 0.02M, solutions of which were prepared in the aqueous medium. Only in case of $PdCl_2$ slight acidic solution was prepared (0.002M HCl), which was

because of low solubility of $PdCl_2$ in water. Doping was done for 4 hours. Redoped PPy was then filtered and dried under vacuum.

2.3.2. Electrochemical synthesis of Conducting Polymers

Gold coated glass substrates were used as electrodes for the electrochemical polymerization of pyrrole and aniline. Prior to gold deposition, one side of these glass plates were coated with a thin layer of PVB/SBS polymer using dip coating technique. Gold deposition was carried out in a Hind Hivac Vacuum coating unit (model 12 A4D) using thermal evaporation method on glass substrates. Electrodes were made by cutting the gold coated glass substrates in to 3cm X 2cm size. Air drying silver paste was then applied on one end to achieve electrical contact.

The electrochemical deposition was carried out in a singe compartment cell with three electrodes system. The setup is shown in the *figure 2.1.* The working electrode was gold substrate while the counter electrode was a platinum foil. Reference electrode used was saturated calomel electrode (SCE) connected through the salt bridge containing agar-agar/ KCl mixture. Under normal conditions, the electrolyte was monomer along with an oxidizing agent in appropriate concentrations. Electrochemical deposition was carried out by chronoamperometric technique at a constant applied potential against SCE. The electrolyte medium in most of the cases was distilled water.

In case of CuPc incorporated Pani film, 1:1 NMP: H_2O was used as electrolyte medium. Potential applied was 900mV for 180 seconds. Oxidizing agent used incase of Pani preparation was HCl.

In case of PPy polymerization potential of 700mV was applied. Oxidizing agent used was H_2SO_4. Deposition time for PPy was 120 seconds.

Conducting polymer films of different roughness were prepared by using cyclic voltammetry technique. Cyclic voltammetry was run with different scan rates.

Doping of PPy films:

Electrochemically prepared PPy films were undoped by applying negative potential of

‘–700mV‘ for 60seconds. These films were redoped with different transition metal doping agents viz. $CuCl_2$, $ZrCl_4$, $MnCl_2$ etc. Doping concentrations were varied from 0 to 0.02M.

2.4. CHARACTERIZATION OF THE POLYMER

2.4.1. Infrared (IR) Spectroscopy

Infrared (IR) studies were carried out in order to confirm the incorporation of phthalocyanine in the conducting polymer or doping of polymers with different transition metal dopants. IR studies were also carried out to characterize the different frequencies of the parent conducting polymer. The powder samples were mulled with dry potassium bromide crystals and pellets were made. These pellets were mounted in the IR cell in the conventional way to record the IR spectra using Model BioRad-175C. The characteristic absorption bands obtained were tabulated and compared with known literature data.

2.4.2. X-Ray Diffraction studies.

The conducting polymer synthesized by chemical route generally has semicrystalline in nature, whereas the conducting polymer prepared by electrochemical route is amorphous in nature. The structure of the various modified polymer was investigated by WAXD; using a powder X-ray diffractometer (Phillips PW 1830 model) using CuK□ source and □ Ni filter. All the scans are recorded in the 2□ region of 10-60 at a scan rate of 4 /min. From the 2□ value for the reflections, d values were calculated using Bragg’s equation.

$$2d \sin\square = n\square$$

From the datas obtained from the XRD, R value i.e., the inter-chain separation of different modified polymer is calculated.

2.4.3. UV-Vis analysis

The conducting polymers synthesized by chemical route are characterized by UV-Vis technique. Formation of complex during insitu polymerization was also investigated

using UV-Vis method. The instrument used was Spectroelectrochemical analyzer HR 2000-CG from Ocean Optics, USA.

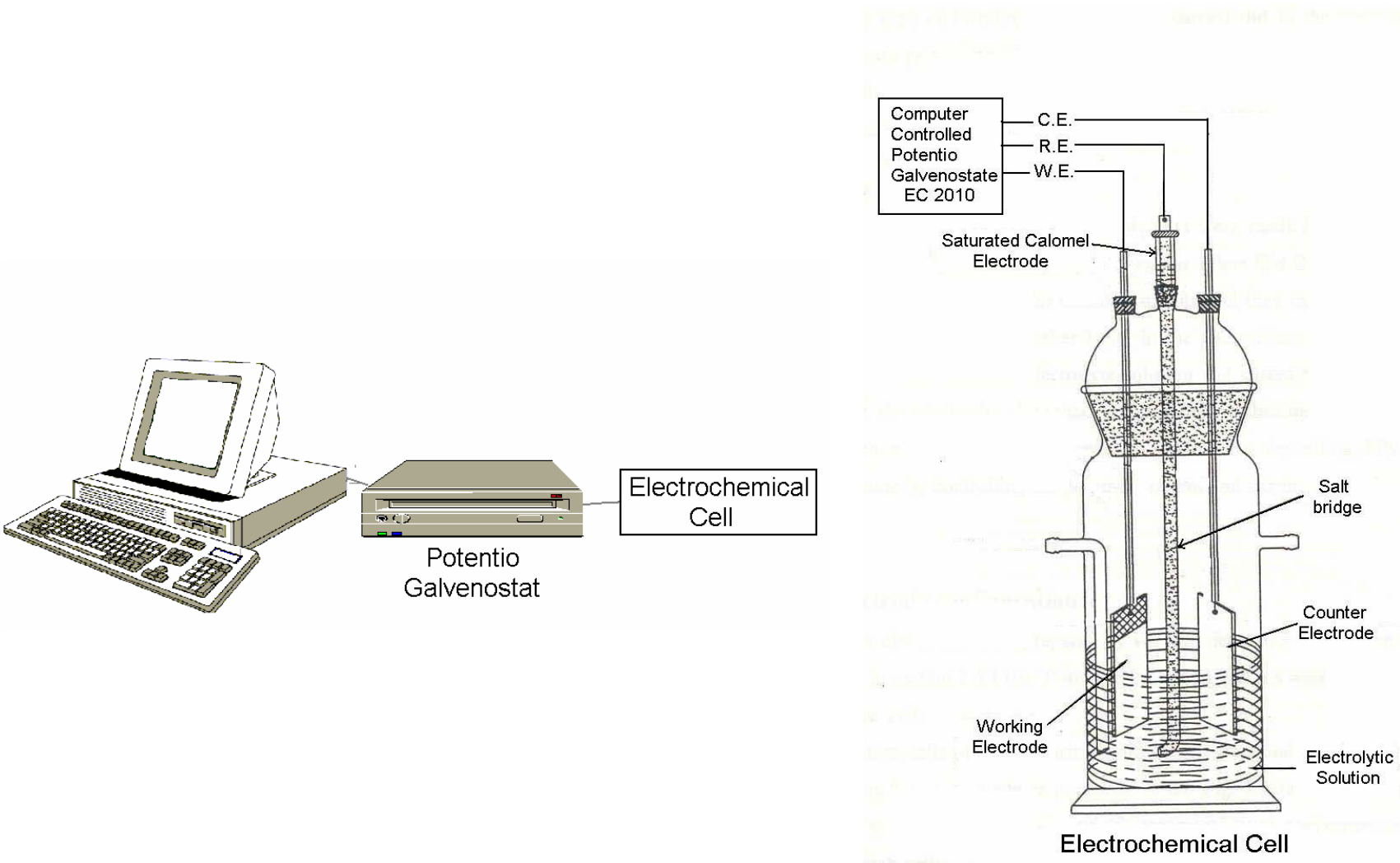

Figure 2.1: Complete Electrochemical Setup

2.4.4. X-Ray Photoelectron Spectroscopy (XPS)/ESCA studies

X-ray photoelectron spectroscopy is a surface specific as well as surface sensitive technique. Surface specific techniques are concerned with a maximum sampling depth of 5-10 nm. Whereas surface sensitive techniques can probe up to 100nm. When ESCA deals with polymer, the technique can be regarded as the surface sensitive technique. XPS is concerned with a special form of photoemission, namely the ejection of electron from a core level by x-ray photons of energy h□. When a surface is irradiated with soft x-ray photons, electrons from inner shells get ejected with KE equal to

$$KE = h\square - BE - \square - S.$$

h□ is x-ray energy, BE is the binding energy of the photo ejected electron, □ if the work function of the spectrometer, S is the correction term for surface charging. XPS is a plot of photoelectron intensity vs. KE (or BE) of the photoelectron. The BE may be regarded as an Ionization energy of the atom for the particular shell involved. XPS is capable of elemental analysis since no two atoms in the periodic table exhibit the same set of BE's. Quantitative analysis can also be performed by wide scans, in which all the available KE range is explored. Higher spectral resolution and more quantitative analysis are performed by detailed or narrow KE (or BE) scan. From the peak position in the XPS information about the chemical species can be obtained. Information about the chemical environment and the redox state can be determined from the BE shift, i.e. chemical shift. From the ratio of the peak area stoichiometry of the chemical species can be found out. The information about unsaturation or □□* transition can also be obtained from the shakeup satellite region of the spectra.

From XPS changes in the BE of core electrons because of chemical environment can be determined. Photoelectron peak intensity is directly proportional to the atomic concentration in the sample.

The intensity of electrons I, emitted from a depth d is given by the Beer-Lamberts equation,

$$I = I_0 \exp(-d / \square \sin\square)$$

Where I_0 = the intensity from the clean substrate.

- □ = Inelastic mean free path (the value is function of Kinetic energy (KE) of the emitted electrons)
- □= Angle subtended by the sample surface.

X-Ray photoelectron spectra were recorded using V. G. Scientific ESCA-3 MK II spectrometer and in ESCA 3000. X-ray source used were Al-K□ (1486.6eV) and Mg-K□(1253.6eV). All the spectra were recorded under identical conditions at 50eV pass energy, 4 mm slit and vacuum was 10^{-9} Torr. The instrumental resolution obtained for the Au 4f7/2 levels under this condition is 1.6eV (Full Width at Half Maximum-FWHM).

2.4.5. Electron Spin Resonance Spectroscopy:

ESR spectroscopy involves detecting and making semi quantitative measurements of unpaired electrons that occur in organic free radicals and in certain valence states of transition metals. For organic free radicals in solution, the structure of the radical can also be deduced. Principle: The unpaired electron has magnetic moment that can exist in two energy states. Transitions in a magnetic field can be induced by irradiation with microwave radiation of the proper frequency. The absorbed energy is detected and plotted as the first derivative of absorption in relation to the applied field. Information on the structure or the concentration of the species containing the unpaired electron is obtained from the position, number and intensity of the peaks. If sufficient concentration is present in a sample, ESR spectroscopy can detect the presence of stable free radicals or certain valence states of transition metal ions. To detect signal in ordinary matter it is necessary to subject the sample to some energetic process that will break chemical bonds. Such processes include irradiating with ultraviolet light or x-ray, chemical reactions, mechanical grinding or stretching. ESR spectroscopy was done in the Hiroshima University, Japan.

2.4.6. Scanning Electron Microscopy

SEM studies were performed to investigate the surface morphology or microstructure of the samples. Leica Stereoscan 440 model manufactured by M/S Leica Cambridge Ltd., U.K. was used for analysis. The conducting polymer films deposited on the gold coated

glass substrate were silver pasted on the sample holder. Usual method of gold coating was not done as these samples are already in the conducting state. The micrographs of the samples with 10KV EHT and 25 PA beam current were recorded by a 35mm camera attached on the high resolution recording unit.

2.5.CHARACTERIZATION OF PRODUCT

2.5.1. Gas Chromatography(GC) analysis

Chromatography is a separation method in which the components of a sample partition between two phases: one of these phases is a stationary bed with large surface area and the other is a gas, which percolates through the stationary bed. The sample id vaporized and carried by the mobile gas phase (the carrier gas) through the column. Samples partition into the stationary liquid phase, based on their solubilities at the given temperature. The components of the sample (solutes or analytes) separate from one another based on their relative vapor pressures and affinities for the stationary bed. Gas chromatography is the premier technique for separation and analysis of volatile compounds. It has been used to analyze gases, liquids and solids. Solids are usually dissolved in volatile solvents for analysis. Both organic and inorganic materials can be analyzed by this method. In gas chromatography gas is the moving phase. GC analysis was done by using HP 6890 model. 0.5µl of the sample was taken for injection in the column.

2.5.2. Infrared (IR) analysis

The different products obtained in the decene and nitrobenzene reactions are characterized by IR technique. The liquid samples were placed in between the NaCl crystals and IR spectra was recorded using Biorad-175C. The absorption bands were compared with the data given in the literature.

2.5.3. UV-Vis analysis

The different products obtained in the electrochemical reduction of nitrobenzene reaction were analyzed by UV-Vis technique also. The instrument used was Spectroelectrochemical analyzer HR 2000-CG from Ocean Optics, USA.

2.6. PROPERTY MEASUREMENTS

2.6.1 Conductivity measurements:

The conductivity measurements were carried out by a two-probe technique recorded by a Keithley Electrometer 614 model. Samples were tested in a surface cell as well as in a sandwich cell form schematically represented in *figure 2.2* . Pellets were also used in the case of pure conducting polymers. The specific resistivity was calculated as,

$$\rho = RA/l$$

Hence $\sigma = 1/\rho$

Where ρ is its resistivity, A is the cross sectional area, l is the thickness, R is the sample resistance and σ is the conductivity.

2.6.2. Temperature dependence of Conductivity.

The interdigited electrodes were placed in the sample holders as shown in the figure…. The apparatus consists of a sample holder that was enclosed in an electromagnetic shielded cell, which in turn was mounted inside a glass jacket, which could be sealed and connected to a rotary pump. A small heater was mounted close to the film or pellet and using a suitable control device controlled the rise in the temperature to 4°/min. The temperature was varied from room temperature to 90° C. The change in the conductivity was noted with respect to the temperature. From the temperature – conductivity data activation energy was determined using Arrhenius equation.

2.6.3. Cyclic Voltammetry

The electrocatalytic properties of the modified conducting polymers were investigated by running cyclic voltammetry. Electrochemical oxidation-reduction reactions were carried out using Potentio-galvenostat EC 2010 model. Cyclic voltammograms were run usually at a scan rate of 50mV/s. The working electrodes were the modified conducting polymers, Pt was the counter electrode and SCE was the reference electrode in every case.

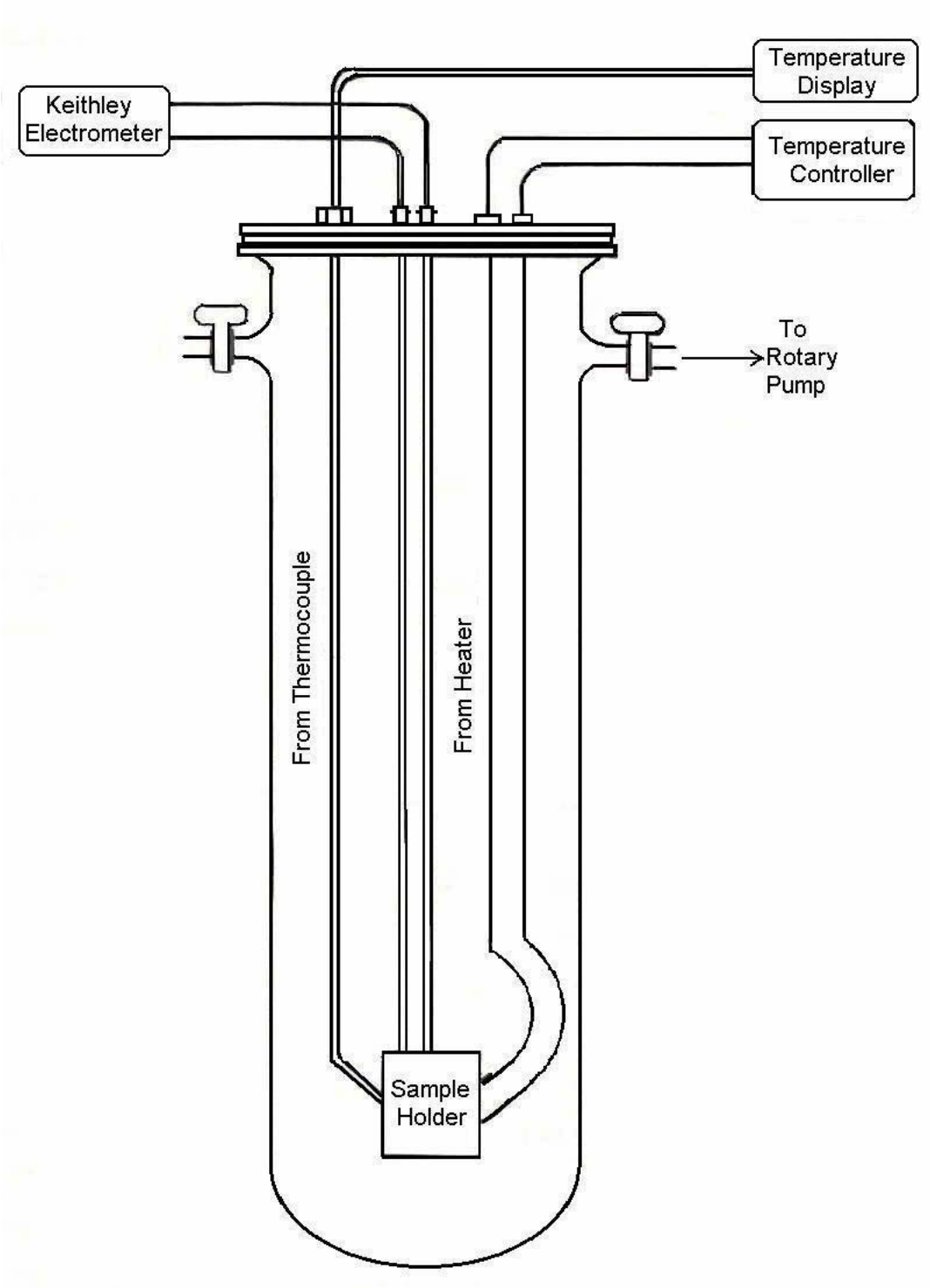

Figure 2.2: Schematic representation of Conductivity measurement Apparatus

2.8. CHEMICAL OXIDATION OF ALKENE

For chemical reaction, reaction set up as shown in the schematic diagram (*figure 2.3.)* was used. The reaction setup consisted of a two-necked round bottom flask connected to a condenser. The condenser was connected to oxygen bladder through two-way connector. The round bottom flask was kept on oil bath, which was heated by using temperature-controlled hot plate.

For the reaction, 40 ml of acetonitrile was taken in the RBF. To the RBF containing acetonitrile, varying quantity of conducting catalyst was taken. The mixture was then allowed to heat at 80 degree centigrade with constant stirring for an hour. Oxygen supply was kept on using inlet through condenser. After one hour required quantity of reactant was added to the reaction mixture. After adding reactant all the inlets and outlets were closed properly. This was kept for varying time ranging from 12 hrs, 24 hrs, 30 hrs, 48 hrs, 60 hrs and 72 hrs.

After the reaction was over the reaction mixture was filtered through the Whatmann filter paper followed by silica gel column to separate the catalyst from the mixture. Then it was eluted by acetonitrile.

This solution was then concentrated using rotavapor. While concentrating, acetonitrile solvent was removed from the reaction mixture leaving behind product and unreacted reactants. Products formed in the reaction were characterized using GC and IR techniques.

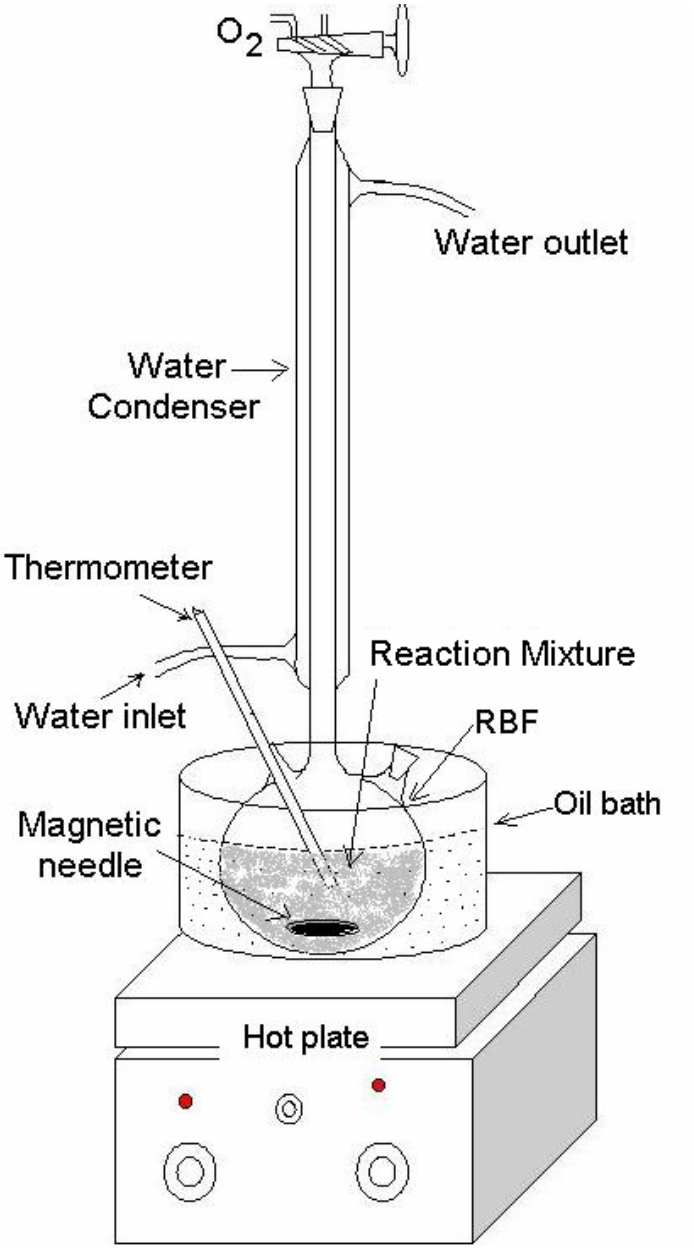

Figure 2.3: Reaction setup for chemical reaction

Chapter III

ELECTROCATALYTIC OXIDATION OF METHANOL USING MODIFIED CONDUCTING POLYPYRROLE

3.1 INTRODUCTION

Interest is growing in the field of methanol electrochemical oxidation due to its use as a fuel in the direct methanol fuel cell. Drawbacks of petroleum fueled internal combustion engines, like air pollution in the urban areas, global warming and decreasing sources has lead to the research and development of alternative energy sources. Among the various types of alternative energy sources fuel cells are considered to be clean and silent, which provides high-energy conversion efficiency when compared with other power devices. Extensive research on DMFC's have been carried out mainly aiming at improving its poor performance due to the slow methanol oxidation kinetics on the anode catalysts. Slow methanol oxidation is due to self-poisoning of the surface of the electrodes by reaction intermediates such as CO, which are formed during stepwise dehydrogenation of methanol.[1-29]

In the present study conducting polypyrrole electrodes doped with different dopant ions were used in order to investigate and to improve the performance of the electrode towards methanol electro-oxidation. Various conditions like reaction temperature, scan rate etc were varied. The preparation, characterization of electro-catalyst and the investigation of catalytic properties of these various PPy doped films are described in this chapter. Various relations of electrocatalytic activity with different parameters like electronegativity of dopant ions are also established.

3.2 EXPERIMENTAL:

3.2.1. Synthesis and Modification of PPy

Among the various methods available for polymerization of pyrrole, electrochemical, chemical, vapor phase techniques are the most extensively studied technique. In the current study PPy was synthesized by two methods viz. chemical polymerization and electrochemical polymerization technique. Both the polymerization techniques are simple and are possible in aqueous medium.

3.2.1.1 Chemical Synthesis of Polypyrrole

Chemically synthesized PPy polymer:

In general, pyrrole have been prepared in the past using various oxidizing agents like H_2O_2 in acetic acid, PbO_2, $FeCl_3$, HNO_2, O_3 etc. In the present study, chemical polymerization of pyrrole, $FeCl_3$ was used as oxidizing agent. In the polymerization reaction of pyrrole, it was observed that as soon as the $FeCl_3$ was added to the reaction mixture, the colour changed almost instantaneously in aqueous medium. Polymerization of pyrrole by chemical route in various solvent mediums had been reported by Machida and Miyata.[30] There was increase in temperature after the reaction was started, which was the indication of an auto acceleration reaction and exothermic system. The color of polypyrrole obtained was dark green / black. The yield obtained in the present case was 50-60%. The reaction proceeds as

$$3mPy + nFeCl_3 \longrightarrow m(Py_3Cl) + nFeCl_2 + (n-m)HCl$$

which gives PPy doped with Cl^-. In order to dope PPy with other dopants, it has to be first undoped and then further doped with desired species.

Undoping of Polypyrrole powder

The PPy powder obtained was then undoped completely in order to remove completely the oxidizing agent (Cl^-) which gets incorporated during synthesis. Undoping could also be regarded as the reduction of polypyrrole from its oxidized and conducting state. Undoping of polypyrrole was done by placing PPy powder in the 2M NH_4OH solution for 4 hours and filtered using Whatman filter paper no 1. It was then washed thoroughly distilled water to remove ammonia and obtain pH of 7. The brown coloured powder was then dried in ambient followed by vacuum drying.

Doping of PPy powder

The undoped PPy powder obtained was then redoped with different doping agents viz. $PdCl_2$, $ZrCl_4$, $CoCl_2$, $NiCl_2$, $CuCl_2$, $FeCl_3$ and $MnCl_2$. Molarity of dopant ions in the solutions were 0.003, 0.006, 0.012, 0.02, for each case, which were prepared in the

aqueous medium. Only in case of $PdCl_2$ slight acidic solution was prepared (0.002mM HCl), which was because of low solubility of $PdCl_2$ in water. PPy powder was dispersed in these and kept for doping for 4 hours. Redoped PPy was then filtered and dried under vacuum. These differently doped powders were then used for further study.

3.2.1.2. Electrochemical synthesis of Polypyrrole

On gold-coated glass plate electrochemical polymerization of pyrrole was carried out in a three electrodes single compartment cell. Electrochemical polymerization was done using Pt foil as counter electrode, SCE as reference electrode and gold-coated glass plates as a working electrode. The typical electrolyte solution contains 0.1 M pyrrole and 0.1M H_2SO_4 in 150 ml distilled water. The deposition of polymeric films was carried out with the help of computer controlled potentio-galvenostat [Vibrant EC 2010 model] at fixed potential of 700mV and time of polymerization 120 sec. These films were then rinsed with water and then stored in the dessicator. Detail procedure of the electro-polymerization was mentioned in the chapter II.

Undoping of Polypyrrole films

Electrochemically polymerized PPy films as obtained above were undoped by applying negative potential to the films. The electrochemical cell contained aqueous solution of 0.1M H_2SO_4 and the potential applied was -700mV (cathodic) for 60 sec. Application of potential for longer time causes cracking/pealing of the film. The undoping of polypyrrole films could also be done by dipping the films in 0.1M ammonia solution for 30 min.

Doping of polypyrrole films

Undoped electrochemically prepared PPy films were then redoped externally with different doping agents like $PdCl_2$, $CuCl_2$, $ZrCl_4$ etc. Concentration of dopant ion in the solution was varied from 0 to 20mM. These films were doped by dipping them in aqueous solution (slightly acidic with 2mM HCl in case of $PdCl_2$). Doping was done for 2 hours followed by draining the excess liquid and drying

.

3. 2. 2. Modification of PPy electrodes by different techniques.

a) Modification by insitu doping during polymerization.

In the insitu method, the pyrrole monomer was first complexed with the dopant salt and then incorporated in the polypyrrole during polymerization process. This was carried out as follows: in 100 ml distilled water 0.8ml H_2SO_4 and 0.5ml of pyrrole were added and stirred properly. In another beaker 50 ml of distilled water was taken and the desired doping agent was first dissolved. Then to this solution 0.5 ml of pyrrole was added and allowed to form complex (for 10 mins). The solution of this complex was then added to electrochemical cell as above and electrochemical polymerization was done as before under similar conditions (700mV SCE, 120s). Concentrations of doping agents were varied from 0 to 20 mM in the solution. In case of $PdCl_2$ and $FeCl_3$ during the complex formation, chemical polymerization may get initiated. In order to avoid rapid polymerization of pyrrole acetonitrile was chosen as the medium for electrochemical polymerization.

b) Ion beam irradiation

In order to form PPy complexes with $PdCl_2$ using dry technique, ion beam irradiation was used. Modification of PPy electrodes was done by ion beam irradiation technique. Irradiation was carried out at Nuclear Science Center, New Delhi. The films were irradiated with 120MeV Au^+ beam at a dose of 10^{12} ions/cm^2. PPy film electrodes doped with different concentration of $PdCl_2$ (by external technique) were subjected to ion beam irradiation and these films were used as anode in the electro-catalytic oxidation of methanol.

c) Surface roughening

Roughening of the PPy film electrodes were done while depositing the films. Films of different roughness were prepared using cyclic voltammetry instead of chronoamperometry technique. Scan rate while running cyclic voltammetry was varied during deposition for getting films of varying roughness. Scan rates for deposition were 25mV/s, 30mV/s, 40mV/s, 50mV/s, 60 mV/s, 100mV/s. Deposition time was same for all the films.

d) Deposition time

PPy film electrodes with varying thickness were also prepared. For varying thickness, deposition time while running chronoamperometry was varied. Different deposition times were 50s, 75s, 100s, 125s, 150s, and 200s.

3.2.3. Electro-Catalytic Oxidation of Methanol

Electrochemical oxidation of methanol was carried out using these different PPy electrodes. The electrochemical cell contained 150 ml distilled water and 0.1M $HClO_4$ electrolyte, with varying methanol concentration from 0.01M to 0.5M in each case. The reaction was carried out in acidic media which is (here $HClO_4$) generally preferred since carbonate residues are not formed in this electrolyte.[31] The overall reaction for methanol electrooxidation can be shown as follows,

$$CH_3OH + H_2O \rightarrow CO_2 + 6H^+ + 6e^-$$

Cyclic voltammetry was run to study the catalytic activity of the electrodes. PPy electrodes were used as working electrode where as Platinum electrode of 1 sq. cm.
area was used as counter electrode. Reference electrode used in this process was Standard Calomel Electrode (SCE).

3.2.4. Percentage Conversion Calculation.

From the CV's, the peak current in *m Amps* and peak area (area CDE in *Figure 3.1*) under the curve was estimated for the MeOH oxidation. The total charge passed in the reaction time interval for methanol oxidation was estimated from the area under the curve (taking in to account the scan rate for converting voltage scale to time scale). Following the Faraday's law, the molar conversion can be calculated which can then be transformed in terms of weight percentage conversion in the reaction time. This weight when divided by density of methanol and volume in ml of methanol reactant taken for reaction volume in ml of methanol conversion can be calculated. As, complete methanol oxidation process is a six-electron process, for percentage conversion during that time; the term

obtained in the above calculation has to be divided by 6. A typical CV is shown below to illustrate the calculation of percentage conversion of the reactant to the product.

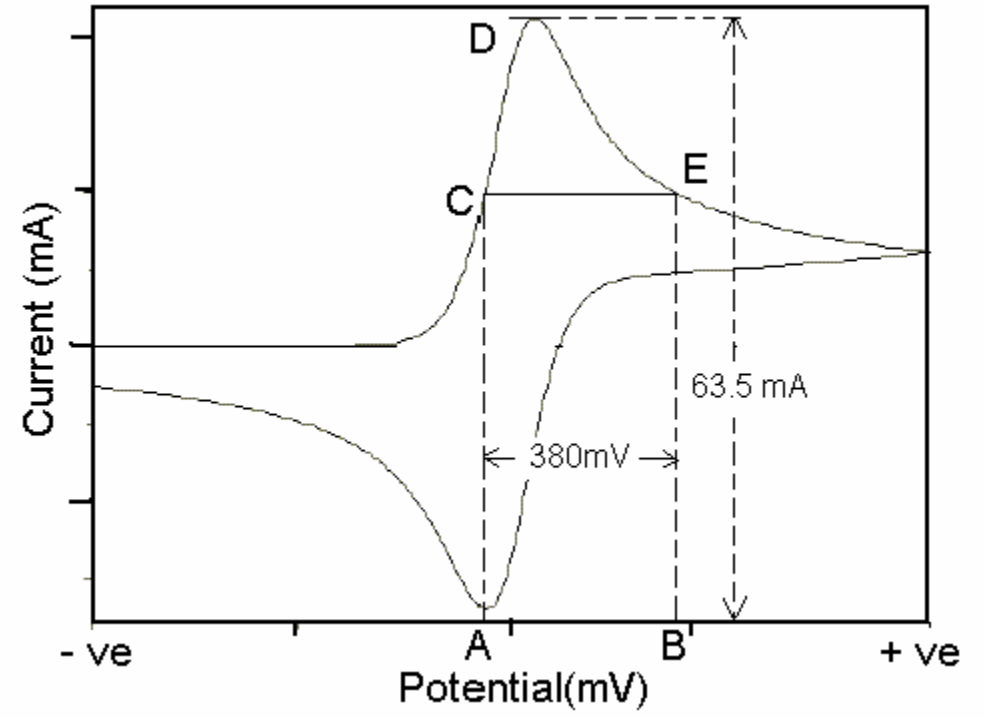

Figure 3.1: Schematic representation of a CV showing calculation of percentage conversion

In the above cyclic voltammogram

Peak Current = 63,500 μ amps = 63.5 m amps

Scan rate = 50 mV/s

The time of reaction (time interval between A to B) = 380/50 = 7.6 s

Charge (Q) = I × t = 63.5 × 7.6 = 482.6 m Amp. S = 482.6 m Coulombs

n = Q/F = 482.6 / 96540 (Faraday's Law)

= $4.9989 \times 10^{-3} \times 32$ (MW of methanol = 32)

= 0.15996mg

= 0.15996 / 0.79 (Density of methanol = 0.79 g/cc)

= 0.20248 ml

= (0.20248 × 100) / (0.606 × 6) %

= 5.568 % of conversion in 7.6 seconds.

Therefore in 10 seconds the conversion will be

= 5.568 × 10 / 7.6

= 7.32 %

Conversion per minute for methanol oxidation was calculated and presented in the following studies.

3.3. RESULT AND DISCUSSION:

3.3.1.Characterisation Of the Modified Conducting Polypyrrole

3.3.1.1. Infra red (FT- IR) spectroscopy studies:

IR spectra of the different doped PPy powders was run. For that purpose these different doped powders were mixed with KBr powder and pellets were prepared. The spectrum for powders is shown in the *figure 3.2*. The undoped PPy spectrum essentially conforms to the polypyrrole spectra reported in literature. [32-39]

A comparison of the IR spectroscopic data of undoped and doped PPy shows that doping produces dramatic changes in the spectra which reflect drastic changes of the molecular structure of the material. In conducting polymers doping generates extra string bands in the infrared spectra generally called 'doping induced bands' or 'bipolaron bands'. In the case of PPy the infrared spectrum after doping consists of some strong bands near 2365 cm^{-1}, 1560 cm^{-1}, 1210 cm^{-1}, 1050 cm^{-1} and 930 cm^{-1} accompanied by many other weaker bands. In the spectrum of the doped material all bands appear to be broader whereas incase of undoped PPy peaks are weak and ill defined. The assignment of IR absorption bands is shown in the *table 3.1*.

It could be seen from the figure that major changes in the IR spectra occur for the bands in the region of 1200 cm^{-1} — 1100 cm^{-1} which are associated with C–N vibrations. These changes in the intensity as well as group vibrational frequency could be due to the complex formation of pyrrole and the dopant molecule.

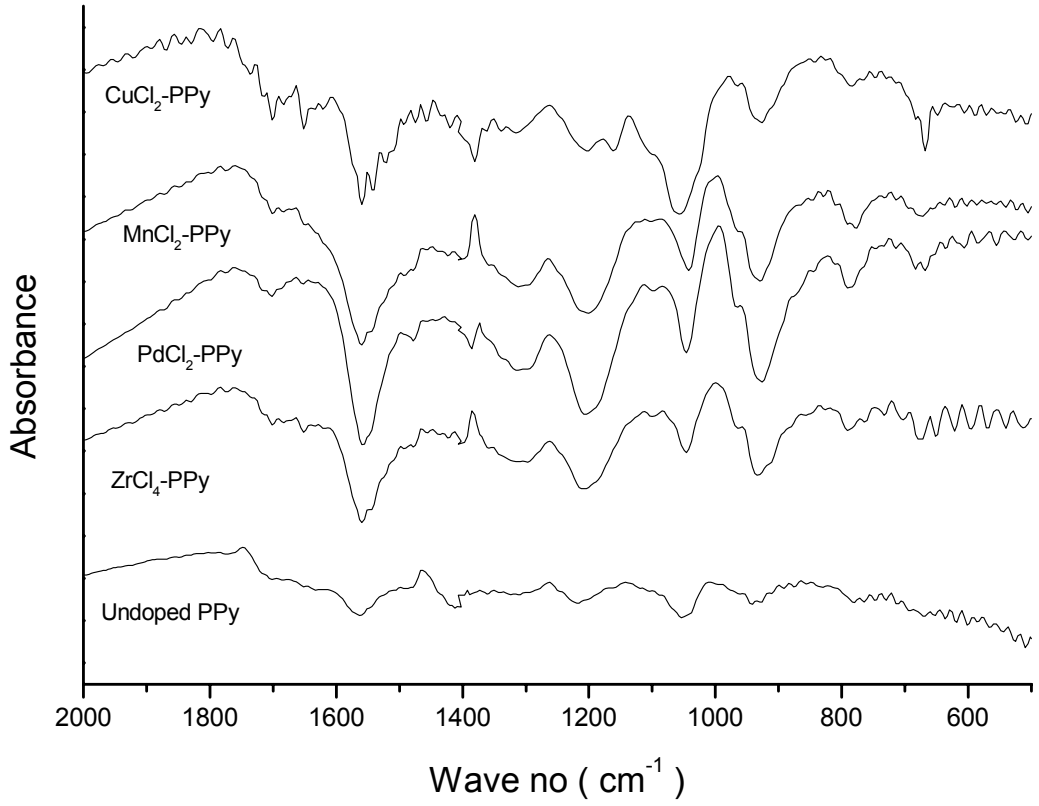

Figure 3.2: FT-IR spectra of different PPy doped powders

3.3.1.2. XRD Studies Of the Conducting Polypyrrole Doped with Different Agents.

XRD studies of the polypyrrole doped with different doping agents were also studied. X-ray diffraction studies shows that the polypyrrole is mainly amorphous in nature as shown in the *Figure 3.3.* Typical XRD for three dopants viz. $ZrCl_4$, $CoCl_2$ and $CuCl_2$ along with undoped PPy are shown, although it has been recorded for all. PPy has been reported to be mainly amorphous with very little structure in the XRD pattern. There may be few reflection occurring at 2θ of about 26°, however, change in the position of the maximum intensity of the amorphous halo with the dopant ion was observed.

Dedoped	**$ZrCl_4$ doped PPy**	**$PdCl_2$ doped PPy**	**$MnCl_2$ doped PPy**	**$FeCl_3$ doped PPy**	**$CuCl_2$ doped PPy**	**$NiCl_2$ doped PPy**	**Assignment**
-	790(w)	790(w)	790(w)	780(w)	790(m)	780(w)	C-H out of plane bending
930(w)	930(m)	930(s)	930(s)	930(s)	926(s)	930(w)	C-H out of plane bending
1053(m)	1045(s)	1045(s)	1050(s)	1050(s)	1050(s)	1050(s)	C=C stretching
1210(w)	1210(br)	1200(br)	1200(br)	1200(br)	1200(w)	1200(w)	C=N stretching, C-H in plane vibration
1300(w)	1300(br)	1300(br)	1300(br)	1300(br)	1300(w)	1300(w)	C-N stretching
1385(w)	1385(br)	1385(br)	1385(br)	1385(w)	1385(w)	1385(w)	C-N, C-C vibration
1400(w)	1405(w)	1405(w)	1405(w)	1405(w)	1407(m)	1405(w)	Pyrrole ring stretch
-	1540(w)	1540(w)	1540(w)	1540(w)	1540(w)	1540(w)	C=C stretching
1560(m)	1560(s)	1560(s)	1560(s)	1560(s)	1560(s)	1560(s)	N-H bending, C=C stretching of PPy
-	1640(vw)	1640(vw)	1640(vw)	1640(vw)	1640(vw)	1640(vw)	C=N stretching

Table 3.1: Table of FT-IR assignment for different PPy doped powders

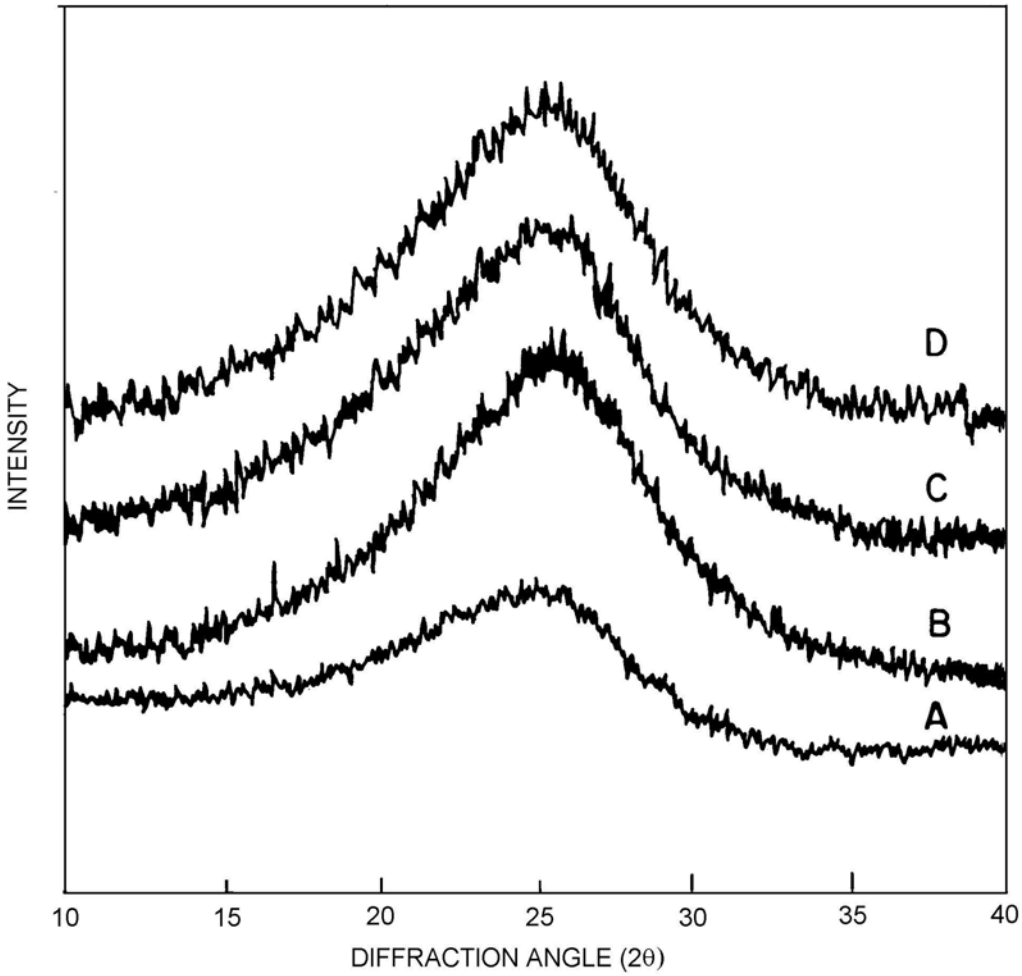

Figure 3.3: XRD spectra of different PPy doped powders (A) Undoped PPy, (B) $ZrCl_4$ doped PPy, (C) $CoCl_2$ doped PPy and (D) $CuCl_2$ doped PPy

On the other hand it may be interesting to note that the position of peaks of these amorphous halos depend on the dopant present. Average interchain separation can be estimated from these maxima using the relation* [40-43]

$$R = \frac{5}{8}\left[\frac{\lambda}{\sin\theta}\right]$$

Where λ is the x-ray wavelength of CuKα and θ is the diffraction angle at the maximum intensity in the amorphous halo. All these parameters are tabulated for PPy containing different dopant ions in *table-3.2.*

Doping Agents	2θ	Inter Chain separation (A^0)
$FeCl_3$	25.8	4.405
$NiCl_2$	25.5	4.3629
$CuCl_2$	25.5	4.3629
$CoCl_2$	25.8	4.3128
$ZrCl_4$	26.0	4.2803
$MnCl_2$	25.3	4.3128
$PdCl_2$	26.5	4.2009

Table 3.2: Table of XRD data of PPy doped powders

3.3.1.3. X-ray Photoelectron Spectroscopy studies

In order to monitor the changes occurring due to doping of PPy powders with different dopant ions X-ray photoelectron spectroscopy (XPS) were run for the undoped and different doped powders. XPS spectrum of C1s, N1s, Cl2p and respective dopant ions were recorded, but only the deconvoluted XPS graphs of C1s and N1s were shown in the *figure 3.5(A) and 3.5(B)* respectively.

As in the XPS study of different doped PPy powders, Cl2p core level spectrum is observed; it reveals the presence of the dopant ion, which is the proof of doping in the PPy powders. It can be seen from the *figure 3.5.(A),* which are the spectra of different doped PPy powders that C1s core level spectra are not symmetric on the higher BE side of the peak, which is assigned to the 'disorder effect'. This disorder effect might be due to cross-linked, chain terminating or non α-α′ bonded carbons as well as carbon in partially saturated rings. A schematic representation of N1s and C1s core level spectrum showing different components is given below.

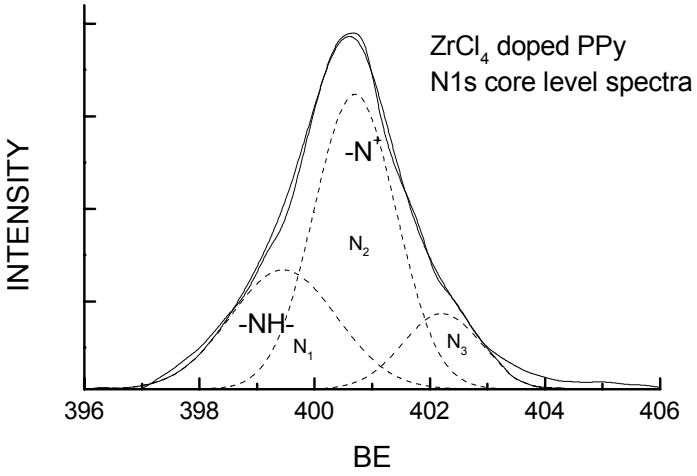

Figure 3.4 (A): Schematic representation of N1s core level spectrum showing different components

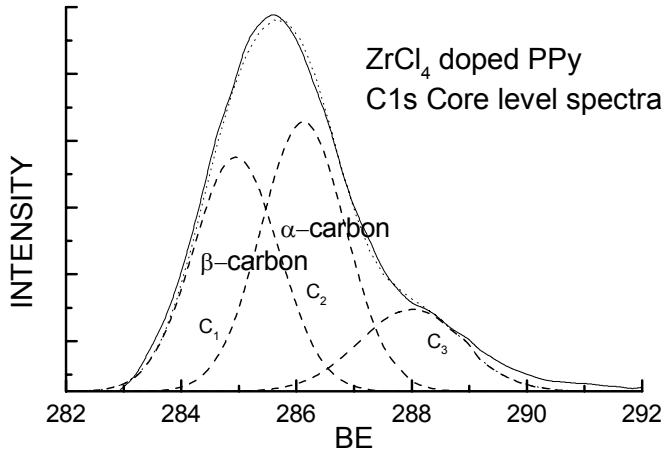

Figure 3.4.B: Schematic representation of C1s core level spectrum showing different components

Table 3.3: Table of Energy splitting C and C for different doped Polypyrrole powder

Sample name	C	C	Energy splitting of C and C
Dedoped	284.6	285.8	1.2
$ZrCl_4$	284.6	285.72	1.12
$PdCl_2$	284.6	285.7	1.1
$MnCl_2$	284.6	285.8	1.2
$FeCl_3$	284.6	285.66	1.06
$CoCl_2$	284.6	285.76	1.16
$CuCl_2$	284.6	285.67	1.07
$NiCl_2$	284.6	285.83	1.23

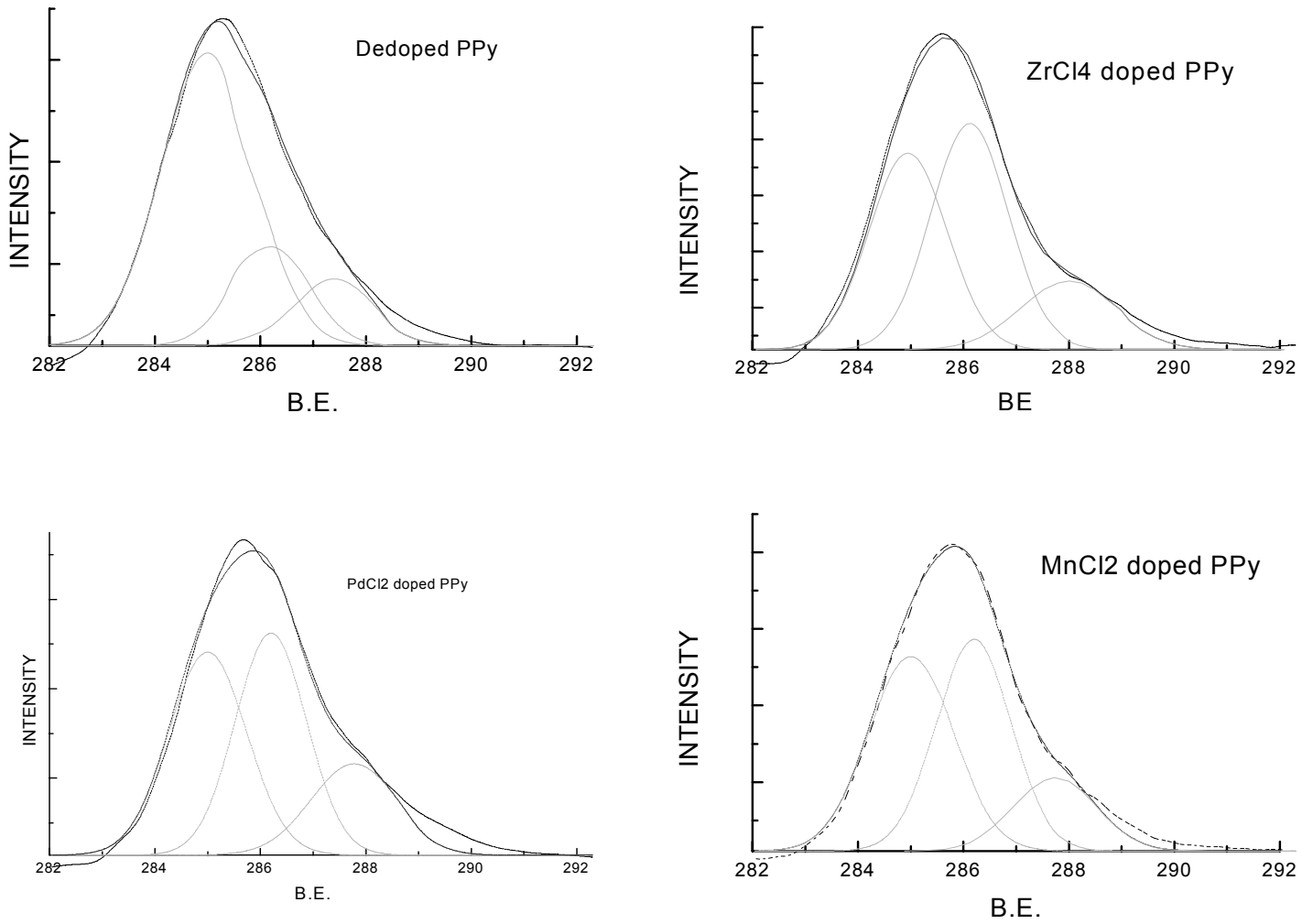

Figure 3.5.A : XPS of C1s core level spectra of different PPy doped powders

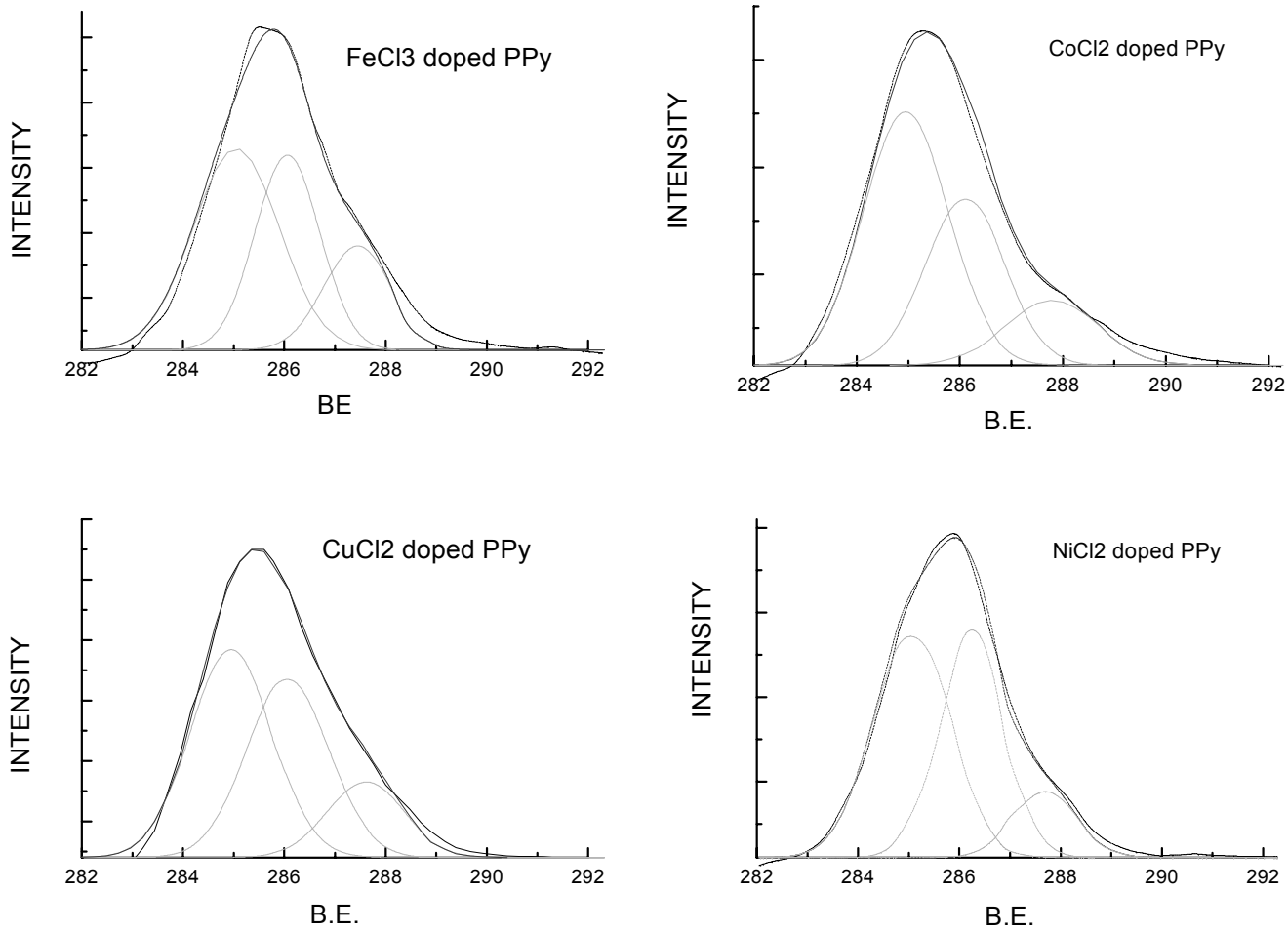

Figure 3.5.A : XPS of C1s core level spectra of different PPy doped powders

Parameters	**Dedoped**	**$ZrCl_4$**	**PdC_2**	**$MnCl_2$**	**$FeCl_3$**	**$CoCl_2$**	**$CuCl_2$**	**$NiCl_2$**
Xc1	284.6	284.6	284.6	284.6	284.6	284.6	284.6	284.6
W1	1.75	1.48	1.45	1.58	1.7	1.565	1.6	1.5
A1	67.9	38.86	40	42.67	46.8	54.54	45.45	47.69
Xc2	285.8	285.72	285.7	285.2	285.66	285.76	285.67	285.83
W2	1.42	1.47	1.32	1.4	1.25	1.4	1.60	1.26
A2	18.7	44.39	40	41.42	34.68	34.04	38.96	41.03
Xc3	287	287.6	287.4	287.34	287.05	287.47	287.21	287.3
W3	1.5	1.82	1.62	1.58	1.32	1.64	1.5	1.25
A3	13.36	16.74	20	15.89	19.1	16.16	15.58	11.78
A2+A3	32.06	61.13	60	53.35	53.78	50.2	54.54	52.81

Table 3.4.A: Table of BE, FWHM, and percentage area contribution of C1s core level spectra of different PPy doped powders

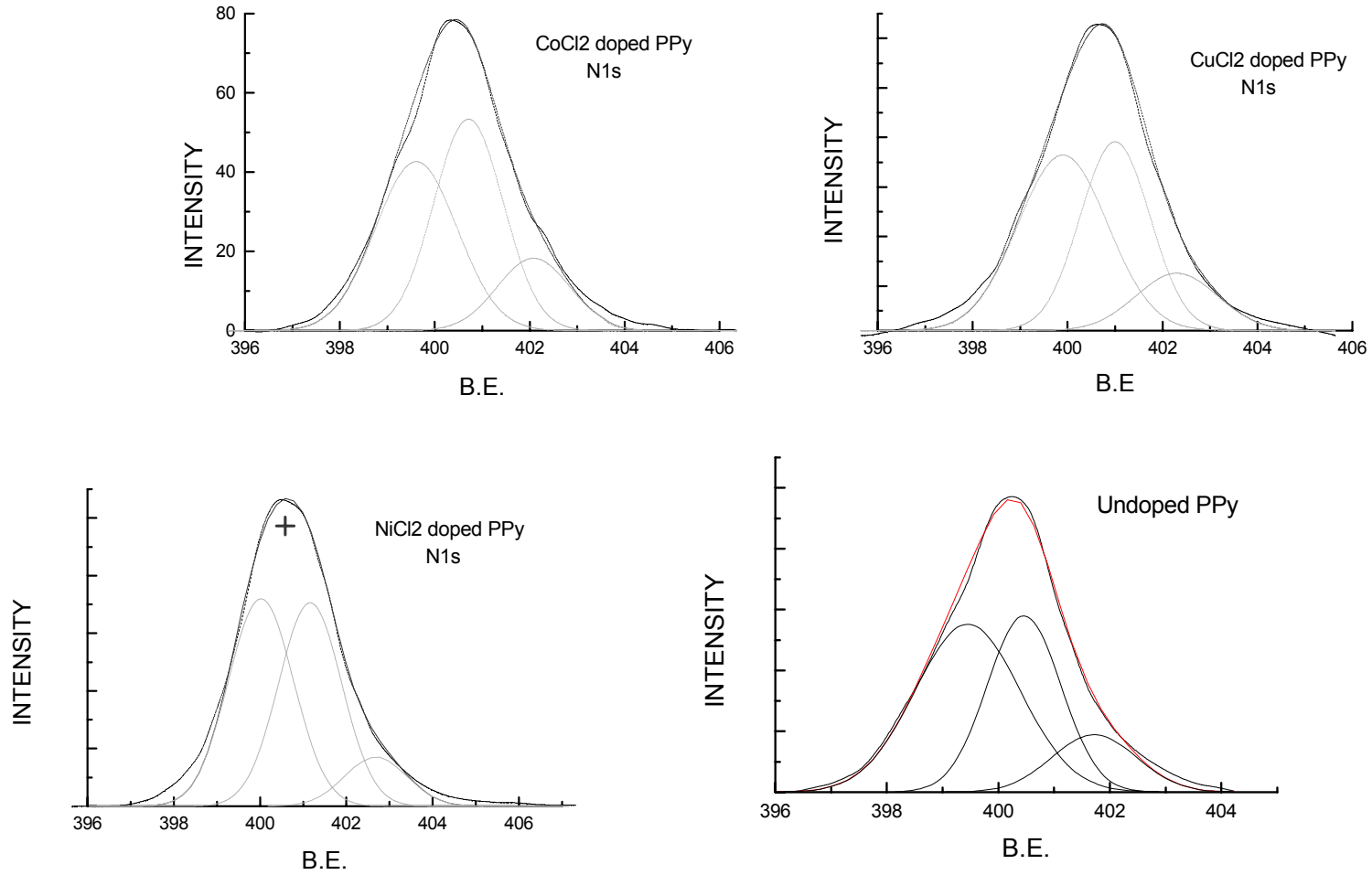

Figure 3.5.B : XPS of N1s core level spectra of different PPy doped powders

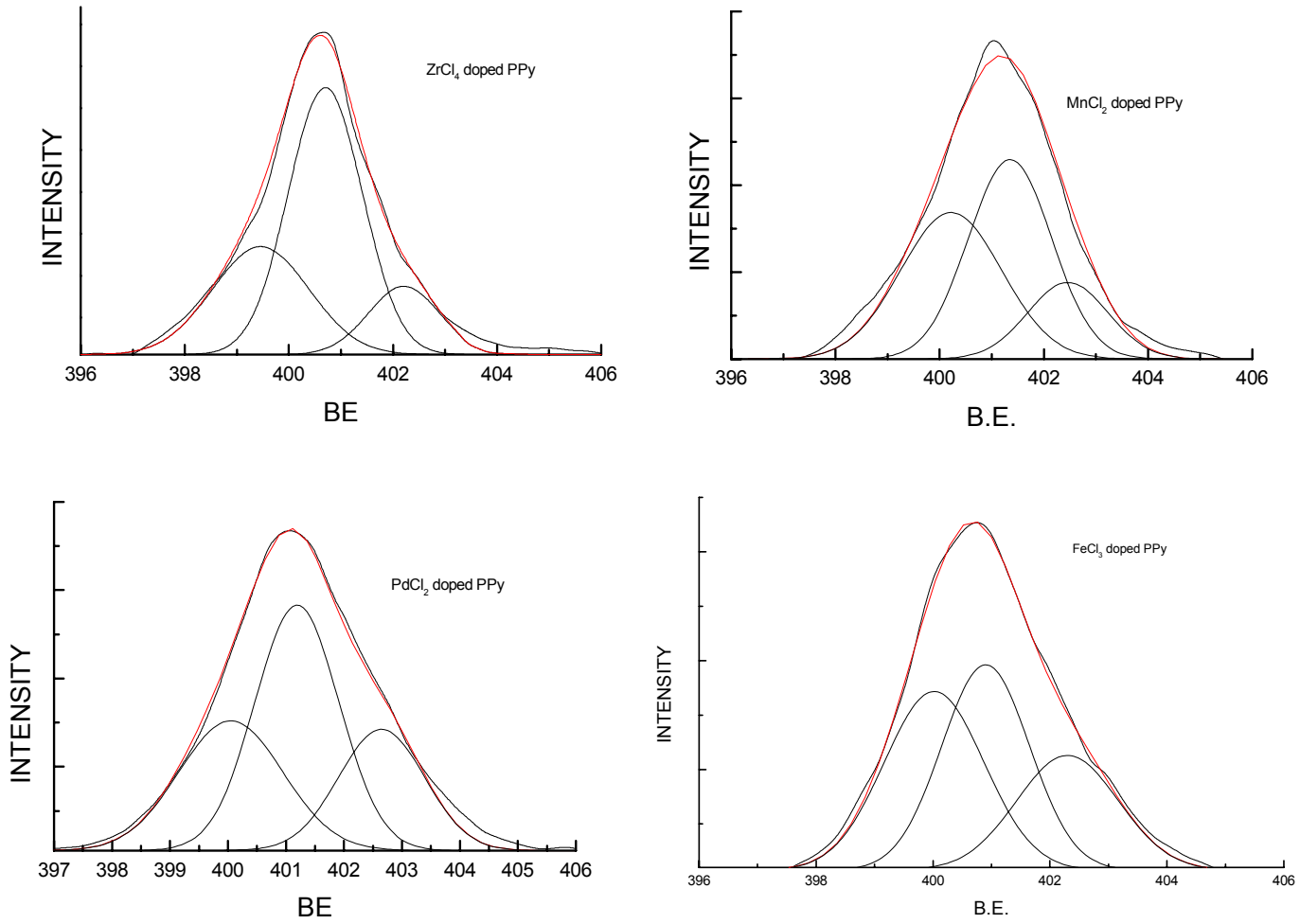

Figure 3.5.B : XPS of N1s core level spectra of different PPy doped powders

Parameters	**Dedoped**	**$ZrCl_4$**	**PdC_2**	**$FeCl_3$**	**$MnCl_2$**	**$CoCl_2$**	**$CuCl_2$**	**$NiCl_2$**
XN1	399.05	399.06	399.65	399.62	399.82	399.21	399.5	399.62
FWHM1	1.88	1.84	1.79	1.7	1.94	1.7	1.87	1.49
A1	49.62	29.7	30.28	37.63	39.42	40.88	46.93	45.95
XN2	400.06	399.3	400.79	400.5	400.95	400.31	400.6	400.76
FWHM2	1.32	1.4	1.45	1.5	1.6	1.44	1.44	1.44
A2	36.64	56.44	46.33	38.17	44.23	43.55	39.11	43.58
XN3	401.32	401.81	402.25	401.9	402.06	401.68	401.9	402.48
FWHM3	1.52	1.34	1.48	1.74	1.54	1.52	1.7	1.45
A3	13.74	13.86	23.39	24.19	16.35	15.55	13.97	10.47
A2+A3	50.38	70.4	69.72	62.36	60.58	59.1	53.08	54.05

Table 3.4.B : Table of BE, FWHM, and percentage area contribution of N1s core level spectra of different PPy doped powders

XPS of C1s core level spectra can be deconvoluted in to three components. The line at the lowest B.E. is due to β-carbon, whereas the second component is due to the α- carbon as shown in the representative figure below. In all the different doped samples the α-carbons have a slightly higher line width than the β-carbons. This is mainly because of the fact that PPy is α-α′ linked and also might be due to the deviations from the ideal planner conjugated chain.

It can be noted that the splitting between α and β carbon is in the range of 1-1.2 which is given in the *Table 3.3.* Joo et al had suggested the splitting as 0.94eV, whereas Pfluger had reported it as 0.9eV. These results agree with the observed energy separation of pyrrole monomer. [44-47]

The peaks of C1s core level spectra could be assigned as follows. The lowest BE peak which is fixed at 284.6eV is due the neutral C, which are C–C or C–H covalent bonded species and it assigned as the carbon of polypyrrole chain. The second peak, which appears in the range of 285.6eV- 285.8eV for different doped PPy powders, might be due to the C–N bonded C and which is not adjacent to the dopant ion and this C is

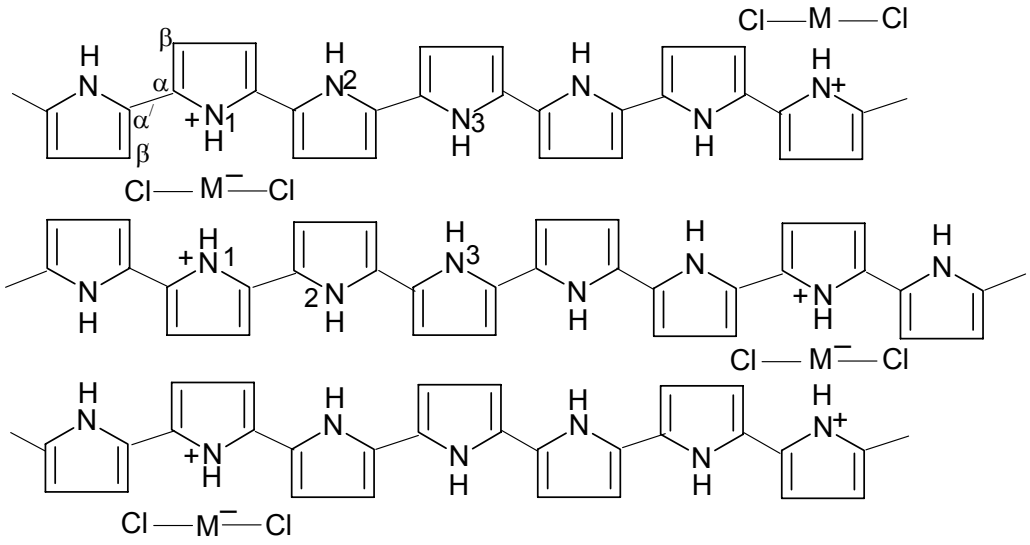

Figure 3.6: Proposed structure of doped PPy powder

assigned as the carbon. The peak in the higher BE region might be due to the carbon i.e. the highly charged C bonded to N of the polypyrrole which is close to M as shown in

the schematic representation (*Figure 3.6*) of doped polypyrrole powder, where M is the dopant ion.

In the *figure 3.5.B* deconvoluted N1s core level spectra are shown. As in the case of C1s core level spectra, in case of N1s spectra also the peaks are asymmetric on the higher BE value. In contrast to the C1s line, the structures on the high BE side of N peaks are sufficiently well resolved. Structural disorder is not believed to be the reason of the shoulder of N1s peak, since polymerization defects directly affect carbon spectrum much more than the nitrogen spectrum. These three nitrogen components after deconvolution are assigned to the three electrostatically inequivalent groups of N atoms. As it is known that the dopant anions bear localized charge, and these anions are located in between polypyrrole chains, they produce electric fields at the nitrogen sites, making the atoms near to the anion more positively charged than the other. The deconvoluted component appearing around 399eV in every case is assigned to the neutral N. The two nitrogen species at higher BE of N1s core level spectrum are assigned to the charged species –NH– and N^+ respectively and the peak at the lower BE is due to the imine like N atom (–N=).

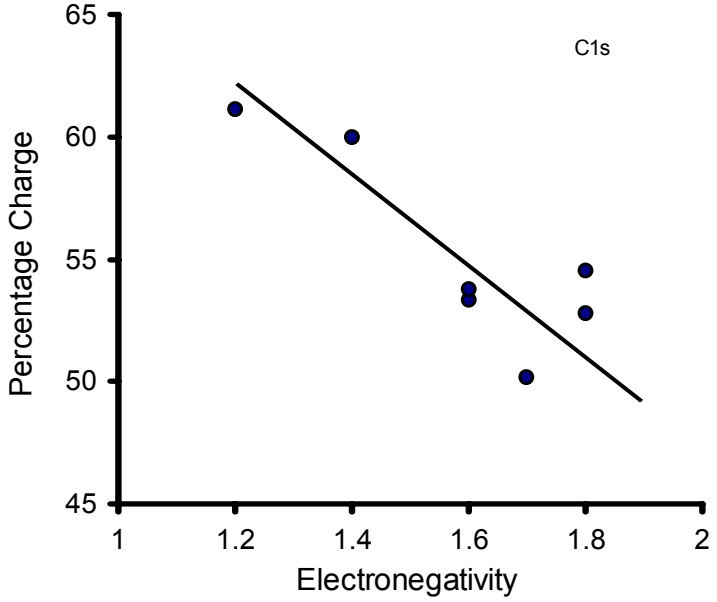

Figure 3.7: Graph of percentage charge in C1s core level spectra against electronegativity of the dopants

Sample Name	Electronegativity	*Percentage Charge*
Dedoped		32.1
$ZrCl_4$	1.2	61.1
$PdCl_2$	1.4	60.0
$MnCl_2$	1.6	53.3
$FeCl_3$	1.6	53.8
$CoCl_2$	1.7	50.2
$CuCl_2$	1.8	54.5
$NiCl_2$	1.8	52.8

Table 3.5: Table of percentage charge (C1s) against electronegativity of different doped PPy powders

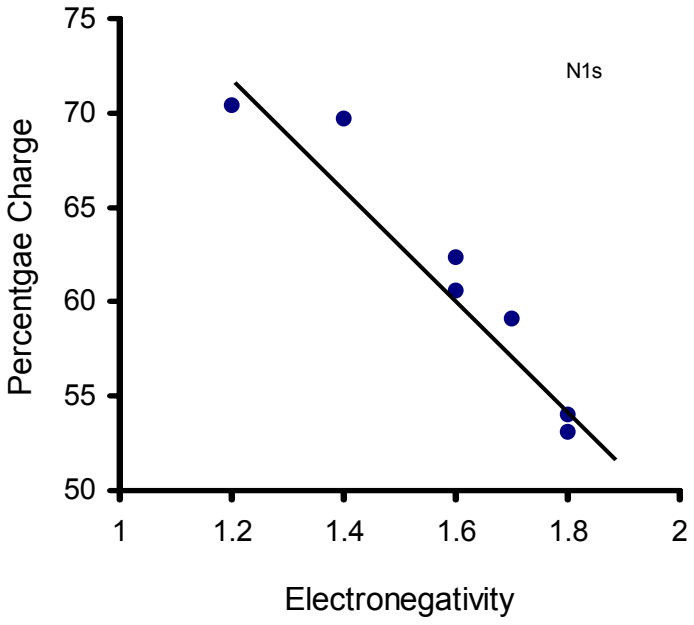

Figure 3.8: Graph of percentage charge in N1s core level spectra against electronegativity of the dopants

Sample Name	Electronegativity	Percentage Charge
Dedoped		50.3
$ZrCl_4$	1.2	70.4
$PdCl_2$	1.4	69.7
$MnCl_2$	1.6	60.6
$FeCl_3$	1.6	62.3
$CoCl_2$	1.7	59.1
$NiCl_2$	1.8	54.0
$CuCl_2$	1.8	53.1

Table 3.6: Table of percentage charge (N1s) against electronegativity of different doped PPy powders

During undoping with ammonia deprotonation of the sample take place prior to doping. –NH– is obtained from the reduction of the deprotonated structure and is susceptible to reoxidation by electron acceptor such as halogens. The high energy peaks i.e. N^+ is due to the doped nitrogen species and the doping level can be expressed as the share of N^+ groups in the polymer.

The BE positions, FWHM (full width at half maximum) and percentage area contribution for various charged species of C1s and N1s core levels were compared with undoped PPy sample and presented in the *table 3.4.A and 3.4.B* respectively.

The components which appear due the surface charging effects, the BE's are referenced to the C1s neutral carbon peak at 284.6. It could be seen from the table that for doped samples, both C1s and N1s the contribution of charged species are more compared to the undoped powder and for undoped sample percentage of neutral component is maximum.

An interesting feature could be observed, if percentage charge contribution for C1s is plotted against electronegativity of the dopant ions as shown in the *figure 3.*7. From the

graph it could be observed that percentage of charged species depends on the electronegativity of the dopant ions, which decreases with the increase in the electronegativity of the dopant ions. Same trend was observed for N1s core level spectra also which is shown in the *figure 3.8***.**

Following salient observations emerge from above.

- The percentage contribution of charged species i.e. –NH– and $–N^+$ species depends on the electronegativity of the dopant ions, which decreases with the increase in the electronegativity of the dopant ions.
- Percentage of doping is higher in case of lower electronegative doping agent like $ZrCl_4$, $PdCl_2$ as doping level can be expressed as the share of $–N^+$ groups in the polymer.
- Based on all the above observation existence of one dopant per three/four pyrrole rings is proposed which is given in the figure above (*Figure 3.6*). [44-51]

3.3.1.4. Measurement of Electrical Property

The PPy powders as synthesized above were compression moulded at an applied pressure of 3 tons for 1 minute. The room temperature electrical conductivity of different samples was calculated by measuring resistance using Keithley electrometer 614 model as described in the chapter-II.

The effect of dopant ion on the overall conductivity behavior in polypyrrole was observed. The room temperature conductivity for dedoped polypyrrole sample was found to be $9.14x10^{-8}$S while it increased to a value of $1.1x10^{-6}$S when the PPy was doped with $ZrCl_4$.

The temperature dependence of conductivity for these pellets was also measured in the temperature range of 30 to 90°C. The activation energy for conduction was then estimated from the Arrhenius plots of these data using curve fitting procedure, and slopes of the linear portions of the graphs. The increase in conductivity with temperature was obvious for conducting polymer, which might be due to thermal activation process. The electrical conductivity in the doped PPy powders might be associated with excitation of

the mobile π-electrons from the valence band containing HOMO (Highest Occupied Molecular Orbital) to the conduction band containing LUMO (Lowest Unoccupied Molecular Orbital) and the charge hopping between the polymer chains. To explain the conduction mechanism in the conducting polymers, the concept of polaron and bipolaron was introduced. Low level of oxidation of the polymer gives polaron and higher level of oxidation gives bipolaron. Both polarons and bipolarons were mobile and could move along the polymer chain by the rearrangement of double and single bonds in the conjugated system. Conduction by polarons and bipolarons was supposed to be the dominant factor which determine the mechanism of charge transport in polymer with non-degenarate ground states. The magnitude of the conductivity was determined by the number of charge carriers available for conduction and the rate at which they move i.e. mobility. In conducting polymers which could be considered as semiconductor the charge carrier concentration increased with increasing temperature. Since the charge carrier concentration was much more temperature dependent than the mobility, therefore it was the dominant factor and conductivity increased with increase in temperature. Hence, it may be surmised that the activation energy for conduction is associated with thermal excitation of charge carriers from the impurity levels.

Name of dopants	Electronegativity	Room temperature Conductivity (S/cm)	Activation Energy (eV)
$ZrCl_4$	1.2	$1.1X10^{-6}$	0.246
$PdCl_2$	1.4	$7X10^{-5}$	0.256
$MnCl_2$	1.6	$4.2X10^{-8}$	0.32
$FeCl_3$	1.6	$3.3X10^{-7}$	0.379
$CoCl_2$	1.7	$4.4X10^{-8}$	0.353
$CuCl_2$	1.8	$3X10^{-7}$	0.398
$NiCl_2$	1.8	$6X10^{-7}$	0.412

Table 3.7: Table of dopants with their electronegativities, R.T. conductivities and activation energies

From the temperature dependence of conductivity data, activation energy (ΔE) for conduction for each doped sample was calculated using Arrhenius equation which was given in the *table 3.7*. It could be seen that activation energy (□E) value was less in case

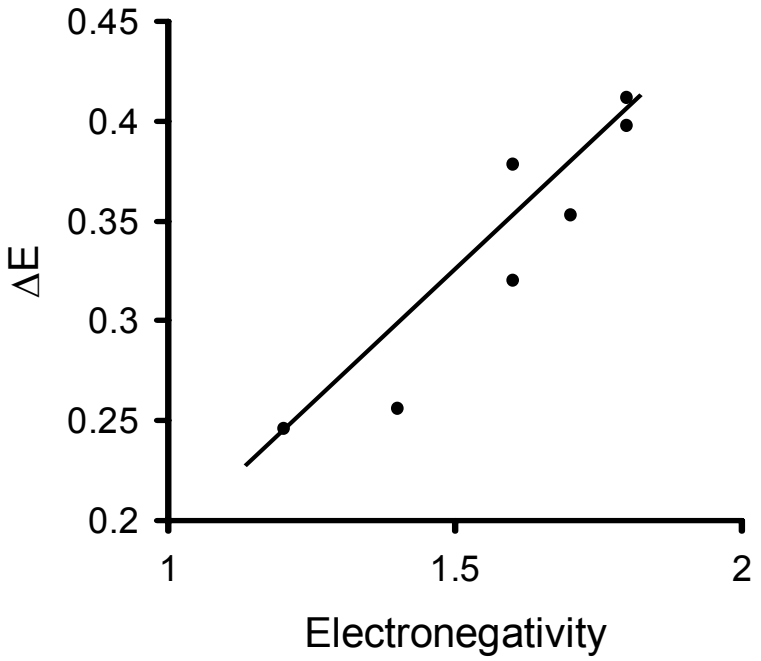

Figure 3.9: Graph of Activation energy in eV against electronegativity of the dopants

of PPy doped with $NiCl_2$, $CuCl_2$ whereas it is high in case of PPy doped with $ZrCl_4$. A graph of □E vs. electronegativity of the transition metal dopant ion was plotted which is given in the *figure 3.9*. From the graph it was observed that the activation energy of doped PPy powders was inversely related to the electronegativity of the dopant ions, i.e. for PPy doped with higher electronegative transition metal salts activation energy is lower and for lower electronegativity it is higher.

3.3.1.5. ESR Study of Different PPy Doped Powder

ESR study of the different doped PPy powders were done, spectrograms of which is shown in *figure 3.10*. From the figure it could be observed that narrow line width was observed incases of $NiCl_2$, $MnCl_2$ and $ZrCl_4$ (few Gauss width). This probably might be

due to the high mobile polarons along the polymer chains. Table of N(s) values of different doped PPy powders obtained from the spectra were given in the *table 3.8.*

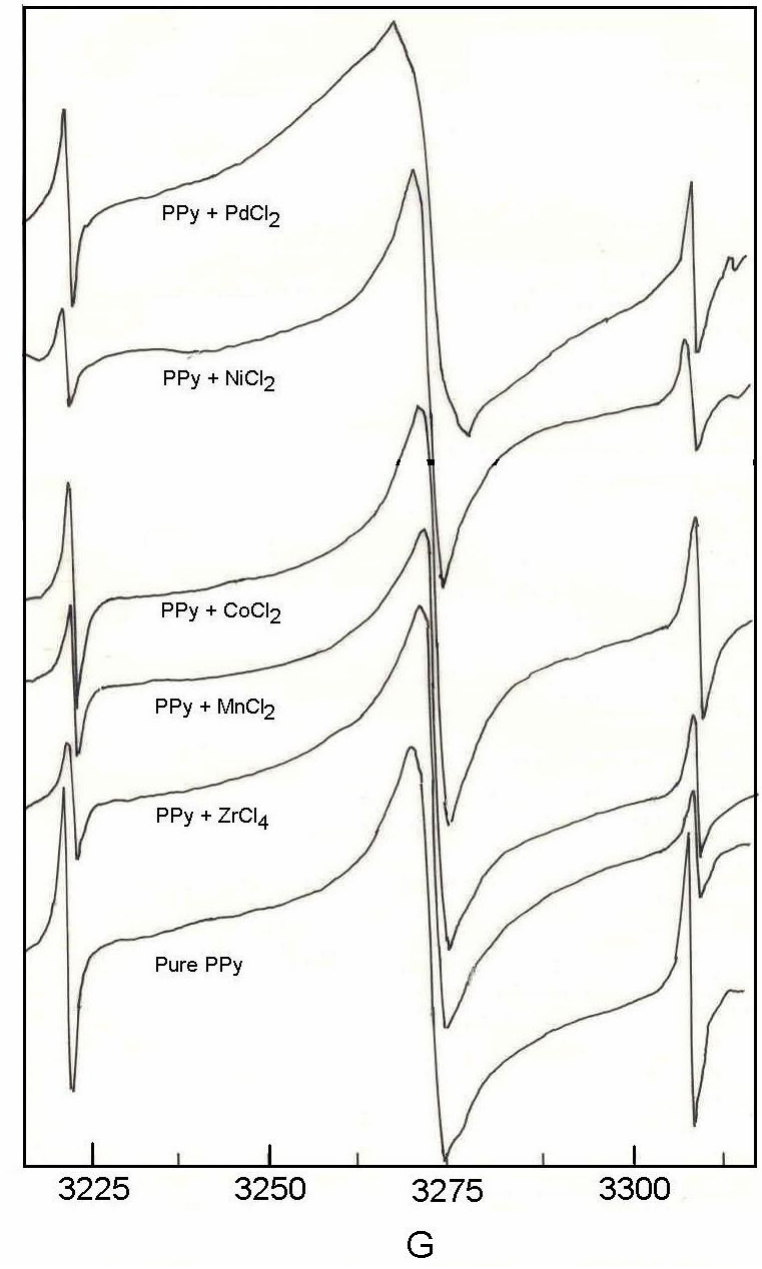

Figure 3.10: ESR of different doped PPy powder

From the table it could be seen that PPy doped with $ZrCl_4$ has maximum N(s) value. It could also be seen that higher electronegative dopant ions like Co(1.35), Ni(2.3) had lower N(s) value and lower electronegative dopant ions like Zr (27.67) had higher N(s) value. Graph for N(s) against electronegativity of the dopant ion was plotted, which was

shown in the *figure 3.11***.** From the figure it could be observed that N(s) value was dependent on the electro-negativity of the dopant and it decrease with the increase in electronegativity. This clearly shows that the dopant ion generates free/mobile carriers, the density of which is dependent on the additional impurity states created within the bandgap. [52-56]

Doping Agent	Electronegativity	Absolute N(s) value
$ZrCl_4$	1.2	27.67
$PdCl_2$	1.4	9.38
$FeCl_3$	1.6	2.907
$MnCl_2$	1.6	2.09
$CoCl_2$	1.7	1.35
$NiCl_2$	1.8	2.3

Table 3.8: Table of doping agents, their electronegativity with absolute N(s) value from ESR data

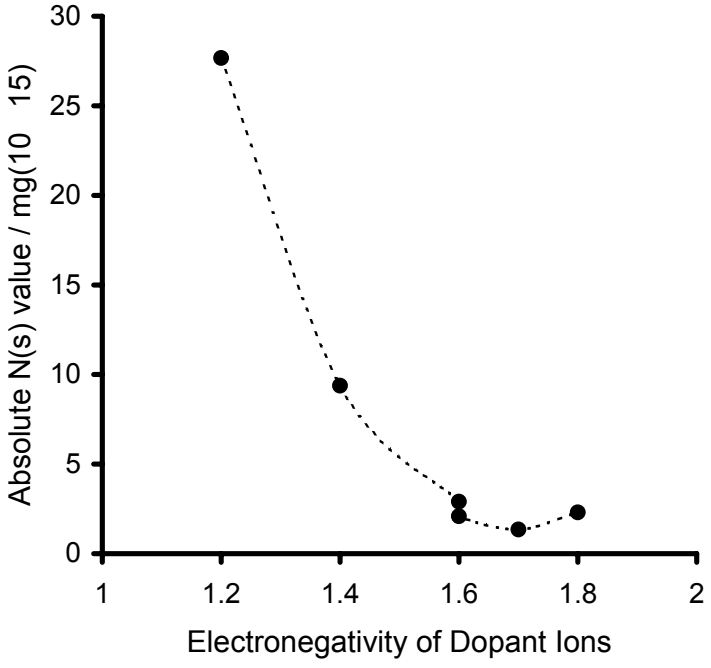

Figure 3.11: Graph of Absolute N(s) value against electronegativity of dopant ions

3.3.1.6. Cyclic Voltammetry study on Complex formation.

The CV's for undoped and PPy doped externally and internally with $ZrCl_4$ were shown in the *Figure 3.12*. The electrochemical cell consisted of 150ml distilled water and 0.1M H_2SO_4. CV (a) in the figure corresponds to the undoped PPy whereas (b) and (c) corresponds to the exsitu and insitu doped PPy respectively. It was seen in the CVs for later two cases were broad whereas for undoped PPy it was narrow. Cyclic voltammetry study could also be the indicative of complexation. Higuchi et al suggested the complexation of polyaniline with $CuCl_2$ by this method.[57] As it was known that the wave shape in CV of any complex was broader. These results appear to be accounted for by the complexation, which was considered to raise the catalytic activity giving rise to broader CV than the original case.

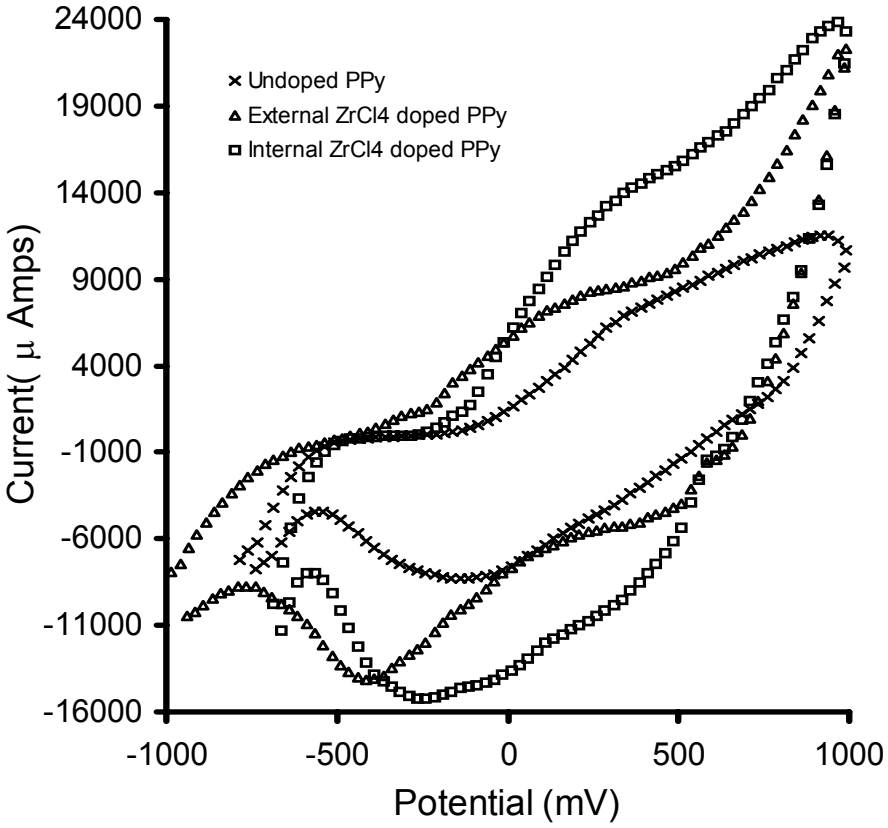

Figure 3.12: CV's of PPy doped external and internal with $ZrCl_4$ along with undoped one in presence of 0.1M H_2SO_4 in the electrolyte

Co-ordination of transition metals to the nitrogen atoms of PPy affords the complex formation, in which transition metals are considered to interact through a π-conjugate

chain. The characteristics of π-conjugate polymers are reflected on the complexes, which are expected to provide a novel catalytic system. It was suggested by various authors that complexation with copper (II) chloride or Iron (II) chloride affords a more efficient synthetic metal catalyst in the dehydrogenation reaction. The complex catalyst consisting of Pd(II) acetate and PPy or Pani is capable of inducing the Wacker oxidation. [58-60]

3.3.2. Electrochemical Oxidation of Methanol

3.3.2.1. Conducting polymer coated electrodes for the electro-chemical oxidation of methanol:

The conducting PPy coated electrodes were employed for electrochemical oxidation of methanol. The *figure 3.13* shows CV's for (a) bare Pt or Au electrode; (b) PPy coated electrode and (c) PPy with $PdCl_2$ for methanol oxidation reaction. The electrochemical

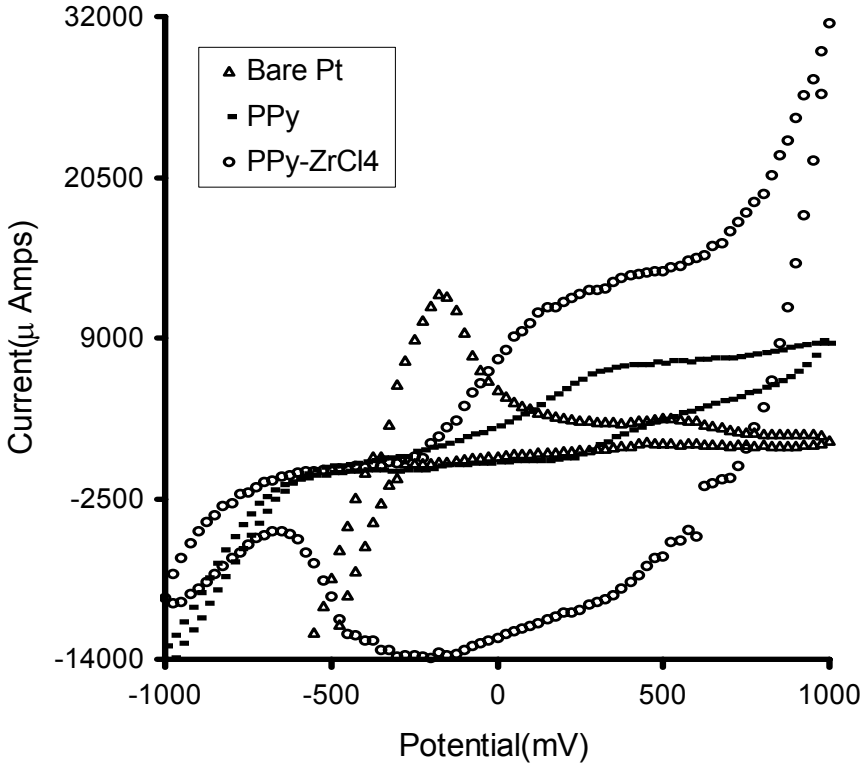

Figure 3.13 : CV's of electrochemical oxidation of methanol (0.1M) using bare Pt, PPy and PPy doped with $ZrCl_4$ electrodes

activity in these cases was clearly seen to enhance with the modification of electrodes as evidenced by enhancement of current. In order to identify the nature and origin of the

anodic current, the concentration of methanol (reactant) in the electrolyte was increased from 0.01 to 0.5 M and the CV was recorded for each using $PdCl_2$ doped PPy coated electrode as shown in *Figure 3.14.* It could be seen that there was a distinct peak appearing at 500mV (SCE) and the anodic current at this potential increased with the

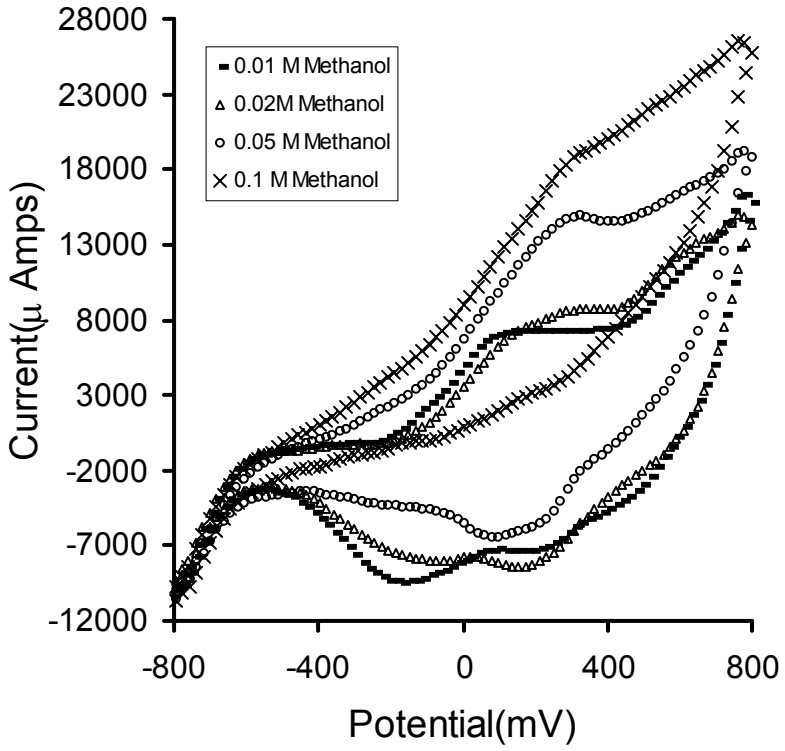

Figure 3.14: CV's of electrochemical oxidation of methanol using 0.006M $PdCl_2$ doped PPy electrode for varying concentration of reactant

increase in concentration of methanol. Thus anodic peak current at 500 mV is associated with the oxidation of methanol, which is in agreement with electro-oxidation potential reported for this reactant.

The CV's for PPy films doped with other dopants were also run to confirm the dependence of anodic current on reactant concentration in the electrochemical reaction.

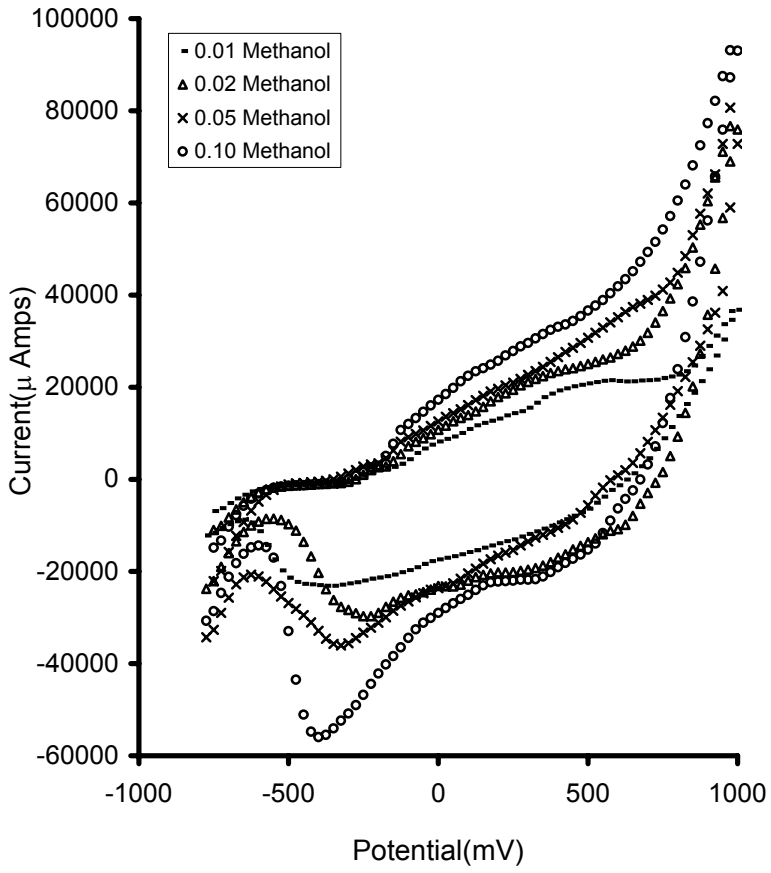

Figure 3.15: CV's of electrochemical oxidation of methanol using $ZrCl_4$ doped PPy electrodes for varying concentration of reactant.

CV's of the $ZrCl_4$ doped PPy shown in the *figure 3.15* and similar trend can be observed, i.e. anodic peak current at 500mV was dependent on the concentration of the reactant. It may be of interest to note that addition of methanol to the electrolyte may in fact increase its resistance and if there was no reaction, the current would reduce. However the current is increasing with MeOH concentration. [61-65]

3.3.2.2. Effect of doping agents in the PPy electrodes on the electrochemical Oxidation of Methanol.

As it was seen that PPy films modified by transition metal doping agents show good catalytic activity, it was essential to find out the most suitable dopant ion for the electro-oxidation of methanol. Further experiments were performed employing transition metal

salts of different electronegativities, e.g. $PdCl_2$, $CoCl_2$, $NiCl_2$ etc. as dopant for that purpose. From the CV's it could be seen that there was an increase in the anodic peak current when PPy films were in the doped state as compared to the undoped state, which was depicted in the *figure 3.16.* Tremendous increase in peak current for PPy films doped with $ZrCl_4$ electrodes followed by $PdCl_2$ doped electrodes was observed. If peak currents of PPy doped with different doping agents was correlated with electronegativity

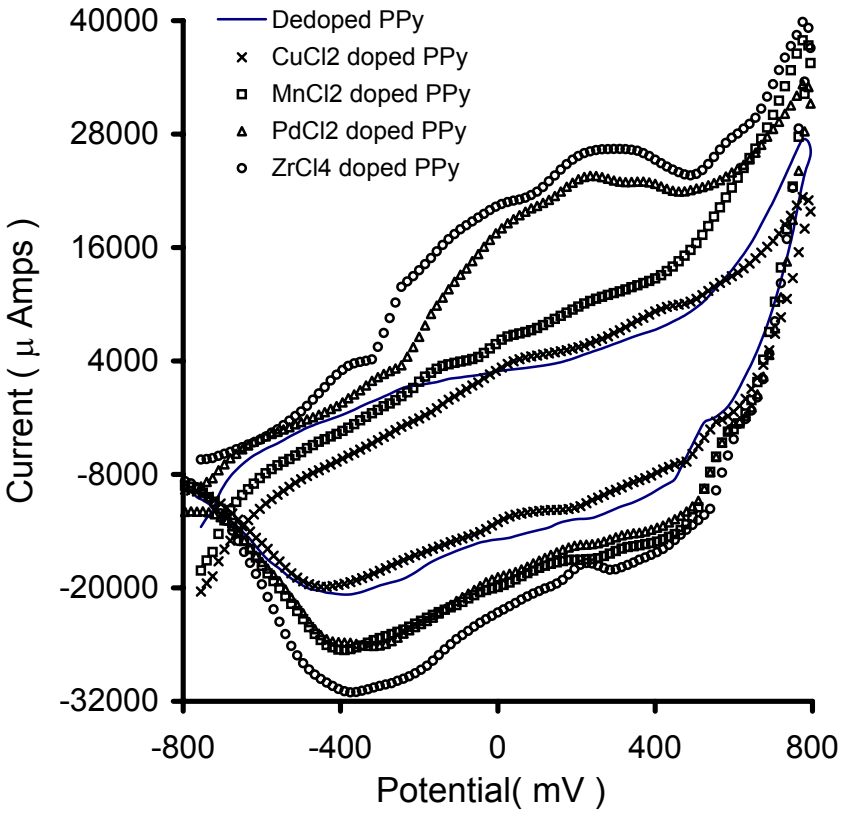

Figure 3.16: CV's of electrochemical oxidation of methanol (0.1M) using different PPy modified electrodes.

of the dopant ions and a graph of anodic peak current vs. electronegativity was plotted a relation could be seen which was shown in the *figure 3.17.* From the graph it could be seen that as the electronegativity of the dopant ion increased peak current decreased i.e., with increase in electronegativity catalytic activity decreases.

In order to investigate the reason for the better catalytic activity of the PPy doped with lower electronegative dopant ions towards methanol electrooxidation, energy level of the

each dopant ions with respect to PPy was calculated. Electrical properties of the PPy doped with different ions were measured in order to obtain the position of the impurity levels with respect to the valence / conduction band. From the temperature dependence of conductivity the activation energy (in eV) was estimated for each sample, which was

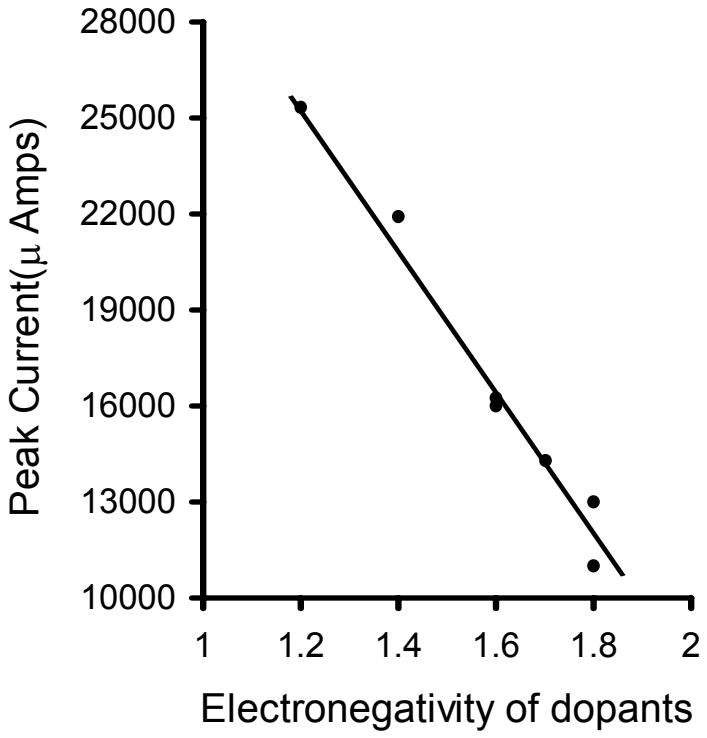

Figure 3.17: Graph of Peak current against electronegativity of the dopant ions

shown in the *Table 3.7*. The impurity doping level was placed above the uppermost valence level. The energy level representation for these electrodes with respect to PPy in contact with MeOH containing electrolyte and gold backing layer is shown in the *Figure 3.18.*

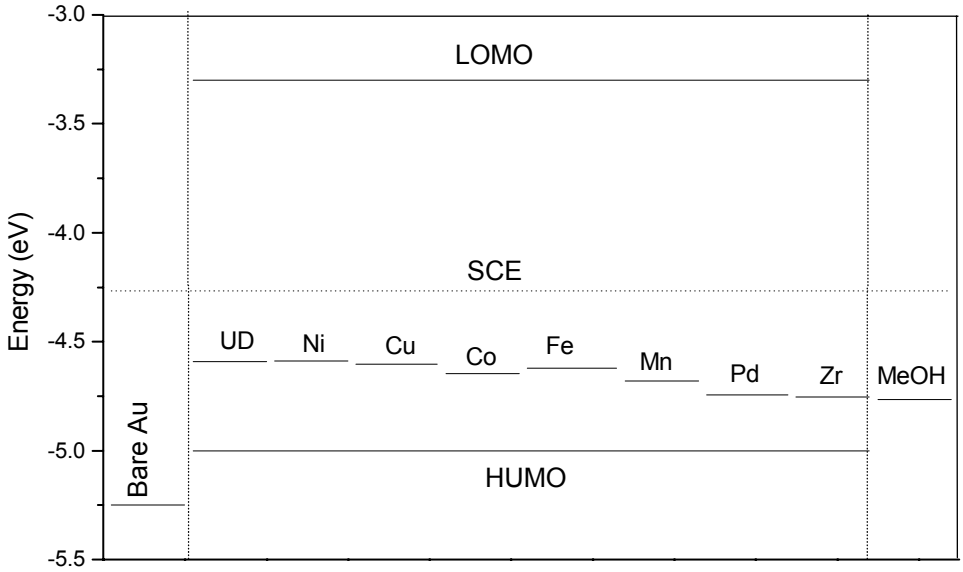

Figure 3.18: Energy level representation of PPy modified electrodes in contact with methanol

It could be seen from the energy level representation that for PPy doped with $ZrCl_4$ electrodes, it was easier for electrons to be transferred from the reactant methanol to the electrode than in other cases. The electron transport from electrolyte to electrode or hole transport from electrode to reactant leads to the oxidation of MeOH in presence of O_2.

$$CH_3OH + O_2 \xrightarrow{-e} HCOOH + H_2O, \text{ and so forth.....}$$
$$\text{and finally to } CO_2 \uparrow$$

In the methanol electrochemical oxidation reaction the primary rate determining step appears to be controlled by the charge transport at the anode. Hence, the energy level of the dopant in the polymer appears to be very important in the electro-oxidation process using conducting polymers.[66,67]

It was observed that the electrocatalytic activity towards methanol oxidation was dependent on the quality factor Q/R [Q is the percentage charge species calculated from the XPS data and R is the inter-chain separation obtained from the XRD data]. Quality

factor is defined as the charge transfer efficiency which is directly proportional to the charge in the polymer chain and is inversely proportional to the inter planer distance between the polymer chains. Data of quality factors of different dopants have been given in the *table no. 3.9.* It was observed that with the increase of quality factor of the dopants the catalytic activity towards methanol oxidation increased, graph of which was given in the graphs below. *Figure 3.19* and *figure 3.20* are the graphs of peak current vs. quality factors of different dopants calculated from C1s and N1s respectively. It was also observed that the quality factor was dependent on the electronegativity of the dopants, which was shown in the *figure 3.21* and *figure 3.22. Figure 3.21* and *figure 3.22* are the graphs of quality factors of different dopants calculated from C1s and N1s respectively vs. electronegativity of dopants.

Dopant Ion	Electro negativity	R Inter planner distance	Q (N) = N2+N3	Q/R (From N1s)	Q(C) = C2+C3	Q/R (From C1s)	Peak Current (m Amps)
$ZrCl_4$	1.2	4.28	70.4	16.45	61.13	14.28	25.35
$PdCl_2$	1.4	4.2	69.7	16.6	60	14.29	21.9
$FeCl_3$	1.6	4.31	62.36	14.46	53.78	12.47	16.2
$MnCl_2$	1.6	4.41	60.58	13.75	53.35	12.11	16.25
$CoCl_2$	1.7	4.346	59.1	13.60	50.2	11.55	14.3
$NiCl_2$	1.8	4.363	54.05	12.39	54.54	12.5	13
$CuCl_2$	1.8	4.363	53.05	12.16	52.81	12.1	11

Table 3.9: Table of quality factors of different dopants

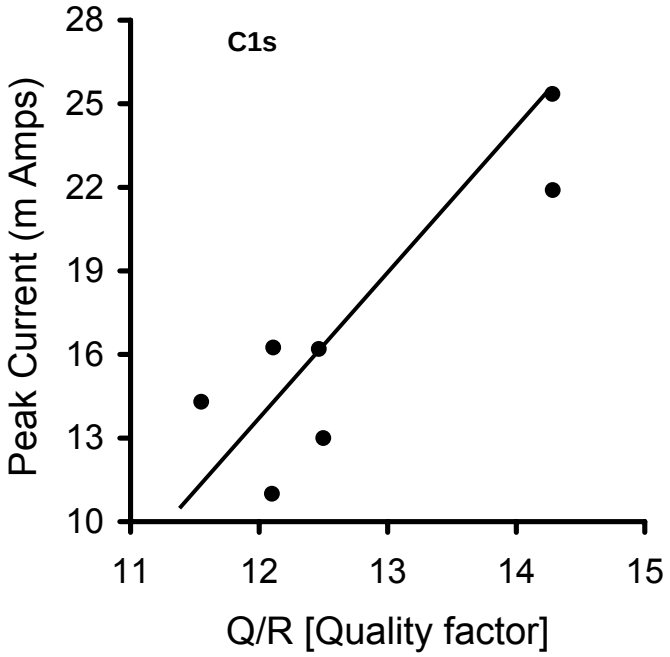

Figure 3.19: Graph of peak current for methanol oxidation vs. quality factor

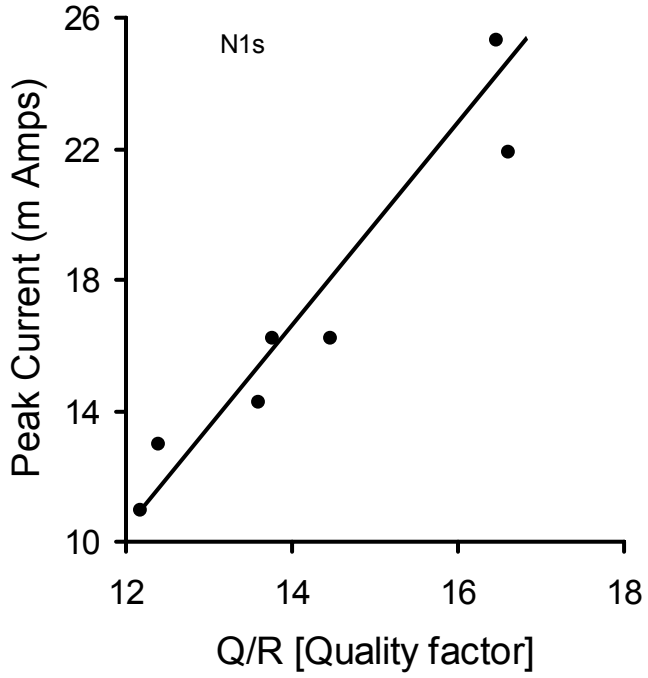

Figure 3.20: Graph of peak current for methanol oxidation vs. quality factor

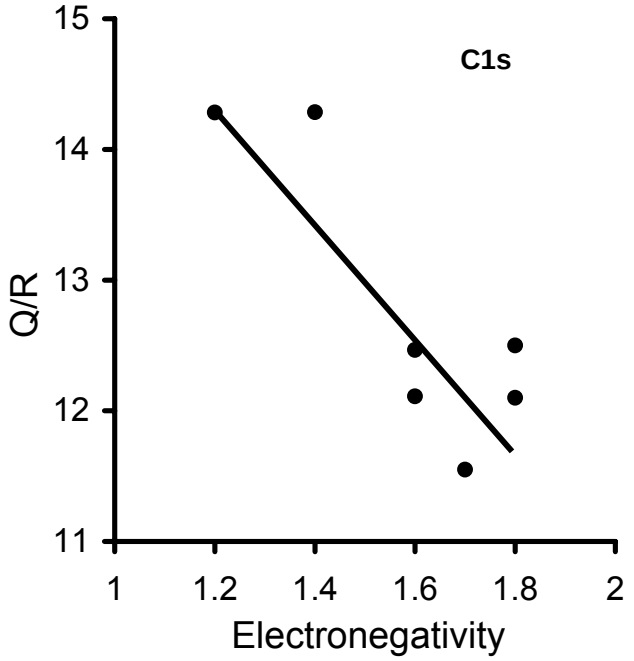

Figure 3.21: Graph of Q/R vs. electronegativity of the dopants

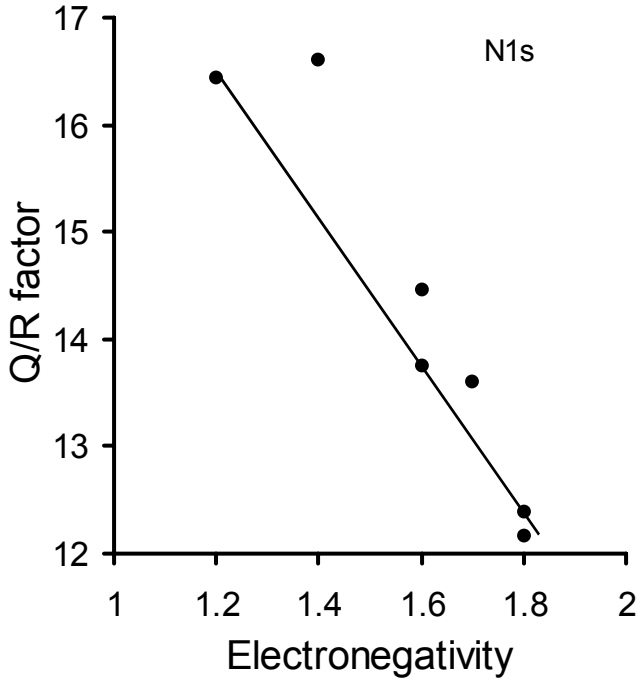

Figure 3.22: Graph of Q/R vs. electronegativity of the dopants

It was clear from the energy level representation that the charge transport process plays an important role in the electro-catalytic oxidation of methanol using different modified PPy electrodes. Further studies were carried out to find out the best dopant ion concentration of various doping agents. For that purpose PPy films doped with varying concentrations of doping agents were employed as working electrodes. Dopant ion concentration was varied from 0.003M, 0.006M, 0.009M 0.012M, 0.02M. *Figure. 3.23* represents the CV's of PPy doped with various concentrations of $PdCl_2$ electrodes. CV's of other dopant ions viz. $NiCl_2$, $CuCl_2$, $FeCl_3$ etc were also run but not shown. The undoped PPy also showed some catalytic activity towards methanol oxidation but when these were doped with different concentration of $PdCl_2$, tremendous jump in the catalytic activity was observed which was evident from the *figure 3.23.* From the CV's it could be observed that for PPy electrodes doped with 0.006M showed maximum electro-catalytic activity among various concentration of dopant ion $PdCl_2$. A graph of peak current against various concentrations of dopant ions for PPy doped with $PdCl_2$ and $ZrCl_4$ are plotted which is shown in the *figure 3.24.* From the graph it could be seen that for both the dopant ions 0.006M is the optimum concentration i.e. 0.006M doped PPy showed maximum catalytic activity. Earlier some groups had shown that in case of polyaniline catalyzed reactions catalytic activity increased with the increase of protonic acid doping.[68,69] However, here in the present study it could be seen that there was an optimum concentration for methanol oxidation and further increase in the dopant ion conc. results in the decrease in the catalytic activity. These findings can be explained on the basis of the various processes involved in catalytic activity of the electrode; adsorption of the reactant and /or oxygen, charge transfer at the interface, redox process. The number of available sites on the catalyst will play crucial role in deciding the maximum activity. For a given number of sites, there will be optimum concentration of the reactant for which maximum yield is obtained. Thus, the dopant concentration and reactant that can be adsorbed will lead have to be optimum for maximum yield.

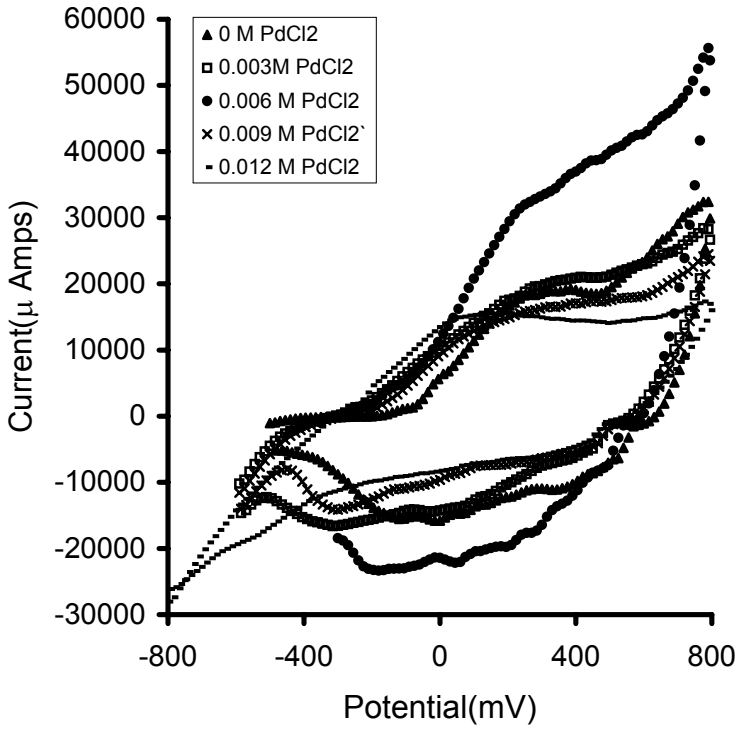

Figure 3.23: CV's of electrochemical oxidation of methanol using different $PdCl_2$ doped PPy electrodes

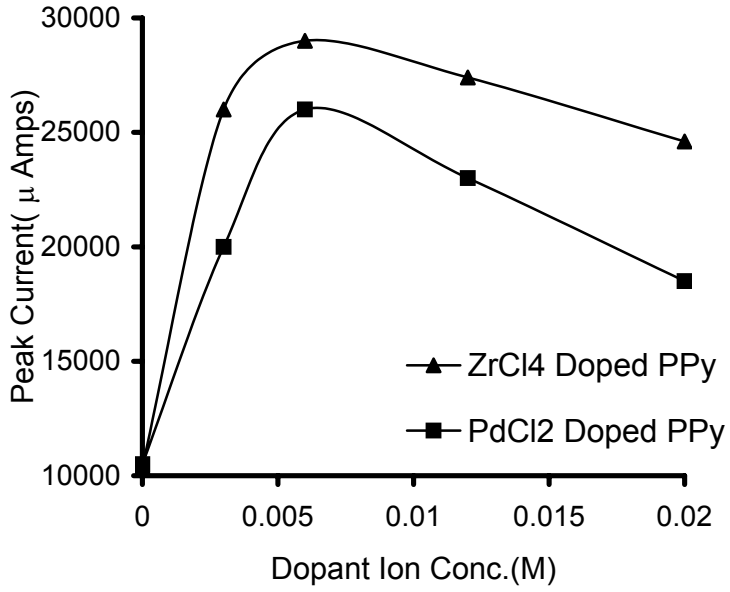

Figure 3.24: Graph of peak current for methanol oxidation vs. dopant ion concentration of $ZrCl_4$ and $PdCl_2$ doped PPy electrodes.

3.3.2.3. Estimation of conversion of methanol in electrooxidation.

The overall electro-catalytic oxidation of methanol is given below,

$$CH_3OH + H_2O \longrightarrow CO_2 + 6H^+ + 6e^-$$

which is six electron transfer process, details of which is described in the chapter I.

Since the electrooxidation of MeOH will depend on the amount of charge transferred, the percentage conversion can be estimated from the total charge consumed. Percentage methanol conversion per minute to the product was calculated using Faraday's equation. Details' regarding calculation is illustrated schematically in the chapter II. Percentage methanol conversion is given in the **table no 3.10**

Deposition time (sec)	Percentage conversion
50	8.1
75	11.6
100	13.7
125	17.3
150	18.8
200	28.6

Temperature (°C)	***Percentage conversion***
10	23.1
25	31.2
40	33.6
50	37.7

Scan Rate (mV/s)	Percentage conversion
25	16.6
33	22.8
40	24.8
50	31.8
66.6	34.6
100	51.2

Electrode (Exsitu doped)	**Percentage conversion**

Dedoped PPy	4
$ZrCl_4$ doped PPy	17.5
$PdCl_2$ doped PPy	15.2
$MnCl_2$ doped PPy	11.3
$FeCl_3$ doped PPy	10.5
$CoCl_2$ doped PPy	9.9
$NiCl_2$ doped PPy	9
$CuCl_2$ doped PPy	7.6

Electrode (Insitu doped)	**Percentage conversion**
$ZrCl_4$ doped PPy	43.9
$PdCl_2$ doped PPy	8.3
$MnCl_2$ doped PPy	27.7
$FeCl_3$ doped PPy	24.9
$CoCl_2$ doped PPy	31.5
$NiCl_2$ doped PPy	29.8
$CuCl_2$ doped PPy	29.4

Table 3.10: Tables of percentage conversion of methanol in the electrocatalytic oxidation reaction

It could be seen from the table that for bare platinum electrode which is normally taken as standard electrode percentage methanol conversion is 5 % per minute while incase of PPy modified with different techniques better methanol conversion was observed. The percentage methanol conversion to the product for PPy doped externally with $ZrCl_4$ is 17.5% per minute whereas for insitu doped one it is 43.95% per minute.

3.3.2.4. Kinetic study of Methanol electrochemical oxidation.

Varying methanol concentration

Kinetics of methanol electrooxidation was studied by plotting Tafel plots. CV's of PPy doped with 0.006M $PdCl_2$ electrodes for varying methanol concentration were used to

plot Tafel plot. In the entire concentration range the reaction rate increased with increasing methanol concentration

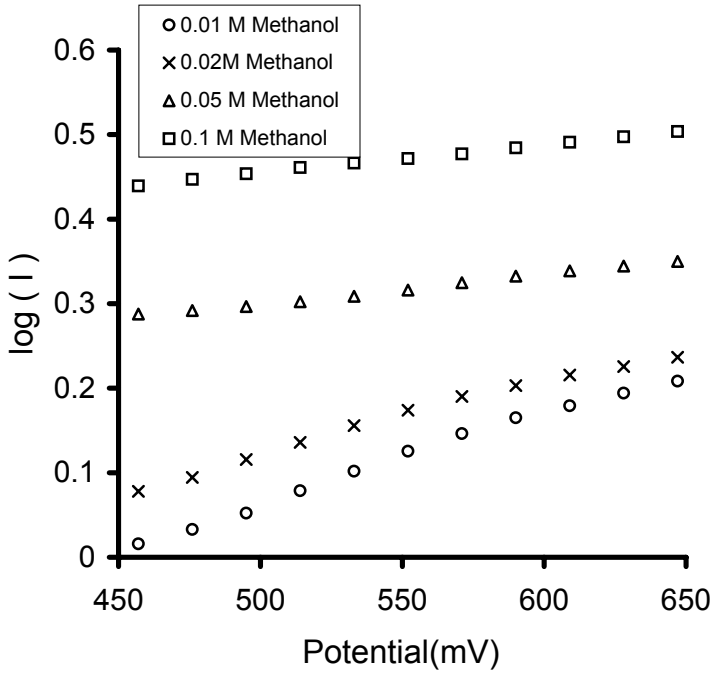

Figure 3.25 : Graph of log I vs. potential for methanol electrochemical oxidation

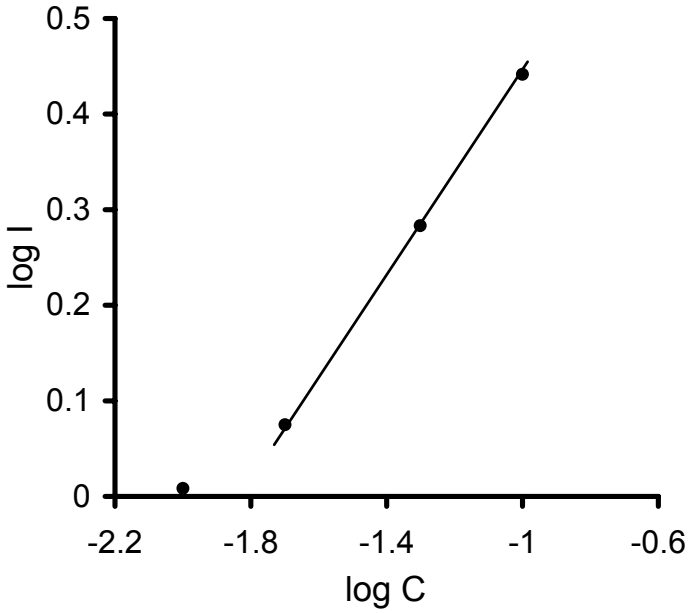

Figure 3.26: Graph of log I vs. log C

Figure 3.25 is the graph of log I (mA/cm^2) against potential in the anodic potential range for different concentrations of methanol in the electrolyte. Potential range taken for plotting Tafel plot is 450mV to 650mV. From the plot of log I vs. potential, intercepts of the straight lines was found out. Then graph of log I vs. log C (concentration in mole) was plotted and slope of the straight line obtained was found out. Graph of log I vs. log C is shown in the *figure 3.26*. Slope of the straight line is found out to be 0.52, which implies that methanol oxidation follows half order kinetics with respect to methanol. The same value was reported by Bagotzky et al for smooth Pt and Pt black and by Gojkovic et al for carbon supported PtRu electrodes.[70,71]

Temperature variation

Effect of temperature on the oxidation of methanol was also studied. Temperature dependence reaction was carried out also to study kinetics of the reaction. Various temperatures of the reactions were 10°C, 25°C, 40°C and 50°C. From the CV's dependence of peak current with temperature was observed, i.e. electro-catalytic activity of the electrodes toward methanol oxidation increases with temperature of the reaction. This could be due to the availability of the dissolved oxygen. Blais et al had studied temperature dependence of the electro-oxidation of the irreversibly chemisorbed As on the Pt(111) electrodes. They had suggested that an increase in temperature led to charge distribution, both on the anodic and cathodic sides. On the anodic side peak current decreased and broadened, whereas on the cathodic side the change was less dramatic.[72] Whereas Schmidt et al. had studied temperature effect on the formic acid oxidation on Pt(111) and Pt(111)/$Bi_{irrev.}$ They had suggested that with the increase in temperature, rate of the reaction increased and hence rise in the peak current was observed. They had suggested that with the increase in temperature the adsorption of OH_{ad} increased, which was the crucial step in the electro-oxidation for formic acid oxidation.[73] In case of methanol oxidation also OH_{ad} was the crucial step. Here in our study, with increase in the temperature OH_{ads} might increase and resulting in the increase in the rate of oxidation reaction. Fiçicioğlu et al had studied temperature effect on electro-oxidation of methanol on platinum doped polyaniline electrode, who reported an increase in the rate of electro-oxidation with temperature.[74]

Kinetics of the methanol electrooxidation was also studied with the help of temperature variation electrochemical reaction. From the temperature dependence cyclic voltammograms log current vs. potential was plotted which is shown in the *figure 3.27*. Intercepts from the above graph is found out and log I vs. 1/T is plotted using these datas which is given in the *figure 3.28*. With the help of the slope obtained from the above mentioned plot activation energy for methanol electrooxidation was calculated using Arrhenius equation. Activation energy for methanol electrooxidation was found out to be 0.24eV.

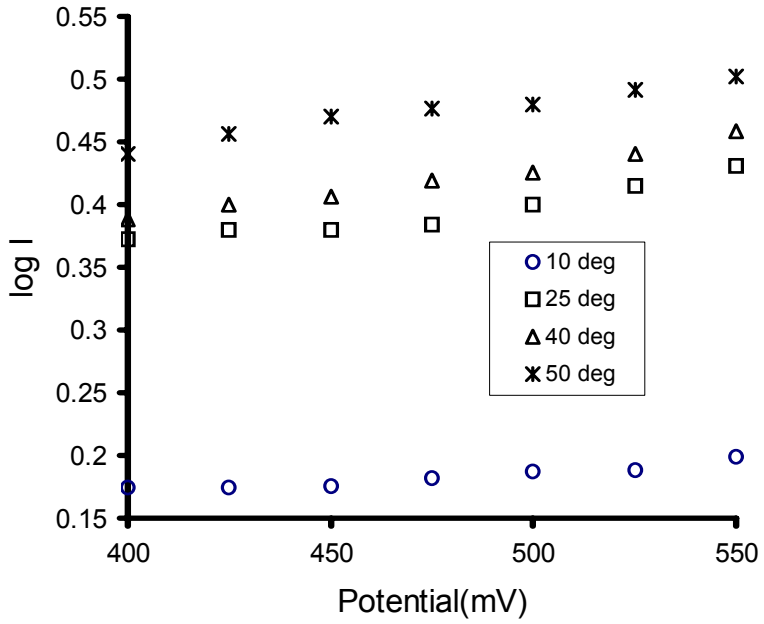

Figure 3.27: Graph of log I vs. Potential for methanol electrochemical oxidation at different temperature

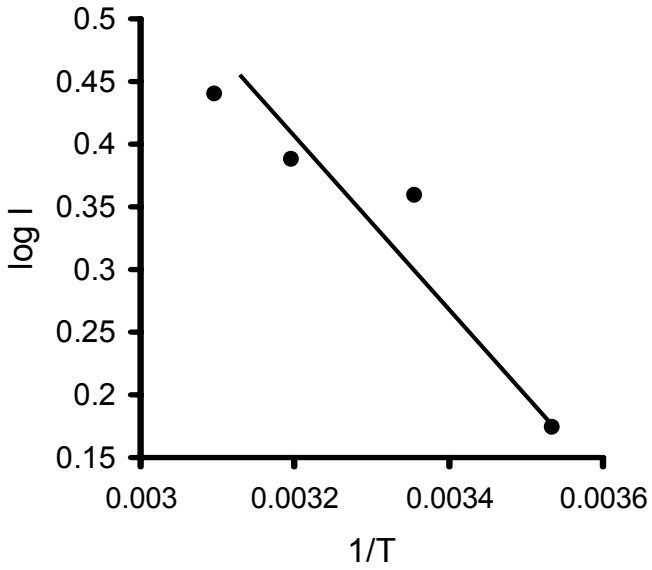

Figure 3.28: Graph of log I vs. 1/T for methanol electrochemical oxidation reaction

3.3.3. Modification of PPy electrodes by different techniques.

It has been observed that conducting PPy electrodes externally doped with different transition metal dopant ions are effective in the electrocatalytic oxidation of methanol. Hence, further modification of conducting polymer electrodes was necessary to improve the electrocatalytic activity towards methanol electrooxidation. Modification of the electrodes were done by,

3.3.3.1. Insitu doping

Conducting PPy electrodes modified by doping internally with different dopant ions i.e. insitu doped PPy electrodes were employed to study the electrocatalytic activity of methanol oxidation. CV's for different insitu doped PPy films were shown in the *Figure 3.29.*

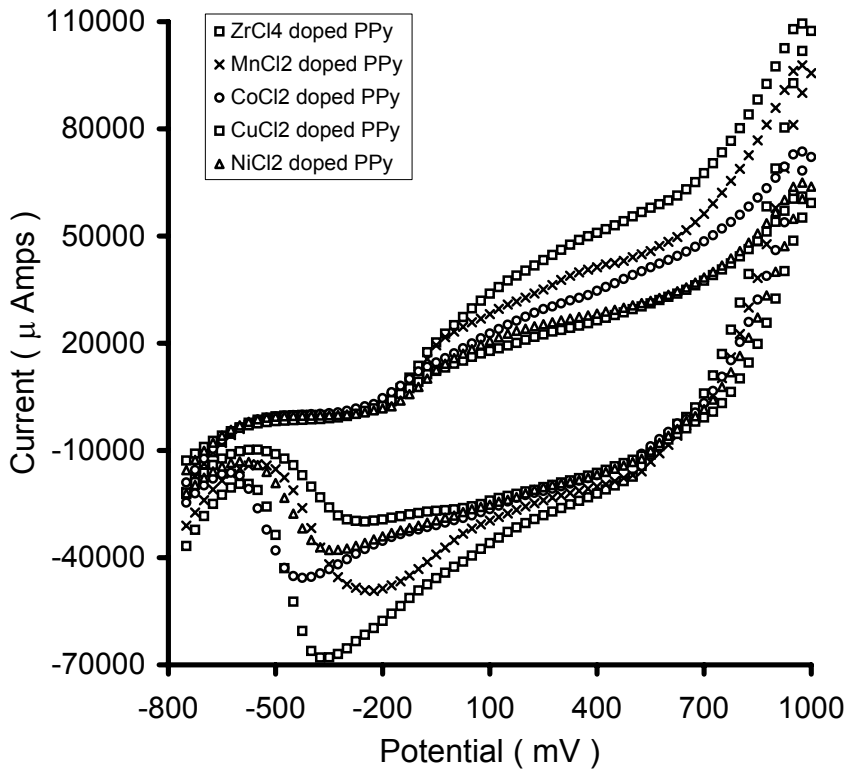

Figure 3.29: CV's of electrochemical oxidation of methanol (0.1M) using insitu doped PPy electrodes

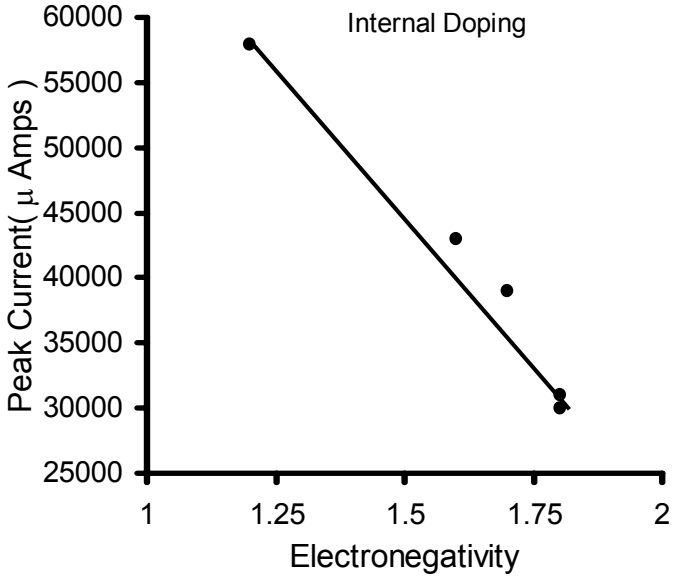

Figure 3.30: Graph of peak current vs. electronegativity of the dopants for insitu doped PPy electrodes

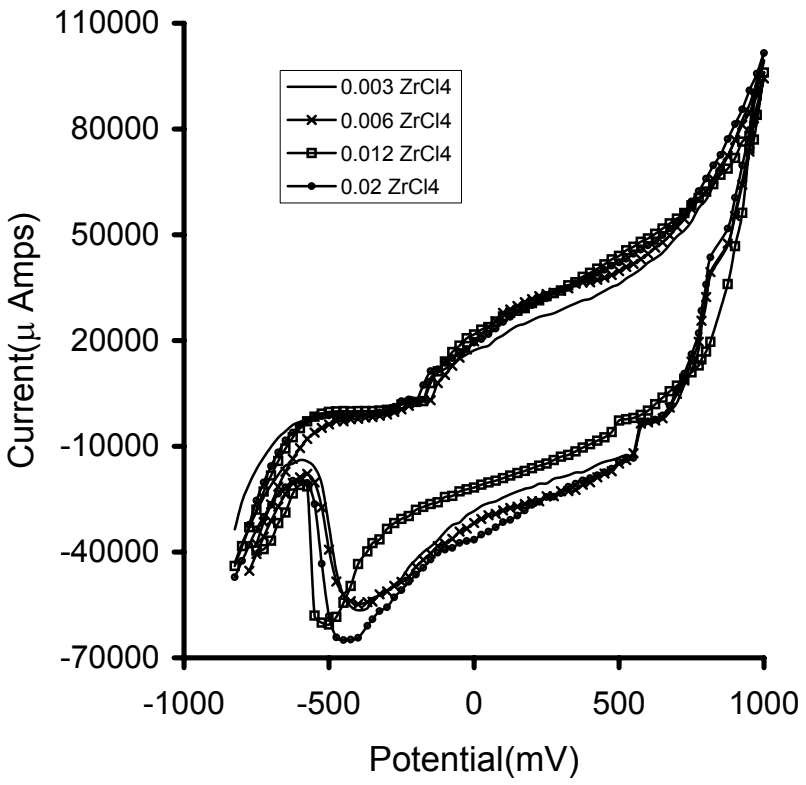

Figure 3.31: CV's of electrochemical oxidation of methanol (0.1M) using different doping concentration of insitu doped $ZrCl_4$-PPy

From the CV's similar trend as shown by the external dopant was observed i.e. PPy insitu doped with lower electronegative dopants viz. $ZrCl_4$ showed maximum catalytic activity, whereas for higher electronegative dopant it is the least, graph for which is shown in the *Figure 3.30*. Cyclic voltammetry study of PPy films insitu doped with various concentration of $ZrCl_4$ (0.003M, 0.006M, 0.012M, 0.02M) in 0.1M methanol concentration were also run which was presented in the *Figure 3.31.* CV's for other dopant ions were also run but not shown here. Graph of peak current as a function of concentration of $ZrCl_4$ dopant ion for both exsitu doped and insitu doped electrodes are shown in the *Figure 3.32.* It was observed from the graph that insitu doped samples are much more electrocatalytically active than the exsitu samples. It was also observed that for insitu doped PPy, 0.012M dopant concentration gave maximum catalytic activity towards methanol oxidation whereas for exsitu one it was 0.006M dopant concentration.

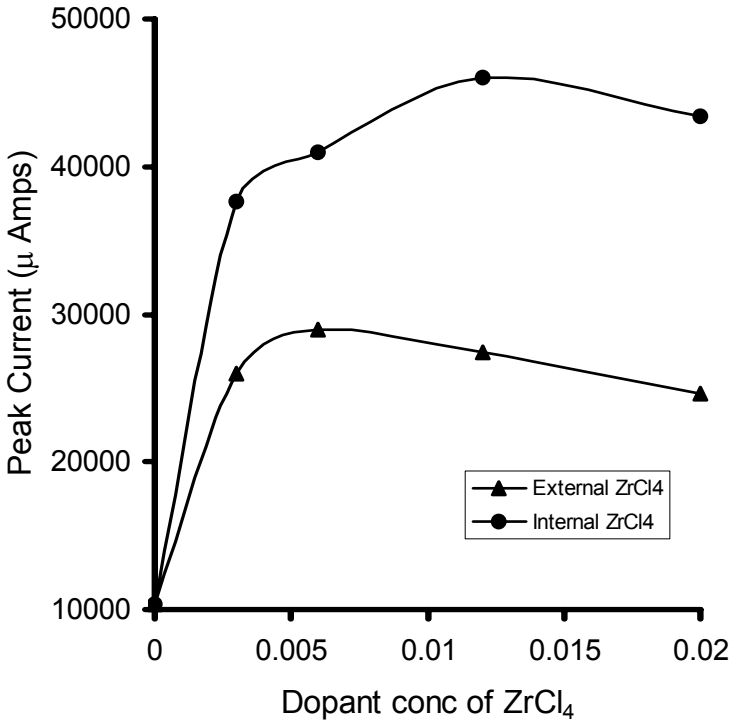

Figure 3.32: Graph of peak current for methanol using insitu and exsitu $ZrCl_4$ doped PPy electrodes

In order to bring out the differences in the PPy samples doped externally and those prepared by insitu doping method detailed studies were carried out with XRD, UV-Vis, IR, and XPS techniques.

XRD study

The in situ doped PPy polymers were synthesized by first making a complex between pyrrole and the dopant ion. It was noticed that such a complex formation not only takes place but it also fairly stable prior to electrochemical polymerization. This was evidenced by crystallizing out the complex from the solution and recording XRD scan at various intervals. *Figure 3.33* shows the XRD scans for the complex of pyrrole –$ZrCl_4$ taken at (b) 24 hrs and (c) 140hrs. The XRD for $ZrCl_4$ alone and PPy doped with $ZrCl_4$ are also shown for comparison. It is clearly evident that a complex is formed. The XRD pattern of pyrrole with $ZrCl_4$ having entirely different crystal structure as compared to original $ZrCl_4$ or the amorphous PPy polymer. This complex was used for subsequent

electrochemical polymerization, which took place within few minutes. Hence, the stability of the complex prior to ECP was established.

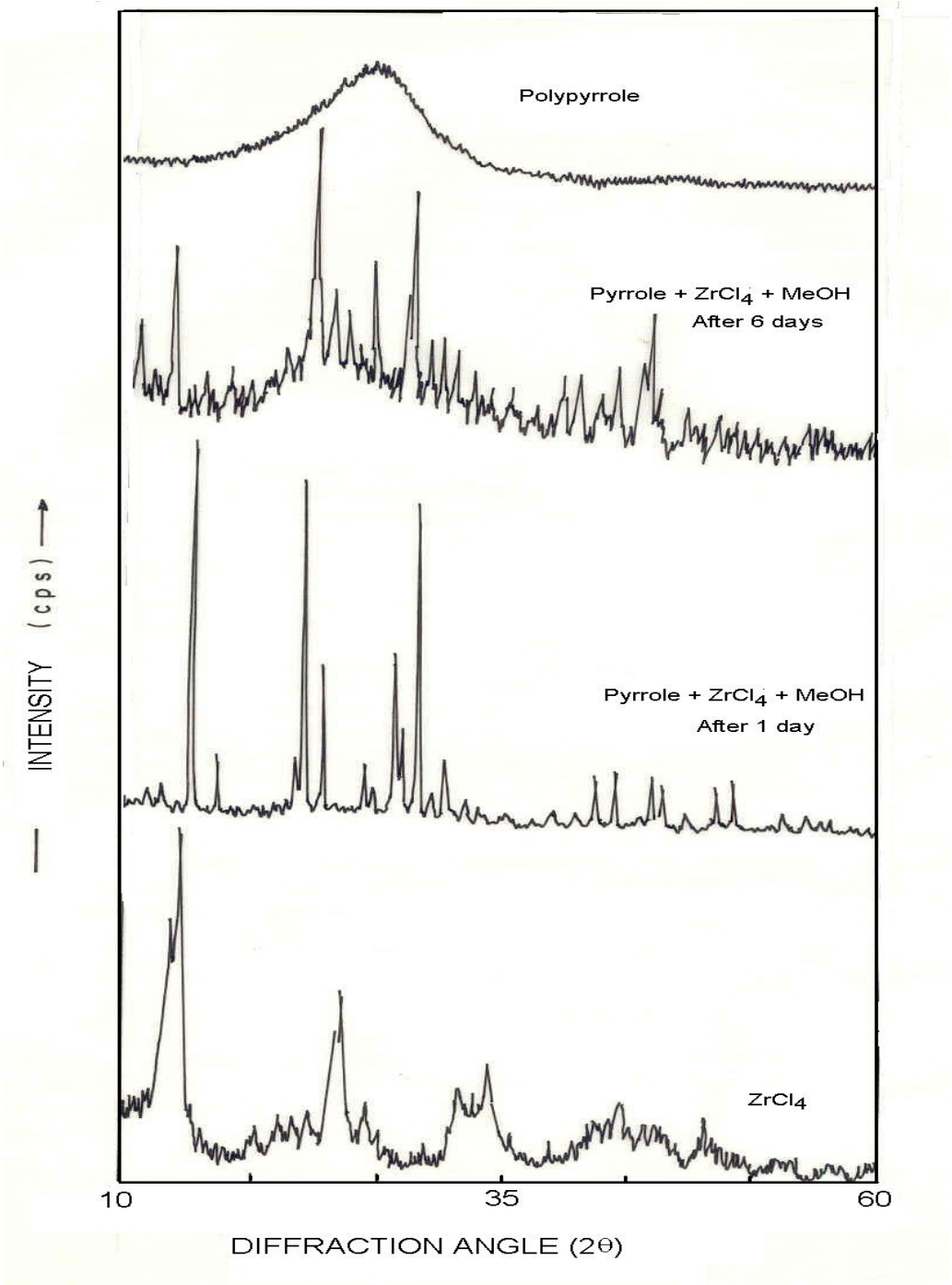

Figure 3.33: XRD of reaction of pyrrole and ZCl_4 in methanol at different time intervals

UV-Vis studies

UV visible spectra were run for the confirmation of complex formation prior to insitu doping of polypyrrole. The UV-Vis spectra of solution of $ZrCl_4$ + pyrrole in methanol

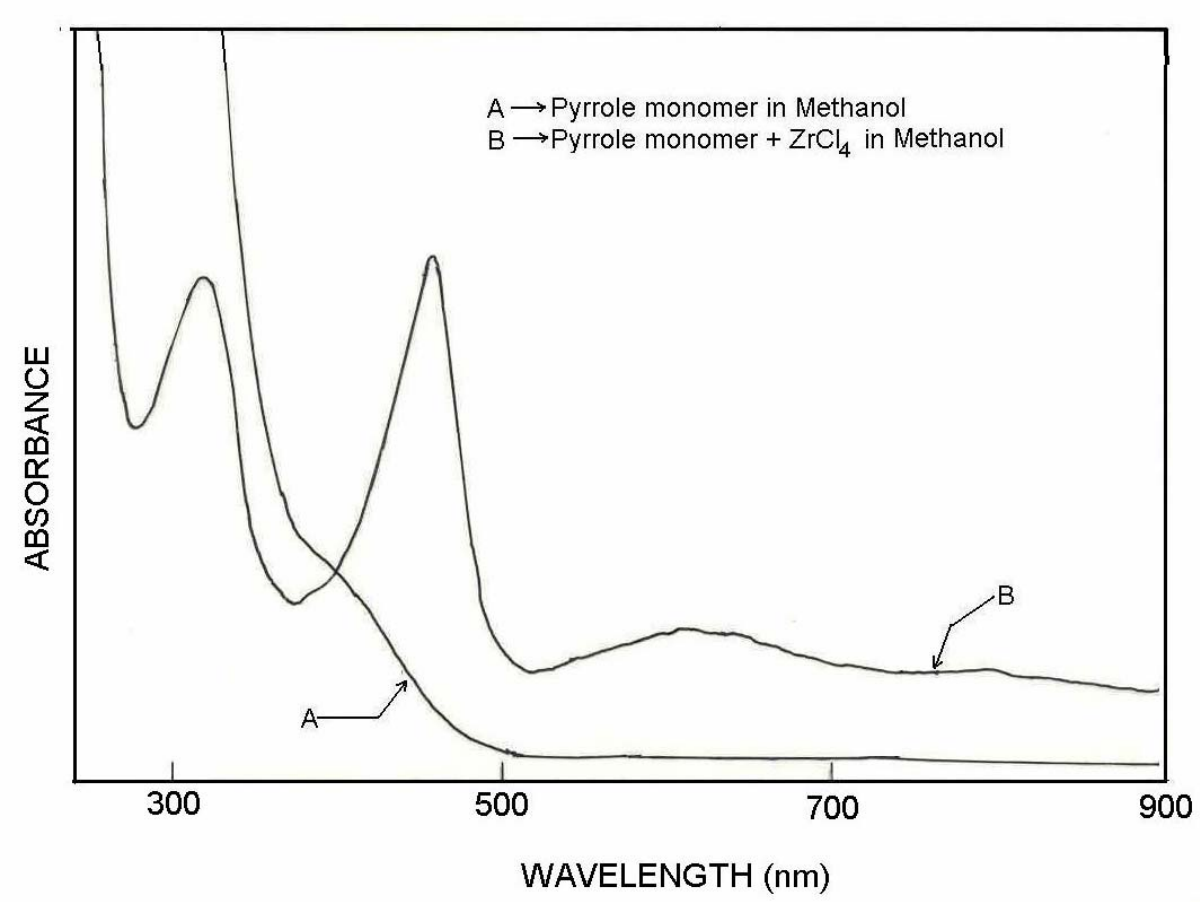

Figure 3.34: UV-Vis spectra of complex formation reaction

together with pyrrole solution alone is shown in the *figure 3.34.* It could be seen that for pyrrole-ZrCl4 complex the new peaks at 300nm, 450nm and 600 nm were observed whereas only the UV region absorption is seen in case of pyrrole.75

FT-IR studies

For the confirmation of complex formation during insitu doping of polypyrrole with $ZrCl_4$, IR spectra for solutions of the mixture of $ZrCl_4$ and pyrrole in methanol for various

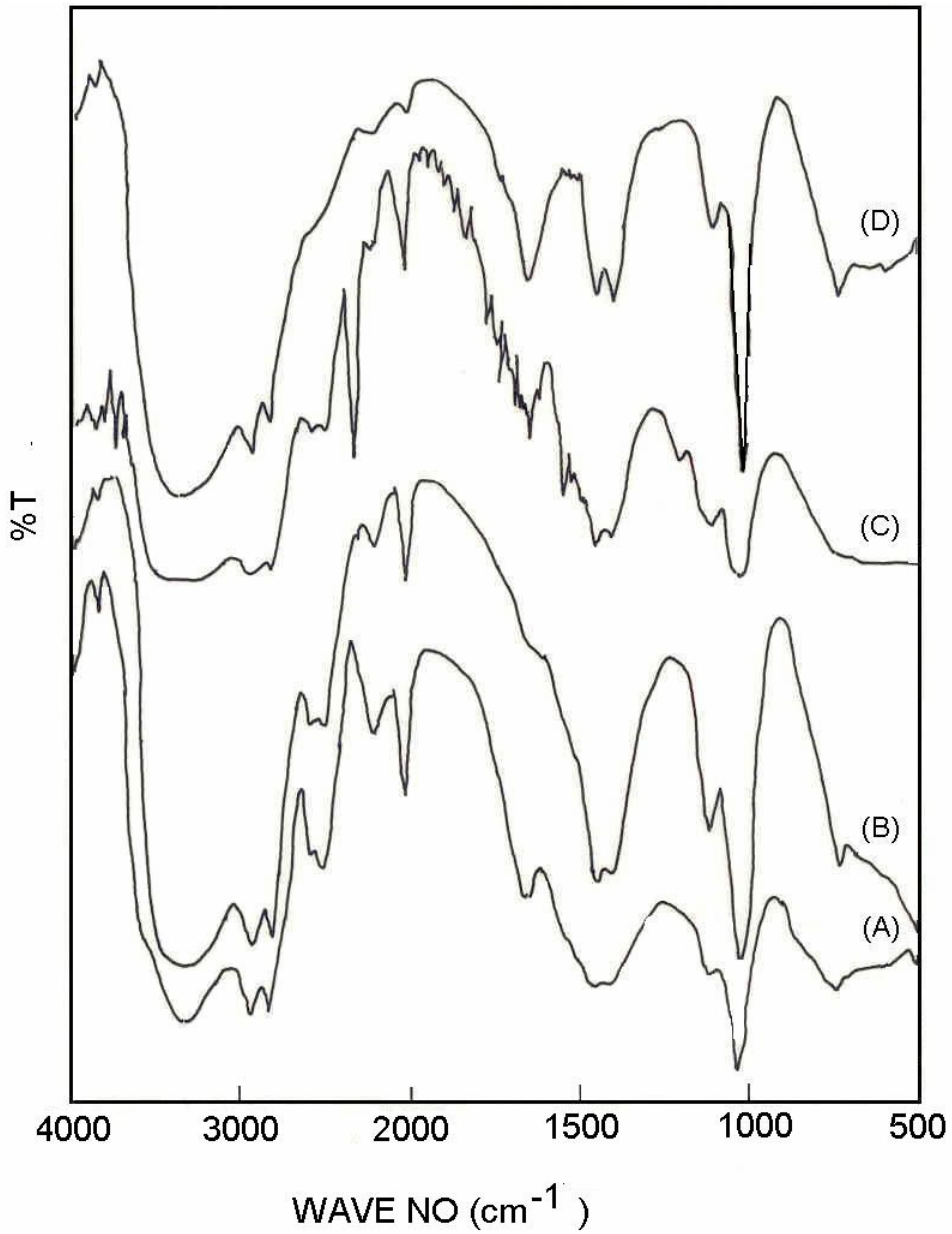

Figure 3.35 : FT-IR of complex formation reaction[(A)Pyrrole(Py)+MeOH, (B)Py+MeOH+$ZrCl_4$ (3hrs), (C) Py+MeOH+$ZrCl_4$ (2 days) (D) PyMeOH+$ZrCl_4$ (3 days)]

time intervals was run. IR spectrogram of various time intervals (3hrs, 36hrs and 72hrs are shown here) was shown in the *figure 3.35*. The IR assignment table for these was given in the *table no 3.11*

IR peak positions	*Assignment*	**Pyrrole+ methanol**	**Pyrrole+ $ZrCl_4$ in methanol**		
			3hrs	**36hrs**	**72hrs**
736	CH_2-NH-CH_2	w	w	vw	w
1028	C-N stretching	s	vs	s	vs
1114	CH_2-NH-CH_2	w	m	m	m
1417	O-H bending	br	s	s	s
1653	N-C=N,C=N, Primary amine	w	vw	m	s
2040		s	s	s	w
2221	C=C	s	m	m	w
2521	CH_2-CH_2	s	m	m	w
2833	C-H stretching (CH_2)	m	m	br	m
3330	-NH Stretching	br	br	br	br

Table 3.11: Table of IR assignments for the peaks of the spectra of different time intervals

In the figure it could be seen that peak at 1028 cm^{-1} is very small in case of only pyrrole in methanol, but the peak becomes sharp in case of solutions of pyrrole and $ZrCl_4$ mixture in methanol. It could also be seen that intensity of the peak gets sharper and prominent after 72 hours. Peak at 1028 cm^{-1} is due to the C-N stretching. For the solution of 36 hours, distinct difference in the peak positions, their size, shape and intensity is observed. Peak in the 1417 cm^{-1} is due to the O-H bending which is broad in the pyrrole methanol mixture whereas it becomes sharp in the initial stage and at 36 hrs and 72 hrs the peak become separated and small distinct peak is seen. This may be due to the O-H of reaction medium methanol. Peak in the region 1653 cm^{-1} is due to N-H bending which becomes prominent after 36 hours of reaction. Peak at 3330cm^{-1} is due to N-H symmetric stretching.

XPS studies

It has been confirmed from the UV-Vis, XRD, IR studies that prior to electrochemical insitu polymerization complex of pyrrole with dopant ions take place. Further, XPS was

also run for the confirmation of complex formation prior to insitu doping of polypyrrole. For that $ZrCl_4$ and pyrrole solution was prepared in methanol. Initial colorless solution turns to green after sometime. This solution was allowed to evaporate at room temperature to get crystals. XPS of this crystal was run. The deconvoluted XPS graphs of C1s, N1s, Cl2p and Zr core level were shown in *the figure 3.36*.

In the C1s core level spectrum, unlike spectrum of different doped PPy powders which is described in the earlier part of this chapter, the shape of the spectrum was symmetric, which is due to the absent of 'disorder effect'. Disorder effect is generally found in the polymer samples. Peak position, FWHM and percentage area of deconvoluted components of C1s and N1s is given in the *table 3.12.* and *3.13.*

It can be noted from the *table 3.12* that the splitting between α and β carbon is found to be 1.25eV, whereas various reports say the energy separation of α and β carbon for pyrrole monomer as well as polypyrrole polymer to be around 0.9eV. This observed α and β carbon splitting value disagree with the reported values. This higher splitting value might be attributed to the formation of highly charged environment at carbon and due to which carbons get shifted to the higher energy value. It could be observed from the table for C1s core level spectrum that the percentage of charged species is quite high. The percentage contribution of the deconvoluted peak appearing at 285.85 eV is 49.23% whereas for the peak appearing at 287.1 eV is 12.3%.

Complex of $ZrCl_4$-Pyrrole in methanol			
Carbon	**Peak positions**	**FWHM**	**% Area**
C1(α)	284.6	1.5	38.46
C2(β)	285.85	1.62	49.23
C3	287.1	1.5	12.3

Table 3.12: Table of C1s core level spectra of the pyrrole –$ZrCl_4$ complex

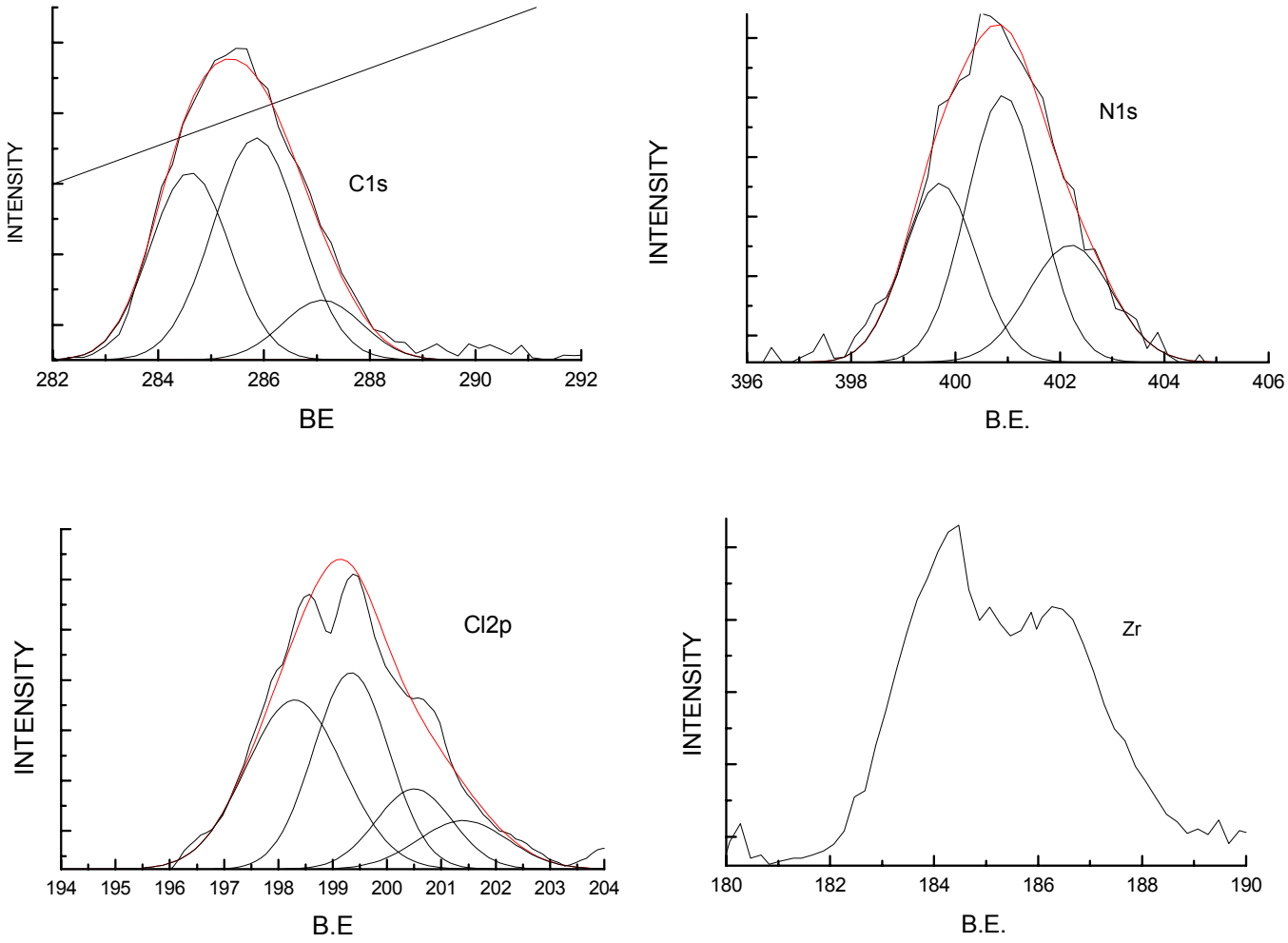

Figure 3.36: XPS of the different core levels of C1s, N1S, Cl2p and Zr

In case of N1s core level spectrum the percentage of charged species is quite high. The percentage contribution of the deconvoluted peak appearing at 400.95 eV is 46.41% and for the peak at 402.2 eV is 23.04% which are due to –NH– and $–N^+$ respectively.

Complex of $ZrCl_4$-Pyrrole in methanol			
Nitrogen	**Peak positions**	**FWHM**	**% Area**
N1	399.7	1.38	30.54
N2	400.95	1.4	46.41
N3	402.2	1.58	23.04

Table 3.13: Table of N1s core level spectra of the pyrrole –$ZrCl_4$ complex

Complex of $ZrCl_4$-Pyrrole in methanol			
Cl_{2p}	**Peak position**	**FWHM**	**% area**
Cl_1	198.3	1.78	39.27
Cl_2	199.34	1.39	35.6
Cl_3	200.5	1.4	14.7
Cl_4	201.4	1.65	10.47

Table 3.14: Table of Cl2p core level spectra of the pyrrole –$ZrCl_4$ complex

It could be observed from the XPS core level spectrum of Zr of the complex that peak is broad. The peak position separation for 3d5/2 and 3d3/2 is also high as compared to the reported. The peak positions of 3d5/2 and 3d3/2 are 184.43 eV and 186.39eV respectively. [76-78]

To make a comparative study of electrocatalytic activity of the insitu doped electrodes with exsitu ones, CV's for PPy insitu as well as exsitu doped with $ZrCl_4$ along with undoped PPy films were run for methanol electrooxidation, which is shown in the *figure 3.37.*

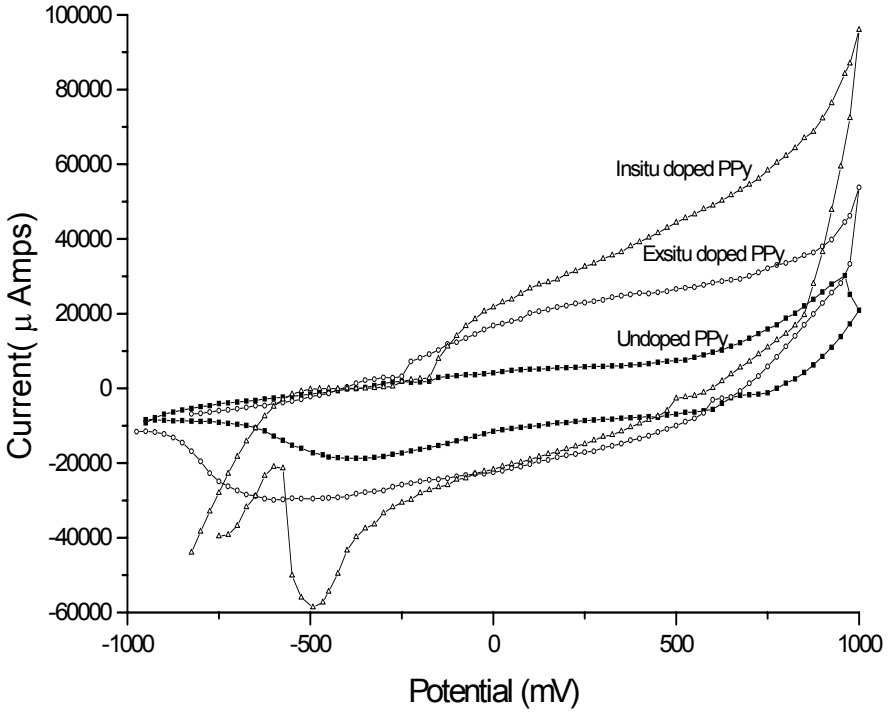

Figure 3.37 : CV's of electrochemical oxidation methanol (0.1M) using undoped PPy, exsitu doped and insitu doped PPy electrodes.

Name of Doping Agents	Peak Current (Amps)	
	Externally doped PPy	Internally doped Ppy
$ZrCl_4$	25350	63500
$PdCl_2$	21900	-
$FeCl_3$	16250	-
$MnCl_2$	16000	40000
$CoCl_2$	14300	45500
$CuCl_2$	13000	42500
$NiCl_2$	11000	43000

Table 3.15 : Table of Peak currents of electrochemical oxidation of methanol using exsitu and insitu doped PPy electrodes

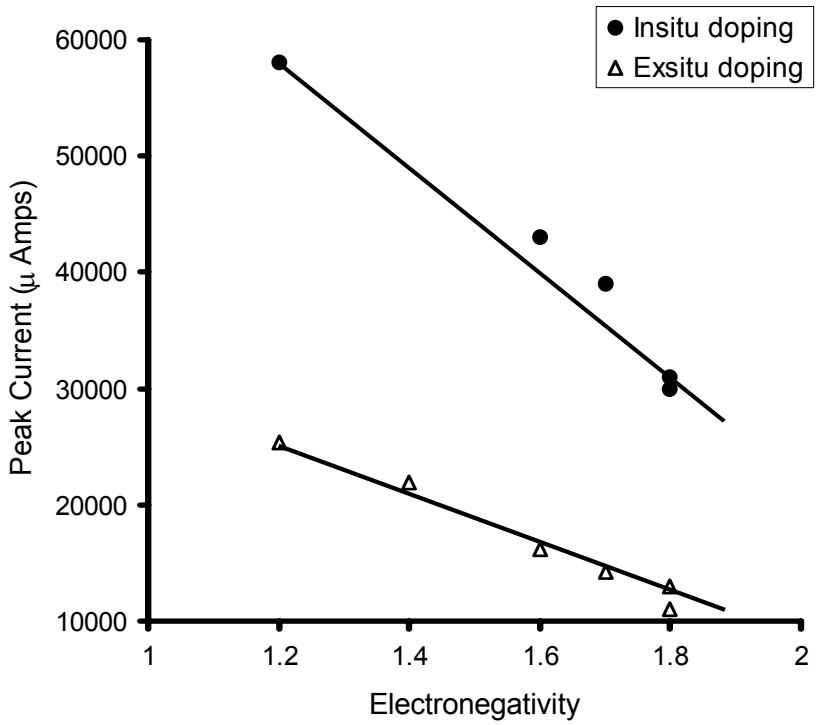

Figure 3.38: Graph of peak current for the electrochemical oxidation of methanol using insitu and exsitu doped PPy electrodes vs. electronegativity of dopants

It was seen from the CV's that there was tremendous increase of current in the anodic region when internally doped PPy films were used, whereas there was slight change in case of externally doped PPy as compared to the undoped film. Table of peak current of various insitu and exsitu doped PPy for methanol oxidation is given in the *table no 3.15* . From the graph of peak current against electronegativity (*figure 3.38)* individual dopant ions it could be seen that incase of internal doping there was tremendous increase in the peak current compared to the external doping. This enhancement in catalytic activity might be due to the better complexation prior to electrochemical polymerization. It may be noted that in the case of $PdCl_2$ and $FeCl_3$, the addition of pyrrole gave almost instantaneously PPy formation and hence were not investigated for electrochemical deposition.

In order to monitor the changes occurring in external and internal doping, the Diffused Reflectance Spectrogram (DRS) and XPS of the films were recorded.

DRS of the dedoped PPy along with external and internal $ZrCl_4$ doped PPy were run and spectrogram of which is shown in the *Figure-3.39.* IR assignment was presented in the *table 3.16*

From the IR assignment it could be seen that, the weak peak at 1617 cm^{-1} in the external doped which is due to the C=N stretching got shifted to 1614 cm^{-1} in case of insitu doped and this peak is absent in the dedoped PPy. 1525cm^{-1} which is due to the C–N stretching polypyrrole ring is strong in case of insitu doped and very weak for dedoped PPy whereas it got shifted and appears at 1487cm^{-1} in the exsitu doped. Peak in the region of 1260 cm^{-1} to 1290cm^{-1} is due to C – C, C – N, medium in case of insitu doped whereas it is weak in case of exsitu and undoped samples.

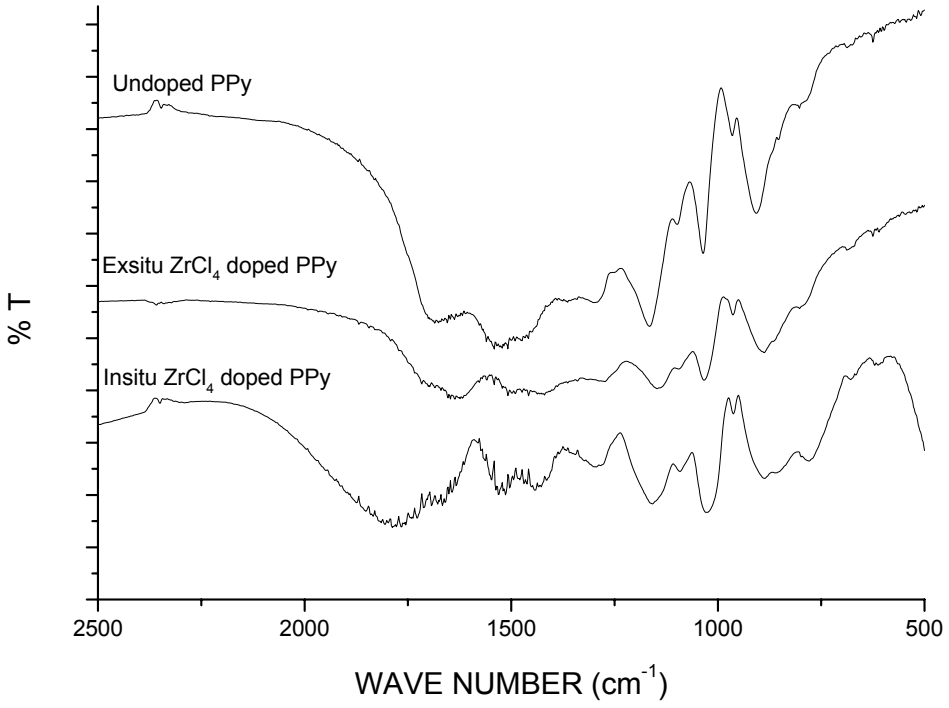

Figure 3.39 : FT-IR spectra of undoped, exsitu and insitu doped PPy

Peak in the region of 1140cm^{-1} to 1160cm^{-1} is due to C – H plane deformation. In case of undoped and insitu doped PPy peak appears at 1159 cm^{-1} and they are sharp whereas incase of exsitu doped a weak peak appears at 1142 cm^{-1}. Peak at 1033cm-1 is due to N–H plane deformation it is strong in case of undoped sample and in case of exsitu doped it is medium, whereas in case of insitu doped PPy this peak got shifted to 1042cm^{-1} and it is strong.

Undoped PPy	External Doping	Internal Doping	Assignment
-	-	1768(br)	
1680(br)	1690(w)	1690(vw)	C=C ring stretching
	1617(w)	1614(w)	C=N stretching
1525(w)	-	1525(m)	C=N, C-N stretching
1469(w)	1487(w)	-	C-N stretching of polypyrrole
-	1413(vw)	1439(w)	N-H deformation
1286(w)	1265(vw)	1286(m)	C-C, C-N
1159(s)	1142(w)	1159(m)	C-H in plane deformation
1033(s)	1033(w)	1025(s)	N-H in plane deformation, Ring vibration of pyrrole
956(m)	956(m)	956(m)	Ring vibration of pyrrole
878(m)	878(br)	878(br)	C-H bending
780(vw)	780(vw)	780(m)	Ring vibration of pyrrole

Table 3.16: IR assignment table for undoped PPy, Exsitu and insitu doped PPy

Peak in the region of 800 - 780cm^{-1}is due to the ring vibration of pyrrole, which is weak in case of dedoped and exsitu doped PPy, whereas it is broad in case of insitu doped PPy. More intense bands and shift of bands are seen in case of insitu doped PPy, which are due to the complexation pyrrole with the $ZrCl_4$ prior to polymerization.[79]

XPS of $ZrCl_4$ external and internal doped PPy films are shown in the *Figure 3.40* which depict the core level spectra for C1s, N1s, Cl_{2p} and Zr. The curves designated by symbols (a) and (b) correspond to the spectra of exsitu and insitu doped PPy respectively. The

broad core level spectra are the indicative of the various components, and these components are obtained by deconvolution of the same. On comparing these various spectra **(***see Table-3.17)* it is seen that there is additional contribution from the charged species in all cases (the intensity of those component peaks at higher B.E. increases) .

In the *figure 3.40 (B)* spectra of N (1s) atom is shown. N (1s) core level spectra of exsitu doped PPy appearing at 399.8 eV got shifted to 399.9 eV in case of insitu doped PPy which is due to the =N—. Peak at higher B.E.'s are due to the charge species —NH— and N^+ respectively. Peak due to —NH— species appears at 400.8 eV and 401.4 eV for exsitu and insitu doped PPy respectively. The peak due to N^+ appears at 402.35 and 402.8 for exsitu and insitu doped PPy respectively. Percentage peak area due to the charge species incase of exsitu and insitu are 40.19(36.64, 3.55) and 62.27(47.6, 14.67) respectively. In the insitu doped PPy the area of charged species is much more than the exsitu doped which can be seen very clearly from the figure.

In case of exsitu doped PPy, the contribution due to the imine like nitrogen atom (=N—) component is higher. This suggests that significant deprotonation of PPy has occurred. Since deprotonation involves exclusively transformation of —N^+ to =N— groups. Deprotonation took place during dedoping of the sample prior to external doping. Whereas in case of insitu doped PPy, contribution due to —NH— and —N^+ are more. The high energy peaks i.e. N^+ is due to the doped nitrogen species and the doping level can be expressed as the share of N^+ groups in the polymer. More the percentage of charged species indicates the formation of polarons and bipolarons in the polymer chain.

From all the observations it could be predicted that substantial complex formation appears to take place in case of insitu doped PPy by co-ordination between Zr and nitrogen atom.

Figure 3.40(A)

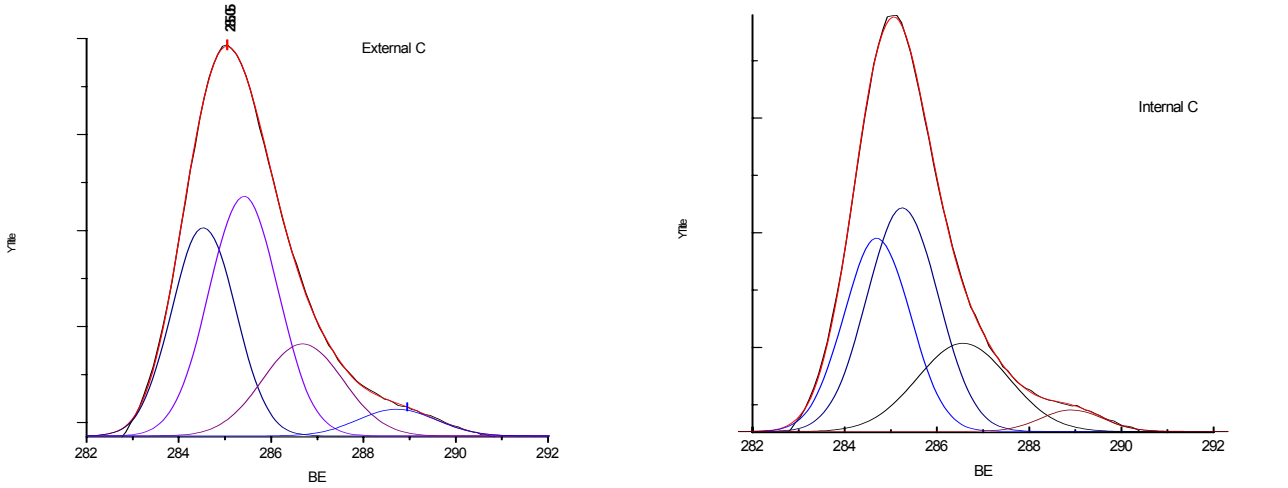

Figure 3.40(B)

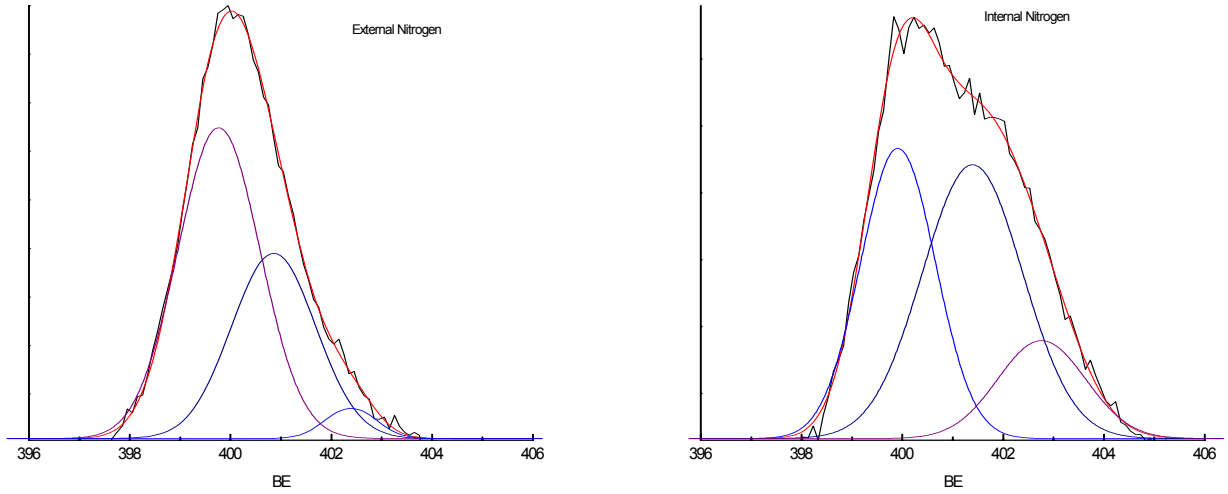

Figure 3.40 (C)

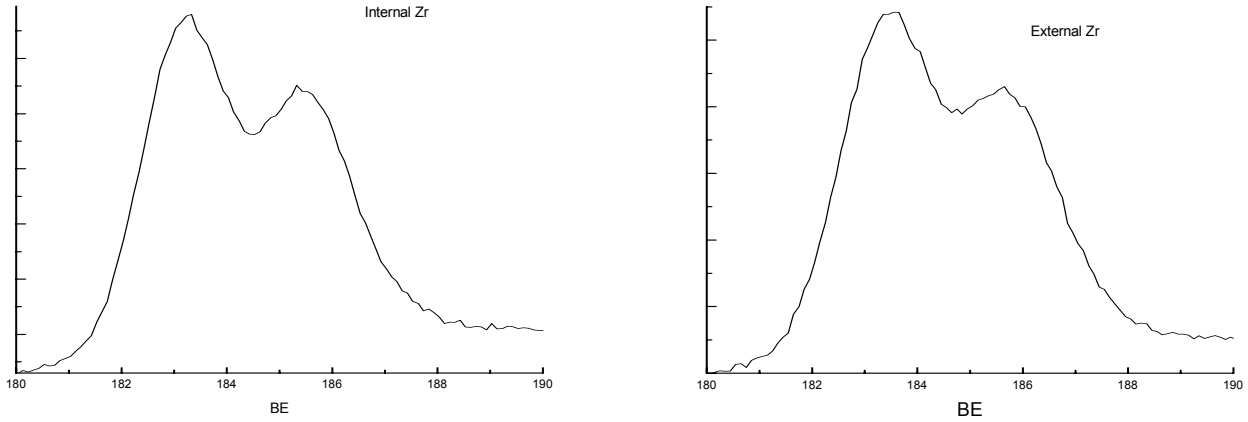

Figure 3.40 (D)

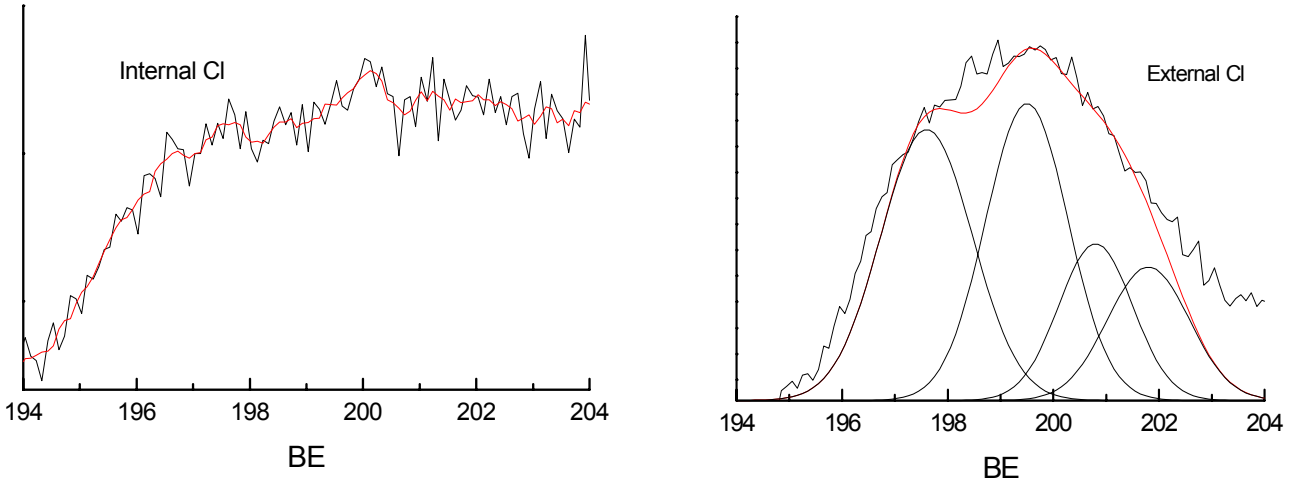

Core Level		External Doping		Internal Doping	
		B.E.(eV)	%Area	B.E.(eV)	%Area
C1s	C1	284.6	34.6	284.6	34.4
	C2	285.4	43.65	285.3	42.6
	C3	286.6	21.74	286.7	23.01
N1s	N1	399.8	59.8	399.93	37.7
	N2	400.8	36.64	401.4	47.6
	N3	402.35	3.55	402.8	14.67
Zr	3d5/2	183.4	-	183.13	-
	3d3/2	185.6	-	185.44	-
Cl	Cl2p	Peak observed		No Peak observed	

Table 3.17: Table of XPS data for exsitu and insitu doped PPy films

In the *figure 3.40 (D)* the XPS of Cl atom is given. In the exsitu doped PPy, Cl atom's spectra is prominent whereas in case of insitu doped PPy, Cl spectra not visible which may be due to that the exsitu doping is surface level modification whereas in case of insitu doping Cl atom has gone inside the matrix and forms a better complex. Thus, insitu doping leads to better complexation of the Zr atoms with the N of the PPy structure. In case of insitu doping there is a possibility of Zr atoms going inside the polymer matrix and better mixing with the polymer matrix leading to higher amount of complex formation. [80-85]

3.3.3.2. Roughness of films.

As surface of the electrode plays an important role in the electrocatalytic reactions, conducting PPy electrodes of varying roughness were prepared. *Figure 3.41* shows the SEM for the polypyrrole deposited at three scan rates : 20 mV/s, 30 mV/ s and 60 mV/s. It is evident that the film surface goes from very smooth to very rough as the scan rate is increased. This is mainly associated with the high current or the rate of deposition of the film. These films were then doped with $ZrCl_4$ and employed to study the effect on electrooxidation of methanol. Electrochemical study of these electrodes for methanol oxidation was carried out, CV's of which is shown in *Figure 3.42*.Graph of Peak Current vs. varying scan rate for deposition i.e. varying roughness is plotted and is shown in the *figure 3.43.* It was observed that as the roughness of the film increases electro-catalytic activity towards methanol oxidation increases. Increase in catalytic activity with

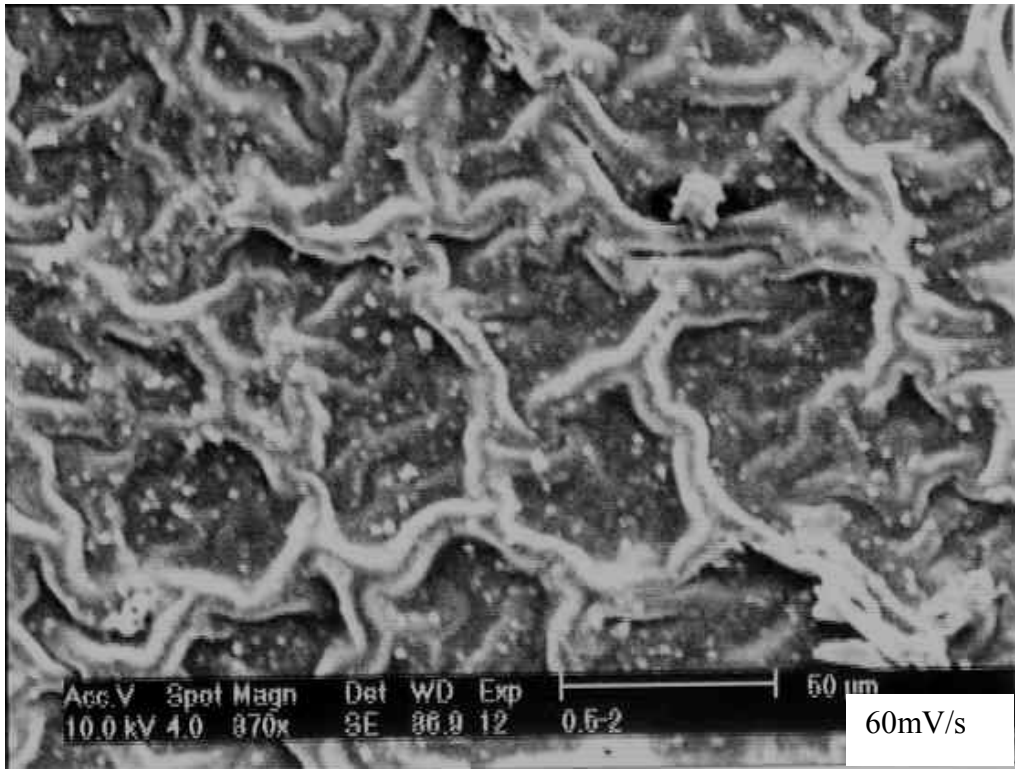

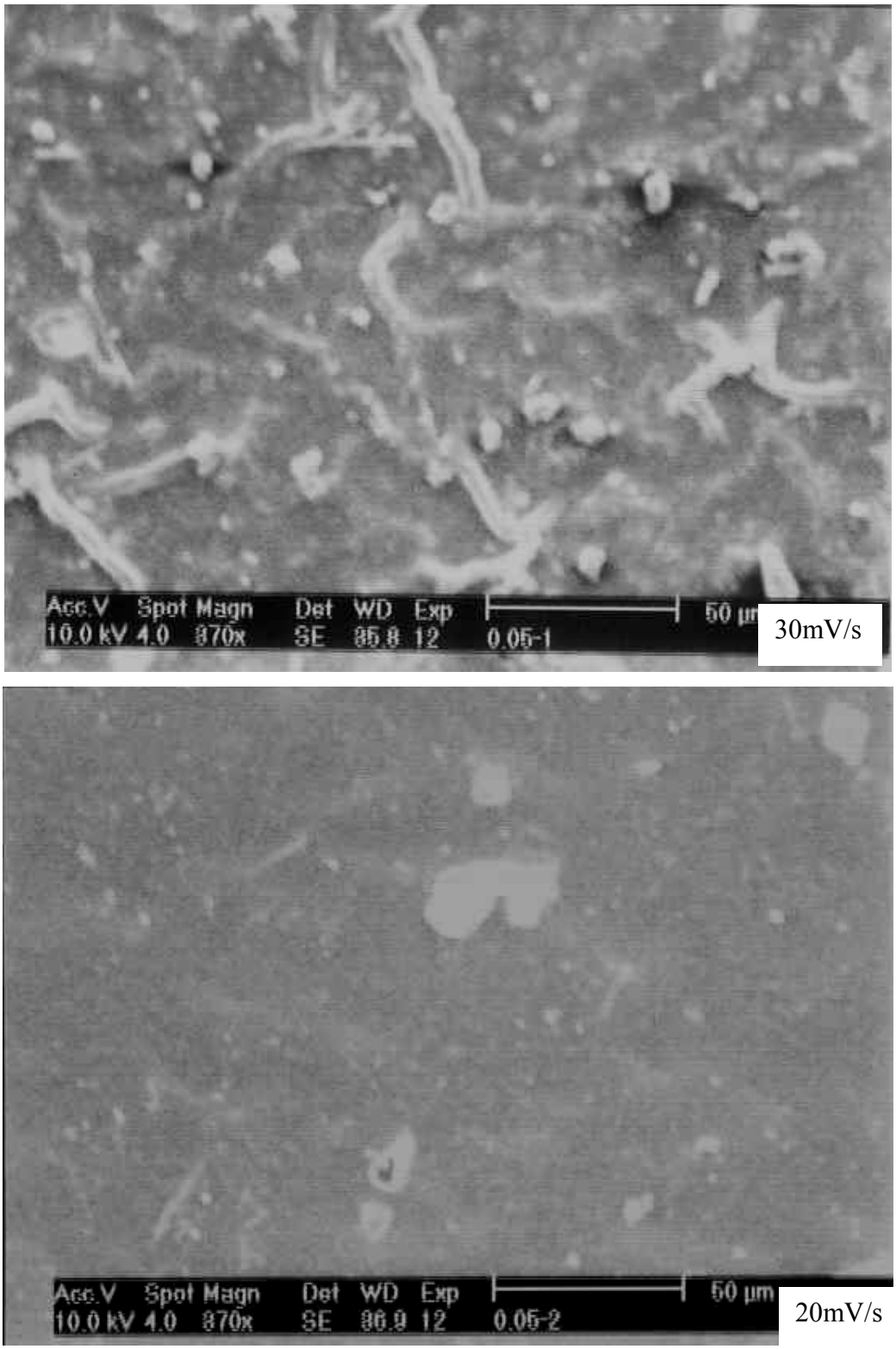

Figure 3.41: SEM images of PPy films of different scan rates showing roughness variation.

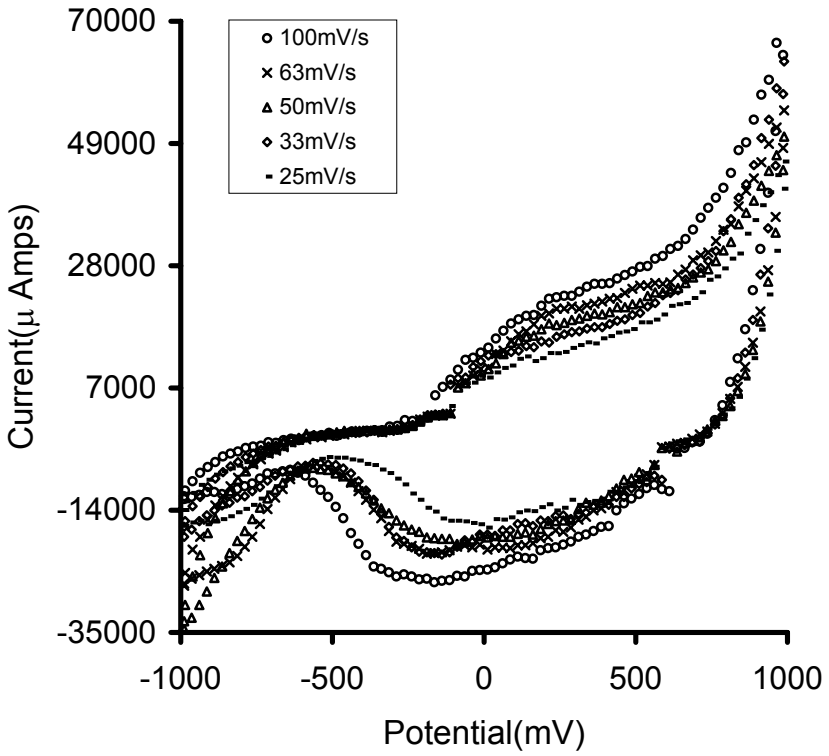

Figure 3.42: CV's of electrochemical oxidation of methanol using films of varying roughness

roughness might be due to the fact that with roughness surface area increased. With roughness porosity of the film increased and because of which there was increase in the catalytic site for interaction with the reactant. Various authors had suggested that conducting polymers hosting metallic particles were of special importance because of the facile flow of electronic charge through the polymer matrix. Many investigators have reported the advantage of incorporating metallic particles into porous matrices which increases the specific surface area of these materials and thus to increase the catalytic activity of the electrode [86-90]

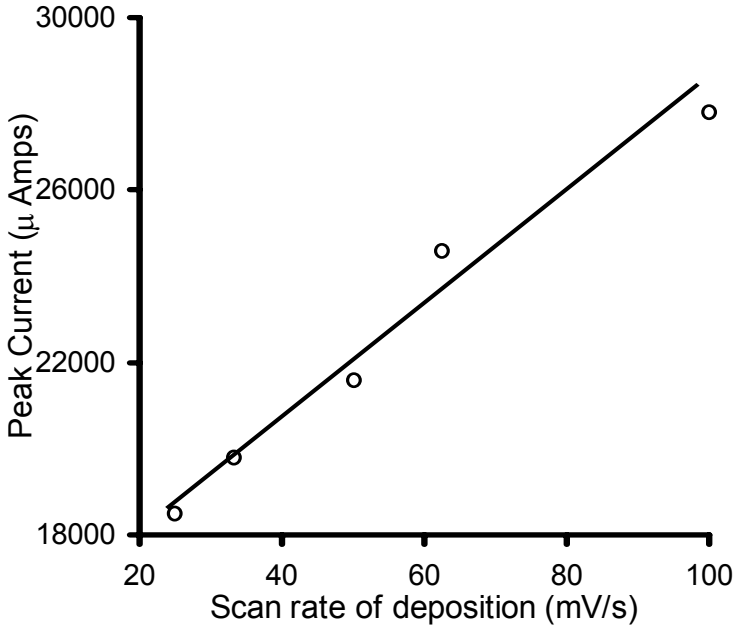

Figure 3.43: Graph of peak current for methanol oxidation vs. scan rate of deposition

3.3.3.3. Thickness of film

As it was observed in the earlier experiment that with roughness of the conducting PPy electrodes catalytic activity increases, hence it is also necessary to study the effect of thickness of the film on electrocatalytic activity. For that purpose PPy films of varying thickness were prepared and were doped with $ZrCl_4$. Electrocatalytic studies were done with these electrodes and CV's for which is shown in the *figure:3.44***.** From the CV's peak current against time for deposition was plotted which is shown in the *figure 3.45.* It could be concluded that with increase in thickness of the films peak current increases. Whereas K.H. Xue et al. suggested that in case of Pt / PPy / GC electrode, thickness of the PPy film was not sensitive towards the electro-catalysis of methanol oxidation.[91]Fiçicioğlu et al had studied Pt doped polyaniline film on the electro-oxidation

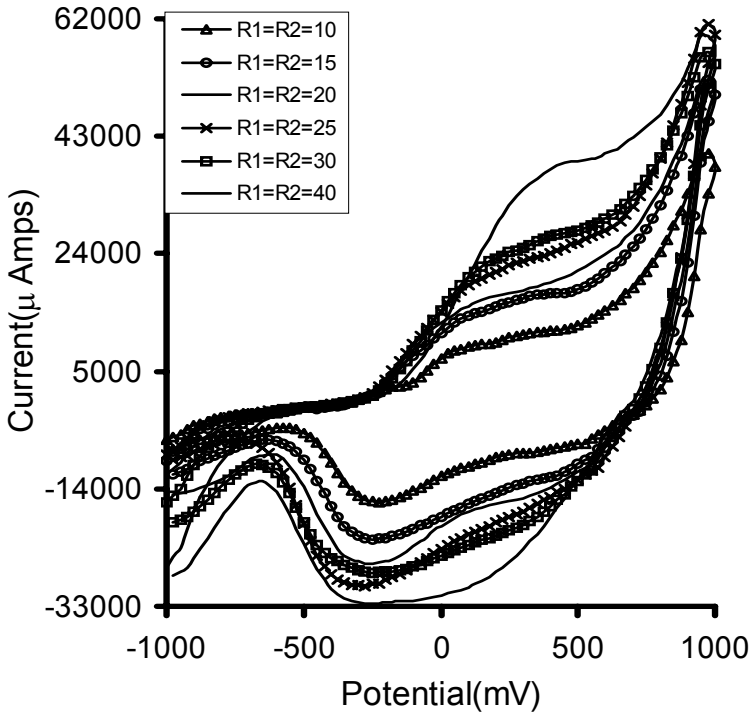

Figure 3.44: CV's for electrochemical oxidation of methanol using films of varying thickness

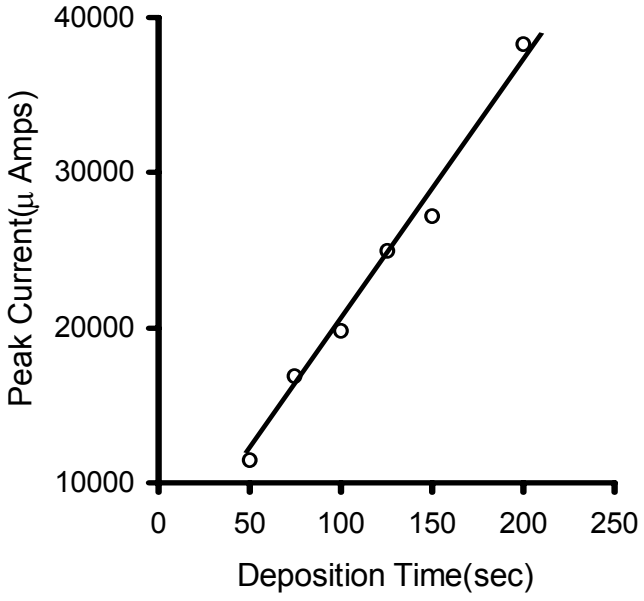

Figure 3.45: Graph of Peak Current for methanol oxidation vs. PPy deposition time

of methanol where they reported electro-oxidation of methanol on the thicker polyaniline film was diffusion controlled whereas for polyaniline film of less thickness the adsorption step was the rate determining step.[92] This could be explained on the basis of higher surface area provided by the thicker film. The increasing porosity with increasing film thickness allowed the Pt particles to be deposited in a regular style giving the maximum possible surface area for the oxidation of methanol, where the diffusion of molecules to the surface of the electrode determine the rate of reaction. Here in the present study electrocatalytic activity was directly related to the thickness of the PPy film. This might be due to the fact that with thickness of films the rate of electron transport through the polymer matrix and the rate of diffusion of substrates through the polymer matrix increased and in case of thicker films availability of higher surface area is more compared to the films of less thickness.

3.3.3.4. Ion beam irradiated PPy electrodes:

To improve the electrocatalytic activity, PPy films were also modified by ion beam irradiation technique. PPy films thus modified by ion beam irradiation were used for methanol electro-oxidation. *Figure 3.46* is the CV's for oxidation of methanol using unirradiated and irradiated PPy films (for 0.01M methanol concentration) in the electrolyte (cv's for other concentrations were also recorded but not shown here). It was seen that irradiated samples were more electro-catalytic active towards methanol oxidation than the unirradiated samples. The rise in the current in the anodic region after irradiation is quite evident. This increase in the anodic current is tremendously enhanced when the PPy films are incorporated with $PdCl_2$ which is already seen in the earlier parts of the chapter. It may be noted that there was only a slight change in the current after PPy films are chemically treated with $PdCl_2$ but dramatic changes were observed in the current after the ion beam exposure of the samples which can be seen in the *figure 3.47.*

In order to monitor the changes occurring due to ion beam irradiation, the XPS of the films were recorded. *Fig. 3.48 (A) to (D)* depict the core level spectra for C1s, N1s, Cl2p and $Pd3d_{5/2}$ of these films. The curves designated by symbols (a) and (b) correspond to the spectra before and after ion beam irradiation respectively.

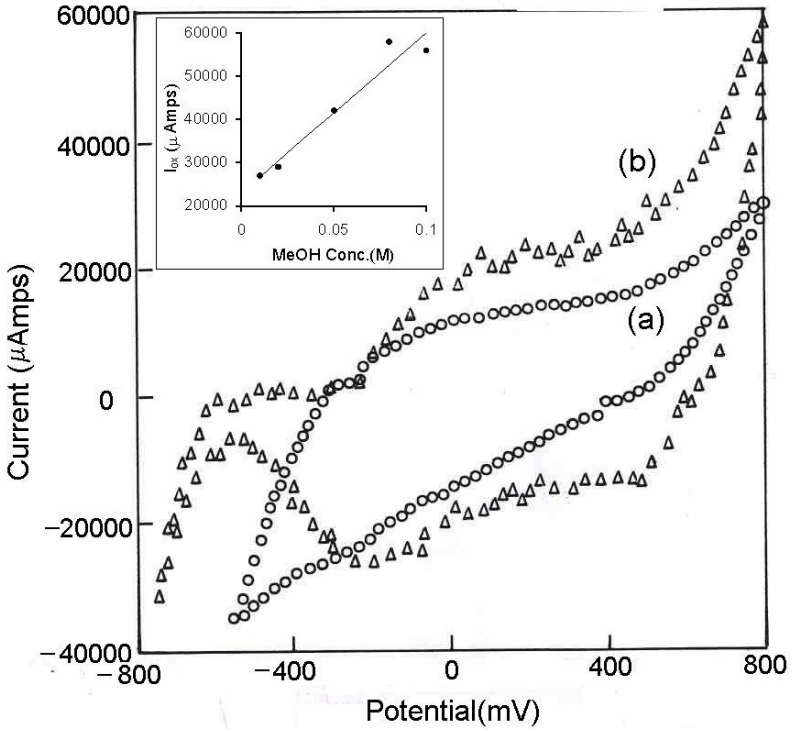

Figure :3.46
CV's of oxidation of methanol (0.01M) using
(a) unirradiated
(b) irradiated PPy electrode. Inset shows increase in anodic current with methanol

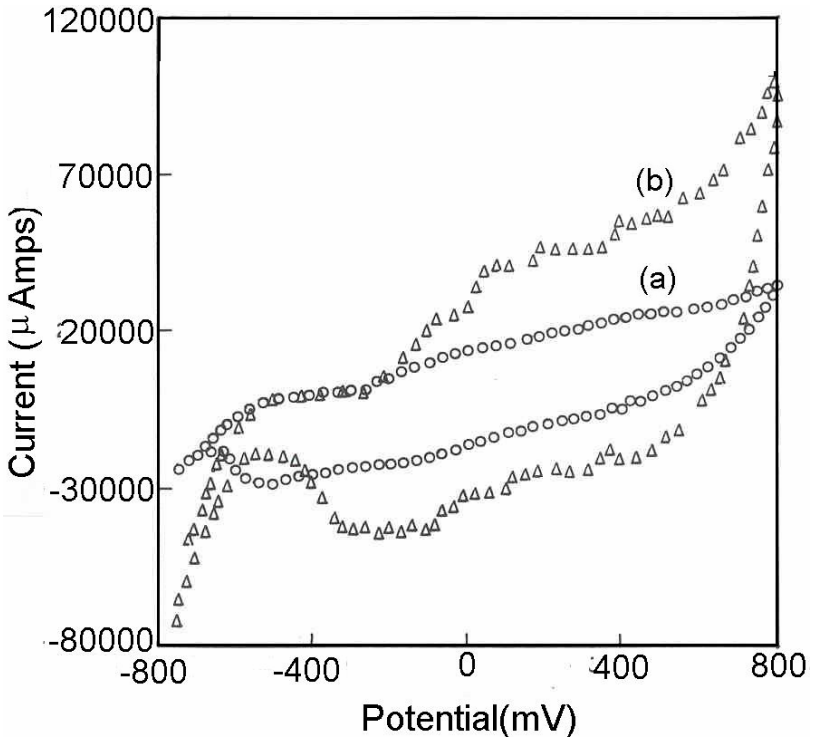

Figure:3.47
CV's of PPy electrodes doped with $PdCl_2$ (0.006M) for 0.01M methanol. The curves (a) and (b) correspond to sample without and after ion beam irradiation, respectively

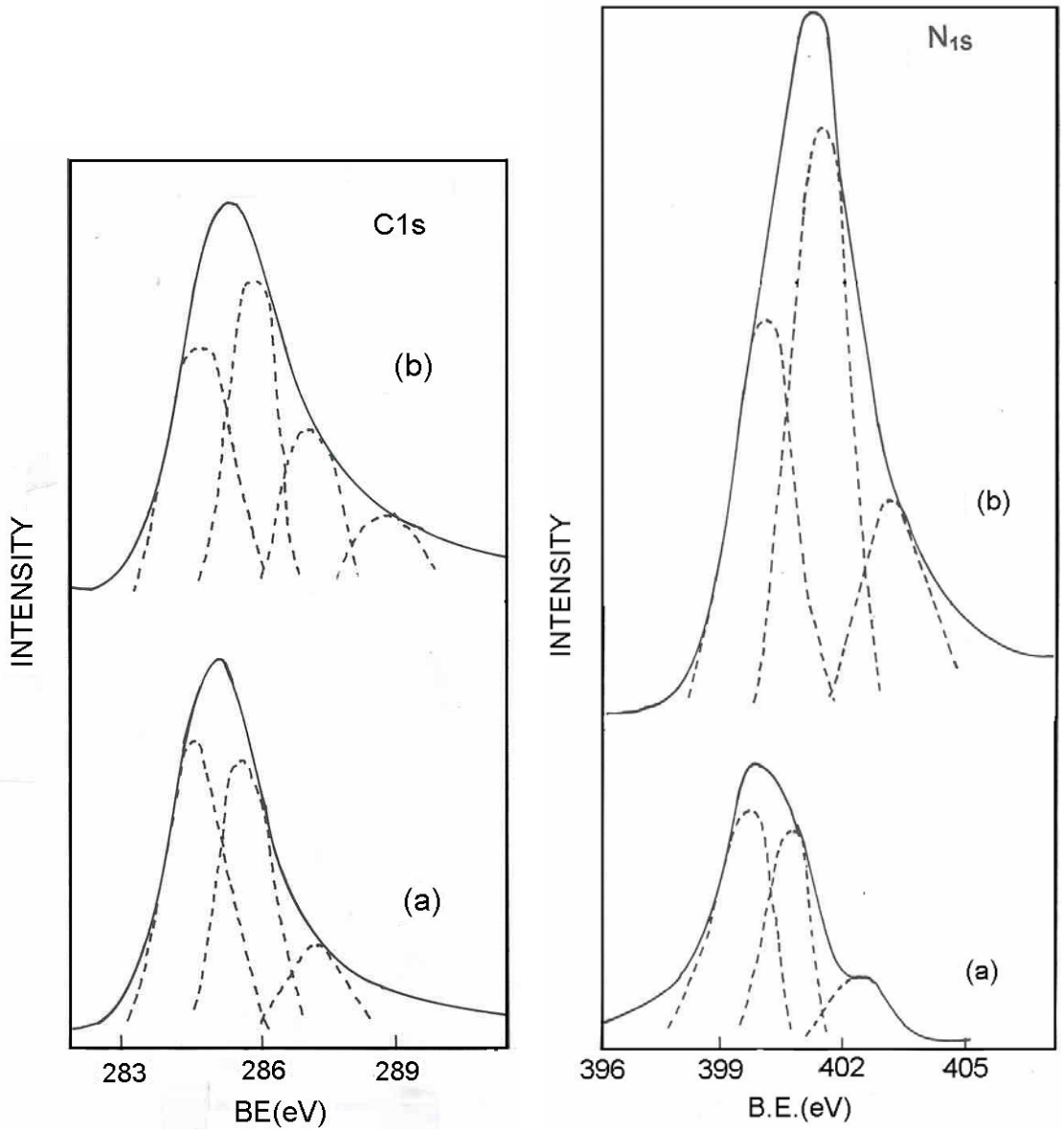

Figure. 3.48(A) **Figure: 3.48(B)**

Figure 3.48: High resolution X-ray photoelectron spectra for (C) C1s and (D) N1s,. The curves designated as (a) and (b) correspond to sample before and after ion beam irradiation

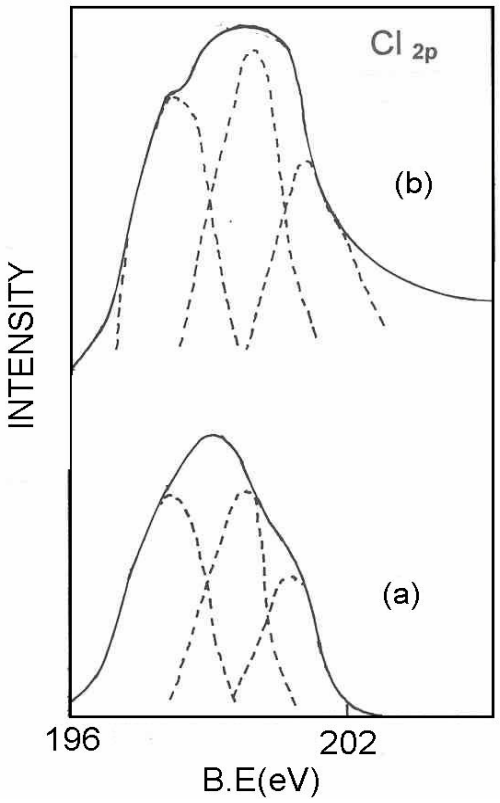

Figure: 3.48(C)
X-ray photoelectron spectra for Cl2p .
(a) Before irradiation
(b) After irradiation

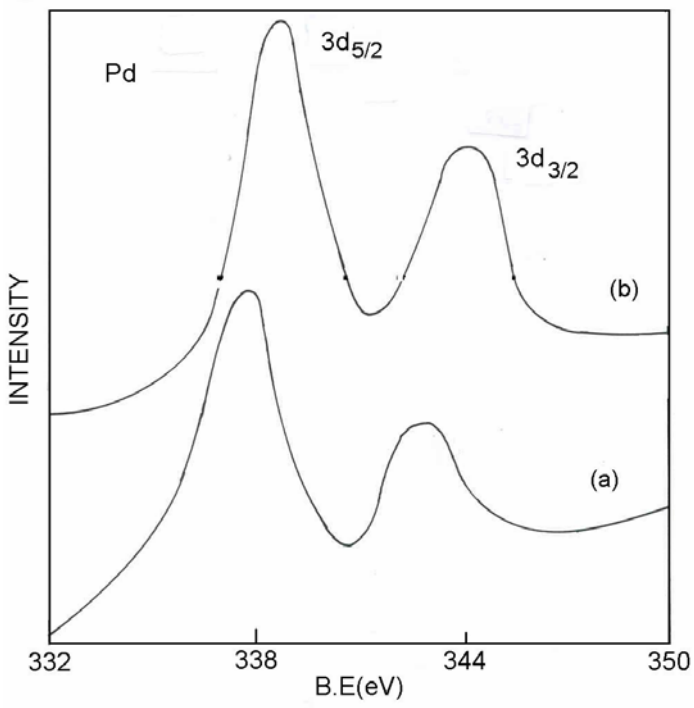

Figure: 3.48(D)
X-ray photoelectron spectra for Pd $3d_{5/2}$ and Pd $3d_{3/2}$.
(a) Before irradiation
(b) After irradiation

The various core levels show very broad spectra indicative of number of components which were obtained by de-convolution of the same. These have been indicated by dotted lines in the figures. Such components are usually observed for conducting polymers and these have been well documented in literature. On comparing these various spectra *(see Table-3.18),* it may be seen that there is additional contribution from the charged species in all cases (the intensity of those component peaks at higher B.E. increases) .

Core Level		**Before Irradiation**		**After Irradiation**	
		B.E. (eV)	**%Area**	**B.E. (eV)**	**%Area**
C_{1s}	**C_1**	284.6	46.5	284.7	37.6
	C_2	285.5	38.7	285.7	31.1
	C_3	287.2	14.8	287.1	19.2
	C_4	-	0	288.1	12.1
N_{1s}	**N_1**	399.7	50.5	400.1	32.9
	N_2	400.7	33.4	401.5	45.9
	N_3	402.5	16.1	403.2	21.2
Cl_{2p}	**Cl_1**	198.0	42.9	198.3	34.5
	Cl_2	199.8	36.3	200.2	39.3
	Cl_3	200.8	20.8	201.4	26.2
Pd	**$3d_{5/2}$**	337.6	-	338.7	-
	$3d_{3/2}$	342.9	-	344.6	-

Table 3.18: XPS data for PPy doped with $PdCl_2$ films before and after irradiation

It may also be noted that the N1s peak intensity in the un-irradiated samples was weak but it became quite prominent after ion beam irradiation. Also, the Pd spectra show a slight shift in B.E. values; the 3d5/2 peak appears at 337.6 eV for un-irradiated films while it is at 338.3 eV with corresponding shift of the 3d3/2 component as well. These various observations suggest that the PPy films chemically treated with $PdCl_2$ do not form completely doped system but contain some amount of the dopant salt at the surface level. These ions are pushed deeper into the films and get fully mixed after ion beam irradiation. This results in bringing the nitrogen species to the surface which were otherwise shielded by the Pd ions giving rise to higher intensity of the N1s peak. Further, substantial complex formation appears to take place by co-ordination between Pd and nitrogen atoms since there is shift of Pd 3d5/2 peak to higher B.E. values which are similar to those observed for palladium - pyridine complexes. Thus, ion beam irradiation of these films leads to essentially pushing the Pd ions deeper and mixing better with the polymer matrix leading to higher amount of complex formation. Such Pd complexes with nitrogen containing hetero-compounds are well known to be excellent catalysts for oxidation of organic compounds including Wackers process.

Thus, these studies show that ion beam mixing of conducting polymers with the dopant species can lead to materials having better electro-catalytic properties than those prepared by mere chemical doping.[93-98]

3.4. CONCLUSION:

These various studies on the electro-catalytic activity of conducting polymer viz. PPy doped films for the methanol oxidation clearly bring out the various processes involved in the catalytic efficiency of such materials. Although PPy by itself shows some activity towards methanol oxidation, specific dopants bring about much better efficiency. The role of different dopant ions on the catalytic activity of PPy was therefore studied in detail. The enhancement was more pronounced when PPy films were doped with less electronegative elements like $ZrCl_4$ than $NiCl_2$. Studies on the conducting polypyrrole

modified with different doping agents show that electronegativity of the dopant agents play an important role in the electro oxidation process. In order to establish a relationship of the nature of dopant ions with electrocatalytic efficiency, the dopant incorporated PPy was thoroughly characterized by different techniques. There were significant changes seen in the average inter-chain distance (derived from XRD) as well as the extent of charge transferred (derived from XPS) with the type of dopant used. The activation energy for the charge transport also changed considerably with the types of dopant present. These various findings suggested that the charge transport in the conducting polymer as well as the charge transfer from polymer to the reactant would be extremely important in the electro-catalytic activity. In order to explain these observations, a model has been proposed with the help of energy level diagram for the different dopant ions with respect to PPy in contact with the reactant in the electrolyte. This energy level representation brings out clearly the importance of the charge (electron/hole) transport process in the electro-oxidation reaction. It is known that conducting polymers in the doped state are p-type semiconductors with the additional impurity state created within the band gap as estimated from the activation energy. The electrocatalytic behaviour of any material depends on various factors such as (a) the position of the energy levels of the reactive species and the electrode material, (b) charge transfer process across the interface of electrode and electrolyte, (c) diffusion of the reactants into /near the electrode surface and (d)ionic mobility. In the present case, the factors (c) and (d) are common to all cases and hence the reasons (a) and (b) appear to be most relevant. It is seen that in the electrooxidation processes, for PPy doped with $ZrCl_4$ electrodes, it is easier for electrons to be transferred from the reactant methanol to the electrode than in other cases. The electron transport from electrolyte to electrode or hole transport from electrode to reactant leads to the oxidation of MeOH in presence of O_2 as

$$CH_3OH + O_2 \xrightarrow{-e} HCOOH + H_2O, \text{ and so forth.....}$$

$$\text{and finally to } CO_2 \uparrow$$

In the above reaction the primary rate determining step appears to be controlled by the charge transport at the anode. Hence, the energy level of the dopant in the polymer appears to be very important in the electro-oxidation process using conducting polymers. The kinetic studies for methanol oxidation indicated that the electrocatalytic activity of these polymers is similar to that reported for other electrodes (Pt, Pt/Rh etc.) but with an added advantage that the activation energy is lower and charge transfer efficiency is higher. The role of surface roughness of the electrodes, ion beam modifications etc. has also been brought forward which give indication to the other important factors such as surface area, number of active sites etc. involved in the electro-catalysis.

The studies of the electrooxidation of methanol with insitu doped PPy electrodes show their higher catalytic activity as compared to the exsitu doped ones. Higher activity is explained on the basis of better complexation in case of insitu doped PPy electrodes which is proved in the different characterization studies. One can define a quality factor (Q/R) for these materials where Q is the percentage of charged species as noted by XPS and R is the average interchain separation as determined from XRD which controls the charge transfer process. It is seen that higher Q/R factor lead to higher electro-catalytic activity.

Overall it can be concluded that even though redox properties shown by the conducting polymers is the basis of the catalytic activity, the actual catalytic efficiency depends on the position of energy levels of the reactive species and the electrode material and the charge transfer process across the interface of electrode and electrolyte appears the main rate determining factor. Further, the extent of complexation, surface roughness, thickness, and temperature also play important role in the electrocatalytic reactions using modified conducting polymers.

3.5. REFERENCE

1. S. Wasmus, A. Kuver, J. Electroanal. Chem. *461 (1999) 14*.
2. A. K. Shukla, M. K. Ravikumar, K. S. Gandhi; J. Solid State Electrochem *2(1998)117*
3. B. D. McNicol, D. A. J. Rand, K. R. Williams, J. Power Sources *83 (1999) 15*.
4. M. Baldauf, W. Preidel, J. Power Sources *84(1999)161.*
5. T. Hatanaka, N. Hasegawa, A. Kamiya, M. Kawasumi, Y. Morimoto, K. Kawahara; Fuel *81 (2002) 2173*.
6. A. Kelaidopoulou, E. Abelidou and G. Kokkinidis, J. App. Electrochem; *29(1991)1255*.
7. C. S. C. Bose and K. Rajeshwar; J.Electroanal. Chem. *333(1992) 235*.
8. C. T. Hable and M. S.Wrighton, Langmuir *7(1991)1305*
9. J. W. Sobczak, B. Lesiak, A. Jablonski, A. Kosinski, W. Palczewska; Polish J. Chem; *69(1995)1732*
10. M. D. Macia´, E. Herrero, J. M. Feliu, J. Electroanal. Chem, *554-555(2003)25*
11. P. J. Kulesza, M. Matczak, A. Wolkiewicz, B. Grzybowska, M. Galkowski, M. A. Malik, A. Wieckowski, Electrochim Acta, *44 (1999) 2131*
12. V. N. Andreev, M. A. Spitsyn, V. E. Kazarinov, Russian J. Electrochem. *32(1996)1307.*
13. V. N. Andreev, Russian J. Electrochem. *35(7) (1999) 735.*
14. E. Buttner, R. Holze, J. Electroanal. Chem, *508 (2001)150*.
15. İ. Becerik, F. Kadirgan, J. Electrochem. Soc, *148(5) (2001)D49*.
16. H. Li, T. F. Guarr; J. Electroanal. Chem; *317(1991)189.*
17. R. Aydin, F. Koleli; J. Electroanal. Chem,; *535(2002)107*.
18. S. C. Thomas, X. Ren, S. Gottesfeld, P. Zelenay; Electrochim. Acta. *47(2002) 3741.*
19. İ. Becerik, S. Suzer, F. Kadirgan, J. Electroanal. Chem. *502 (2001) 118.*
20. G. Tourillon; F. Garnier, J. Phys. Chem. *88 (1984) 5281.*

21. A. S. Arico, A. K. Shukla, K. M. El-Khatib, P. Creti, V. Antonucci; J. Appl. Electrochem. *29(1999)671*
22. A. Hamnett, Catalysis Today; *38 (1997) 445*.
23. G. T. Burstein, C. J. Barnett, A. R. Kucernak, K. R. Williams; Catalysis Today; *38 (1997) 425.*
24. P. V. Samant, J. B. Fernandes; J. Power Sources; *79 (1999)114*.
25. W. H. L. Valbuena, V. A. Paganin, E. R. Gonzalez; Electrochim Acta *47(2002)3715.*
26. K. Ramya, K. S. Dhathathreyan; J. Electroanal. Chem.; *542 (2003) 109.*
27. J. Yu, P. Cheng, Z. Ma, B. Yi; Electrochim. Acta *48(2003)1537*
28. S. S. Sandhu, R. O. Crowther, S. C. Krishnan, J. P. Fellner, Electrochim. Acta *48(2003)2295*
29. C. Lamy, E. M. Belsir, J-M. Leger; J. Appl. Electrochem, *31(2001)799.*
30. S. Machida, S. Miyata, A. Techgumpuch, Synthetic Metal; *31(1989)311*.
31. T. Frelink, W. Visscher, J. A. R. van Veen; J. Electroanal. Chem. *382(1995) 65.*
32. B. Tian and G. Zerbi; J. Chem. Phys. *92(1990)6*
33. B. Street, Hand book of Conducting Polymer (Dekker, New York,1986),vol.1, p.256.
34. G. Zotti, G. Schiavon, S. Zecchin, G. D'Aprano; Synth. Metals *80(1996)35*
35. X. Li, M. Huang, L. Wang, M. Zhu, A. Menner, J. Springer; Synth. Metals *123(2001)435*
36. B. San, M. Talu; Synth. Metals *94(1998)221*
37. W. Su, J. O. Iroh; Synth. Metals *95(1998)159*
38. Stanley Jasne, Encyclopedia of Polymer Science & Engineering, Vol.13 Polypyrrole, p-42; John Wiley & Sons, USA, 1988
39. K. Yakushi, L. J. Lauchlan, T. C. Clarke and G. B.Street; J. Chem. Phys.*79(1983)4774*
40. Alexander L. E, " X-ray Diffraction Methods in Polymer Science", John Wiley, New York, p 379 (1969).
41. K. Cheah, M. Forsyth, V. -T. Truong; Synth. Metals *101 (1999)19*.
42. P. Lemon, J. Haigh; Mat. Research Bull. *34(1999) 665.*

43. K. Cheah, M. Forsyth, V. -T. Truong; Synth. Metals *94 (1998) 215.*
44. J. Joo, J. K. Lee, J. S. Baeck, K. H. Kim, E. J. Oh, J. Epstein Synth. Metal *117(2001) 45*.
45. P. Pfluger and G. B. Street J. Chem. Phys *80 (1984) 544*
46. P. Pfluger and G. B. Street Polym. Prepr. *23(1982)122*
47. D. T. Clark and D. M. J. Lilley, Chem. Phys.Lett. *9(1971)234*
48. K. L. Tan, B. T. G. Tan, E. T. Kang and K. G. Neoh; J. Chem. Phys. *94 (8) (1991)5382.*
49. S. W. Huang, K. G. Neoh, E. T. Kang, H. S. Han and K. L. Tan; J. Mater. Chem. *8(8) (1998)1743.*
50. M. Hasik, A. Bernasik, A. Adamczyk, G. Malata, K. Kowalski, J. Camra; Euro. Poly. Journal. *39 (2003)1669*.
51. E. T. Kang, K. G. Neoh, Y. K. Ong, K. L. Tan, and B. T. G. Tan; Macromolecules *24(1991)2822.*
52. V. M. Kobryanskii, S. A. Arnautov and M. V. Motyakin; Synth. Metal *69 (1995) 221.*
53. F. Genoud, M. Nechtschein, M. F. Planche and J. C. Thieblemont Synth. Metal *69(1995)339.*
54. Y. Harima, Y. Kunugi, K. Yamashita, M. Shiotani; Chem Phys. Lett. *317(2000)310*
55. A. Neudeck, A. Petr, L. Dunsch; Synth.Metals.*107 (1999) 143*
56. M. Scharli, H. Keiss, G. Harbeka, W. Berlinger, K. W. Blazey, K. A. Muller; Synth. Metals. *22 (1988) 317.*
57. M. Higuchi, I. Ikeda and T. Hirao; J. Org. Chem. *62(1997)1072*
58. T. Hirao, M. Higuchi, I. Ikeda, Y. Ohshiro; J.Chem.Soc., Chem Commun. *(1993) 194.*
59. M. Higuchi, D. Imoda, T. Hirao; Macromolecules *29(1996)8277.*
60. T. Hirao, M. Higuchi, B. Hatano, I. Ikeda; Tetrahedron Lett. *36(1995)5925.*
61. S. Radhakrishnan, A. Adhikari and D. K. Awasthi; Chem. Phys. Lett. *341 (2001) 518.*

62. T. Komura, T. Kobayashi, T. Yamaguchi, K. Takahashi; J. Electroanal. Chem. *454(1998)145.*

63. S. Wasmus and W. Vielstich; J. Appl. Electrochem. *23(1993) 120.*

64. S. Chang, L. H. Leung and M. J. Weaver; J. Phys. Chem. *94(1990)6013.*

65. E. Herrero, K. Franaszczuk and A. Wieckowski; J.Phys. Chem. *98(1994)6013.*

66. A. Armanta, I. Toyoshima , M. Enyo, Electrochim Acta *37 (1992) 1317.*

67. P. Argyropoulos, K. Scott, W. M. Taama, Electrochim. Acta. *44(1999)3575.*

68. G. Venugopal, X. Quan, G.E. Johnson, F.M. Houlihan, E. Chin, O. Nalamasu, Chem. Mater. *7(1995)271.*

69. M. Higuchi, I. Ikeda and T. Hirao; J. Org. Chem. *62(1997)1072*

70. V. S. Bagotzky and Yu. B. Vassilyev; Electrochim.Acta. *12 (1967)1323.*

71. S. Lj. Gojkovic, T. R. Vidakovic, D. R. Durovic; Electrochim. Acta. *48 (2003)3607*

72. S. Blais, G. Jerkiewicz, E. Herrero and J. M. Feliu; Langmuir. *17(2001)3030.*

73. T. J. Schmidt, R. J. Behm, B. N. Grgur, N. M. Markovic and P. N. Ross, Jr; Langmuir. *16(2000)8159.*

74. F. Fiçicioğlu and F. Kadirgan; J. Electroanal. Chem. *430(1997)179.*

75. A. O. Patil, A. J. Heeger and F. Wudl; Chemical Reviews, *88(1988)184*

76. S. Hwu, R. P. Ziebarth, S. von Winbush, J. E. Ford, and J. D. Corbett; Inorg. Chem. *25(1986)283.*

77. J. A. Garcia, A. Guette, A. Medrano, C. Labrugere, M. Rico, M. Lahaye, R. Sanchez, A. Martinez, R.J. Rodriguez; Vacuum *64 (2002)343.*

78. Y. Miyagawa, S. Nakao, K. Baba, R. Hatada, M. Ikeyama, S. Miyagawa; Surface and Coatings Technology *103–104 (1998) 323*

79. Theory and Practicals of Infrared Spectroscopy; Herman A. Szymanski, Plenum press, 1964, NY.

80. T. Komura, T. Kobayashi, T.Yamaguti K.Takahashi, J.Electroanal.Chem. *454(1998) 145.*

81. E. T. Kang , K. Neo , K.L.Tan, Adv.Poly.Sci., *106 (1993) 136.*

82. K. L. Tan, B. T. G. Tan, E. T. Kang and K. G. Neoh; J. Chem. Phys. *94(8)(1991) 5382.*

83. S. W. Huang, K. G. Neoh, E. T. Kang, H. S. Han and K. L. Tan; J. Mater. Chem. *8 (8)(1998)1743.*

84. M. Hasik, A. Bernasik, A. Adamczyk, G. Malata, K. Kowalski, J. Camra; Euro. Poly. Journal. *39 (2003)1669.*

85. E. T. Kang, K. G. Neoh, Y. K. Ong, K. L. Tan, and B. T. G. Tan; Macromolecules *24(1991)2822.*

86. P. A. Christensen, A. Hamnett, G. L. Troughton, J. Electroanal. Chem.; *362 (1993) 207*.

87. P. A. Christensen, A. Hamnett, J. Munk, G. L. Troughton, J. Electroanal. Chem.; *370 (1994) 251.*

88. H. Hammache, L. Makhloufi, B. Saidani, Synth. Metal, *123(2001)515.*

89. C. S. C. Bose, K. Rajeshwar, J. Electroanal. Chem. *333(1992)235.*

90. C. C. Chen, C. S. C. Bose, K. Rajeshwar, J. Electroanal. Chem. *350(1993)161.*

91. K. H. Xue, C .X . Lai, H. Yang, Y. M. Zhou, S. G. Sun, S. P. Chen, G. Xu, J. Power Sources *75 (1998) 207.*

92. E. T. Kang , K. Neo , K. L. Tan, Adv. Poly. Sci., *106 (1993) 136*

93. S. Radhakrishnan , A. B. Mandale , Synth. Metals, *62 (1994) 217*

94. K. Kishi , F. Kikui, Surf. Sci., *99 (1980) 405*

95. Z. M. Michalska, B. Ostaszewski, J. Zientarska, J. W. Sobeczak, J. Mol. Cat. (A), *129 (1998) 207*

96. S. Herman, M. Wenkin, M. Devillus, J. Mol. Cat. (A), *136 (1998) 59*

97. J. Tsuji , Synthesis *(1984) 369*

98. Y. Fujiwara, T. Jintoku, K. Takaki, Chemtech, October *(1990) 636*

Chapter IV

OXIDATION OF DECENE AND HEXENE USING POLYANILINE AND POLYPYRROLE

4.1. INTRODUCTION

Alkene oxidation is one of the most important fields of research for variety of application of the reaction products. In the conventional route for the oxidation of olefinic double bond to the methyl ketone, palladium based catalyst (Pd^{+2}) is used which is an important industrial process. During the course of the reaction Pd^{+2} is reduced to Pd^{0}, and in the presence of some reoxidant (e.g. $CuCl_2$, $MnCl_2$, $FeCl_3$ etc.) Pd^{0} is converted back to Pd^{+2} and this is known as the Wacker type oxidation. The Wacker process consists of three stoichiometric reactions, as shown below,

$$R-CH=CH_2 + H_2O + PdCl_2 \longrightarrow R-\overset{\overset{O}{\|}}{C}-CH_3 + Pd(0) + 2HCl \quad -----(1)$$

$$Pd(0) + 2CuCl_2 \longrightarrow PdCl_2 + 2CuCl \quad -----(2)$$

$$CuCl + \frac{1}{2}O_2 + 2HCl \longrightarrow 2CuCl_2 + H_2O \quad -----(3)$$

The overall reaction can be given as follows, where, in general, terminal olefins are converted to methyl ketone

$$R-CH=CH_2 + \tfrac{1}{2}O_2 \xrightarrow{PdCl_2, CuCl_2} R-\overset{\overset{O}{\|}}{C}-CH_3$$

These sequential oxidation and reduction reactions constitute a catalytic cycle. A few studies were reported also on the oxidation of olefins in the organic (non-aqueous) medium

Today there is an increasing need for mild aerobic catalytic process due to energy saving and environmental reasons. Most of the known oxidation processes based on molecular oxygen, however required elevated temperature and pressure. Recently, macro cyclic metal complexes, in particular metalloporphyrins, have attracted attention as catalysts in oxidation reactions also.[1-13]

Though palladium is extensively used in the industry, there are some negative aspects for these processes. Palladium catalysts are very costly, these are corrosive when used in

combination with some inorganic salts ($CuCl_2$, $FeCl_3$ etc) and these cannot be easily recovered because of their homogeneous nature (dissolved state). To overcome these drawbacks, research has been continuing for new type of catalyst, such as carbon supported catalysts, nanoparticles etc. Here modified conducting polymers were used as catalyst which may be useful alternative to conventional ones.

During the present investigations, electrochemical oxidation of decene and hexene was carried out using modified conducting polyaniline and polypyrrole electrodes.

Chemical oxidation reaction of decene was also carried out using modified conducting polymer. For chemical oxidation of decene, polyaniline powder modified by incorporating CuPc was used as catalyst.

4.2. EXPERIMENTAL

4.2.1. Synthesis and modification of Polyaniline and Polypyrrole

Among the various methods available for polymerization of aniline and pyrrole, electrochemical and chemical are the most extensively studied techniques. In the current study Pani and PPy were synthesized by two techniques viz. chemical polymerization and electrochemical polymerization technique. Both the techniques were simple and were possible in aqueous medium.

4.2.1.1. Chemical Method

Polyaniline was synthesized chemically and modified by incorporating different concentration of copper phthalocyanine. Synthesis of CuPc incorporated Pani was carried out in the NMP: H_2O, 1:1 mixture.

A. Preparation of Polyaniline

Pani was first synthesized by chemical polymerization route using Ammonium persulphate (APS) as the initiator. In one beaker 5.3g APS was dissolved in 100ml of distilled water. A solution of 5.5ml concentrated HCl was added in 150ml distilled water to which was added 10ml aniline and stirred. Detail procedure of preparation of Polyaniline is described in the chapter-II. The solution was digested for 24 hours and then filtered. The precipitate obtained was then washed with distilled water and dried under

vacuum. Powder obtained was brownish green in colour. The polyaniline thus formed was leuco-emaraldine salt.

B. Preparation of Modified Polyaniline powders incorporated with Copper Phthalocyanine.

In a beaker containing 400ml 1:1 mixture of NMP: H_2O, 44ml of HCl and 40ml aniline was added and mixed thoroughly and allowed to cool. To the above solution desired quantity of copper phthalocyanine green (1%-10% wt w.r.t. aniline monomer) was added and stirred properly to make a homogeneous solution. To this solution APS (21.2 g) solution which was prepared in distilled water was added and stirred. Temperature of the reaction rose due to the exothermic nature of the reaction. It was observed that the colour of the reaction mixture changes from light blue to deep blue and finally to dark green. Change of color is the indication to the propagation of the polymerization reaction. The reaction was carried out for 24 hours. Polymer powder was filtered and washed with water. Detail procedure for the preparation of polyaniline modified with CuPc is described in the Chapter II.

Pure polyaniline without phthalocyanine was also synthesized by the same procedure as described above.

4.2.1.2. Electrochemical Method

A. Polyaniline and polyaniline modified by incorporating CuPc.

Electrochemical synthesis of conducting polyaniline and CuPc incorporated Pani was carried out on the gold coated glass plate electrode in a single compartment three electrode cell using platinum foil as a counter electrode and SCE as reference electrode.

For the preparation of unmodified polyaniline, the typical electrolytic solution consisted of 0.2M aniline (3 ml) and 0.4M HCl (6 ml) in 150 ml distilled water.

In case of preparation of modified polyaniline instead of distilled water, 1:1 NMP:H_2O was taken as reaction medium. To this electrolyte, desired amount of phthalocyanine blue [0%, 1%, 2%, 3% and 4% weight percent with respect to monomer aniline] was added. The electrochemical cell was purged with dry nitrogen gas to remove dissolved oxygen in the electrolyte. Electrochemical deposition of polyaniline was carried out at fixed

potential of 900 mV. Potential was applied for 180 sec, with the help of computer controlled potentio galvenostat [Vibrant EC 2010 model].

Polyaniline films thus prepared were kept for half an hour at room temperature, and these were washed with NMP-H_2O mixture followed by distilled water several times. Immediate washing may cause pealing of the films from the gold-coated plate. These films were then allowed to dry. Films thus prepared were used to study electrocatalytic oxidation of alkenes.

B. Polypyrrole films modified with doping with different transition metal salts.

On the gold deposited glass films polypyrrole films were synthesized electrochemically. These films were then dedoped and redoped with different transition metal doping agents. Insitu doping of PPy films with different doping agents were also carried out which is mentioned in detail in the earlier chapters.

4.2.2. Electrocatalytic oxidation of decene and hexene using conducting polymer electrodes

Modified conducting polymer electrodes were employed for electrochemical oxidation of decene and hexene.

4.2.2.1. Polyaniline modified with CuPc

Polyaniline films modified by incorporating copper phthalocyanine were used as electrodes for the electrocatalytic oxidation of decene and hexene.

i) Decene oxidation:

Conducting polyaniline films modified by incorporating CuPc were used as electrodes in the electro-catalytic oxidation of decene. The electrochemical cell consisted of 0.1M $LiClO_4$, varying concentration of reactant decene in acetonitrile medium in presence of secondary external electrolyte $CuCl_2$ (0.1 M). Decene concentration in the reaction medium was varied from 0 to 0.5M. Potential was cycled between –1000mV to + 1000mV in the electrochemical reaction.

ii) Hexene Oxidation

Conducting polyaniline films modified by incorporating varying concentration of CuPc were also used as electrodes in the electro-catalytic oxidation of hexene. Potential was varied from –1500mV to + 1500mV in the electrochemical reaction. All other conditions were same as mentioned in the earlier part except here in the hexene reaction secondary external electrolyte $CuCl_2$ was not used.

4.2.2.2. Polyaniline films modified with $PdCl_2$

Polyaniline films doped with different concentrations of $PdCl_2$ were used as electrodes for electrochemical oxidation of decene. Dopant ion concentration was varied from 0, 0.003, 0.006, 0.009, 0.012 and 0.02M. The electrochemical cell consisted of 0.1M $LiClO_4$. Secondary external electrolyte $CuCl_2$ was also used in this reaction, which was varied in the solution from 0, 0.01, 0.02, 0.05, 0.08 and 0.1 M. CV's of polyaniline films doped with different concentrations of $PdCl_2$ were run with varying $CuCl_2$ and decene concentration. Potential was varied from -1000mV to +1000mV.

4.2.2.3. Polypyrrole modified with different doping agents.

Polypyrrole films modified both by insitu and exsitu techniques, with different doping agents of different electronegativities, viz. $CuCl_2$, $NiCl_2$, $PdCl_2$, $CoCl_2$, $ZrCl_4$, $MnCl_2$ and $FeCl_3$ were also used as electrodes for alkenes electro-oxidation.

4.2.3. Chemical oxidation of decene

For oxidation of decene Pani powders incorporated with different concentration of CuPc was used as catalyst. For chemical reaction, specially designed reaction set up was used. The reaction setup consisted of a two necked round bottom flask(RBF) connected to a condenser. The condenser was connected to oxygen bladder through two way connector. The round bottom flask was kept on oil bath which was heated by using temperature controlled hot plate, details of which is described in the chapter-II

For the reaction, 40 ml of acetonitrile (HPLC grade Merck) was taken in the RBF. To the RBF containing acetonitrile, varying quantity of conducting polyaniline doped with CuPc was taken. Pani catalyst with different concentration of CuPc were also used for chemical

reaction. The mixture was then allowed to heat at 70 degree centigrade with constant stirring for an hour. Oxygen supply was kept on using inlet through condenser. Magnetic stirrer was used for constant stirring. After one hour, 4ml reactant decene was added to the reaction mixture. After the addition of reactant all the inlets and outlets were closed properly. This was kept for reaction to take place for varying time ranging from 12 hrs, 24 hrs, 30 hrs, 48 hrs, 60 hrs, 72 hrs.

After the reaction was over the reaction mixture was filtered through the whatmann filter paper to separate the conducting polymer catalyst from the mixture. This was then passed through silica gel to get clear solution containing product. Then it was eluted by acetonitrile.

This solution was then concentrated using rotavapor. While concentrating, acetonitrile solvent was removed from the reaction mixture leaving behind product and unreacted reactants. This is because of low boiling point of acetonitrile and high boiling point of the reactant and the assumed products decanol, decaldehyde, decanone and decanoic acid.

This reaction mixture was characterized using GC and IR technique.

4.3. RESULTS AND DISCUSSION:

4.3.1.Characterisation of modified conducting polymers

The conducting polymer modified by different methods was characterized by various techniques in order to confirm the incorporation of active groups, dopants etc.

4.3.1.1.Infrared spectroscopy

FT- IR spectra of Pani, CuPc incorporated Pani along with CuPc is given in the *figure 4.1* The incorporation of phthalocyanine in to the polymer chain was confirmed from the IR studies. The frequency data obtained and their probable assignments are presented in the *Table no 4.1.* The presence of characteristic IR absorption due to quinonoid and benzenoid rings at 1590 cm-1 and 1500cm-1 clearly indicates the presence of these two states in the polymer chain. The benzene ring C-C vibration stretching is observed around 1460cm^{-1}. Pc skeleton peak also observed at 1140cm^{-1} and 950cm^{-1}

From all the assignment given, incorporation of phthalocyanine in to the polymer chain is confirmed. [14-16]

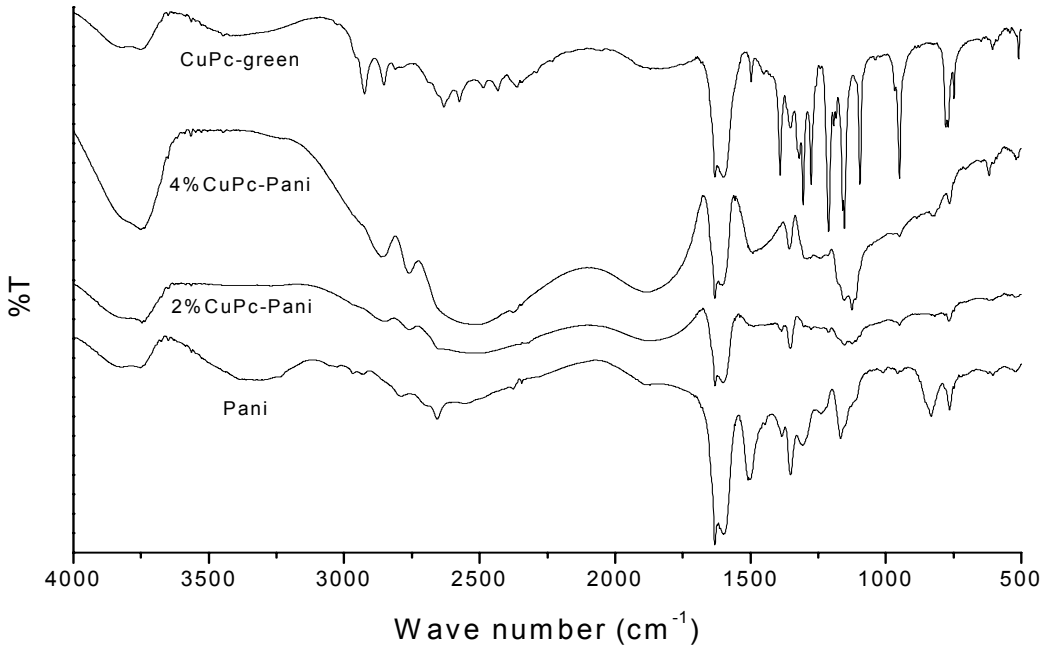

Figure 4.1: FT-IR spectra for Pani, CuPc-Pani along with CuPc green powder

	Pani	2%	4%	CuPc	Assignment
3788	m	m	s	m	
3350	br	--	--	br	NH
1590	s	s	s	s	Quinoid N=Q=N stretching
1500	s	w	m	-	Benzenoid N-B-N stretching
1460	m	w	br		Benzene ring stretching
1385	-	-	-	s	C-N stretching
1350	m	w	w	-	
1300	-	-	-	vs	C-N stretching
1220	-	-	-	vs	C=N stretching
1150	w	w	m	vs	Pc skeleton
940	-	w	w	vs	Pc skeleton
835	m	-	-	-	C-H out of plane deformation
760	m	w	w	s	C-H out of plane bending

*** m = medium, s = strong, w = weak, vs = very strong, br = broad**

Table 4.1 IR assignment of different modified Pani powders

4.3.1.2. UV-Vis studies

The UV-Vis spectrum of polyaniline depends strongly on the oxidation states. *Figure 4.2* shows the optical absorption of polyaniline (in sulphuric acid), polyaniline functionalized

with different concentration of copper phthalocyanine along with copper phthalocyanine green powder in the wavelength range of 200-1000nm. It could be seen that one new broad absorption bands occurring at 500nm which was associated with chlorinated phthalocyanine green moieties. Pure Pani has a broad absorption band occurring beyond 750nm, which is associated with the oxidation/doping of the polymer, giving rise to the polaronic states within the band gap. It is interesting to note that the main absorption band at 300nm of Pani is also affected by the presence of CuPc in the polymer. This can be due to the highly conjugated planar CuPc moieties attached to the main chain as well as high level of dopant present in these polymers as compared to pure Pani. The peak at 300nm is due to B-band. The weak absorption band at about 500nm is due to the vibrational overtones of Q band. Q band is responsible for the intense blue colour of the compound. Q band absorption is due to the □̃□* transition from HOMO a_1u symmetry to the LUMO of e_g symmetry [17,18]

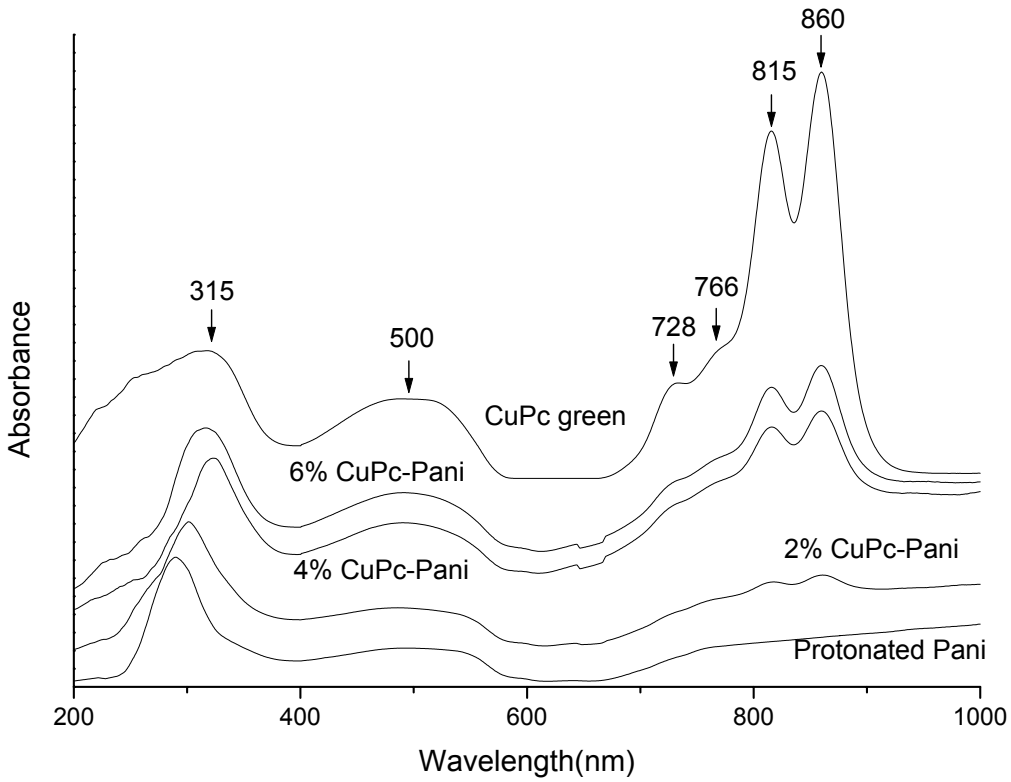

Figure 4.2 : UV-Vis of protonated Pani, 2%CuPc-Pani, 4%CuPc-Pani, 6%CuPc-Pani and Copper Phthalocyanine green in H_2SO_4 medium.

4.3.1.3. X-Ray Diffraction studies

Various workers have studied the synthesis and the structure of Polyaniline. Wang et al reported that with increase in the HCl concentration during preparation of Pani, crystallinity of Pani powder decreases. It was observed that Pani prepared at higher HCl concentration is complete amorphous in nature. Even though emeraldine salt ie. Pani-HCl is partially crystalline, it's base form or undoped Pani ie. emeraldine base is found to be amorphous. It was reported by Pouget et al. that when Pani was doped with HCl, crystalline character increases. In the current study, Pani was modified by incorporating phthalocyanine in the acidic medium. Changes in the nature of the polymer structure with

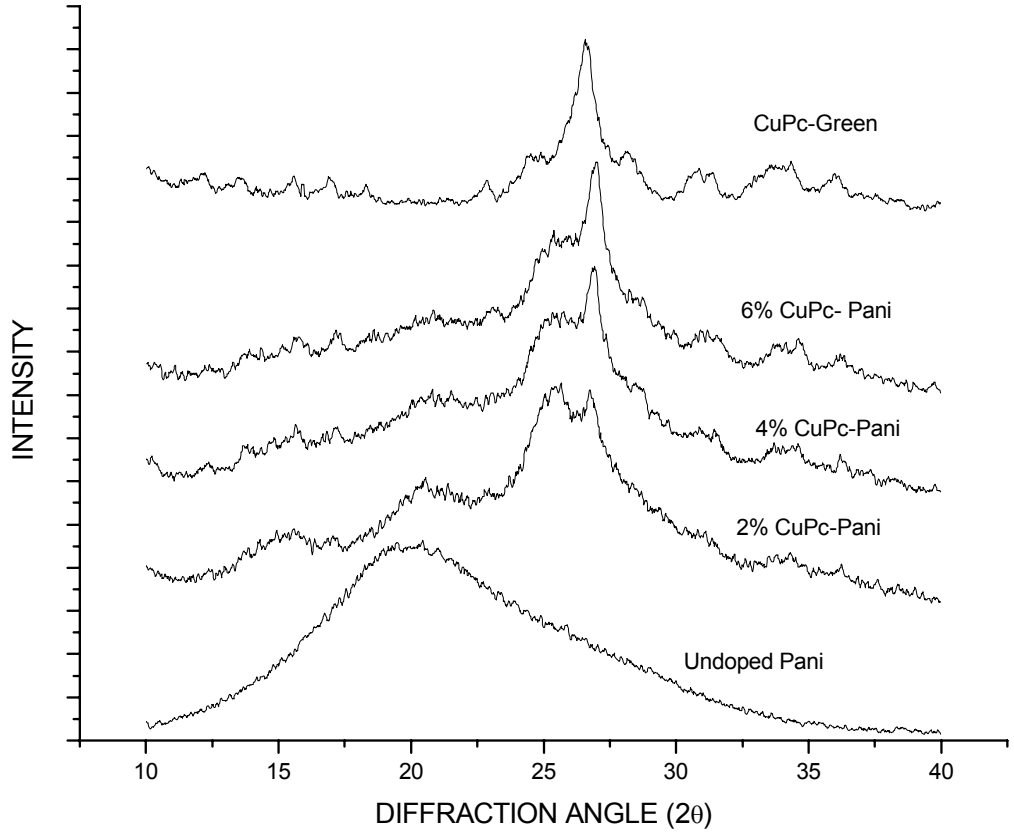

Figure 4.3: XRD of undoped Pani, 2%CuPc-Pani, 4%CuPc-Pani, 6%CuPc-Pani and copper phthalocyanine powder

the incorporation of macro cyclic phthalocyanine in to the Pani polymer matrix was investigated in this chapter. The X-ray diffraction patterns of the different modified Pani

were shown in the *figure 4.3.* The XRD pattern of undoped Pani is fully amorphous in nature having an amorphous halo in the 2θ of 20° which could be seen in the figure. It could be seen from the figure that as the percentage concentration of CuPc increases in the polymer, the peak at 20° decreases, whereas a sharp peak gradually appears in the 2θ of 27°. Some small reflections also appear at 31°, 33.9° and 36°. The XRD patterns indicate that the structure of Pani gets modified with the incorporation of CuPc green in the polymer. Overall crystallinity of the polymer increases and few reflections get enhanced suggesting better order in certain direction.[19,20]

4.3.1.4. X-ray Photoelectron Studies

X-ray photoelectron spectroscopy was run to monitor the changes occurring due to doping in the Pani films as well as Pani powder. XPS studies on chemically and electrochemically synthesized Pani showed the presence of quinonoid imine(-N=), benzenoid amine(-NH-) and positively charged nitrogen (-N^+) and protonated level or percentage protonation of Pani can be quantitatively calculated from the properly curve fitting the different components of the N1s core level spectrum. From the XPS studies one can reveal the presence of co-monomer, dopant ion etc also.

Polyaniline-CuPc powder

For that purpose chemically synthesized Pani and Pani powder incorporated with copper phthalocyanine are used for XPS study. XPS was carried out for the Pani films doped with $PdCl_2$ also along with the undoped one to study the changes occurring due to doping.

XPS studies were carried out for the chemically synthesized Pani and CuPc incorporated Pani powder along with the CuPc green powder, different core level spectra are shown in the *figure 4.4 (A), 4.4(B) and 4.4(C)* In the XPS studies of different modified Pani powders, Cl2p core level spectrum is observed, which reveals the presence of the CuPc and it is the proof of incorporation of CuPc in the Pani powders. In the *figure 4.4(A),* C1s core level spectra of Pani, 4%CuPc incorporated Pani and CuPc alone is shown. From the figure, four species could be seen in each case after deconvolution. The contribution for the neutral carbon specie appears at the lower BE energy which is at 284.6 eV for all the

cases. It is seen that the percentage contribution for neutral C is more than the charged species in case of Pani and the CuPc green powder, but the percentage charged species contribution is more in case of phthalocyanine incorporated Pani powder. These observations are tabulated in the *table no 4.2*.which is the table of C1s core level spectra with BE of various species, their FWHM and percentage area contribution.

The N1s core level spectra of different Pani are given in the *figure 4.4(B)***.** In the Pani powder, three peaks are observed having major contribution from the peak appearing at 399 eV which is due to the neutral species. The N1s spectrum of CuPc green can be deconvoluted in to four peaks which appear at the BE values of 398.4 eV, 400.2 eV, 401.5 eV and 404.1 eV. The peak which appears at 398.4eV is due to the N bearing negative charge. This may be due to the N connected to the Cu atom of copper phthalocyanine. It was observed from the N1s core level spectrum of Pani incorporated with 4%CuPc that there also four peaks appear after deconvolution. Presence of multiple peaks reveals the chemical interaction between the polymeric chain and the phthalocyanine macrocycle. Broadening of peaks also indicates structural changes taking place in case of CuPc incorporated Pani sample. The various data obtained from the N1s core level spectra are given in the *table no 4.3.*

	C1s	**B.E**	**FWHM**	**% Area**
Pani Powder	C1	284.6	1.64	71
	C2	286.18	1.77	22
	C3	287.69	2.04	7
CuPc Powder	C1	284.6	1.8	37.7
	C2	286.03	1.92	31.4
	C3	287.53	1.8	19.1
	C4	290.04	2.16	11.7
4% CuPc-Pani Powder	C1	284.6	2.28	40.7
	C2	286.24	2.04	41.9
	C3	288.96	2.04	10.9
	C4	291.16	2.16	6.5

Table 4.2 : Table of XPS data for C1s core level spectra for different samples

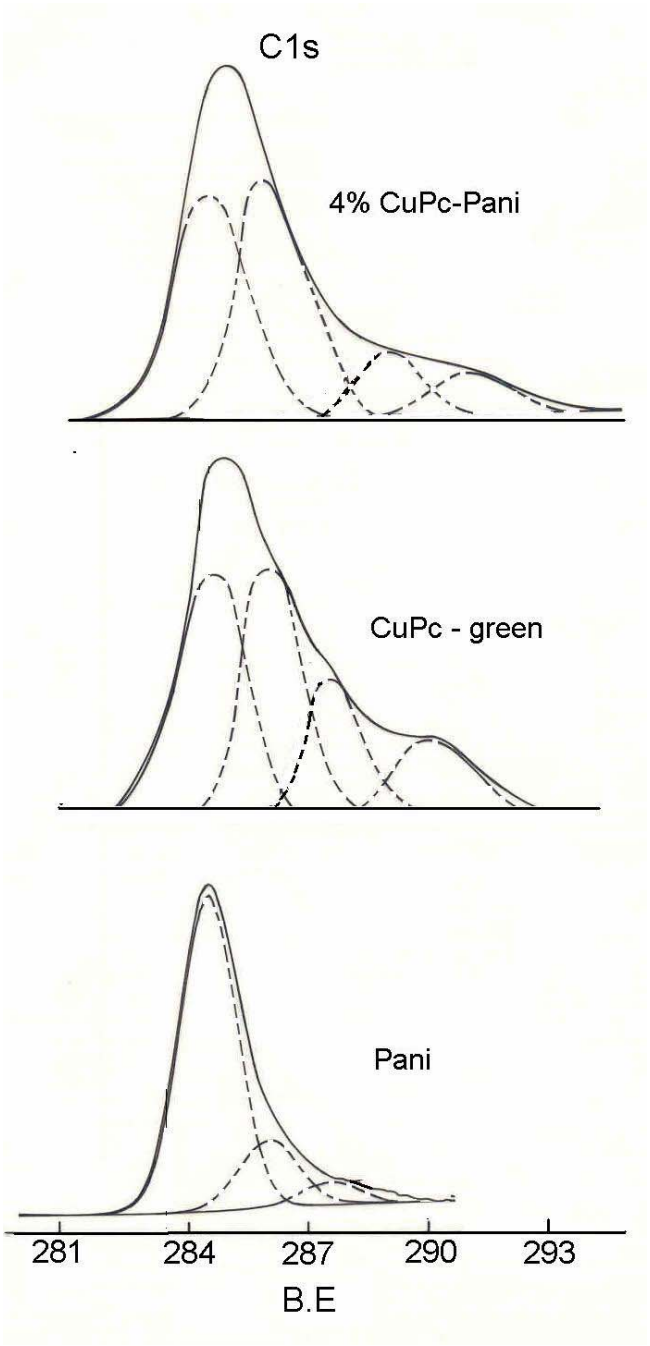

Figure 4.4(A): C1s core level spectra of Pani, Pani incorporated with CuPc and CuPc green powders

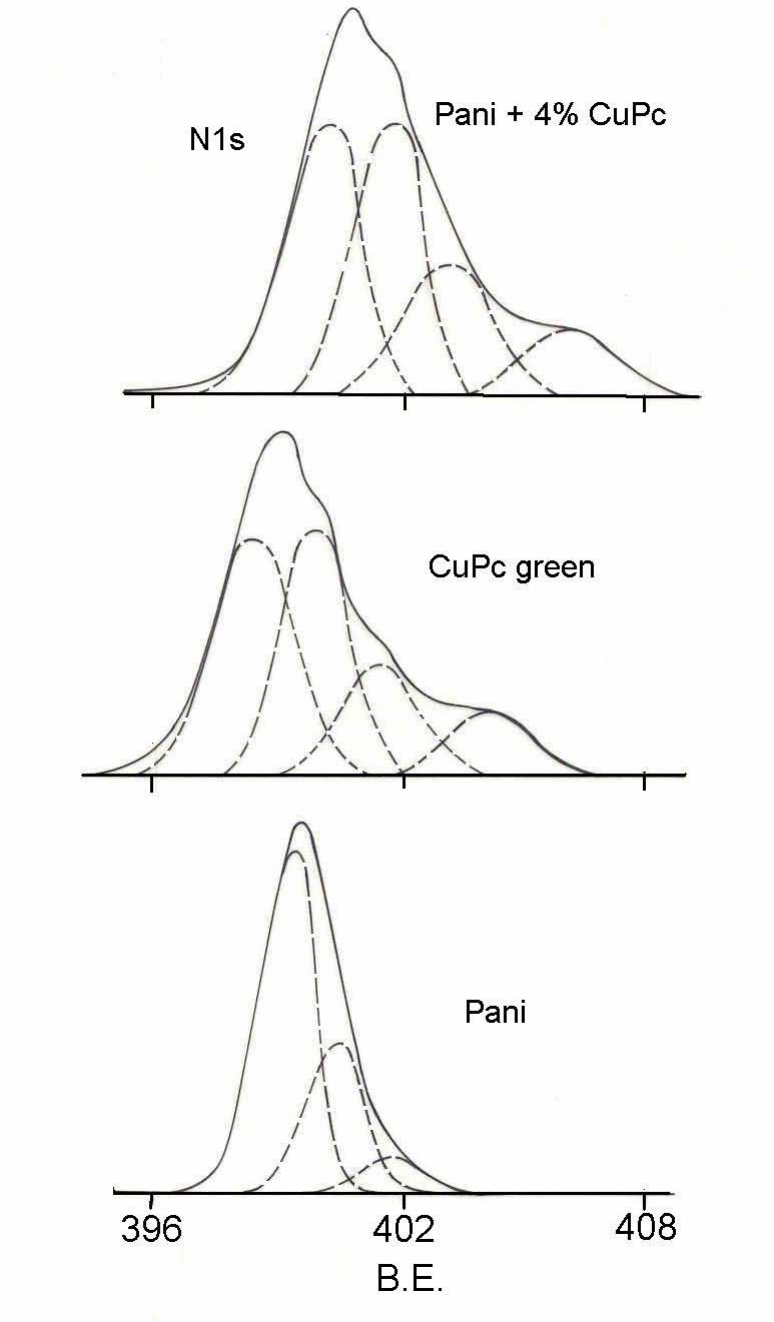

Figure 4.4(B): N1s core level spectra of Pani, Pani incorporated with CuPc and CuPc green powders

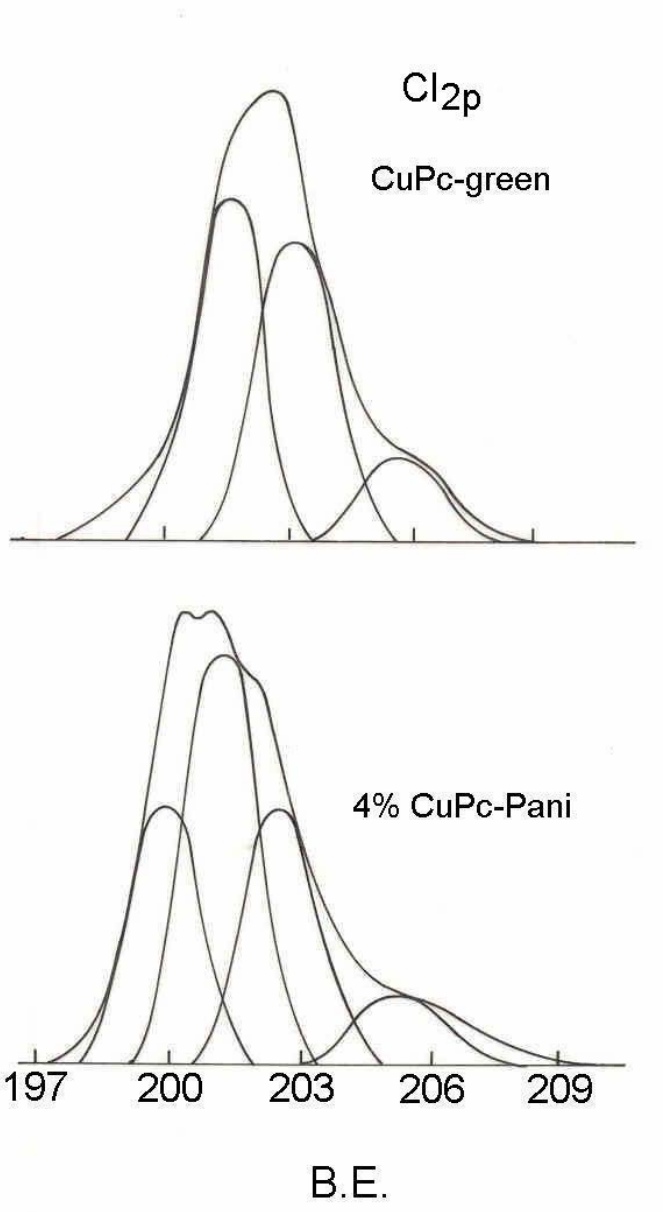

Figure 4.4(C): Cl2p core level spectra of Pani incorporated with CuPc and CuPc green powders

Pani Powder	*N1s*	**B.E**	**FWHM**	**% Area**
	N1	399	1.53	59.6
	N2	400.6	1.74	31.9
	N3	401.72	1.95	8.5
CuPc Powder	N1	398.4	2	36.8
	N2	400.2	1.83	33.8
	N3	401.5	2.1	17.9
	N4	404.1	2.35	10.5
4% CuPc-Pani Powder	N1	399.7	2	35.2
	N2	401.5	2.1	33.5
	N3	402.9	2.4	20.1
	N4	405.8	2.7	11.2

Table 4.3 : Table of XPS data for N1s core level spectra for different samples

	Cl2p	**B.E**	**FWHM**	**% Area**
CuPc Powder	Cl1	201.5	1.92	43.3
	Cl2	203.25	2.25	41.8
	Cl3	205.83	2.3	14.9
4% CuPc-Pani Powder	Cl1	199.85	1.87	26.3
	Cl2	201.05	1.8	39.3
	Cl3	202.2	2.02	26.4
	Cl4	204.87	2.5	8

Table 4.4: Table of XPS data for Cl2p core level spectra for different samples

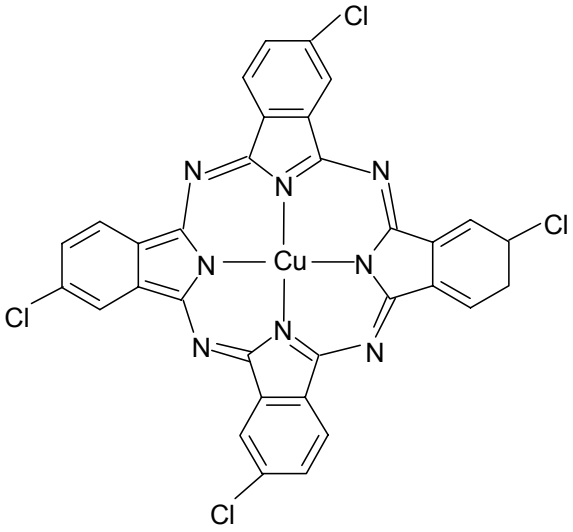

Figure 4.5: Structural representation of Copper Phthalocyanine (green) molecule

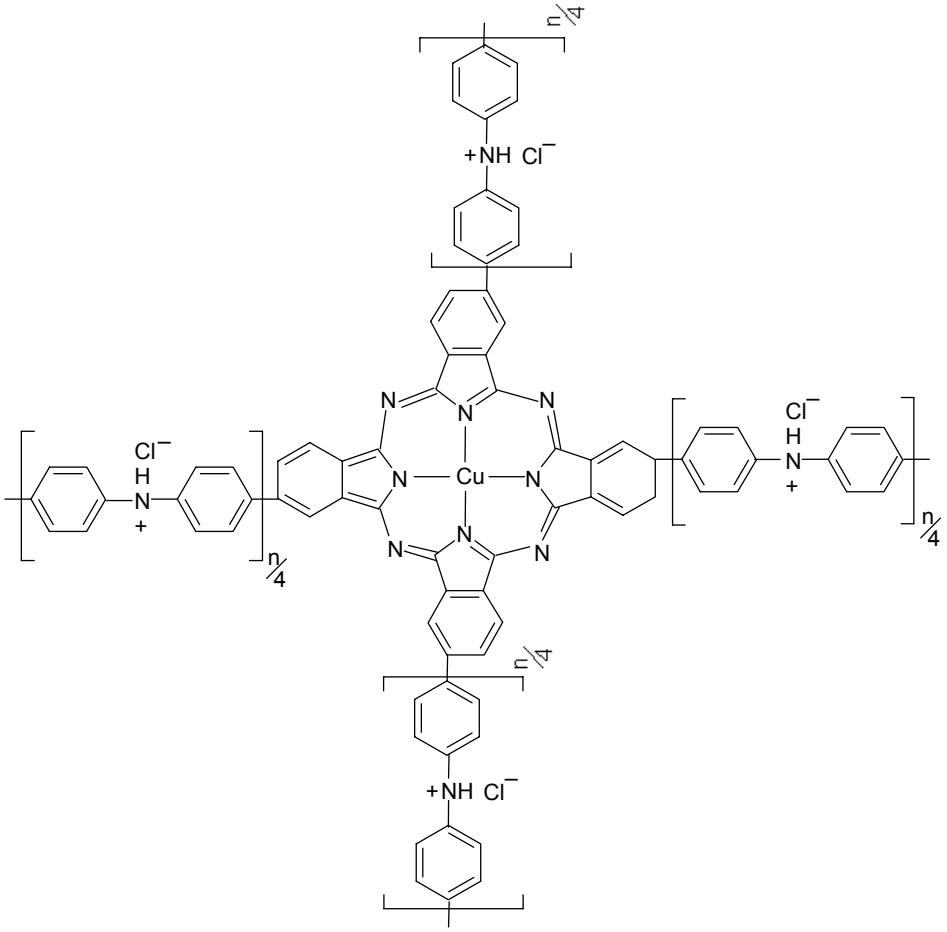

Figure 4.6: Structure of Copper Phthalocyanine incorporated Polyaniline polymer

The core level spectra of chlorine Cl2p for CuPc green and 4% CuPc doped Pani is shown in the *figure 4.4(C)*. The major peak at 203.3 eV in CuPc might be due do the covalently bonded Cl to the phenyl rings. This peak at 203.3 eV is absent in case of CuPc incorporated Pani sample which might be due to the reason that CuPc get attached to the Pani chain through these sites containing Cl atom as shown in the figure below.

Broadening of peak is also observed incase of CuPc incorporated Pani, which indicates the presence of more number of Cl species in the sample. The data obtained from the Cl_{2p} core level studies is presented in the *table no 4.4.* The higher BE obtained in case of CuPc sample might be due to the more degree of conjugation. Comparison of these data indicates that the covalently bonded Cl species decrease while charge Cl atoms increase when chlorophthalocyanine is incorporated in Pani. It is interesting to note that covalently bonded Cl also shows increase in BE than the normal. Chlorine attached to the phenyl ring is reported to appear in the BE of 201 eV, whereas in case of chlorine doped polyvinyl carbazole sample, the Cl_{2p} core level spectra appears at 202.5 eV. There are additional Cl^- species observed in CuPc incorporated Pani. Which can arise from the fact that Cl^- can be present at Pani as well as CuPc sites. Thus the dopant ion can be distributed in these two groups leading to different degree of charge transfer interaction. As degree of conjugation in case of CuPc is still more, the chlorine here is attached to the phenyl ring, which in turn is attached to another heterocyclic ring. Therefore, in case of CuPc, because of degree of the conjugation, the BE of Cl2p core level shifts to the higher BE. From all these studies it can be concluded that the CuPc incorporated polyaniline exists as a mixture of quinonoid - benzenoid type of structure.[21-27]

Polyaniline-$PdCl_2$ doped Films

XPS studies were done for the electrochemically polymerized undoped Pani film along with the $PdCl_2$ doped Pani film. For that purpose, Pani films were electrochemically prepared and then undoped using 0.1M NH_3 solution prior to doping with 0.012M $PdCl_2$ solution. The different core level spectra are shown in the *figure 4.7*

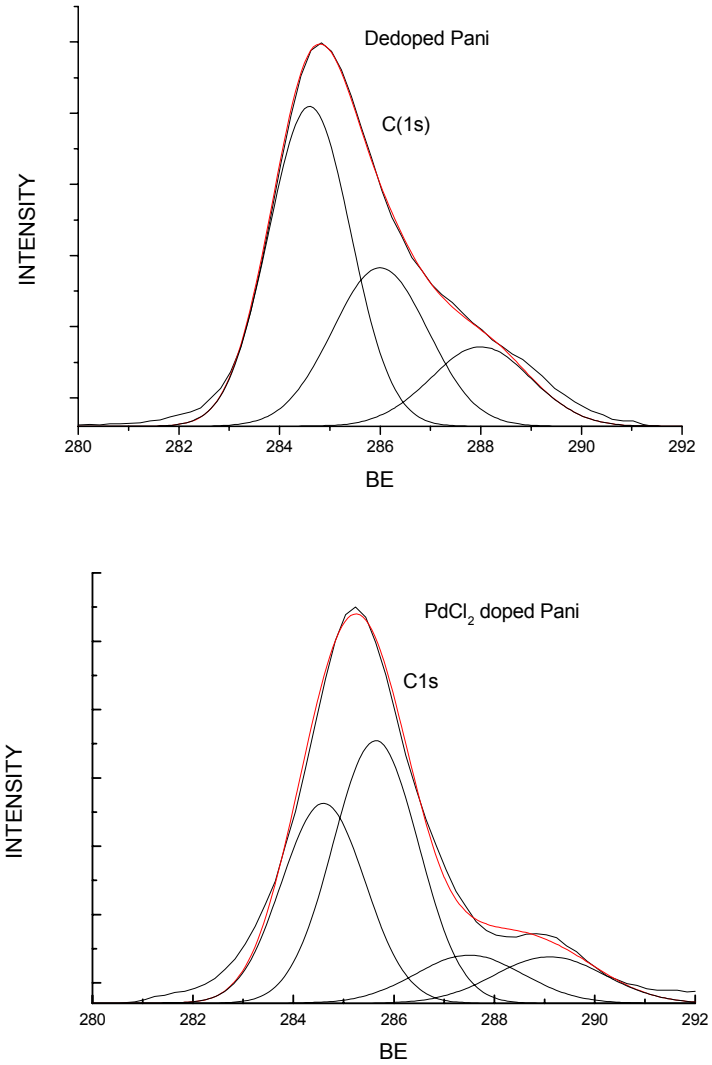

Figure 4.7(A) C1s core level spectra of undoped Pani and $PdCl_2$ doped Pani

Sample Name	Carbon C1s	Peak Position (BE)	FWHM (eV)	% Peak Area
Dedoped Pani	C1	284.6	1.63	53.2
	C2	286	1.9	30.6
	C3	288	2	16.2
$PdCl_2$ doped Pani	C1	284.6	1.66	33.74
	C2	285.64	1.7	45.35
	C3	287.5	2.15	10.51
	C4	289.1	2.2	10.4

Table 4.5: Table of BE position, FWHM and percentage charge of C1s core level spectra of undoped and $PdCl_2$ doped Pani

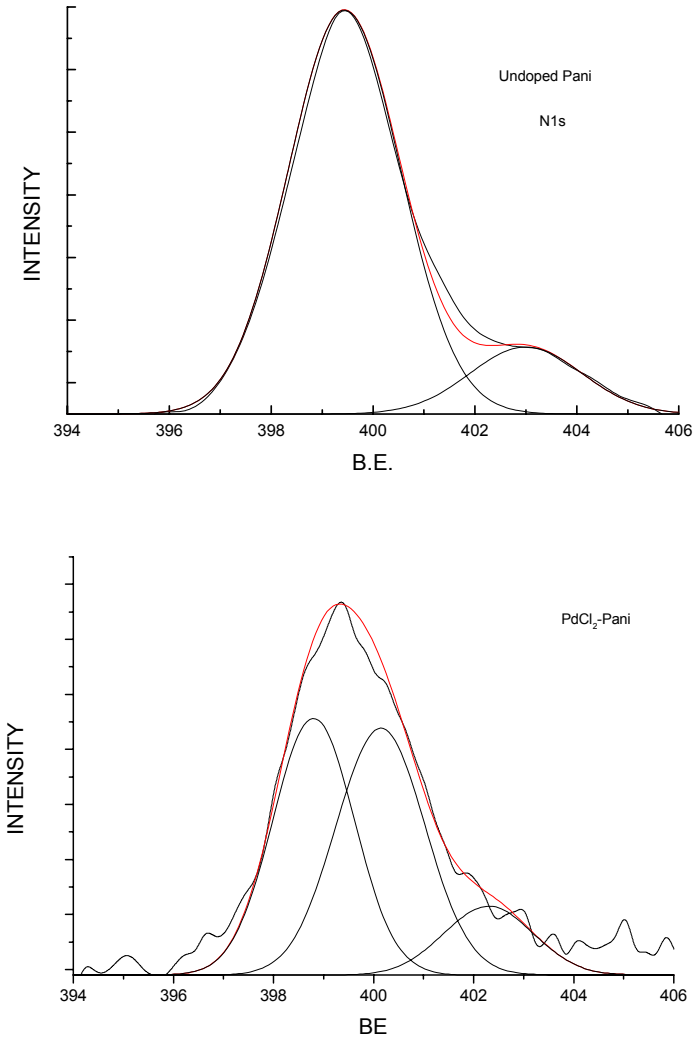

Figure 4.7(B) N1s core level spectra of undoped Pani and $PdCl_2$ doped Pani

Sample Name	Nitrogen N1s	Peak Position (BE)	FWHM (eV)	% Peak Area
Dedoped Pani	N1	399.4	2.2	85.8
	N2	403	2.2	14.2
$PdCl_2$ doped Pani	N1	398.9	1.62	42.7
	N2	400.14	1.77	44.7
	N3	402.3	1.78	12.58

Table 4.6: Table of BE position, FWHM and percentage charge of C1s core level spectra of undoped and $PdCl_2$ doped Pani

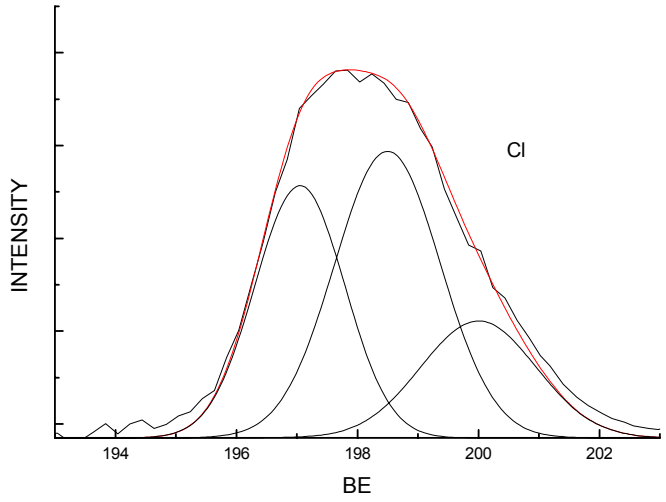

Figure 4.7(C) Cl2p core level spectra of $PdCl_2$ doped Pani

Cl 2p	BE	FWHM	%Area
Cl1	197.05	1.48	34
Cl2	198.5	1.75	45.7
Cl3	200	1.9	20.3

Table 4.7: Table of BE position, FWHM and percentage charge of Cl2p core level spectra of $PdCl_2$ doped Pani

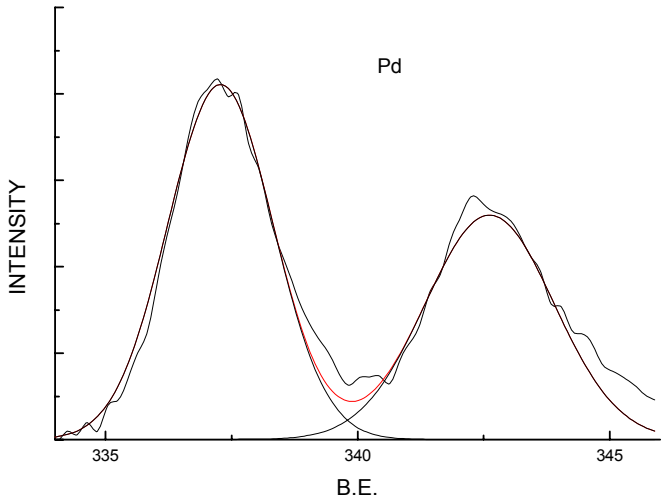

Figure 4.7(D) Cl2p **core level spectra of $PdCl_2$ doped Pani**

Pd	BE	FWHM	%Area
Pd	337.28	2.08	56.4
Pd	342.62	2.55	43.6

Table 4.8: Table of BE position, FWHM and percentage charge of Pd core level spectra of $PdCl_2$ doped Pani

Figure 4.7 (A) is the deconvoluted C1s core level spectra of undoped Pani and $PdCl_2$ doped Pani. From the figure it could be observed that in case of undoped Pani, three components ware seen, whereas for the $PdCl_2$ doped Pani four components were seen after deconvolution of the C1s core level spectra. In the undoped specie the percentage contribution for the neutral specie, ie. peak appearing at 284.6 eV, is more as compared to the $PdCl_2$ doped specie. The percentage charge species in case of undoped and the doped species 46.8% and 66.3% respectively. BE's, FWHM and percentage area contribution of the different components of Carbon C_{1s} core level spectra of both the samples is shown in the *table no 4.5*

The Cl2p core level spectra of $PdCl_2$ doped Pani shows three components at 197.05 eV, 198.5 eV and at 200 eV. The presence of 198.5 eV can be attribute to the Cl^-, since $PdCl_2$ is reported to show similar peak component in this region.[28-34]

4.3.1.5. Measurement of Electrical Properties:

The modified Pani incorporated with phthalocyanine powders as synthesized above were compression molded at an applied pressure of 3 tons for 1 minute. Room temperature conductivity of the pellets was measured using Keithley Electrometer, details of which are mentioned in the chapter II. Graph of room temperature conductivity versus percentage phthalocyanine in the Pani is given in the *figure 4.8.* From the graph it could be observed that with the increase in the percentage phthalocyanine incorporation in Pani polymer, conductivity increases. Phthalocyanine macrocycles have tendency to organize themselves and form stacks in which interaction between the large □-system of the adjacent rings in such a way to give greater conjugation length. Molecular stacking of phthalocyanine allows intermediate interactions necessary for electrical conductivity.

Hence with the increase in the concentration of phthalocyanine, molecular stacking and overlap of orbitals can lead to an increase in the overall conductivity.

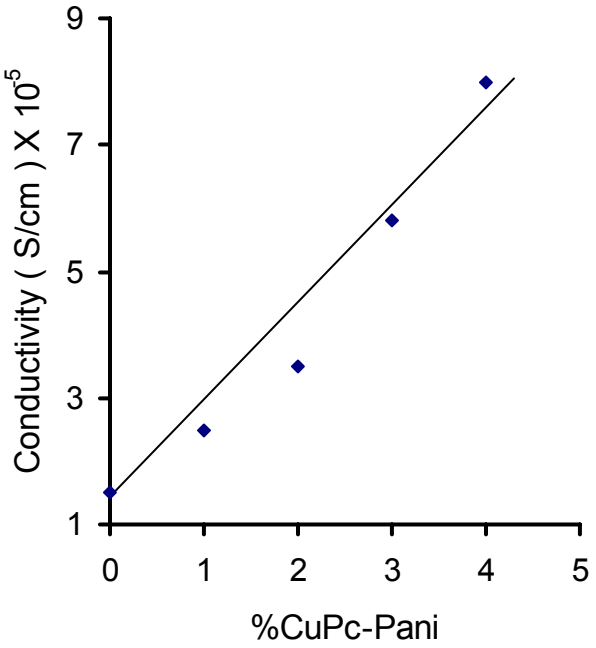

Figure 4.8: Graph of Room temperature conductivity against %CuPc-Pani powder

Percentage Phthalocyanine in Pani	Activation Energy (ΔE) eV
0	0.25
1	0.205
2	0.17
3	0.135
4	0.125

Table 4.9: Table of Activation Energy(ΔE) with % CuPc-Pani

The temperature dependence of conductivity for these pellets was also measured in the temperature range of 30° to 90°C. The activation energy for conduction was then estimated from the Arrhenius plots of these data using curve fitting procedure, and slopes of the linear portions of the graphs. Plot of activation energy (□E) versus phthalocyanine concentration is shown in the *figure.4.9* A gradual decrease in the activation energy was seen with increase in the phthalocyanine concentration. The pure Pani sample has □E

value of 0.25eV whereas 4% CuPc doped Pani has □E value of 0.125 eV. From the results, it could be predicted that by incorporation of phthalocyanine, the thermal excitation of the carriers become easier which either arises from the reduction in the band gap due to higher conjugation or introduction of additional defect/impurity states within the band gap. Further, the movement of charge carriers will be facilitated across the chains due to coupling between the CuPc groups, resulting in greater conductivity and less activation energy value.

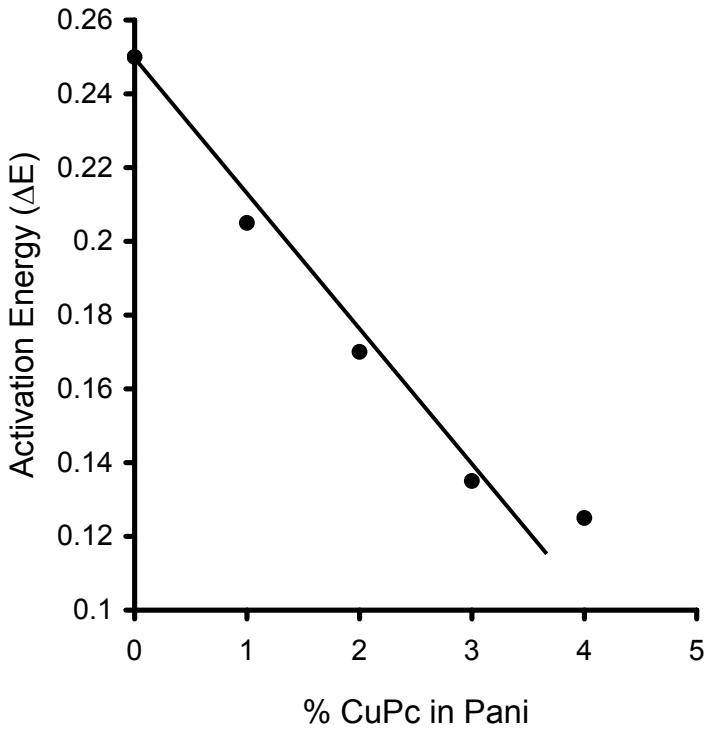

Figure 4.9: Graph of Activation energy against %CuPc-Pani powder

4.3.2. Conducting polymer coated electrodes for the electro-chemical oxidation of alkene:

4.3.2.1. Polyaniline –CuPc system

A) Decene electrochemical oxidation

The modified conducting PAni coated electrodes were employed for the electrochemical oxidation of decene in presence of secondary supporting electrolyte $CuCl_2$ of concentration 0.1M. The *figure 4.10* shows CV's for (a) bare Pt; (b) PAni coated electrode and (c) PAni modified with CuPc for decene oxidation reaction.

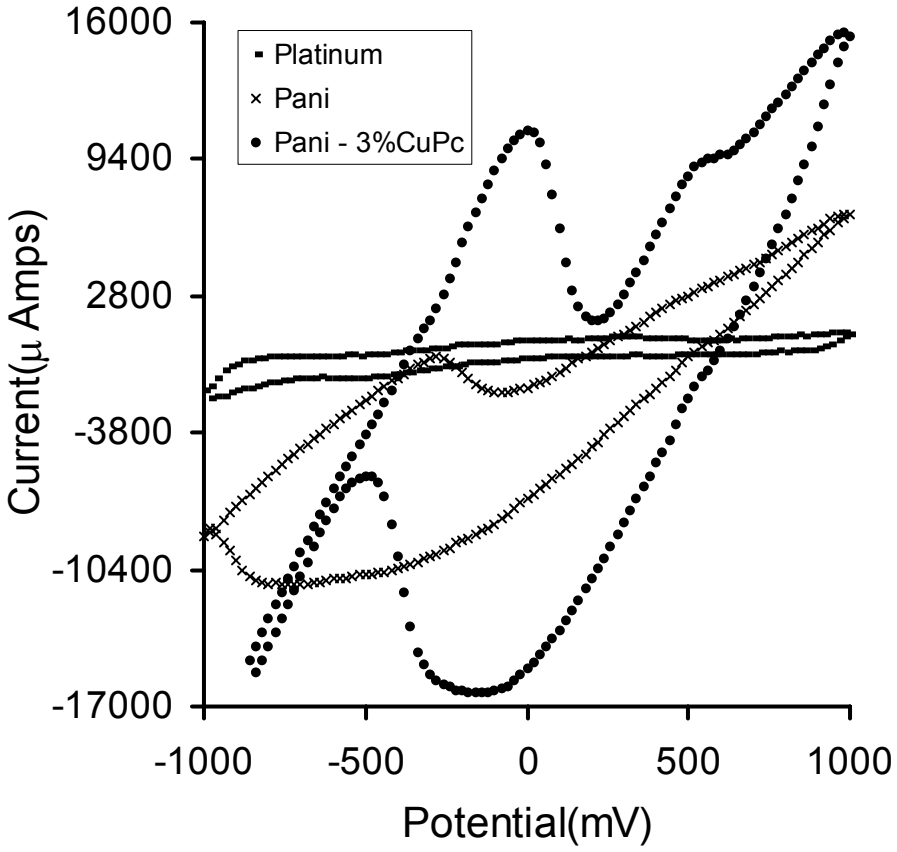

Figure 4.10: CV's of electrochemical oxidation of decene using bare platinum, Pani and CuPc incorporated Pani electrodes containing $CuCl_2$ in the electrolyte

The electrochemical activity in these cases is clearly seen to enhance with the modification of electrodes as evidenced by enhancement of current. In order to identify the nature and origin of the anodic current, the concentration of decene (reactant) was varied in the electrolyte and CV was recorded for each concentration. Reactant decene

concentration was increased from 0.01 to 0.5 M for CuPc modified Pani coated electrode which is shown in *Figure 4.11*. It could be observed that there are two anodic peaks which appear in the CV profile. First one is in the region of –100 mV to 0 mV and the second one at 600 mV. The first peak might be due to the CuPc-$CuCl_2$ interaction as it is independent of the concentration of the reactant decene. The second peak which appeared at 650mV (SCE) and the anodic current at this potential increased with the increase in

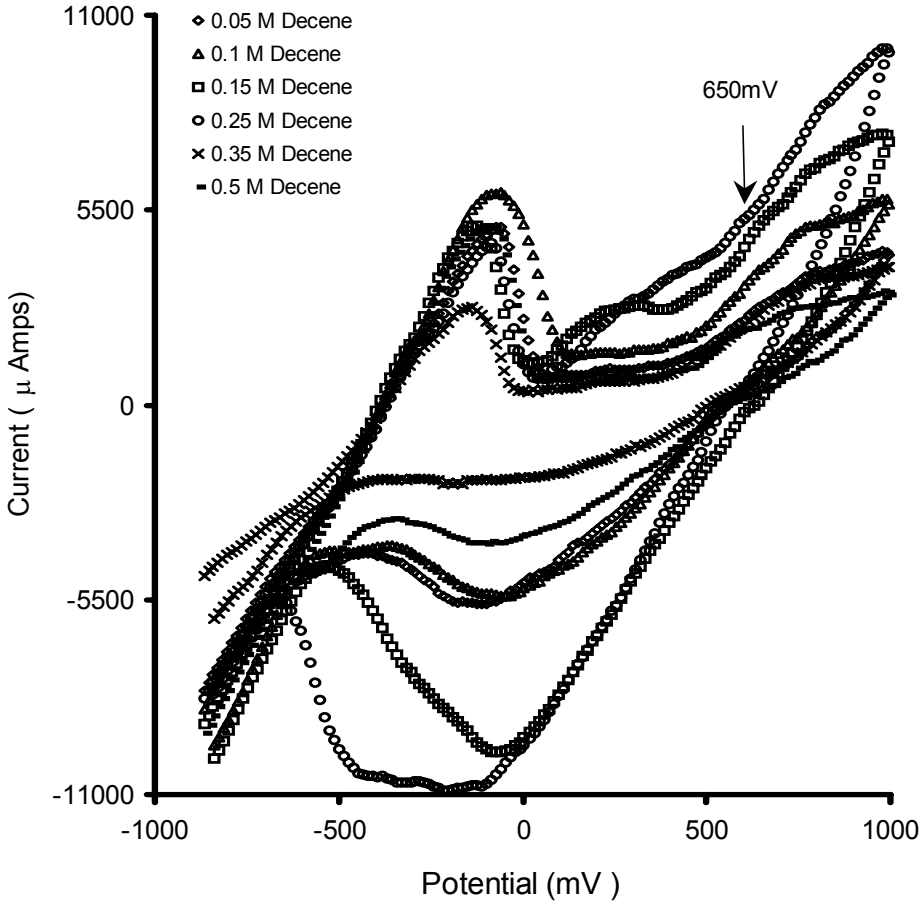

Figure 4.11: CV's of electrochemical oxidation of decene using 1%CuPc-Pani electrode for varying concentration of reactant in presence of 0.1M $CuCl_2$

concentration of decene. Thus anodic peak current at 650 mV is associated with the oxidation of decene. It could also be observed that the peak current increases till 0.25M decene concentration and further increase in the decene concentration, peak current

decreases which is due to the saturation of the reaction medium with reactant. With the further increase in the concentration of reactant, resistance of the medium increases, resulting in the decrease in the peak current. Phase separation was also seen to take place in the electrochemical solution after 0.25M decene concentration, which might prevent mobility of ions from the reactant to the electrodes.

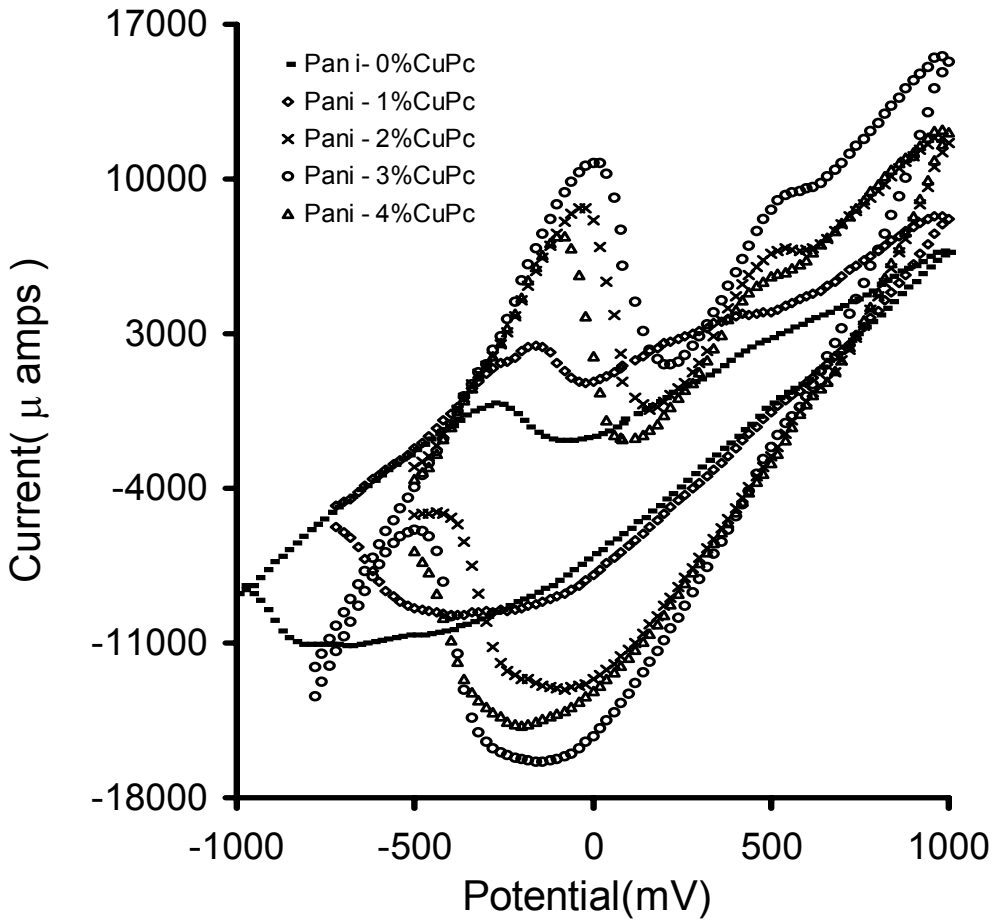

Figure 4.12 : CV's of electrochemical oxidation of decene using Pani modified with varying concentrations of CuPc containing 0.1M decene and 0.1M $CuCl_2$

As it is evident from the above observations that Pani modified with CuPc electrode is electrocatalytically active towards oxidation of decene, further experiments were carried out with varying concentration of CuPc doped Pani electrodes. Electrochemical oxidation reaction using Pani modified with varying concentration of CuPc for 0.1M decene in the

solution was carried out, CV's for which is shown in the *figure 4.12*.CV's indicate 3% CuPc doped Pani to be the optimum for decene oxidation reaction. With the further incorporation of the concentration of the CuPc in the Pani, anodic peak current decreases.

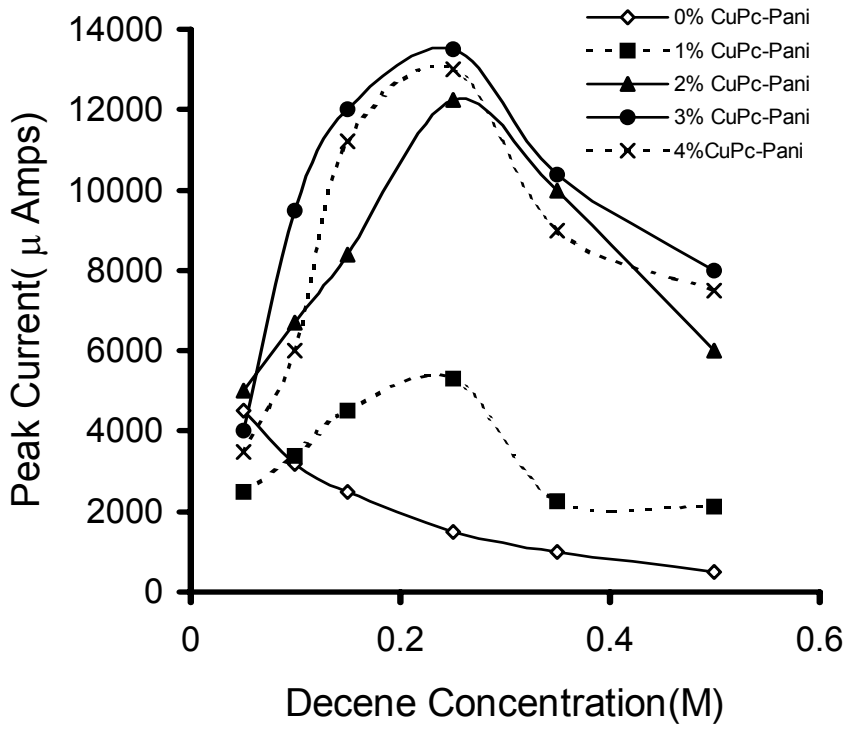

Figure 4.13: Graph of electrochemical oxidation of decene using different CuPc doped Pani electrodes for varying concentration reactant in the electrolyte.

From the CV's it could be observed that for polyaniline film (i.e. 0% CuPc) where the anodic wave is narrower whereas for 1%, 2%, 3% and 4% CuPc doped Pani CV's are broader in shape. It could also be observed that the anodic peak which appeared in the region of –100 mV to 0 mV increased with the increase in the concentration of CuPc in the Pani polymer. CV's of oxidation of decene using different CuPc-Pani electrodes were run for varying concentration of decene, but not shown here, instead graph of peak current against different decene concentrations for various CuPc-Pani electrodes are shown in the *figure 4.13.* From the graph it could be seen that as the percentage of incorporation of CuPc in the Pani increases till 3% catalytic activity increases but further increase in the concentration of CuPc catalytic activity decreases. It could also be observed that 0.25M concentration of decene was the optimum concentration for the

oxidation reaction under present condition. Further increase in the concentration of reactant peak current decreases which is due to the saturation of the reaction medium with reactant, resulting in phase separation which decreases ion mobility in the electrolyte. The variation of anodic current with the concentration of reactant can be explained as follows. For a given electrode there are certain number of sites/cm^2 at which the reactant gets adsorbed. Further the current depends on the resistance of the electrolyte which changes in presence of the reactant such as decene which is non polar. Hence, as the reactant content is increased, the number of sites get covered fully and current become high and reaches the maximum value. However, since the electrolyte conductance decreases the anodic current decreases. Thus for a given experimental condition and the electrode there is an optimum of reactant concentration for highest yield.

B) Hexene electrochemical oxidation

Electrocatalytic oxidation of hexene was also carried out with these CuPc incorporated polyaniline electrodes. CV's for varying concentration of hexene for 4% CuPc doped Pani is shown in the *figure 4.14* to confirm the oxidation process in the electrode. Anodic peak current in the region 600mV, increases with increase in the concentration of hexene indicating dependence of peak current with concentration of hexene. CV's of hexene oxidation for varying CuPc doped with Pani films electrodes is shown in the *figure 4.15.* From the CV's anodic peak current is found out for various concentration of

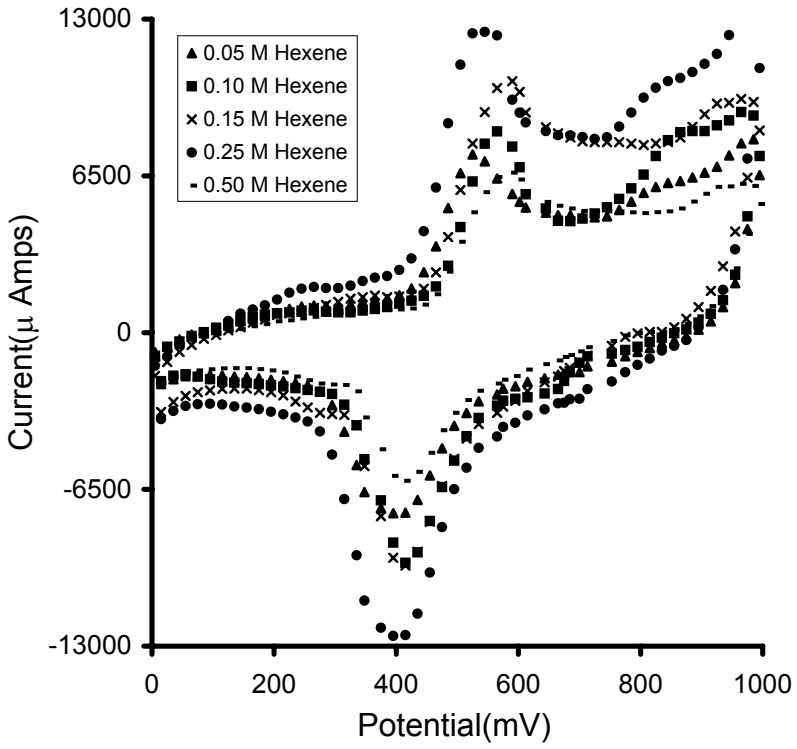

Figure 4.14: CV's of electrochemical oxidation of hexene using 4%CuPc incorporated Pani electrode with varying concentration of reactant.

CuPc-Pani graph of peak current against different concentration of hexene for varying CuPc– Pani electrodes are shown in the *figure 4.16.* In the figure, same trend, as in the case of decene electrochemical reaction, using CuPc-Pani electrode was seen, ie, 0.25M

Figure 4.15 : CV's of electrochemical oxidation of hexene (0.1M) using different Pani modified electrodes

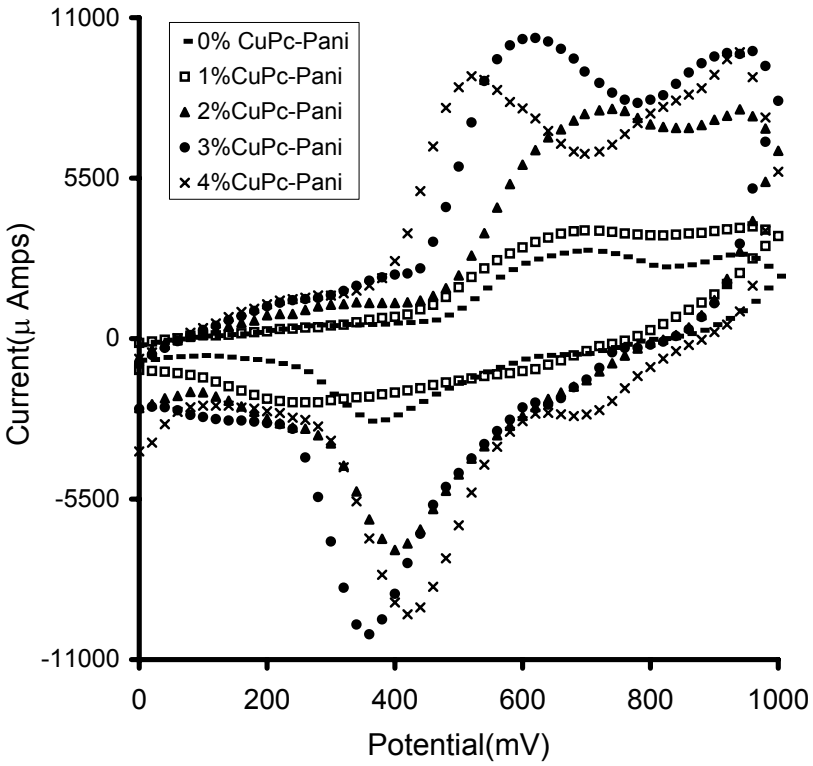

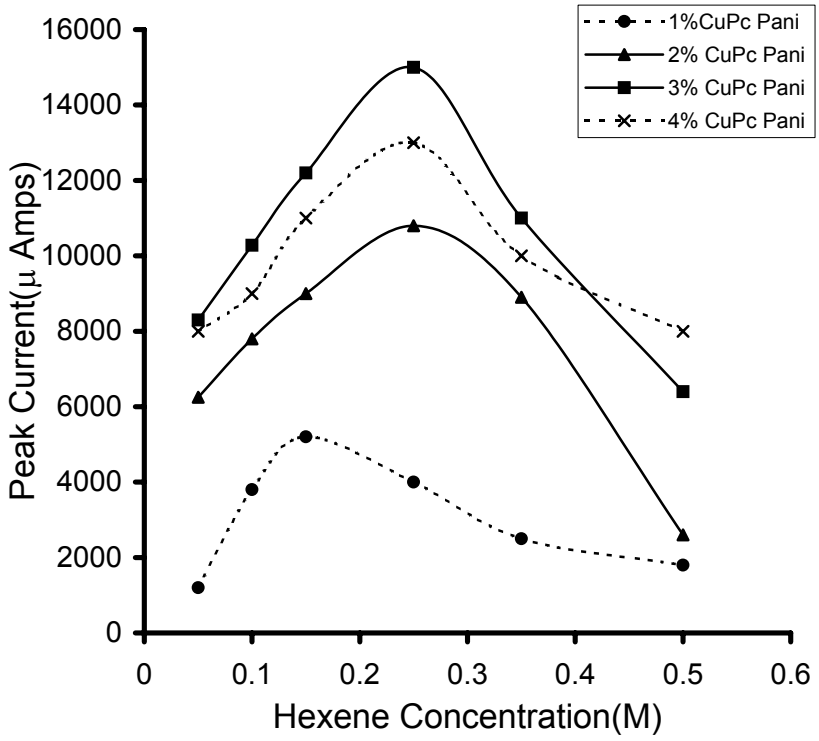

Figure 4.16: Graph of anodic peak current against concentration of hexene in the electrochemical oxidation of hexene using different Pani modified electrodes

is the optimum hexene concentration and 3% CuPc-Pani electrodes are the best electrodes for electrocatalytic oxidation of hexene.

4.3.2.2. Polyaniline doped with $PdCl_2$ electrodes

Conducting polyaniline films were modified by doping with $PdCl_2$ also and catalytic activity of these electrodes towards electrooxidation of decene was studied in presence of $CuCl_2$ in the electrolyte. CV's of the Pani film electrode doped with 0.012M $PdCl_2$ for varying concentration of $CuCl_2$ in the solution of 0.1M decene concentration is shown in the *figure 4.17*. $CuCl_2$ was used in the reaction mixture as it is known that for Wacker type oxidation, where salts of palladium based catalyst (Pd^{+2} salts) is used, Pd^{+2} is reduced to Pd^0 during the course of the reaction and in the presence of some reoxidant (e.g. $CuCl_2$, $MnCl_2$, $FeCl_3$ etc.) Pd^0 is converted back to Pd^{+2}. It was seen in the CV's that with increase in the concentration of $CuCl_2$ in the reaction mixture the peak current at 650 mV increased up to certain concentration of $CuCl_2$ and further increase in the concentration peak current in this region decreased.

$$H_2C = CH_2 + H_2O + PdCl_2 \longrightarrow H_3C - CH = O + Pd(0) + 2HCl$$

$$Pd(0) + 2CuCl_2 \longrightarrow PdCl_2 + 2CuCl$$

$$2CuCl + 2HCl + \frac{1}{2}O_2 \longrightarrow 2CuCl_2 + H_2O$$

$$H_2C = CH_2 + \frac{1}{2}O_2 \longrightarrow H_3C - CH = O$$

It could be observed in the figure that polyaniline doped with $PdCl_2$ also shows some catalytic activity towards decene oxidation, but in presence of $CuCl_2$ in the electrolyte catalytic activity increases tremendously. Here, Wacker type oxidation process can be envisaged in conducting polymer, in which these switch from one oxidation state to another and $CuCl_2$ might help in regenerating the catalyst. A typical reaction scheme is shown below. Pani when doped with $PdCl_2$, it is in the oxidized state and Pd is in the +2 oxidation state. But when this catalyst is used in the oxidation of □-olefin in presence

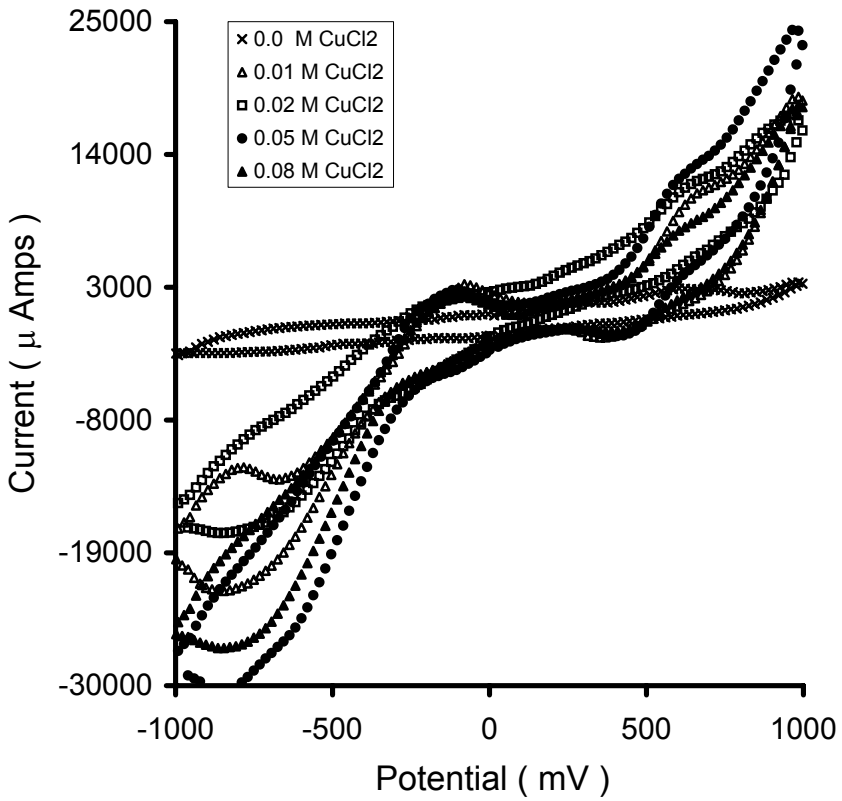

Figure 4.17:CV's of the electrochemical oxidation of decene(0.1M) using 0.012M $PdCl_2$ doped Pani electrode with varying concentration of $CuCl_2$ in the electrolyte

of reoxidant $CuCl_2$, the Pani catalyst oxidizes the reactant, but during the course of the reaction Pani itself gets converted to its reduced state. During the reaction Pd(II) also gets converted to the Pd(0) state. This Pani- Pd in the reduced state, gets reoxidized to it's original oxidation state with the reoxidant $CuCl_2$. Sobczak et al had studied the chemical hydrogenation of alkynes using polyaniline doped with palladium and platinum. Pani powder in the semi-oxidized form ie, emeraldine form was doped by exposing the

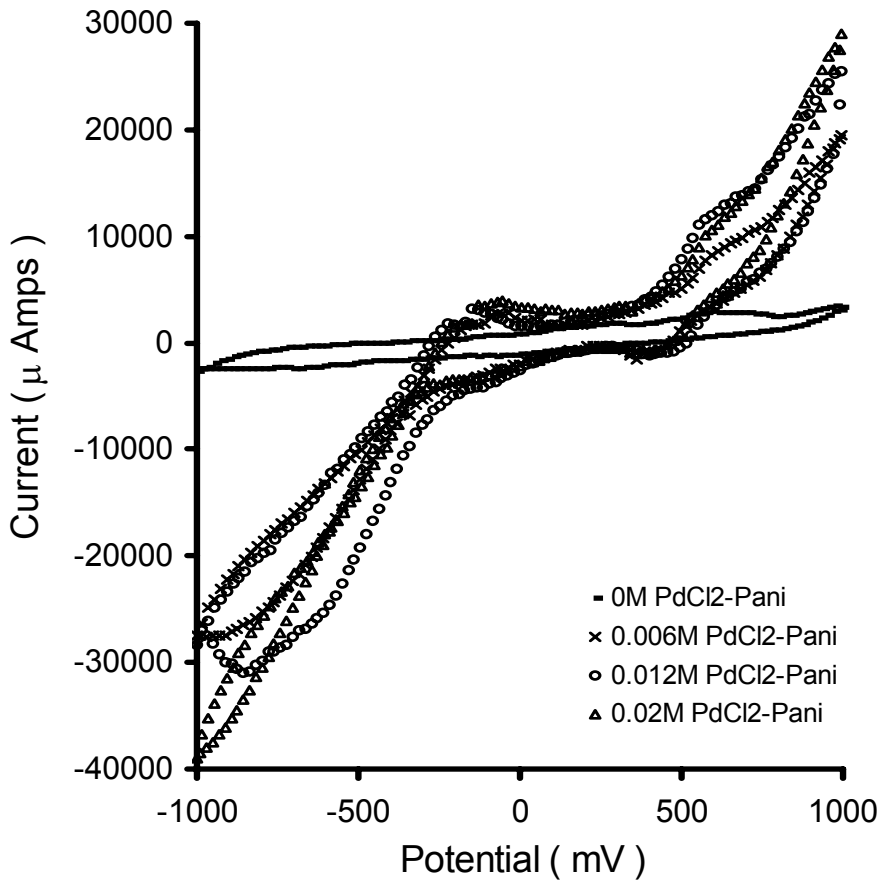

Figure 4.18: CV's of electrochemical oxidation of decene (0.1M) using different $PdCl_2$ doped Pani electrodes in presence of 0.05M CuCl2 in the electrolyte

powder to aqueous solution of H_2PtCl_2 and H_2PdCl_4. They found that these type catalysts were very active and selective in nature. Tsuji et al had reported the oxidation of olefins to ketones in combination with electrooxidation by the catalyst $Pd(OAc)_2$ and benzoquinone. In the oxidation process, Pd^{+2} is reduced to Pd^0, and in presence of reoxidant benzoquinone, Pd^0 oxidized back to Pd^{+2} state. During his process olefin get converted to methyl ketone.

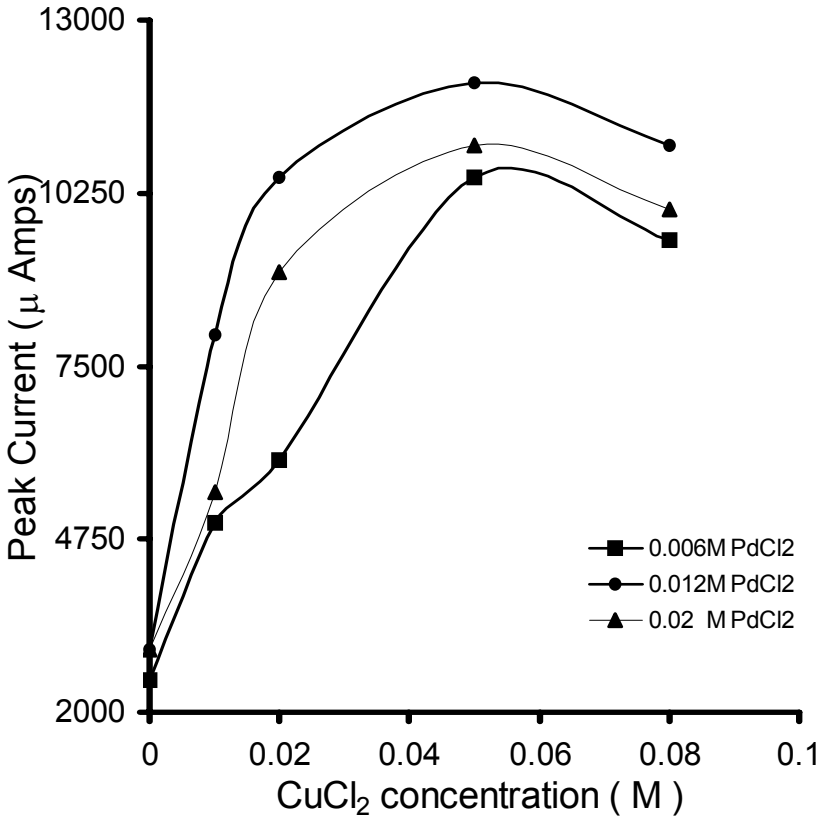

Figure 4.19: Graph of anodic Peak current for decene(0.1M) oxidation using different $PdCl_2$ doped Pani electrodes against $CuCl_2$ concentration in the electrolyte

As it was observed that $PdCl_2$ doped polyaniline was catalytically active in presence of $CuCl_2$, it was essential to find out the optimum concentration of $PdCl_2$ in the polyaniline electrode which gave maximum catalytic activity toward decene oxidation. For that purpose electrochemical oxidation of decene was carried out with varying concentration of $PdCl_2$ doped polyaniline electrodes with different $CuCl_2$ concentration in the solution. Decene concentration was 0.1M in the electrolytic solution. Representative CV's of polyaniline doped with varying concentration of $PdCl_2$ for 0.1 M decene oxidation in presence of 0.05M $CuCl_2$ is shown in the *figure 4.18*. From the CV's it could be observed that 0.012M $PdCl_2$ shows maximum catalytic activity. From the CV's of varying concentration of $PdCl_2$ doped Pani electrodes for different $CuCl_2$ concentration in the

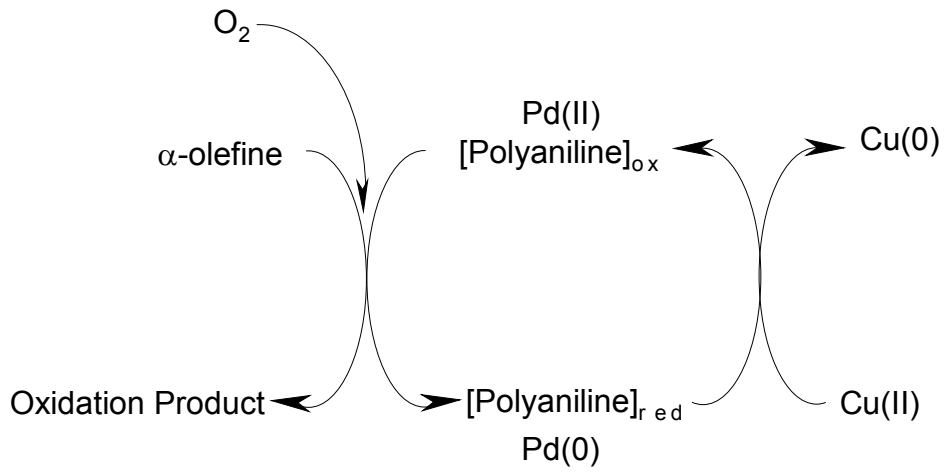

Figure 4.20. Reaction scheme for oxidation of α-olefine with Pani-$PdCl_2$/ $CuCl_2$ system

electrolyte, a graph of peak current against these parameters were plotted which is shown in the *figure 4.19* From the graph it could be seen that 0.012M $PdCl_2$ is best electrocatalyst among these different $PdCl_2$ doped Pani electrodes and 0.05M is the optimum concentration of $CuCl_2$ for different doped electrodes. Hwang et al had carried out electrochemical assisted Wacker oxidation of 1-butene. They used phosphomolybdate as the reoxidant. Several reports are available of using Pd or polymer supported Pd catalyst system for the oxidation processes.[35-45]

4.3.2.3. Polypyrrole doped with different transition metal dopants

The conducting PPy modified with doping externally with dopants of different electronegativities were employed for the electrochemical oxidation of hexene and decene. The *figure 4.21* shows CV's for (a) bare Pt; (b) electrochemically deposited PPy electrode and (c) PPy modified with $ZrCl_4$ for hexene oxidation reaction. The electrochemical activity towards oxidation of hexene in case of modified electrode is clearly seen to enhance as evidenced by enhancement of current. These experiments were carried out in the acetonitrile medium in presence of $HClO_4$ electrolyte. Prior to carrying

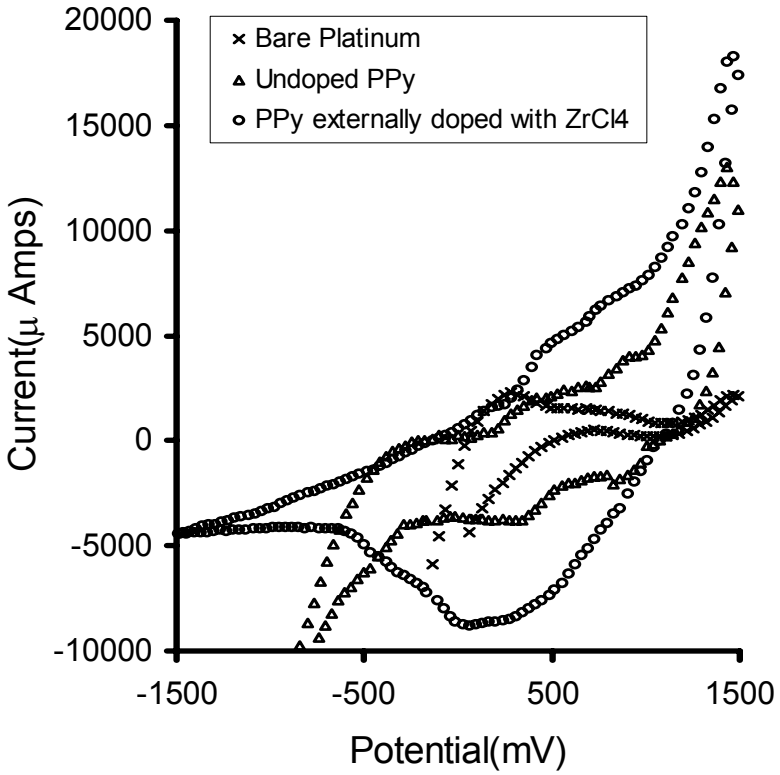

Figure 4.21: CV's of electrochemical oxidation of hexene using bare Pt, undoped PPy and PPy externally doped with $ZrCl_4$ electrodes

out the reaction, oxygen was bubbled through the reaction medium for half and hour. Further reaction was carried out in presence of electrolytes $LiClO_4$ and $HClO_4$ to find out the better electrolyte for oxidation reaction, CV's of which is shown in the *figure 4.22*

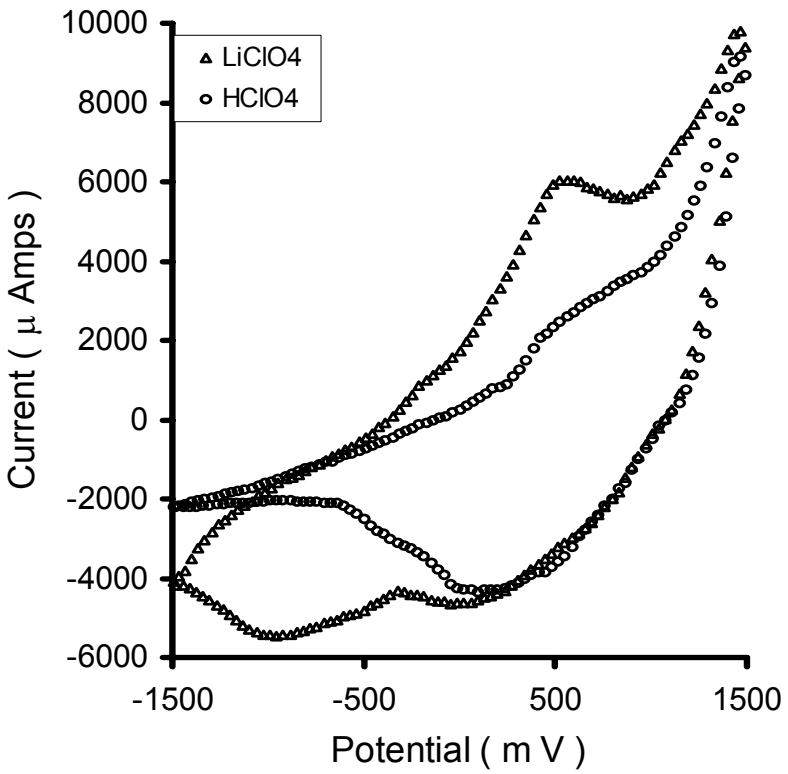

Figure 4.22: CV's of hexene electrochemical oxidation using PPy externally doped with $ZrCl_4$ electrodes in presence of $HClO_4$ and $LiClO_4$ in the electrolyte.

.From the figure it could be observed that even though in presence of $HClO_4$ PPy electrode gives good electrocatalytic activity towards hexene oxidation in acetonitrile medium, $LiClO_4$ gave much better results. It could also be observed that in presence of $LiClO_4$ electrolyte the oxidation peak is more prominent. Hence, further experiments were carried out using $LiClO_4$ electrolyte.

CV's for PPy doped with $ZrCl_4$ for varying concentration of hexene is given in the *figure 4.23.* Increase in peak height with increasing concentration of reactant in the anodic

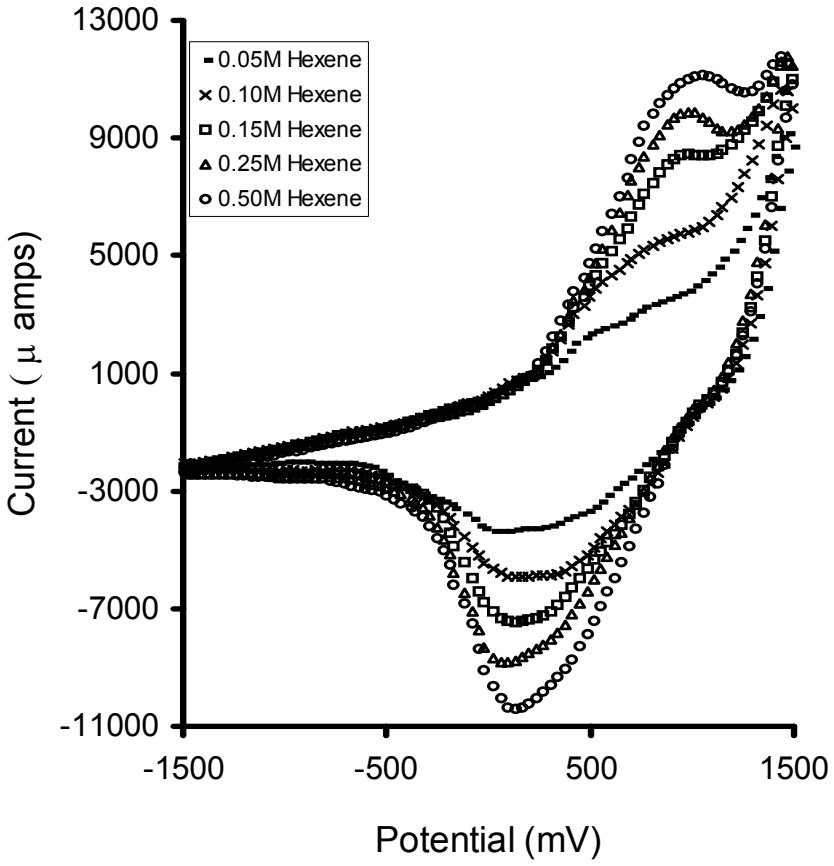

Figure 4.23: CV's of electrochemical oxidation of hexene using PPy externally doped with $ZrCl_4$ electrode for varying concentration of reactant in the electrolyte

region is the evidence for the hexene oxidation which could be seen in the above figure. As it was proved that PPy films modified by transition metal doping agents are catalytically active, it was essential to find out the most suitable dopant ion for electrocatalytic oxidation of hexene. Further experiments were performed employing transition metal salts of different electronegativities vis. $ZrCl_4$, $PdCl_2$, $MnCl_2$, $FeCl_3$, $CoCl_2$, $CuCl_2$ and $NiCl_2$ as the dopant agents. CV's of PPy doped with these doping agents for hexene oxidation is shown in the *figure 4.24.*

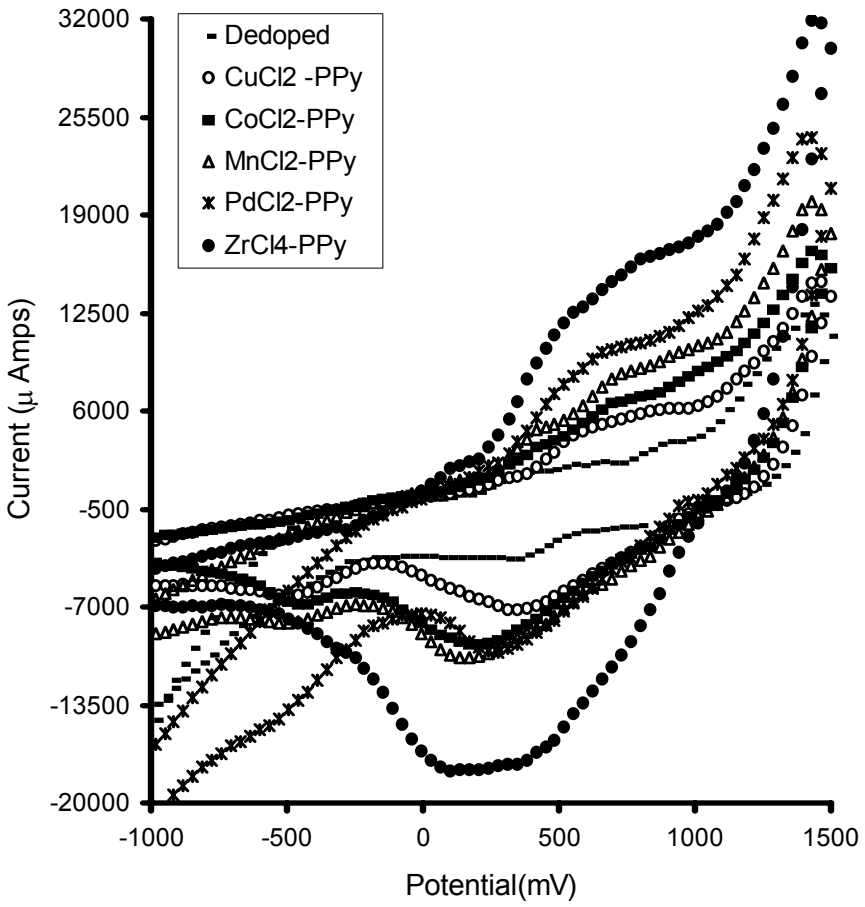

Figure 4.24: CV's of electrochemical oxidation of hexene using different PPy externally modified electrodes

Tremendous increase in the peak current was observed when the PPy films were doped with different dopant agents as compared to the undoped state. Here in the hexene oxidation also lower electronegative dopant ions like $ZrCl_4$ gives maximum catalytic activity whereas the higher electronegative dopant agents like $CuCl_2$ gives lowest catalytic activity towards hexene oxidation, which could be seen in the *graph 4.25* is the plot of peak current for hexene oxidation vs. electronegativity of the different doping agents Similar trend in the catalytic activity was observed in case of methanol oxidation also, which is described in the chapter III..

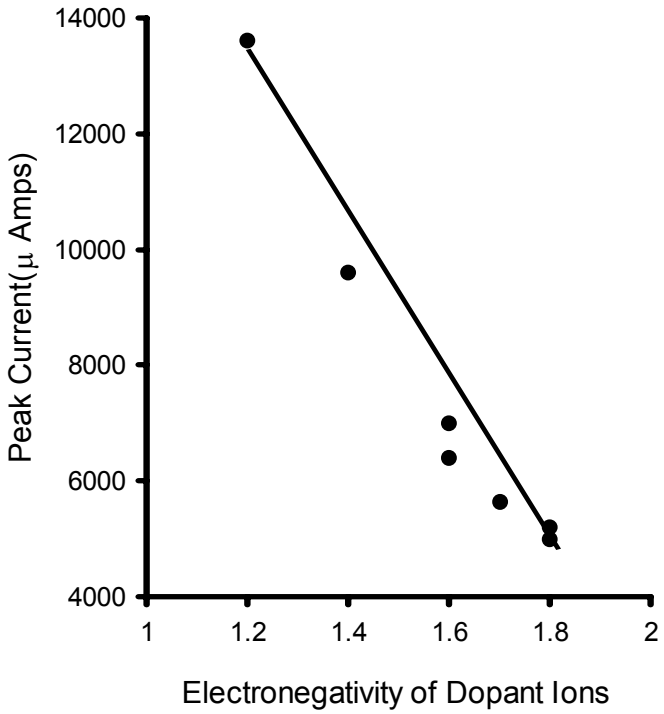

Figure 4.25: Graph of peak current against electronegativity of dopants in the electrochemical oxidation of hexene(0.1M) using different PPy modified electrodes

In order to investigate the reason for the better catalytic activity of the PPy doped with lower electronegative dopant ions towards hexene electrooxidation, energy level of the each dopant ions with respect to PPy was plotted. Electrical properties of the PPy doped with different ions were measured in order to obtain the position of the impurity levels with respect to the valence / conduction band. From the temperature dependence of conductivity the activation energy (in eV) was estimated for each sample which was shown in the *Table 4.10* . The energy level representation for these electrodes with respect to PPy in contact with Hexene containing electrolyte and gold backing layer is shown in the *Figure 4.26.* It could be seen from the energy level representation that for PPy doped with $ZrCl_4$ electrodes, it was easier for electrons to be transferred from the reactant hexene to the electrode than in other cases. The electron transport from electrolyte to electrode or hole transport from electrode to reactant leads to the oxidation of hexene in presence of O_2. In the hexene electro-oxidation reaction also the primary rate determining step appears to be controlled by the charge transport at the anode. Hence, the energy level of the dopant in the polymer appears to be very important in the electro-oxidation process using conducting polymers.

Dopant Ions	**ΔE(eV)**
$ZrCl_4$	0.2462
$PdCl_2$	0.2563
$MnCl_2$	0.32
$FeCl_3$	0.3785
$CoCl_2$	0.3534
$CuCl_2$	0.3979
$NiCl_2$	0.4118

Table 4.10: Table of electronegativity of the dopants with Activation energy in eV.

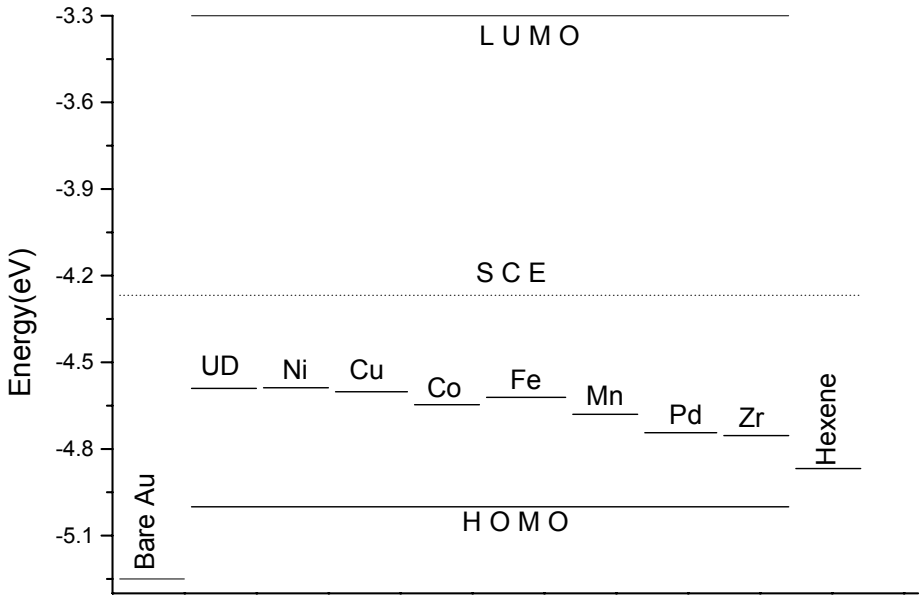

Figure 4.26: Energy level representation of PPy modified electrodes in contact with hexene

Modified polypyrrole electrodes are active towards electrooxidation of decene also. CV's of different concentration of decene for $ZrCl_4$ modified electrode is given in the *figure 4.27.* From the figure it could be observed that with increase in the decene concentration peak current increases which is the evident of electroactive nature of the electrodes towards decene oxidation. Multiple peaks are observed in the CV's of decene oxidation

using $ZrCl_4$ doped PPy films electrodes. Initially at 350mV and 500mV peaks are seen but with time peaks get shifted to the higher potential region. This might be due to the step wise oxidation of decene. In the first step one product is formed, which further gets oxidized to the other products.

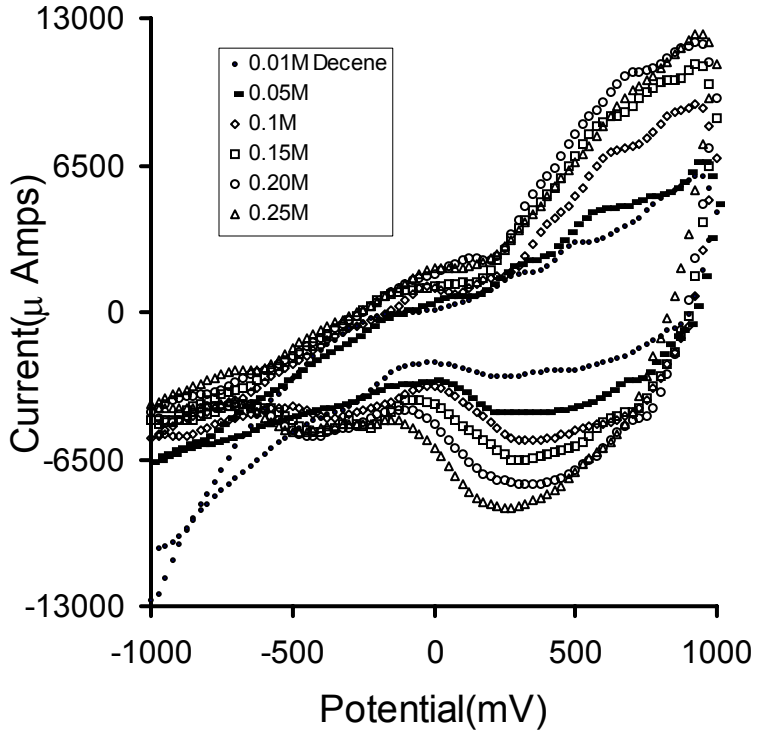

Figure 4.27 : CV's of electrochemical oxidation of decene using PPy externally doped with ZrCl4 electrode with varying concentration of reactant.

PPy films internally doped with various doping agents were also used for the electrooxidation of hexene. CV's of different doping agents is given in the *figure 4.28*. In case of the insitu doped PPy electrodes also lower electronegative dopant ions gives maximum catalytic activity towards hexene oxidation.

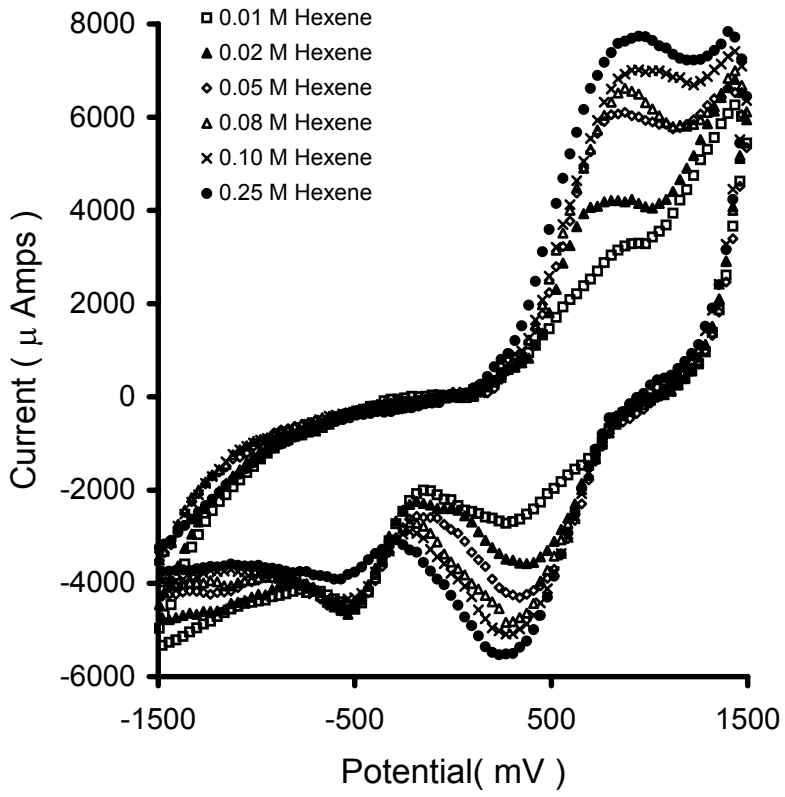

Figure 4.28: CV's of electrochemical oxidation of hexene using PPy insitu modified with $ZrCl_4$ electrode for varying concentration of reactant

4.3.3. Kinetic Study for Decene and Hexene electrochemical oxidation

i. Decene electrochemical oxidation:

(a) Kinetics of decene electrochemical oxidation was carried out using CV's of Pani – CuPc electrodes of varying decene concentration. Slope of the log I vs. log C plot gives α i.e. electron transfer coefficient which is equal to 0.4. Graphs of which are given in the *figure 4.29 A and figure 4.29B*

(b) Electron transfer coefficient for electrochemical oxidation of decene using PPy doped $ZrCl_4$ electrodes was also found out, which is equal to 0.55. Graphs are given in the *figure 4.30A and figure 4.30B*

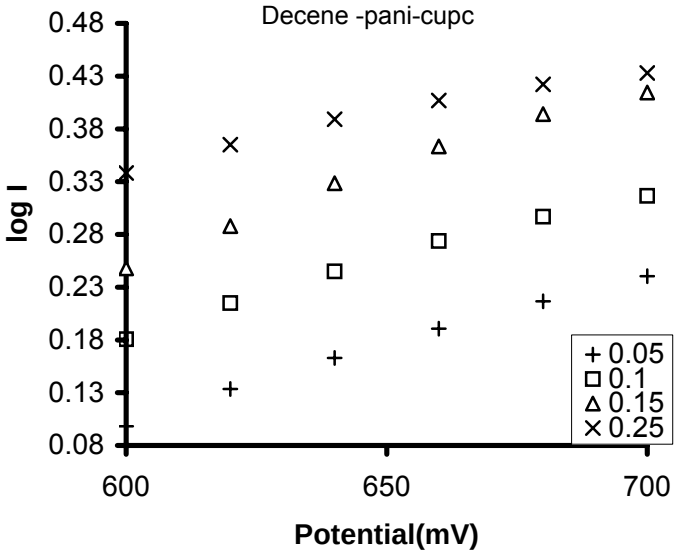

Figure : 4.29(A) Plot of log I vs potential for the electrochemical oxidation of decene using Pani-CuPc electrode

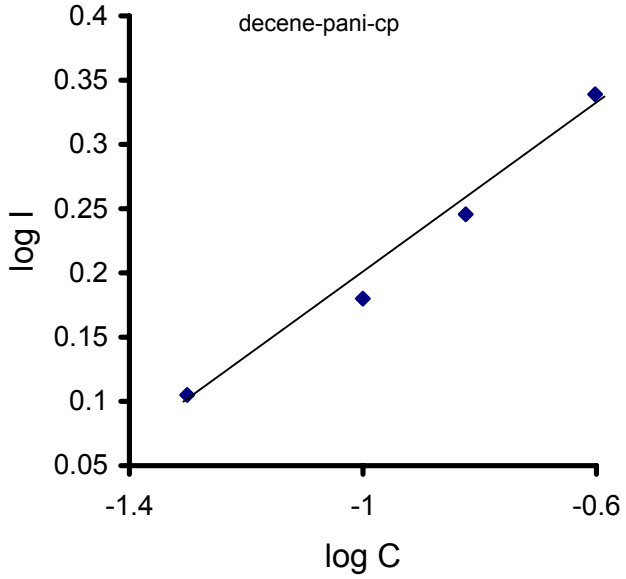

Figure 4.29(B): Graph of log I vs. log C from the data 's of CV's of Decene electrochemical oxidation using Pani-CuPc electrode

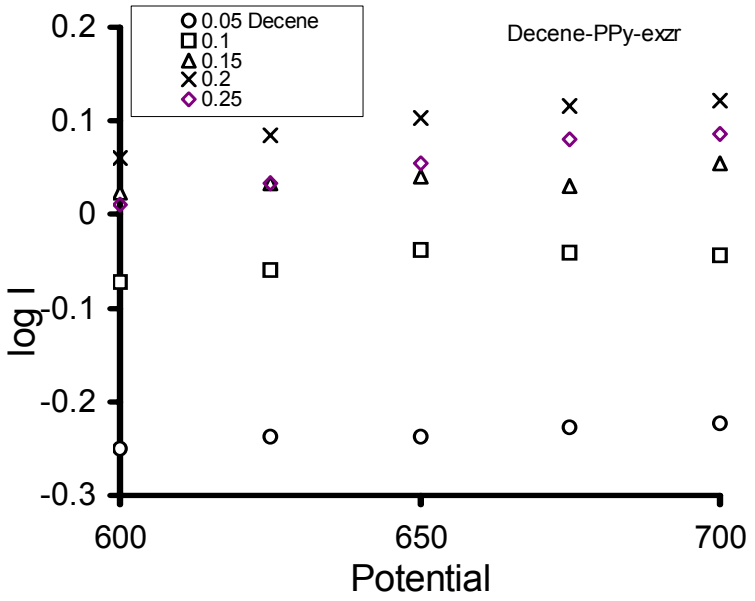

Figure : 4.30(A) Plot of log I vs potential for the electrochemical oxidation of decene using $ZrCl_4$ doped PPy electrode

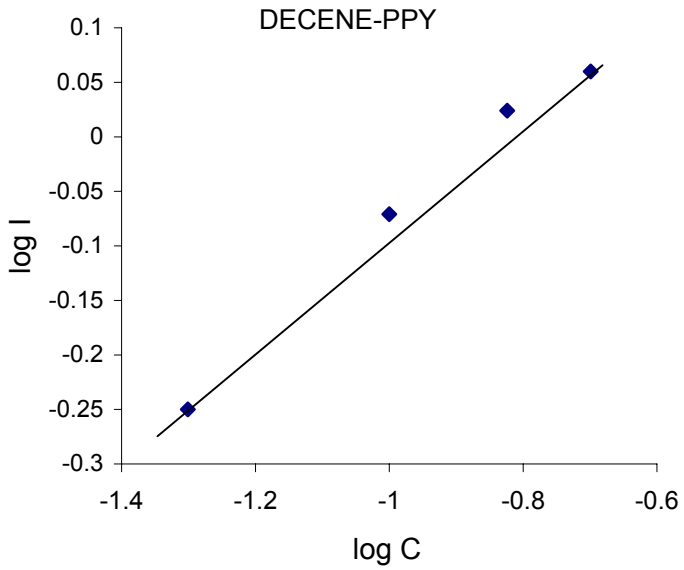

Figure 4.30(B): Graph of log I vs. log C from the data 's of CV's of Decene electrochemical oxidation using $ZrCl_4$ doped PPy electrode

ii. Hexene electrochemical oxidation

For calculating the kinetics data of hexene oxidation, both Pani incorporated with CuPc electrode and PPy externally doped with $ZrCl_4$ electrodes are used

(a) Electron transfer coefficient from the Pani incorporated CuPc was found to be 0.83. Graphs of which are given in the figure 4.31A and figure 4.31B

(b) Electron transfer coefficient for electrochemical oxidation of Hexene using PPy doped $ZrCl_4$ electrodes was also found out, which is equal to 0.7. Graphs are given in the figure 4.32A and figure 4.32B

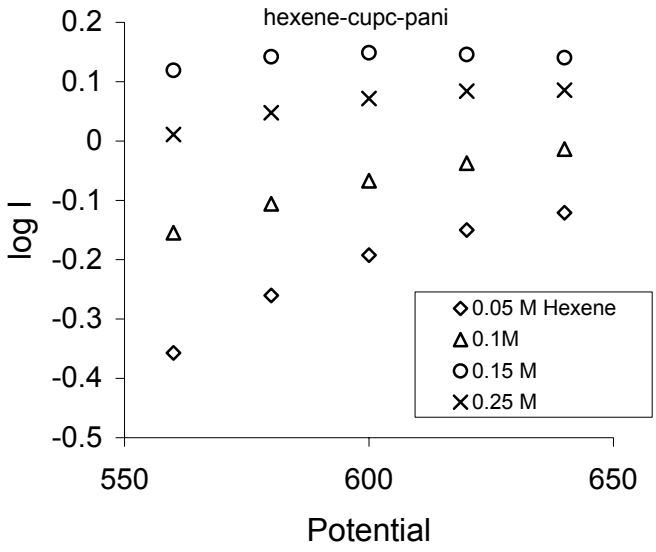

Figure 4.31: (A) Plot of log I vs potential for the electrochemical oxidation of hexene using Pani-3%CuPc electrode

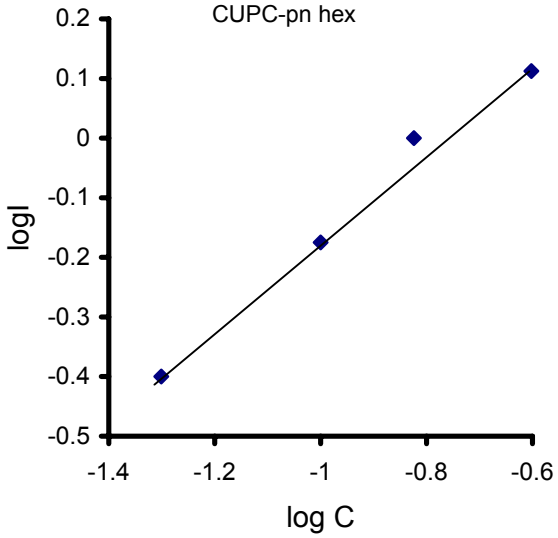

Figure 4.31(B): Graph of log I vs. log C from the data 's of CV's of hexene electrochemical oxidation using Pani-3%CuPc electrode

b. Using $ZrCl_4$ doped PPy electrode

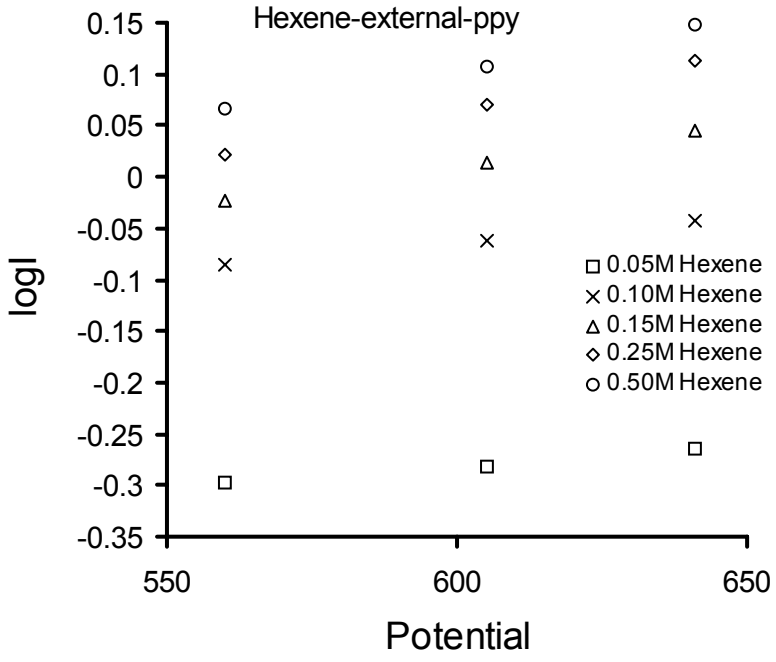

Figure : 4.32(a) Plot of log I vs potential for the electrochemical oxidation of hexene using PPy-$ZrCl_4$ electrode

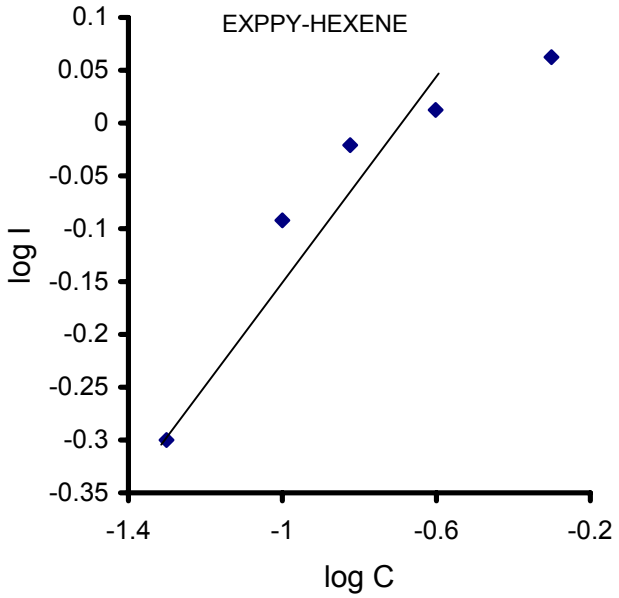

Figure 4.32(B): Graph of log I vs. log C from the data 's of CV's of hexene electrochemical oxidation using PPy-$ZrCl_4$ electrode

4.3.4. Conducting polymer powder for the chemical oxidation of alkene:

As it was observed in the electrochemical study that the modified conducting polyaniline and polypyrrole were catalytically active towards oxidation of decene and hexene, so it was necessary to study the catalytic behavior of these catalyst prepared chemically for the chemical oxidation of alkene. For that purpose Polyaniline powder modified by incorporating CuPc was synthesized chemically and was used as catalysts for the chemical oxidation reactions of decene. Various reaction conditions like temperature, time, catalyst concentration, concentration of CuPc in the catalyst etc was varied. Products obtained were characterized using GC and IR.

Usually alkene oxidation is carried out using $PdCl_2$ as catalyst in presence of some co-catalyst or reoxidant like $CuCl_2$, $FeCl_3$ etc which is commonly known as the Wacker oxidation process.[46-64] However, these catalytic systems are highly corrosive because of its acidic conditions and may cause the formation of chlorinated by-products. To overcome such drawbacks, halide free catalytic systems have also been widely investigated, e.g. combination of benzoquinone[39] and metal phthalocyanine[69], the Pd salt-heteropolyacid system[68] and the Pd salt of polyaniline and polypyrrole system[38,66,67]. Various reports are available about the alkene oxidation. Various aspects of the reactions

have been studied so far by various groups. Usually in the Wacker process methyl ketones are formed but aldehydes, acetates are also reported to form depending on the reaction condition used.[65-69]

Gas chromatography study

Polyaniline powder incorporated with different concentration of Copper phthalocyanine (CuPc) for decene oxidation was run. Concentration of CuPc in polyaniline was varied from 0%-10% weight percentage of monomer aniline. Various reaction conditions such as time, temperature, amount of catalyst was varied. Gas chromatography of all the reactions was run but only the reaction run by the modified polyaniline catalyst containing 2% CuPc for reaction temperature 70º C and reaction time 72 hours was shown in the *figure 4.33(B).* along with the reaction run by using $Pd(OAc)_2$ and $CuCl_2$ catalyst mixture ie Wacker process. Wacker reaction was run for comparison, as it is

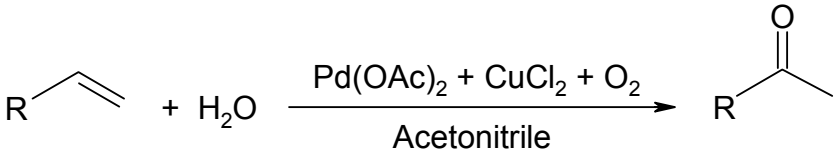

considered to be the standard alkene oxidation reaction and the product of this reaction is methyl ketone. From the GC of standards of oxidation products *[figure 4.33.A]* different retention time was noted, which are 6.31 minute for decanone, 6.41 min for decaldehyde, 6.78 minute for decanol and 7.31 minute for decanoic acid. From the *figure 4.33.B* it could be observed that in the GC for Wacker oxidation process peak at 6.34 minute was dominant. But along with the decanone peak some other peaks are also seen. It was observed that in case of Wacker oxidation reaction decaldehyde (2%), decanol (2.3%) decanoic acid(2%) along with some other side products were also formed. But incase of decene oxidation run by using 2% CuPc-Pani catalyst, it was observed that decanone (32.8%), decaldehyde(5.4%), decanol(19.8%) and decanoic acid (12.8%) were formed as the products. In the 2%CuPc-Pani catalyzed reaction no side product was observed. The peak appearing in the position 5.125 minute is due to the reactant decene, whereas peaks at 1.45 minute, 1.65 minute are due to acetonitrile and water respectively.

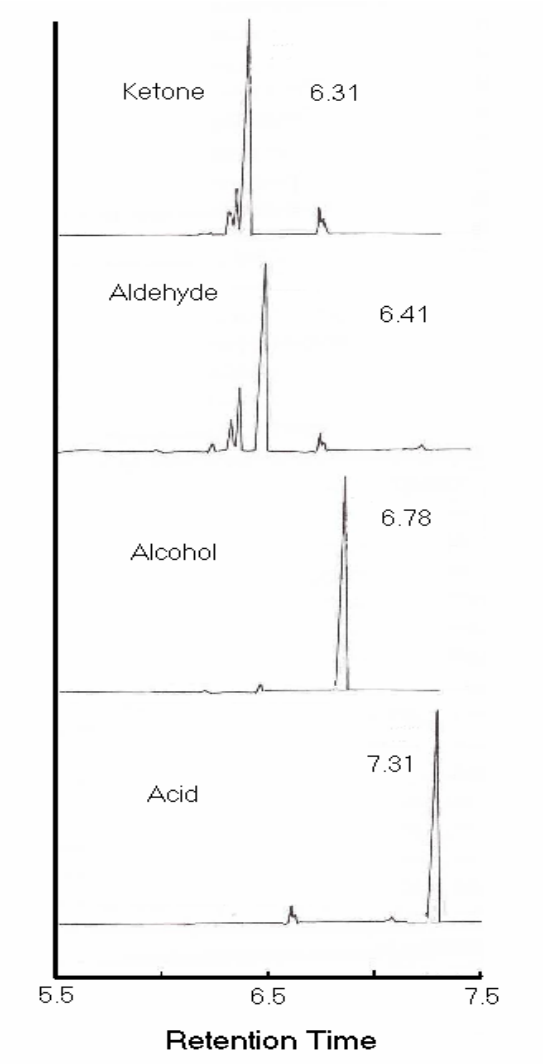

Figure 4.33(A): GC of the standards of the Decene reaction product

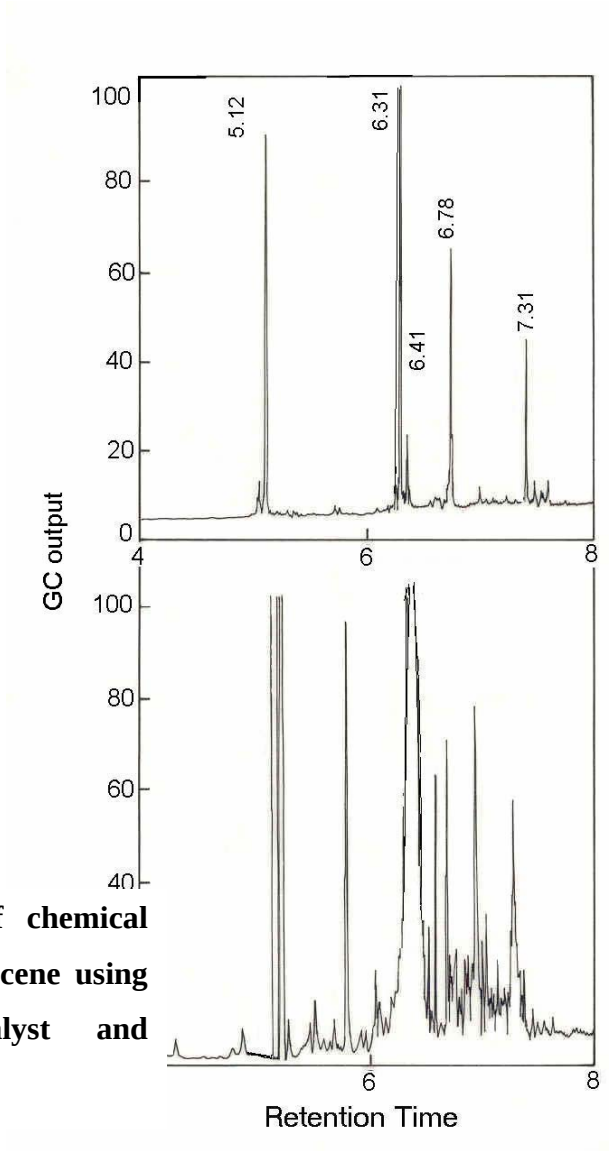

Figure 4.33(B): GC of chemical oxidation reaction of decene using 2% CuPc-Pani catalyst and Wacker catalyst

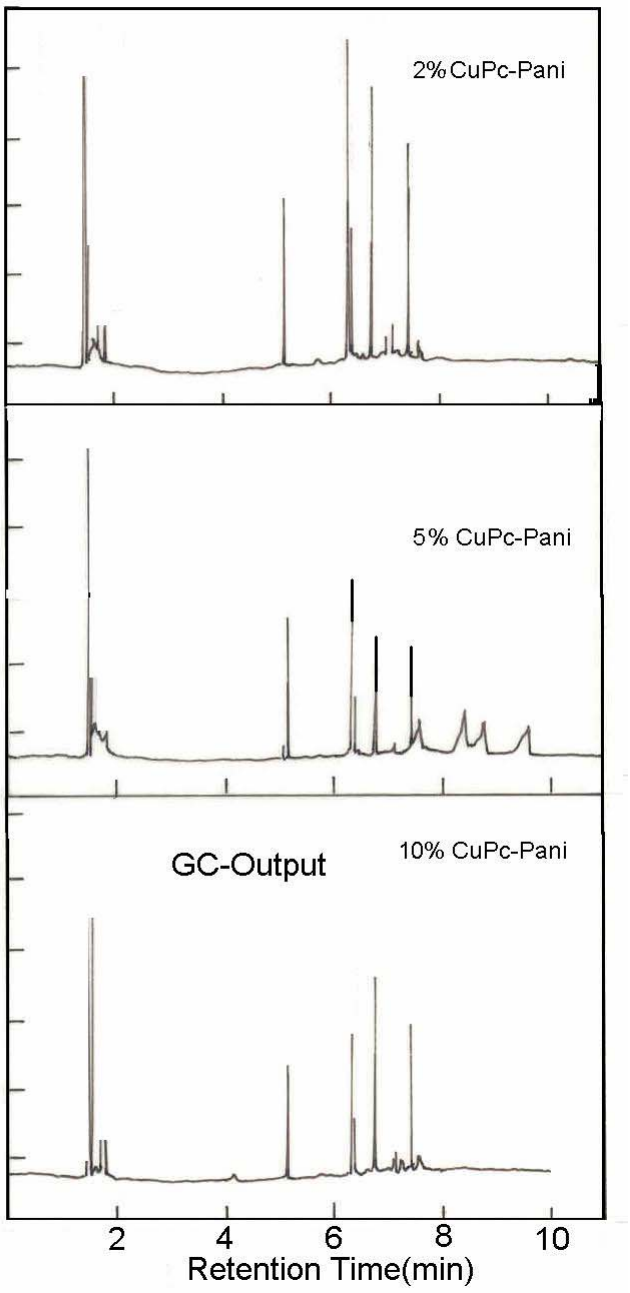

Figure 4.33(C): GC of decene oxidation reaction using 2%, 5%, and 10% CuPc incorporated Pani catalyst

A table of retention time with percentage conversion from GC data of 2%CuPc-Pani and Wacker oxidation process and assignment of the peaks are given in the *table no. 4.11*
As it is seen that the polyaniline powder modified with incorporating CuPc act as catalyst for decene oxidation, so it is essential to find out the optimum percentage of CuPc in the polyaniline which gives maximum percentage conversion. **Figure 4.33(C)** shows the GC of decene oxidation with 2%, 5% and 10% CuPc incorporated polyaniline. From the figure it could be observed that the in all the cases products decanone, decaldehyde, decanol and decanoic acid is formed.

Retention Time	**Percentage conversion (%)**		
	2% CuPc-Pani	**$Pd(OAc)_2$+$CuCl_2$**	**Assignment**
5.12	29.09	15.9	Decene
5.25		16.6	
5.33		9.72	
5.89		3.43	
6.31	32.8	44.6	Decanone
6.41	5.43	2.05	Decaldehyde
6.78	19.78	2.26	Decanol
7.00		2.55	
7.09		1.00	
7.31	12.83	1.9	Decanoic Acid

Table 4.11: Table of percentage conversion of products of oxidation reaction from the GC data

IR spectroscopy for product analysis.

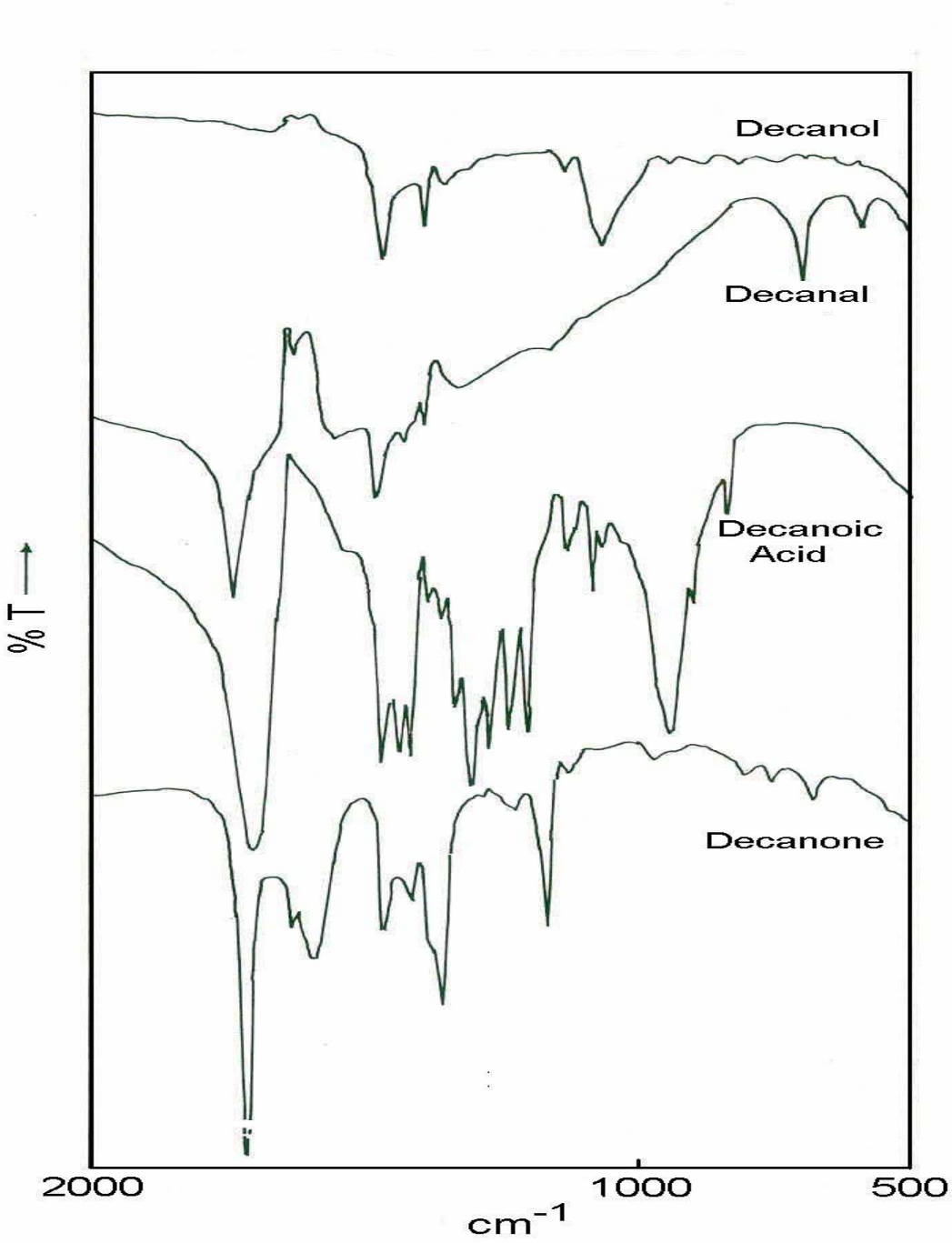

Figure 4.34 (A): FT-IR spectra of decene oxidation reaction products

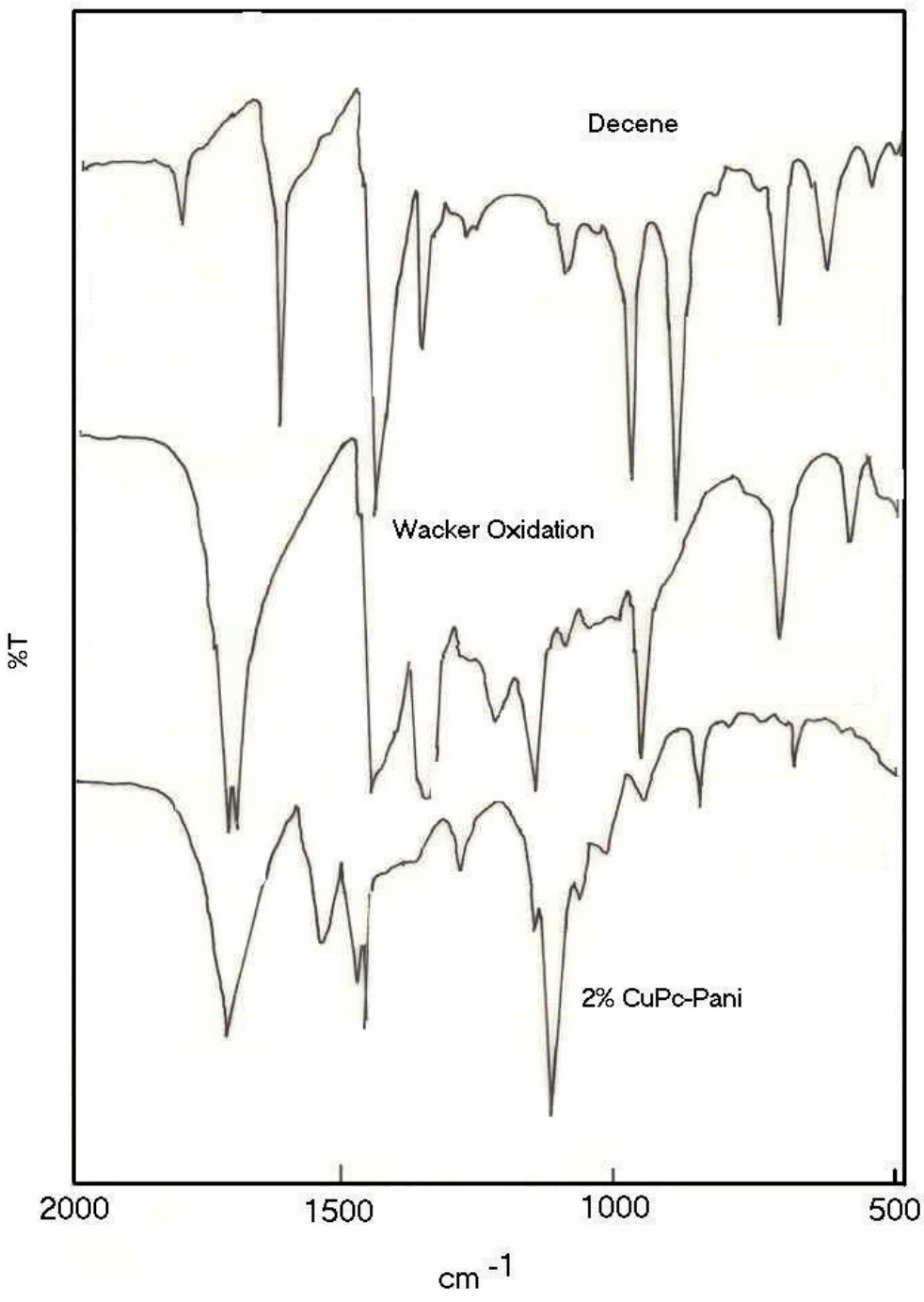

Figure 4.34(B): IR spectra of reactant decene, oxidation reaction carried out with Pani-2% CuPc and Wacker catalyst.

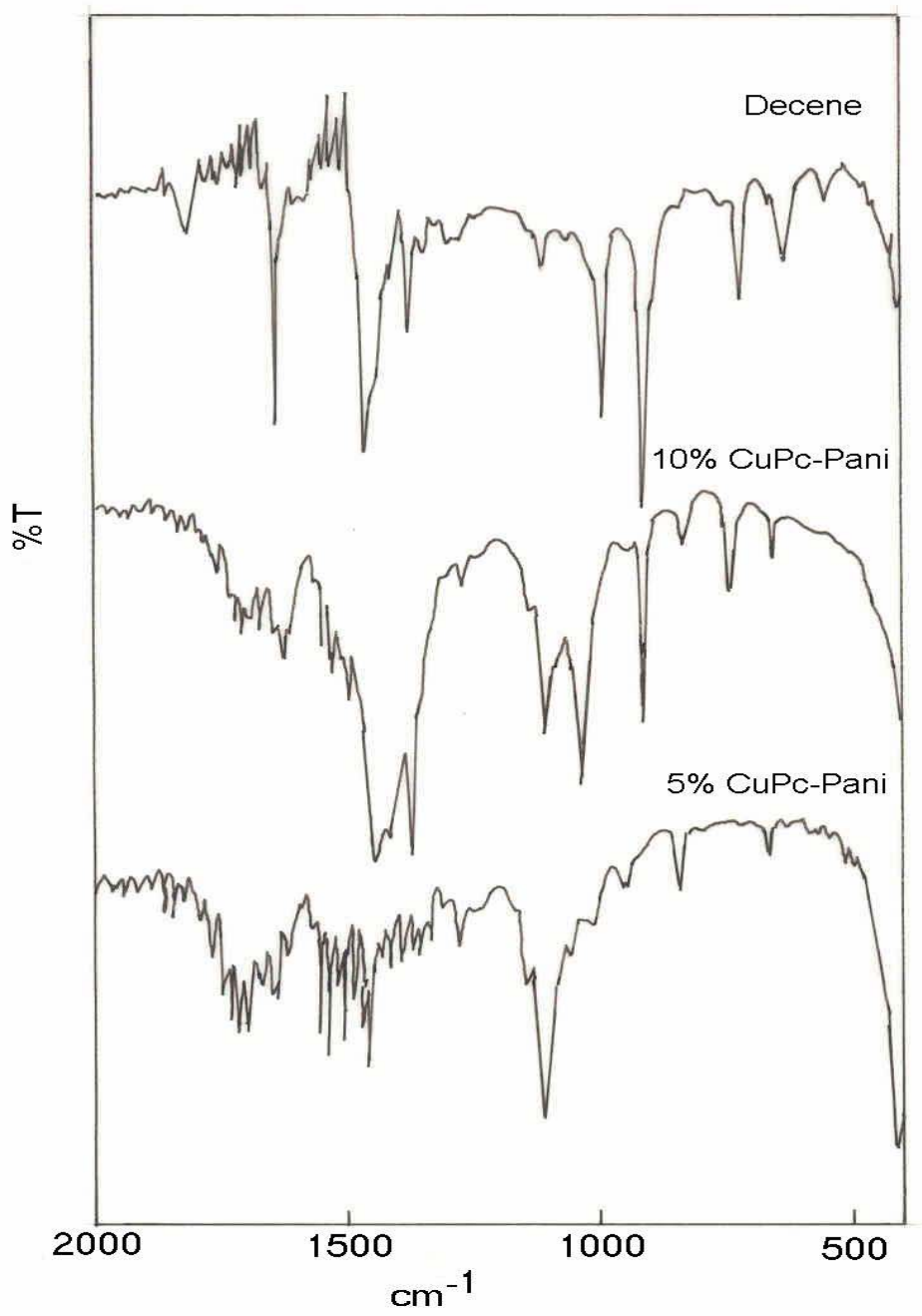

Figure 4.34(C): IR spectra of decene oxidation reactions carried out with 5%CuPc-Pani and 10%CuPc-Pani catalyst along with decene reactant

Peak position	Decene	2% CuPc-Pani	Wacker system	Assignment
1820	m	-	-	
1713	-	s	S	C=O stretching acyclic
1704	-	-	S	C=O stretching, saturated aliphatic COOH acid
1641	s	-	-	C=C multiple bond stretching, non conjugated
1545	-	m-	-	
1471	-	s	-	CH_2 bending
1456	-	s	Br	CH bending
1379	s	-	-	C-CH_3 bending
1360	-	-	S	α-CH_3 bending, C-C-C bending
1287	-	w	-	
1228	-	-	M	
1154	-	w	S	
1118	-	s	-	
1022	-	w	-	
991	s	-	-	
963	-	w	S	
908	s	-	-	
868	-	w	-	
720	s	-	M	Bending vibration of the group-(CH_2)n, where n≥4

Table 4.11: Table for the IR assignments for different decene oxidation reaction

Products formed in the chemical oxidation of decene was analyzed by IR technique also. Different IR spectrum is given in the figure 4.34 (A-C). Figure 4.34(A) is the IR spectrum of the standard decene oxidation products. Figure 4.34(B) is the spectrum of the reactant 1-decene along with the oxidation reaction product of the reactions carried out with the Wacker catalyst and polyaniline doped with 2% CuPc powder. Figure 4.34(C) is the IR spectrum of reaction product carried out with the catalyst 2%, 5% and 10% CuPc doped polyaniline. From the figure 4.34(B), different peak positions were found out and tabulated in the table no 4.9. From the IR assignment it could be seen that in 2% copper phthalocyanine doped Pani catalyst reaction there is a sharp peak at 1713cm^{-1}, which is due to the C = O acyclic stretching. This peak observed in all the CuPc modified catalyzed decene chemical reactions. As there is no peak observed in the region 1740cm^{-1} – 1720cm^{-1}, which is due to the aldehyde C–H stretching, therefore it could be assigned that the reaction product may be a ketone. Peak at 1471 is due to CH_2 bending, peak at 1456cm^{-1} and 1360cm^{-1} are due to CH_2 bending and □-CH_3 and -C–C–C- bending. The peak appearing at 720cm^{-1} is for bending vibration of the group -$(CH_2)_n$- where $n \geq 4$. From all the above discussion, it could be predicted that in the chemical oxidation reaction of decene carried out by modified conducting polymer, the main product is found to be the methyl ketone i.e. decanone along with other oxidation products decanal, decanoic acid and decanol .[14]

4.4. CONCLUSION :

It could be concluded from all the above studies that the conducting polymers Pani and PPy can be used as catalyst for oxidation of higher □-olefins. It could be observed that Pani and PPy films in their original state also show some catalytic activity, but their modified form showed better catalytic activity. Hexene and decene show oxidation peak at 600mV and 650mV respectively which is confirmed from the dependence of height of the peak with concentration of the respective reactants. In the electrooxidation reactions of olefins also, different dopant ions show different catalytic activity which clearly shows the importance of electron/hole transfer process at the electrode interface as the

controlling parameter. It could be observed that for oxidation reaction carried out with modified PPy electrodes, dopants containing less electronegative element like Zr shows maximum catalytic activity. Like methanol oxidation, in case of alkene oxidation also electronegativity of the dopant agents play an important role. With the help of energy level model mechanism of electron/hole transport process in the electrooxidation process is explained. It is seen that in the electrooxidation processes, for PPy doped with $ZrCl_4$ electrodes, it is easier for electrons to be transferred from the reactant hexene or decene to the electrode than in other cases. The electron transport from electrolyte to electrode or hole transport from electrode to reactant leads to the oxidation of olefin to desired products in presence of O_2.

Polyaniline doped with $PdCl_2$ electrodes also showed catalytic activity towards decene oxidation in presence of $CuCl_2$ in the reaction medium. Pani –$PdCl_2$ itself shows some catalytic activity but in presence of $CuCl_2$ in the electrolyte catalytic activity increases tremendously. Wacker type oxidation process can be envisaged in conducting polymer, in which these switch from one oxidation state to another and $CuCl_2$ might help in regenerating the catalyst. $CuCl_2$ was used in the reaction mixture as it is known that for Wacker type oxidation, where salts of palladium based catalyst (Pd^{+2} salts) is used, Pd^{+2} is reduced to Pd^0 during the course of the reaction and in the presence of some reoxidant (e.g. $CuCl_2$, $MnCl_2$, $FeCl_3$ etc.) Pd^0 is converted back to Pd^{+2}.

Studies on the electrooxidation of decene and hexene with CuPc incorporated Pani show their higher catalytic activity as compared to the Pani without CuPc. The catalytic activity gradually increases upto 3% CuPc incorporation, and further increase in the CuPc activity decreases. Higher activity is explained on the basis of better complexation which is proved in the different characterization studies.

From the above studies it could also be concluded that Pani powder modified with CuPc can also be used as catalyst for the chemical oxidation reaction. From the GC and IR studies, formation of product was confirmed.

Overall it can be concluded that even though redox properties shown by the conducting polymers is the basis of the catalytic activity, the efficiency depends on the position of energy levels of the reactive species and the electrode material, and the charge transfer process across the interface of electrode and electrolyte. Further, the extent of complexation also plays important role in the electrocatalytic reactions using modified conducting polymers.

4.5. REFERENCE:

1. W. H. Clement, C. M. Selwitz, J. Org. Chem. *29(1964)241*
2. W. G. Lloyd, B. J. Luberoff, J. Org. Chem *34(1969)3949*
3. D. R. Fahey, E. A. Zuech, J. Org. Chem. *39(1974)3276*
4. F. J. McQuillin, D. G. Parker, J. Chem. Soc, Perkin Trans. *1(1974)809*
5. J. Bobacka, M. Grzeszczuk, A. Ivaska; J.Electroanal.Chem.*427(1997)63*
6. N. Batina, S. A. Chaffins, J. Y. Gui, F. Lu, J. W. McCargar, J. W. Rovang, D. A. Stern, A. T. Hubbard; J. Electroanal. Chem *284 (1990)81*
7. C.-Yu Chen, S.Cheng,Y.O.Su; J. Electroanal. Chem. *487(2000)51*
8. C. N. Pillai and C. Sattinathan; Bull. Catal. Soc. India *7 (1997) 40*
9. B. Vishwanathan; Bull. Catal. Soc. India *7(1997)48*
10. M. Fleischmann and D. Pletcher; Tett. Lett. *60(1968) 6255*
11. A. T. Kuhn, H. Wroblowa, J.O'M Bockris; Trans. Faraday Trans. *63 (1967)1458*
12. N. R. Davies; Nature *(1964) 490*
13. J. O'M. Bockris, H. Wroblowa, E. Gileadi and B. J. Piersma; *61(1965) 2531*
14. "Application of Absorption spectroscopy of organic compounds" by J.R.Dyer, Easter Economy Edition, New Delhi, 1991
15. A. Yasuda and Shimidzu, Synth. Metal, *61(1993)239*
16. B. N. Achar, G. M. Fohlen and J. A. Parker; J. Polym. Sci., Polym. Chem. *20 (1982)2073*
17. Y. Cao, S. Li, Z. xue and D. Guo; Synth. Metal *13 (1986)305*
18. A. R. Inigo, F. P. Xavier, G. J. Goldsmith; Materials Research Bull *32(5),(1997)539*
19. F. S. Wang, J. S. Tang, L. Wang, H. F. Zang &Z. Mo; Mol. Cryst. Liq. Cryst *160(1988)175*
20. J. P. Pouget, M. E. Jozefowicz, A. J. Epstein, X. Tang, A. G. MacDiarmid; Macromolecules. *24 (1991) 779*
21. C. D. Wagner, N. M. Rigers, L. E. Davis, J. F. Moulder, G. E. Muilenberg; **"Handbook of X-ray Photoelectron Spectroscopy"** Perkin-Elmer, Eden prairie, MN 1979.

22. S. Tohiri, G. Safoula and J. C. Bernede; Polym. Degradation and stabilization *60(2,3) (1998)481*
23. S. W. Huang, K. G. Neoh, C. W. Snih, D. S. Lim, E. T. Kang, H. S. Han and K. L. Tan; Synth. Metal; *96(1998)117*
24. D. Zheng, Z. Gao, X. He, F. Zhang, L. Liu; App. Sur. Science *211(2003)24*
25. B. Adolphi, O. Berger. W.-J. Fischer App. Sur. Science; *179 (2001)102*
26. K. T. Park, A. Miller, K. Klier, R. L. Opila, J. E. Rowe; Surf. Science *529(2003)L285*
27. L. Lozzi , L. Ottaviano, F. Rispoli, P. Picozzi, S. Santucci; Surf. Science *433–435(1999)157*
28. J. W. Sobczak, B. Lesiak, A. Jablonski, A. Kosinski and W. Palczewska; Polish J. Chem.*69 (1995) 1732*
29. S. W. Huang, K. G. Neoh, C. W. Snih, D. S. Lim, E. T. Kang, H. S. Han and K. L. Tan; Synth. Metal ; *96 (1998) 117*
30. S. W. Huang, K. G. Neoh, E. T. Kang, H. S. Han and K. L. Tan; J. Mater. Chem., *8 (1998) 1743*
31. S. Hermans, M. Wenkin and M. Devillers; J. Mol. Cat: A Chem. *136 (1998) 59*
32. Z. H. Ma, K. L. Tan and E. T. Kang; Synth. Metal *114(2000)17.*
33. K. L. Tan, B. T. G. Tan, E. T. Kang and K. G. Neoh; Phys. Review B: *39 (1989)8070.*
34. S. Radhakrishnan, A. Adhikari and D. K. Awasthi; Chem. Phys. Lett. *341(2001)518.*
35. J. W. Sobczak, B. Lesiak, A. Jablonski, A. Kosiniski and W. Palczewska; Polish J. Chem., *69(1995)1732*
36. J. Tsuji and M. Minato; Tetrahedron Letters; *28(1987)3683*
37. D. Y. Hwang, S. Y. Ha and S.Kim; Bull. Kor. Chem. Soc. *22(2001)441*
38. A. Drelinkiewicz, M. Hasik and M. Kloc; Cat. Lett. *64(2000)41*
39. J. -E. Backvall, R. B. Hopkins, H. Grennberg, M. M. Mader and A. K. Awasthi; J. Am. Chem. Soc. *112 (1990)5160*
40. P. Henry; J. Am. Chem. Soc. *88 (1966)1595*
41. P. Henry; J. Am. Chem. Soc. *88(1966)1597*

42. J. F. Llopis and F. Colom; Chapter VI-7, Palladium Encyclopedia of Electrochemistry of Elements; Ex. Ed. A. J. Bard, Asso. Ed. H. Lund; Marcel Dekker Inc, New York, 1973
43. J. Perichon, M. Herlem, F. Bobilliart, A. Thiebault, K. Nyberg, Chapter XI-1, Hydrocarbon, Encyclopedia of Electrochemistry of Elements; Ex. Ed. A. J. Bard, Asso. Ed. H. Lund; Marcel Dekker Inc, New York, 1973
44. L. D. Burke, L. C. Nagle; J. Electroanal. Chem. *461(1999)52*
45. M. Liu, Y. Oliver Su; J. Electroanal. Chem. *452 (1998) 113*
46. A D. Silva, M L. Patitucci, H R. Bizzo, E D'Elia, O.A.C. Antunes, Catalysis Communications *3 (2002) 435*
47. E. Karakhanov , A. Maximov, A. Kirillov; J. Mol Cat A: Chemical *157(2000) 25*
48. B Betzemeier, F Lhermitte and P. Knochel Tett Lett *39(1998)6667*
49. N, Donalita D Krystyna Applied Catalysis A: General *159 (1997) 75*
50. A.W. Stobbe-Kreemers, M. van der Zon, M. Makkee, J.J.F. Scholten; J Mol Cat A: Chemical *107 (1996) 247*
51. G. C. Bond and M. Hellier; J. of Catal.*4(1965)1*
52. J. Tsuji, New J. Chem. *24 (2000)127*
53. T.-L. Ho, M. Hua Chang and C.Chen; Tetrahedron Lett. *44 (2003) 6955*
54. J. Tsuji, H. Nagashima, H. Nemoto; Organic Synthesis *62 (1984)9*
55. A. Lambert, E. G. Derouane and I. V. Kozhevnikov ; J of Catalysis, *211(2002) 445*
56. Alexander J. Dyakonov Applied Catalysis B: Environmental *45 (2003) 257*
57. M. Higuchi, I. Ikeda, T. Hirao; J. Org. Chem. *62 (1997) 1072*
58. J. Tsuji; Synthesis *(1984)369*
59. T. Nishimura, N. Kakiuchi, T. Onoue, K. Ohe, S. Uemura; J. Chem. Soc., Perkin Trans.*1 (2000) 1995*
60. T. Hosokawa, T. Nomura, S. -I. Marahashi; J. Organomet. Chem. *551(1998) 387.*
61. L. M. Stephenson, M. J. Grdina, M. Orfanopoulos; Acc.Chem.Res.*13 (1980) 419*
62. C. -G. Jia, F. -Y. Jin, H. -Q. Pan, M. -Y. Huang, Y. -Y. Jiang; Macromol. Chem. Phys. *195 (1994) 751.*
63. J. Tsuji, H. Nagashima, K. Hori; Chem.Lett.*(1980) 257*

64. J. M. Madurro, G. Chiericato Jr., W. F. De Giovani and J. R. Romero; Tett. Lett. *29 (1988) 765.*
65. A. Malinauskas; Synth. Metal *107 (1999) 75*
66. T. Hirao, M. Higuchi, B. Hatano and I. Ikeda; Tetrahedron Lett. *36(1995)5925.*
67. M. Higuchi, S. Yamaguchi and T. Hirao; Synlett *(1996)1213.*
68. E. Monflier, E. Blouet, Y. Barbaux and A. Mortreux; Angew. Chem. Int. Ed. Eng. *33(1994)2100*
69. J. -E. Backvall and R. B. Hopkins; Tetrahedron Lett. *29(1988)2885.*

Chapter V

NITROBENZENE ELECTROREDUCTION USING MODIFIED CONDUCTING POLYPYRROLE

5.1. INTRODUCTION

Charge transfer process from electrolyte to electrode / electrode to electrolyte is the key factor in the electrocatalytic oxidation/reduction process. The extent to which this transfer takes place determines the rate of the reaction. The level of the electrode and the reactant in the energy level, therefore plays main role in deciding activity/selectivity of the electrode. In the present work electrochemical reduction of nitrobenzene, benzaldehyde and acetophenone was carried out to study the effect of above factors in the reaction process. Emphasis has been given to nitrobenzene reduction process to observe the effect of electrode on the reaction.

The reduction of nitro aromatic compounds is of considerable interest because these are common groundwater contaminants and reduction reactions can play a central role in their environmental fate or cleanup. Sources of nitro aromatic contaminants include activities associated with the production or utilization of explosives, dyes, agrichemicals and pesticides. In the year 1898, F. Haber for the first time studied the electrochemical reduction of nitrobenzene. Haber used platinized platinum electrode for the electrochemical reduction of nitrobenzene.

Reduction products of nitrobenzene are nitrosobenzene, phenylhydroxylamine, aniline and coupled products such as azoxy-, azo- and hydrazobenzene. The course of reactions were varied depending on the choice of electrode material, electrode potential and electrolyte solutions.

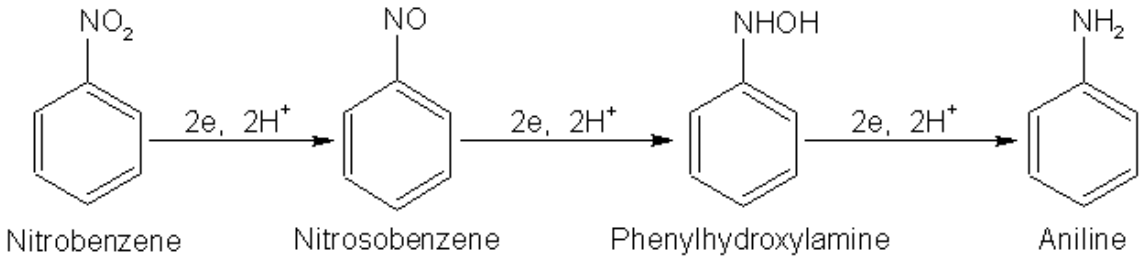

Here in this chapter, studies on electrochemical reduction of nitrobenzene with modified polypyrrole electrodes have been described. Modification of polypyrrole was done by doping with different transition metal salts like $PdCl_2$, $CuCl_2$, $ZrCl_4$, etc. Various reports have been found in the literature about the reduction of nitrobenzene at various electrodes

mainly Pt, Ni, Cu etc.[1-42] Reduction of organic molecules on modified conducting polymers are also found[43-60] but there is hardly any reference found in the literature on using conducting polymer electrodes.[61-63]

Further electrochemical reductions of reactants with different redox potential viz. acetophenone, benzaldehyde and nitrobenzene were carried out at $NiCl_2$ doped PPy electrode also, to find out the dependence of redox potential on the activity of the electrode. It was observed in the earlier chapters that charge transfer process is the important player in the electrochemical reactions. Hence position of the working electrodes in the energy level and the redox potential of the reactants are the important factors which determine the activity of the electrocatalyst, rate of the reaction etc have been tried to show in the present piece of work.

5.2. EXPERIMENTAL

In the current study, among the various methods available for polymerization of pyrrole, electrochemical technique was employed in order to synthesize PPy. This was preferred because all the reactions were carried out in non-aqueous medium which may affect the binder material used for powder/ carbon paste electrodes containing powder PPy.

5.2.1. Electrochemical polymerization

On gold-coated glass plate, electrochemical polymerization of pyrrole was carried out in a three electrodes single compartment cell with the help of computer controlled potentio-galvenostat. These films were then undoped and then redoped with different transition metal salts. Detail procedure of the vacuum deposition, electro-polymerization technique and doping was mentioned in the chapter II.

5.2.2. Modification of PPy films by different techniques

a) Insitu doping during polymerization.

As PPy films doped internally with different transition metal dopant ions shows catalytic activity towards oxidation of methanol as well as in the oxidation of hexene, it is essential to check the catalytic activity of the films for reduction process also.

b) Films of varying roughness

Electrodes of varying surface roughness were also prepared and used for the reduction of nitrobenzene reaction. These were prepared by scanning the potential from 0 to 0.7V (vs. SCE) at various scan rates ranging from 10 mV/s to 75 mV/s.

5.2.3. Electro-Catalytic Reduction of Nitrobenzene

Electrocatalytic reduction process of nitrobenzene proceeds through several intermediate steps. The intermediate reduction products of nitrobenzene are nitrosobenzene and phenylhydroxylamine which finally leads to the formation of aniline. In the reduction process coupled products such as azoxy-, azo- and hydrazobenzene are also reported to form.

In the current study, different modified polypyrrole cathodes were used to study the electrochemical reduction of nitrobenzene. The reactions were carried out in acidic media. The electrochemical cell contained 150 ml acetonitrile and 0.1M $HClO_4$ electrolyte. Nitrobenzene concentration was varied from 0.01M to 0.5M in each case. Cyclic voltammetry method was employed to study the reduction process, which was cycled from –1500mV to +1500mV. In another set of experiments, constant potential was applied at predetermined value for 300 minutes and the products were analyzed by spectroscopic methods.

5.3.RESULT AND DISCUSSION

5.3.1. Characterization of Electrodes

X-ray photoelectron spectroscopy

XPS of PPy films modified by doping externally and internally with $NiCl_2$ are shown in the *Figure 5.1***.** *Figure 5.1.* is the core level spectra for C1s and N1s. The curves designated by symbols (a) and (b) correspond to the spectra of exsitu and insitu doped PPy respectively. Broad core level spectra are seen for these films which are indicative of the various components which are generally seen in the conducting polymers, and these components are obtained by deconvolution of the same. On comparing these various spectra (see Table-1) it is seen that in all the cases there is additional contribution from the charged species (the intensity of those component peaks at higher B.E. increases) .

In the *figure 5.1 (B)* spectra of N (1s) atom is shown. N (1s) core level spectra of exsitu doped PPy appearing at 399.65 eV got shifted to 399.8 eV in case of insitu doped PPy which is due to the =N— formed due to complex formation with metal salts.

Peak at higher B.E.'s are due to the charge species —NH— and N^+ respectively. Peak due to —NH— species appears at 401.2 eV and 401.1 eV for exsitu and insitu doped PPy respectively. The peak due to N^+ appears at 402.1 and 402.7 for exsitu and insitu doped PPy respectively. Percentage peak area due to the charge species incase of exsitu and insitu are 39.79(23.18, 16.61) and 56.79(40.29, 16.5) respectively. In the insitu doped PPy the area of charged species is much more than the exsitu doped which can be seen very clearly from the figure.

In case of exsitu doped PPy, the contribution due to the imine like nitrogen atom (=N—) component is higher. This suggests that significant deprotonation of PPy has occurred. Since deprotonation involves exclusively transformation of —N^+ to =N— groups. Deprotonation took place during dedoping of the sample prior to external doping.

Whereas in case of insitu doped PPy, contribution due to —NH— and —N^+ are more. The high energy peaks i.e. N^+ is due to the doped nitrogen species and the doping level can be expressed as the share of N^+ groups in the polymer. More the percentage of charged species indicates the formation of polarons and bipolarons in the polymer chain.

From all the observations it could be predicted that substantial complex formation appears to take place in case of insitu doped PPy by co-ordination between Ni and nitrogen atoms.

In the exsitu doped PPy, Cl atom's spectra is prominent whereas in case of insitu doped PPy, Cl spectra not visible which may be due to that the exsitu doping is surface level modification whereas in case of insitu doping Cl atom has gone inside the matrix and forms a better complex. Thus, insitu doping leads to better complexation of the Ni atoms with the N of the PPy structure. In case of insitu doping there is a possibility of Ni atoms going inside the polymer matrix and better mixing with the polymer matrix leading to higher amount of complex formation.[64-69]

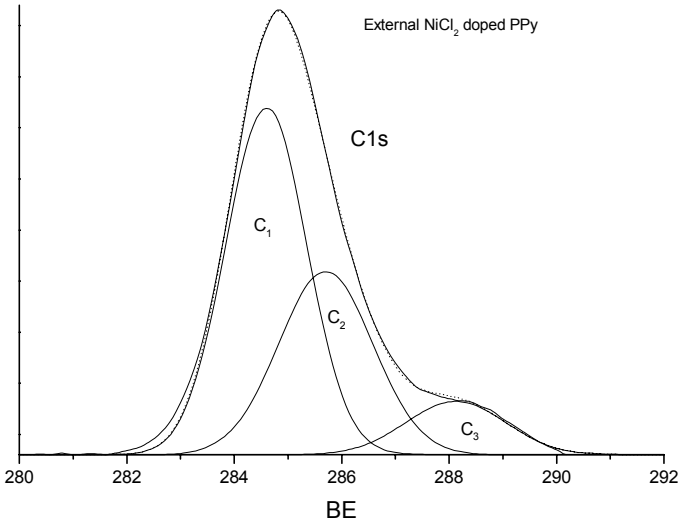

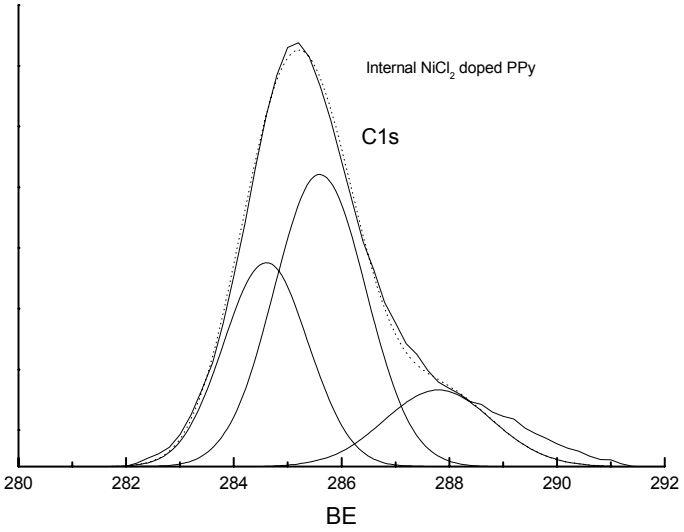

Figure 5.1(A) : XPS core level spectra of C1s species of exsitu and insitu doped PPy films

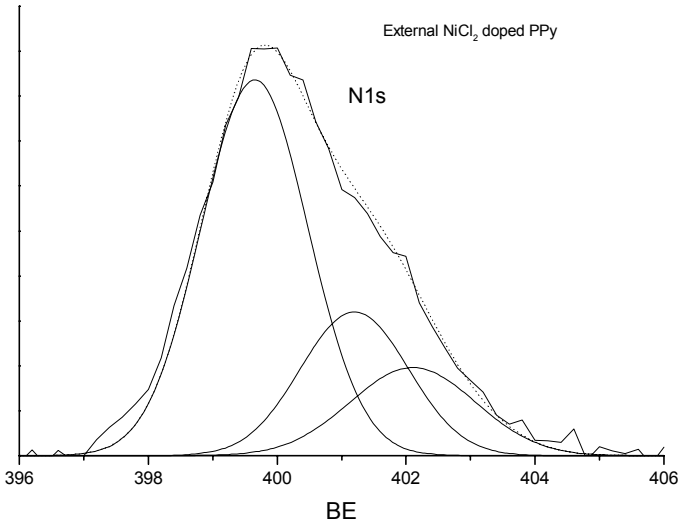

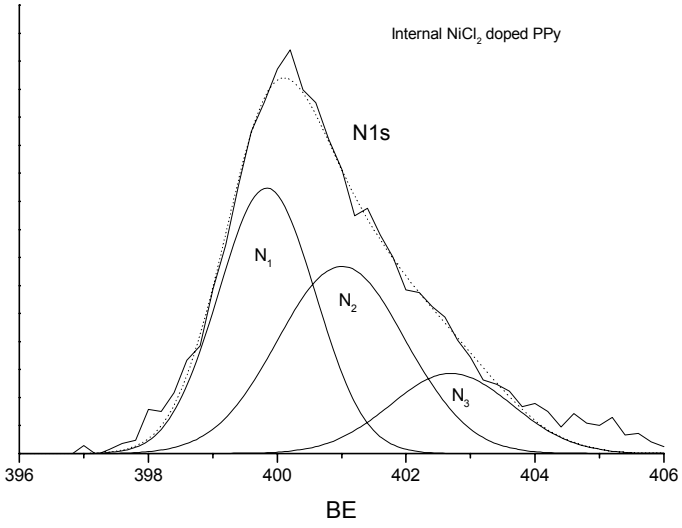

Figure 5.1(A) : XPS core level spectra of N1s species of exsitu and insitu doped PPy films

Core Level		External Doping			Internal Doping		
		B.E.(eV)	FWHM	%Area	B.E.(eV)	FWHM	%Area
C1s	C1	284.6	1.5	55.65	284.6	1.56	32.97
	C2	285.7	1.75	33.95	285.6	1.7	51.25
	C3	288.1	1.83	10.4	287.8	2	15.78
N1s	N1	399.65	1.66	60.2	399.8	1.5	43.2
	N2	401.2	1.67	23.18	401.1	1.98	40.29
	N3	402.1	1.95	16.61	402.7	1.9	16.5

Table 5.1: Table of BE, FWHM and % charge contribution of each components of the exsitu and insitu doped films

5.3.2. Electrochemical reduction of nitrobenzene

5.3.2.1. Conducting polymer coated electrodes for the electro-chemical reduction of nitrobenzene

Conducting polymer coated cathodes were employed for the electrocatalytic reduction of nitrobenzene. As it was reported by various authors that nitrobenzene can be reduced electrochemically both in the acidic as well as alkaline medium,[3,7,41] so it is necessary to find out the suitable reaction medium for modified conducting polymer. For that purpose electrochemical reduction was carried out using these electrodes in acidic and alkaline medium CV's for which is shown in *the figure 5.2***.**

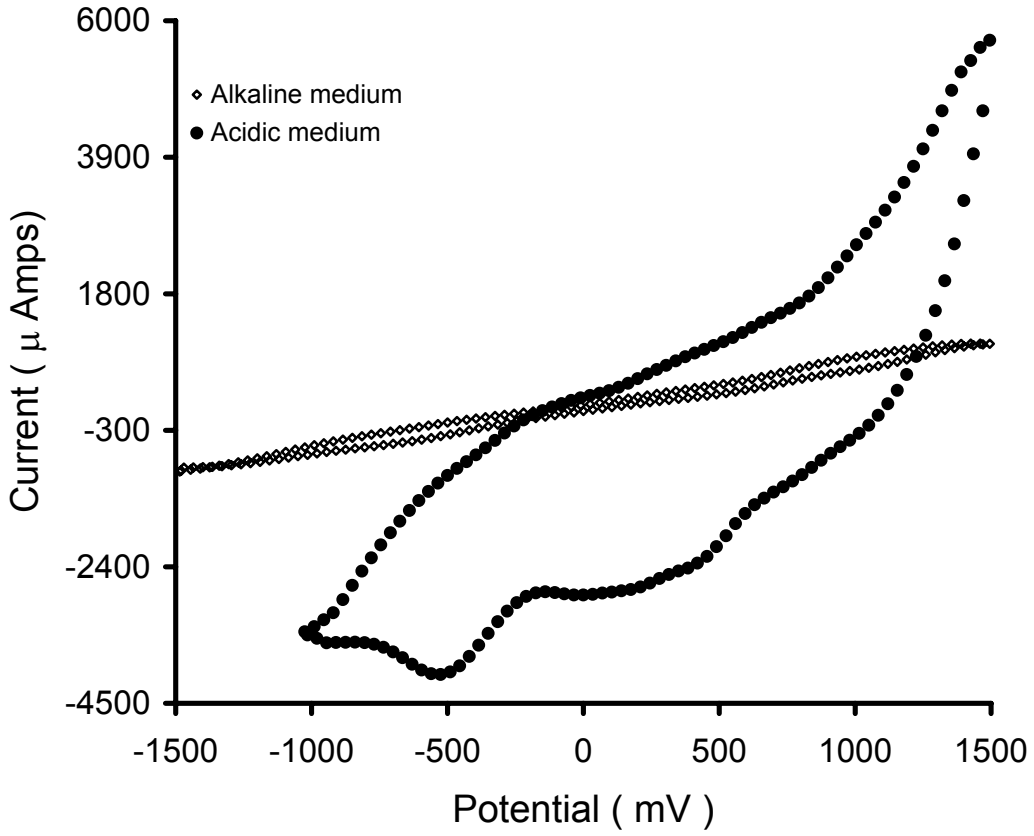

Figure 5.2: CV's of PPy doped with $NiCl_2$ electrodes for the reduction of nitrobenzene in acidic and alkaline medium

It could be seen in the figure that in the acidic medium characteristic voltammogram with cathodic peak was seen. However, when the reaction was carried out in the alkaline medium, no distinct peak in the reduction side could be observed indicating inert nature of the electrode. Absence of reduction peak in this case might be due to the fact that when the $NiCl_2$ modified PPy electrode was immersed in the alkaline electrolytic solution for electroreduction, the conducting polymer film might get undoped leading to the ineffective nature of the PPy electrode.

As it was observed that conducting polymer electrodes were active towards reduction of nitrobenzene in the acidic medium all further experiments were performed in the acidic

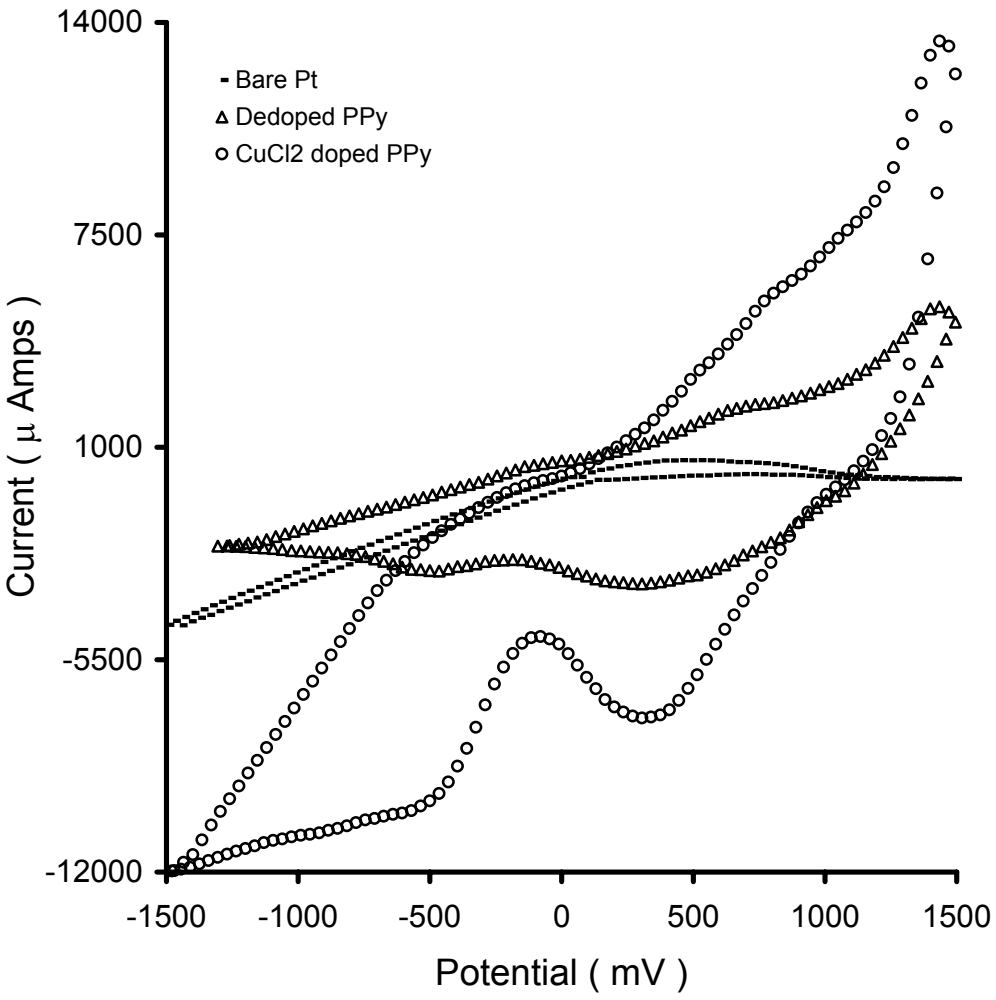

Figure 5.3: CV's of electrochemical reduction of nitrobenzene at Pt, undoped PPy and $CuCl_2$ doped PPy electrodes

medium ie. in presence of 0.1M $HClO_4$. It was observed that the PPy coated electrodes were quite effective in the electrocatalytic reduction of nitrobenzene as compared to bare metal (e.g. Pt) electrodes for reduction process which was proved from the high current values observed CV which is shown in *figure 5.3.* Figure 5.4 is the CV for nitrobenzene reduction with undoped PPy, PPy externally doped with $CuCl_2$ and bare platinum electrodes.

The electrochemical activity shown by modified electrode in the cathodic region is clearly associated with the reduction of nitrobenzene and the reduction process taking place at the cathode. In both undoped PPy and $CuCl_2$ doped PPy electrode reduction peak

at –500 mV was observed. The peak current at –500 mV for $CuCl_2$ doped PPy electrode was five times higher compared to the undoped PPy electrode, confirming the catalytic activity of the modified electrodes. It is interesting to note that although the redoped PPy electrode had initially high resistance value, after dipping in the acidic medium, it became weakly doped with acid and showed conducting properties.

Further experiments were performed increasing the concentration of nitrobenzene (reactant) in the electrolyte from 0.01 to 0.5 M in order to identify the origin and nature of the cathodic current and the CV was recorded for each using doped PPy coated electrode.

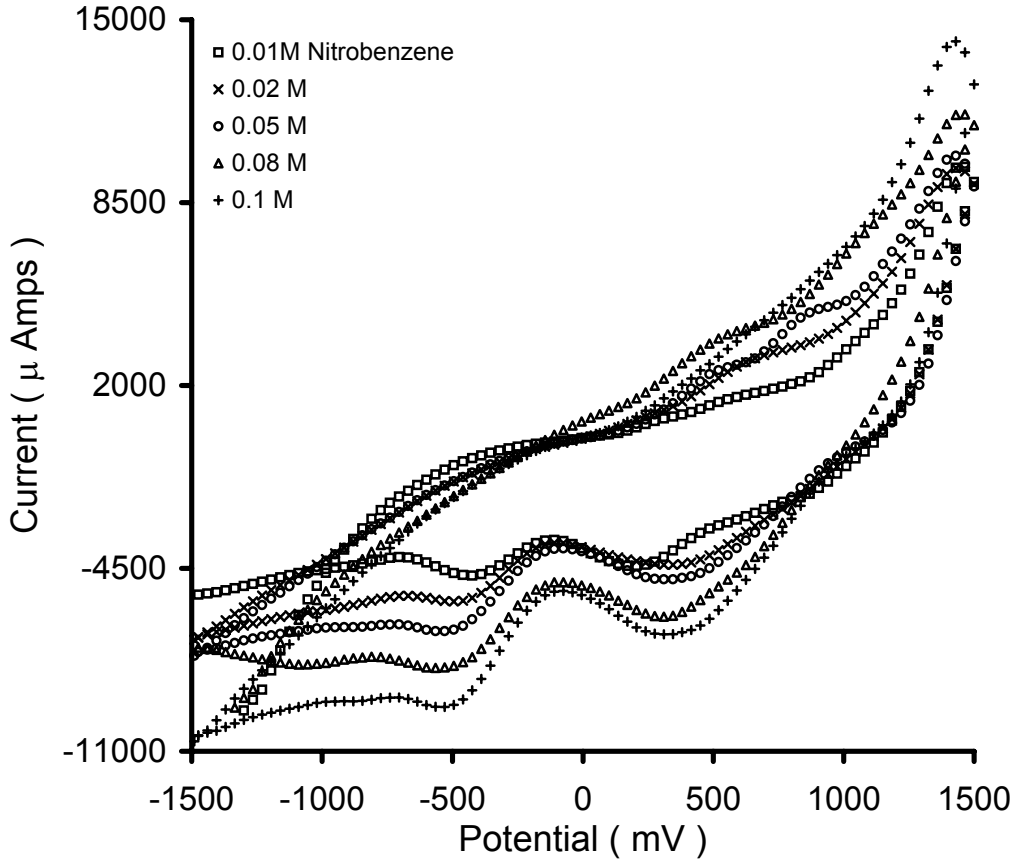

Figure 5.4: CV 's of Nitrobenzene electrochemical reduction with $NiCl_2$ doped PPy electrodes for varying reactant concentration.

Figure 5.4 shows the CV's for these cases recorded in +1500 mV to -1500 mV at scan rate of 50 mV/s. CV profiles show a distinct peak appearing in the region of -500mV

(SCE) and this current in the cathodic potential region increased with the increase in concentration of nitrobenzene. Thus cathodic peak current at -500 mV is associated with the reduction of nitrobenzene, which is in agreement with electro-reduction of this reactant.

Electrochemical studies of PPy films doped with other dopants were also carried out to confirm the dependence of cathodic current on reactant concentration in the electro-reduction reaction of nitrobenzene and similar trend were observed, ie. peak current at -500mV was dependent on the concentration of the reactant.

As already observed, PPy films modified by doping externally with transition metal dopants show good catalytic activity but the efficiency depends on the specific dopant. Hence it was essential to find out the most suitable dopant ion for the electro-reduction of nitrobenzene. A range of dopants were chosen viz. $NiCl_2$, $PdCl_2$, $MnCl_2$, $CoCl_2$, $FeCl_3$, $CuCl_2$, and $ZrCl_4$ and the electrochemical reduction process was studied as before. *Figure 5.5* is the CV's of the electrochemical reduction of nitrobenzene using PPy electrodes containing these dopants. Reactant concentration in the electrolyte was 0.1M in each case. In the CV's it could be observed that there is a distinct peak appearing at -500mV in the cathodic region in each case. Tremendous increase in the peak current for PPy films doped with $NiCl_2$ electrodes followed by $CuCl_2$ doped electrodes was observed.

When peak currents of these PPy doped films was correlated with electronegativity of the dopant ions and a graph of cathodic peak current vs. electronegativity dopants was plotted a relation could be seen which was shown in the *figure 5.6.* Graph shows that higher electronegative dopant ions are catalytically more active towards electrochemical reduction of nitrobenzene as compared to the lower electronegative dopant ions i.e., with increase in electronegativity of the dopant ions catalytic activity increases.

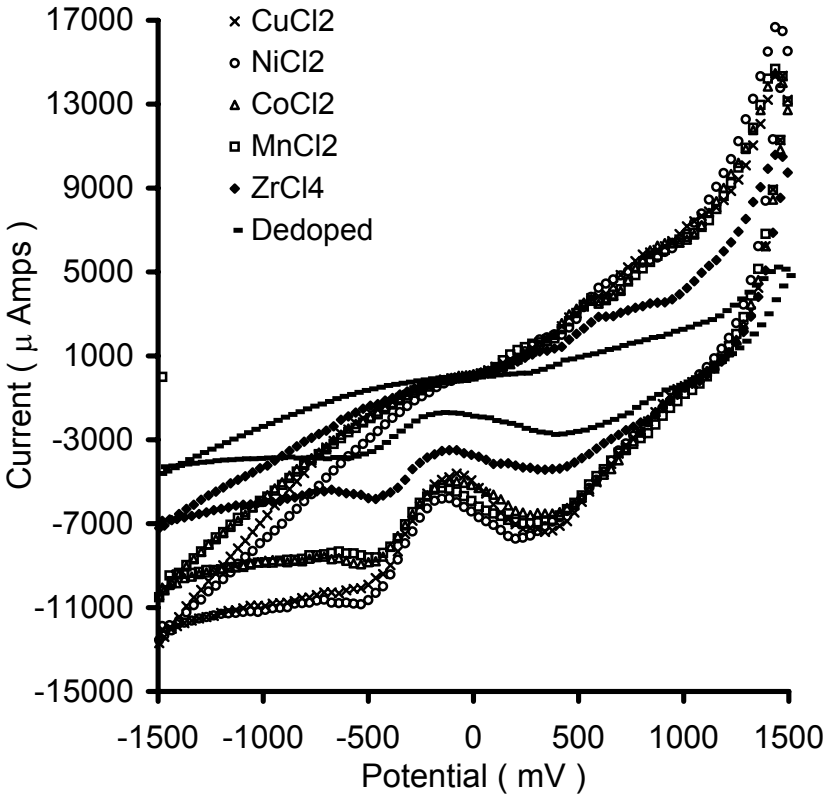

Figure 5.5 : CV's of electrochemical reduction of nitrobenzene with PPy doped with different dopants

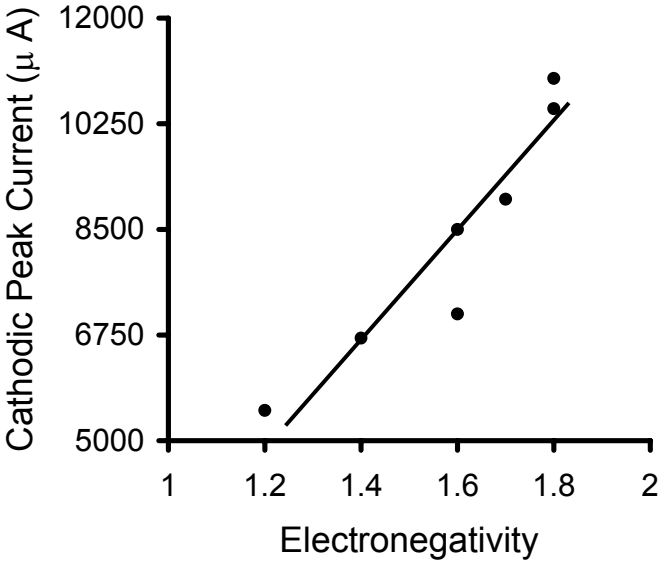

Figure 5. 6: Graph of peak current for electro-reduction of nitrobenzene vs. electronegativity of the dopant ion

5.3.2.2. Energy Level representation of the different doped electrodes with respect to nitrobenzene.

The reason for the better catalytic activity of the PPy doped with higher electronegative dopants ions towards nitrobenzene electro-reduction process was investigated by plotting the energy level of the each dopant ions with respect to PPy. In order to obtain the position of the energy level with respect to the valence / conduction band electrical properties of the PPy doped with different ions were measured. Detail procedure was discussed in the chapter II as well as in the chapter III for discussing the charge transport process in the methanol electrooxidation reaction. The energy level representation for these electrodes with respect to PPy in contact with nitrobenzene containing electrolyte

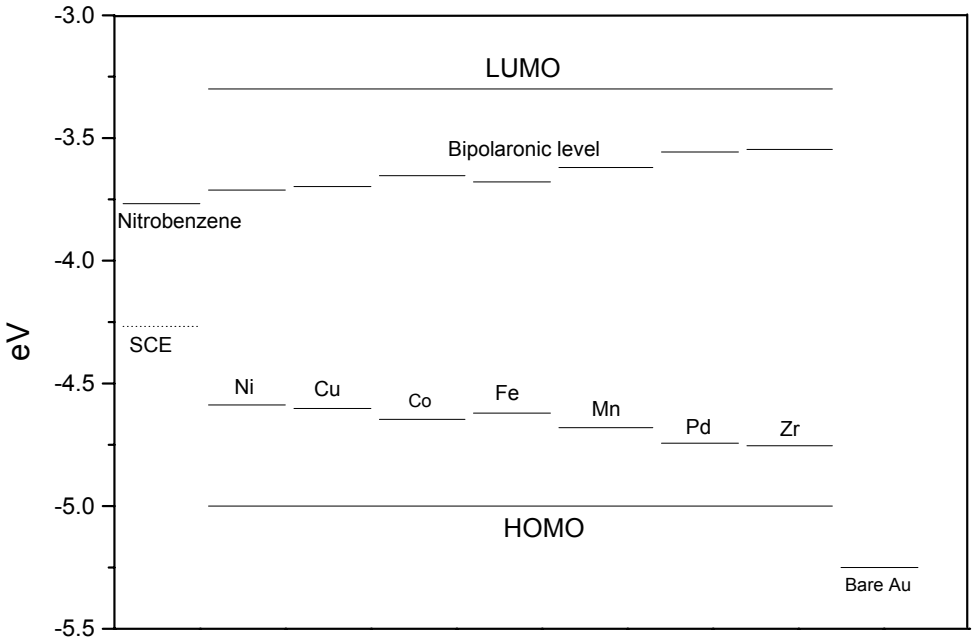

Figure 5.7: Energy level representation of the different modified electrodes in contact with nitrobenzene

and gold backing layer is shown in the *Figure 5.7***.** It could be seen from the energy level representation that for the PPy doped with $NiCl_2$ electrodes, it was easier for holes to be transferred from the electrode to the reactant nitrobenzene than in other cases. The

electron transport from electrode to reactant leads to the reduction of nitrobenzene, which is the opposite of the methanol electrooxidation process.

In the electrochemical reduction of nitrobenzene, as in methanol electrooxidation process, the primary rate-determining step appears to be controlled by the charge transport at the anode. From the discussions above, it is observed that the energy level of the dopant ion in the polymer appears to play an important role in the electroreduction process using conducting polymer.

It was clear from the energy level representation that the charge transport reaction is an important factor and it plays an important role in the electro-catalytic reduction of nitrobenzene using different modified PPy electrodes. Further studies were carried out to find out the best dopant ion concentration of various doping agents. For that purpose PPy doped with varying concentrations doping agents were employed as working electrodes. Dopant ion concentration was varied from 0.003M, 0.006M, 0.012M, and 0.02M. *Figure 5. 8* represents the graph of cathodic peak current against concentration of

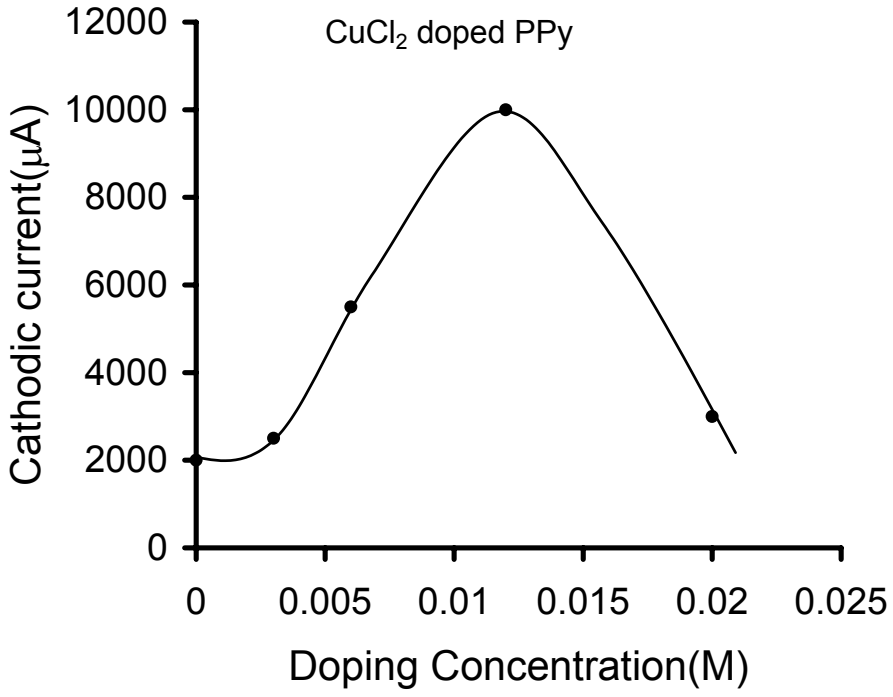

Figure 5.8: Graph of peak current against doping concentration of the reactant for the electrochemical reduction of nitrobenzene at $CuCl_2$ doped PPy electrode

$CuCl_2$ in the electrodes. CV's of other dopant ions viz. $NiCl_2$, $CoCl_2$, $FeCl_3$ etc were also run but not shown. From the graph it could be observed that for PPy electrodes doped with 0.012M showed maximum electro-catalytic activity for nitrobenzene reduction process. These findings suggest that the number of specific sites generated by the doping process and the amount of reactant adsorbed on the surface are optimum under these conditions.

5.3.3. Further modification of electrodes

As it has been observed that the PPy modified electrodes are active towards nitrobenzene reduction, further modification like insitu polymerization, surface roughening, of electrodes were carried out and studied for electrochemical reduction. Various reaction conditions like temperature and scan rate of the reaction also varied for the nitrobenzene reduction.

Insitu polymerization:

Conducting PPy electrodes modified by doping internally with different dopant ions i.e. insitu doped PPy electrodes were employed to study the electroreduction of nitrobenzene. CV's for different insitu doped PPy films were shown in the *Figure 5.9*. CV's show that the insitu doped films were much more electrocatalytically active towards reduction of nitrobenzene than exsitu ones. From the CV's similar trends were observed as in the external doped PPy. To make a comparative study between exsitu and insitu doped films a graph of peak current vs. electronegativity individual dopant ions were plotted which is shown in the *figure 5.10.* It could be seen in the graph that the internally doped PPy electrodes are catalytically more active as compared to the externally doped electrodes.

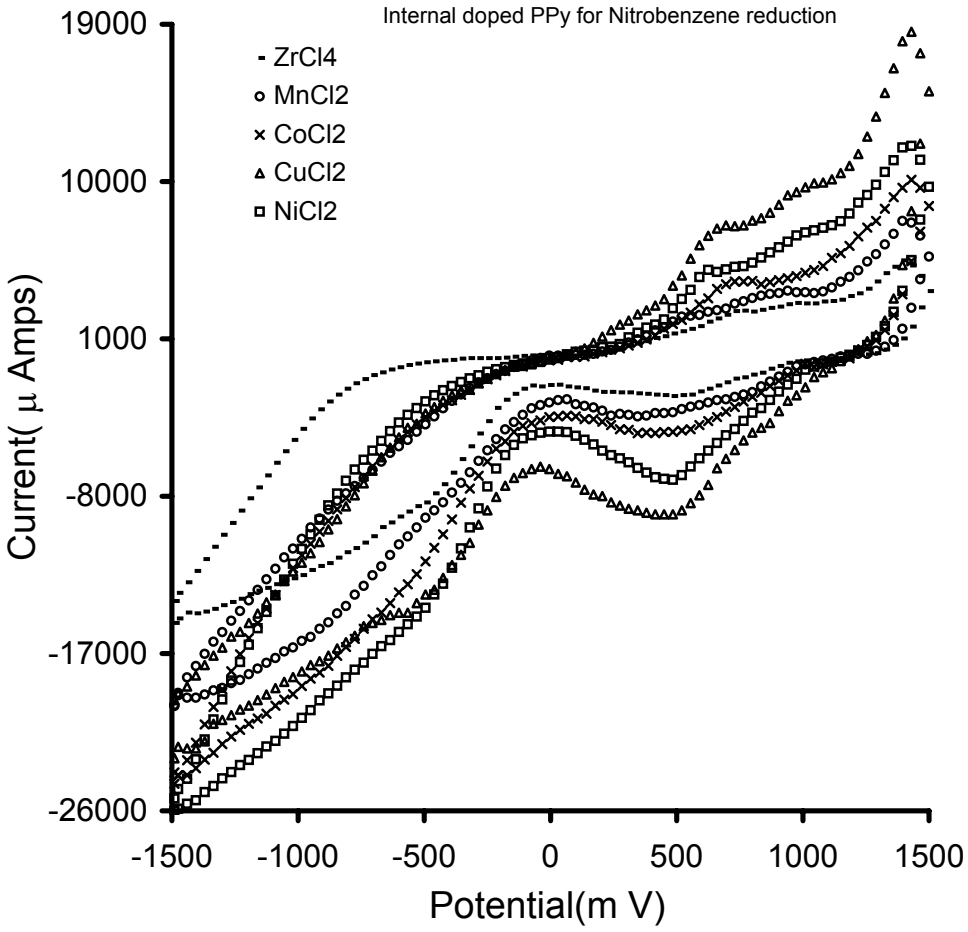

Figure 5.9: CV's for the electroreduction of nitrobenzene with different insitu doped PPy electrodes

This enhancement in catalytic activity in case of internally doped samples is attributed to the better complexation prior to electrochemical polymerization which is proved from the different characterizations carried out for the films details of which is given in the chapter III.

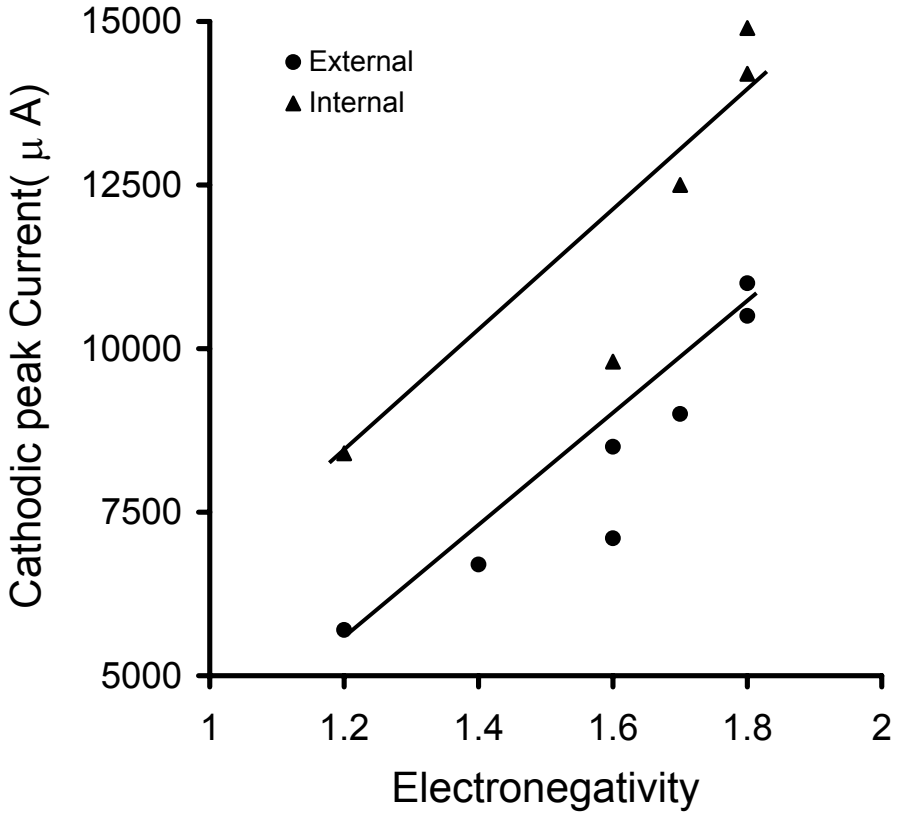

Figure 5.10: Graph of peak current for the electroreduction of nitrobenzene against electronegativity of the dopants in PPy (for both external and internal doping)

Effect of Surface Roughness of PPy films

As it is known that surface morphology of the electrocatalyst plays an important role in the electrochemical reactions, reactions were carried out with conducting PPy electrodes of varying roughness. PPy film electrodes of varying roughness were prepared by varying scanning rate while depositing the films. For getting PPy films of varying roughness cyclic voltammetry technique was employed for electrochemical synthesis instead of commonly used chronoamperommetry technique. These films were then doped with $NiCl_2$ and were employed to study the effect on electroreduction of nitrobenzene. CV's of the films of varying roughness for 0.1 M nitrobenzene is shown in *Figure 5.11*

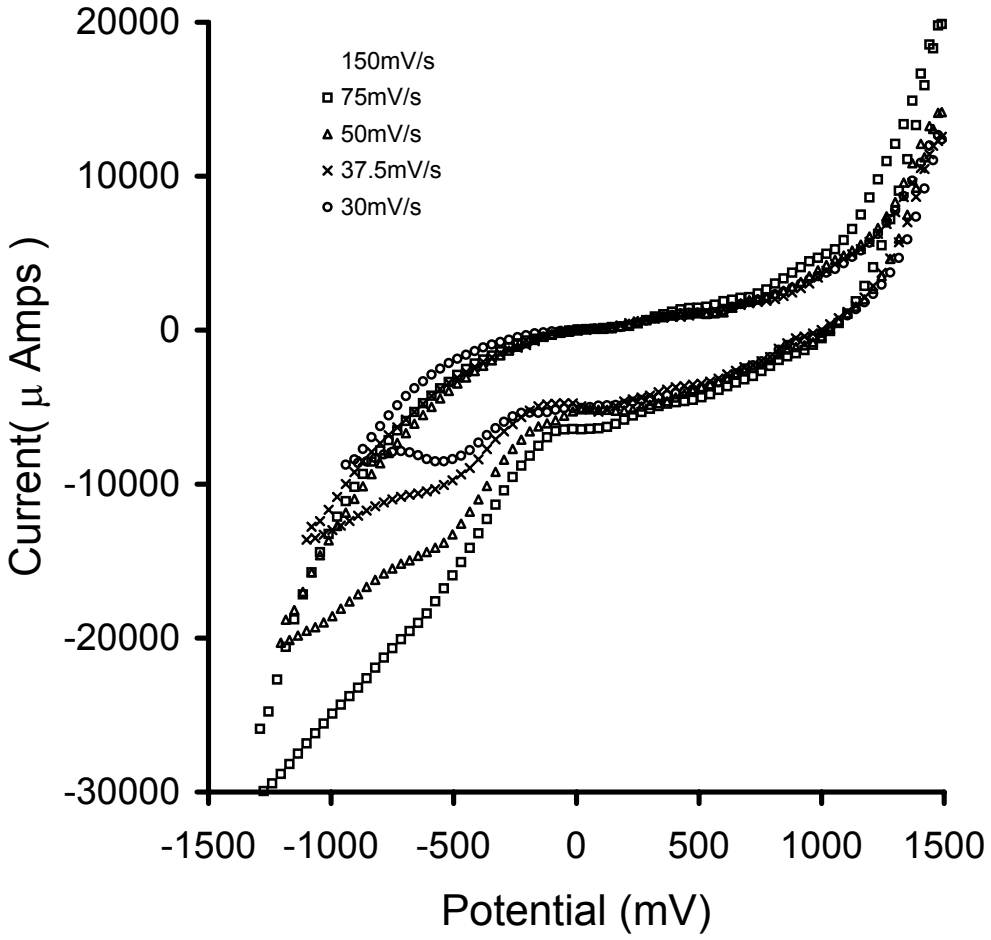

Figure 5.11: CV's of electrochemical reduction of nitrobenzene using films of varying roughness

From the CV's it could be observed that films which are more rough in nature are catalytically more active. As it was seen from the SEM figures that films [Figure 3.41, Chapter III] which are prepared at higher scan rate are more rougher that those prepared at lower scan rate. It could be seen in the figure that as the scan rate of deposition ie. roughness increases electrocatalytic activity towards nitrobenzene reduction increases.

Increase of roughness of the film, surface area and porosity increase resulting in the increase of number of sites for interaction with the reactant which gives rise to improved catalytic activity. This is in agreement with the earlier remarks made regarding the number of available active sites for catalytic process wherein the surface morphology plays an important role.

5.4. KINETIC STUDY OF NITROBENZENE REDUCTION REACTION:

Temperature variation:

Temperature effect on the electroreduction of nitrobenzene was also studied. The various data's obtained from the temperature dependence reaction was used to determine the activation energy of the reaction also. CV's were run for temperatures 5°C, 15°C, 26°C, 35°C and 48°C. From the CV's, cathodic peak current for nitrobenzene reduction vs. temperature of the reaction was plotted which is shown in the *figure 5.12***.** From the graph it could be concluded that rate of the electro-reduction of nitrobenzene reaction is temperature dependent, which increases with temperature of the reaction.

It is known that electrocatalytic reduction process of nitrobenzene is six electron process and proceeds through several intermediate steps. In protic system the electrochemical

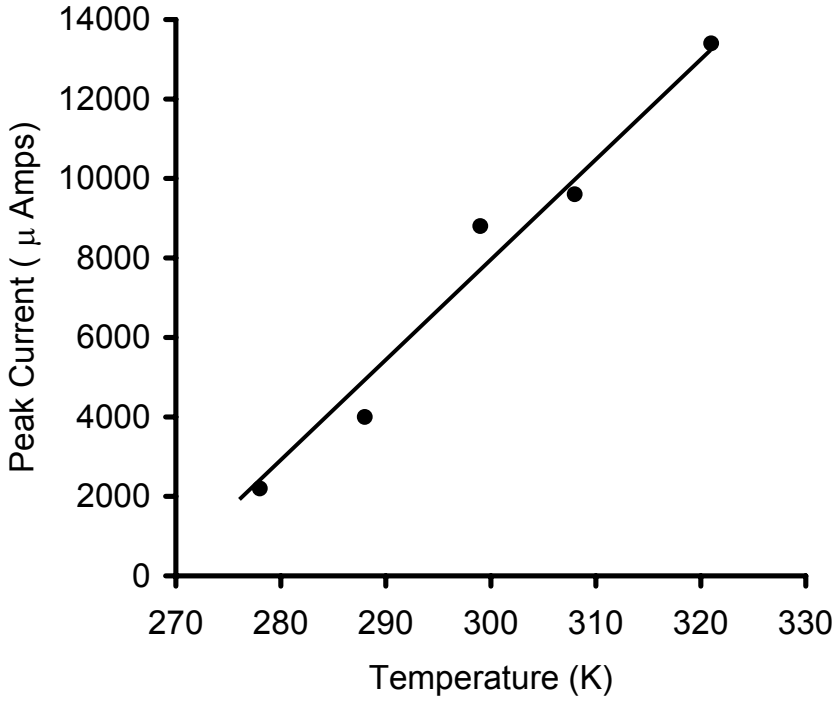

Figure 5.12 : Graph of Peak current vs temperature of the reaction for the electrochemical reduction of nitrobenzene using conducting polymer electrodes

reduction progress through steps as given in the *figure 5.13* which was suggested by Heyrovsky and coworker.[70]

The intermediate reduction products of nitrobenzene are nitrosobenzene and phenylhydroxylamine which finally leads to the formation of aniline.

But at high temperature, in acidic conditions, the intermediate phenylhydroxylamine undergoes rearrangement to form p-aminophenol.[14]

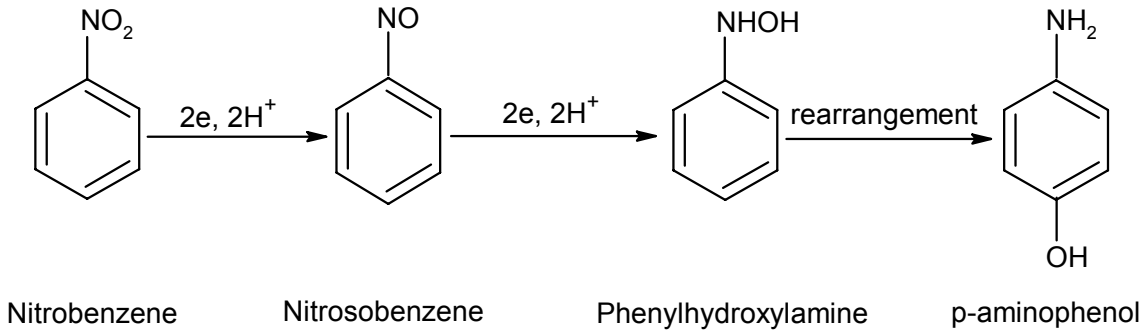

In the present study, when the electrochemical reduction reaction was carried out at higher temperature, it was observed that the electrolytic solution turns to slight red in color, which may be due to the formation of azobenzene derivatives as a result of side/coupling reaction as one of the product of intermediate steps shown in the nitrobenzene reaction scheme in the *figure 5.13.*

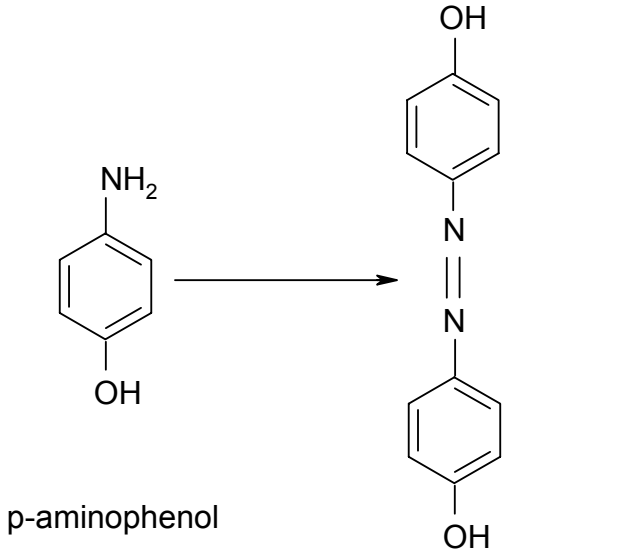

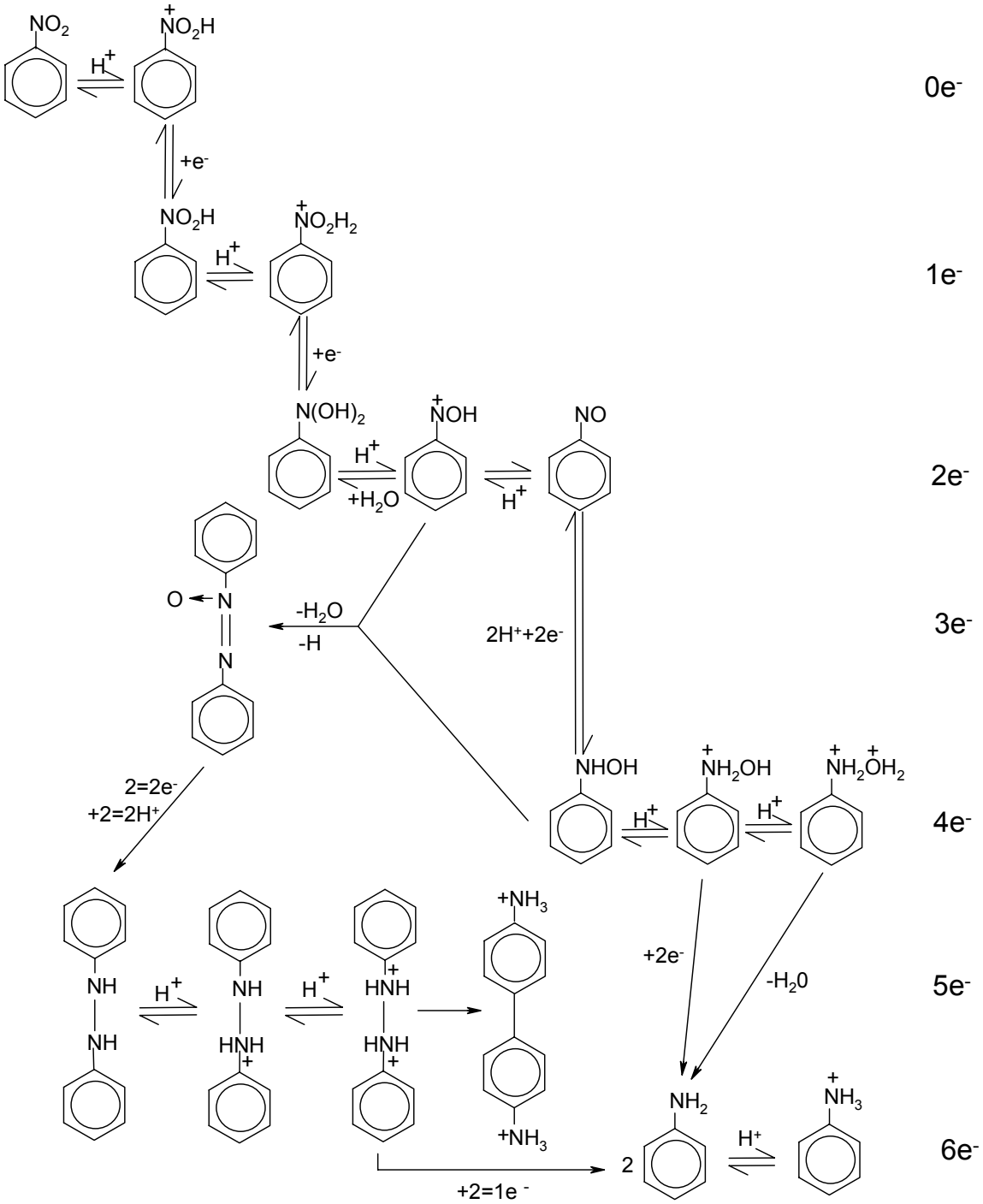

Figure 5.13: Reaction scheme for complete nitrobenzene reduction process.

[Reaction scheme proposed by Heyrovsky and coworker]

It was suggested by Seshadri et al the formation of p-aminophenol at higher temperature as shown in the above reaction which may further undergo couple reaction to form 2,2-dihydroxy azobenzene leading to colored product.

Kinetics of the nitrobenzene electrochemical reduction was also studied with the help of temperature variation CV's. From the temperature dependence cyclic voltammograms log

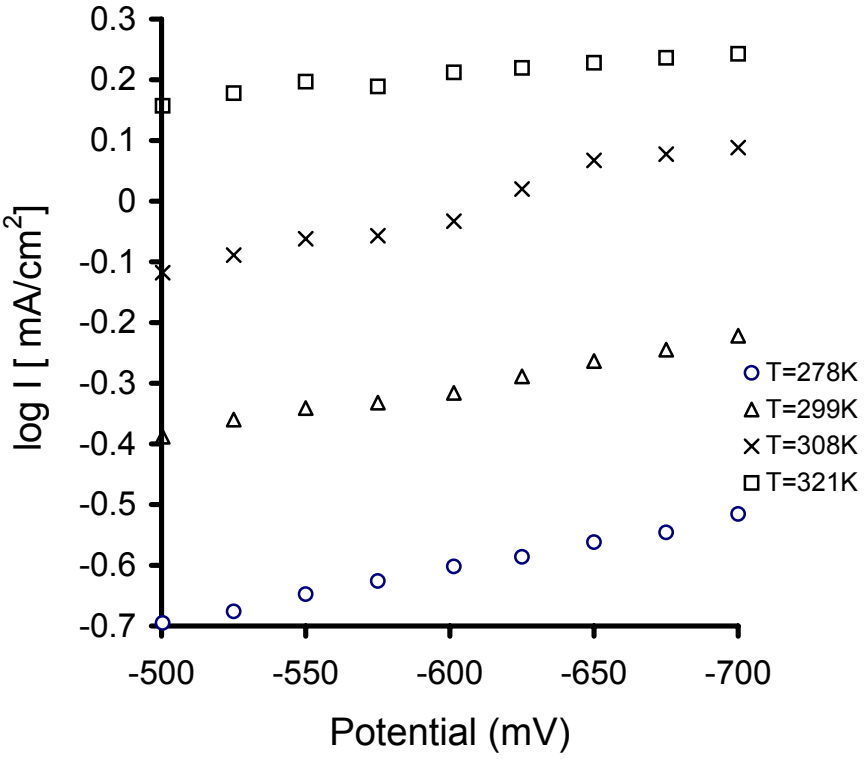

Figure 5.14: Graph of log I against potential for nitrobenzene electrochemical reduction using $NiCl_2$ doped PPy electrodes

current vs. potential was plotted which is shown in the *figure 5.14***.** Intercepts from the above graph is found out and log I vs. 1/T is plotted using these datas. Graph of log I vs. log 1/T is given in the *figure 5.15.* With the help of the slope obtained from the above mentioned plot, activation energy for nitrobenzene electroreduction was calculated using Arrhenius equation. Activation energy for nitrobenzene electrochemical reduction was found out to be 0.52eV.

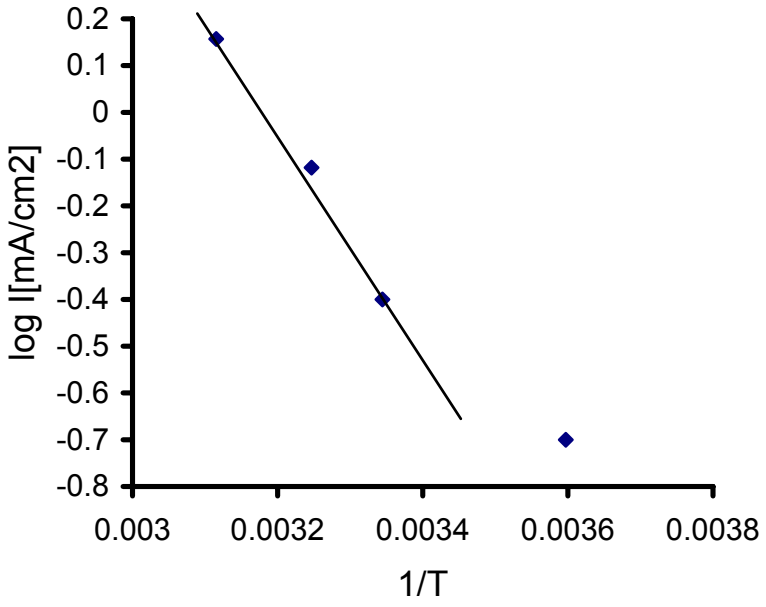

Figure 5.15. Graph of log I vs I/T for electrochemical reduction of nitrobenzene with $NiCl_2$ doped PPy electrodes.

Varying nitrobenzene concentration

Kinetics of nitrobenzene electrochemical reduction was studied by plotting Tafel plots. CV's of PPy doped with $CuCl_2$ electrodes for varying nitrobenzene concentration were used to plot Tafel plot. It was seen in the CV's that for the entire concentration range the reaction rate increased with increasing nitrobenzene concentration.

Figure 5.16. is the graph of log I (mA/cm^2) against potential in the cathodic potential range for different concentrations of nitrobenzene in the electrolyte. Potential range taken for plotting Tafel plot is -200mV to -450mV. From the plot of log I vs. potential, intercepts of the straight lines was found out for plotting the graph of log I vs. log C, which is shown in the *figure 5.17.* Slope of the straight line is found out to be 0.512, which implies that nitrobenzene reduction follows half order kinetics with respect to nitrobenzene.

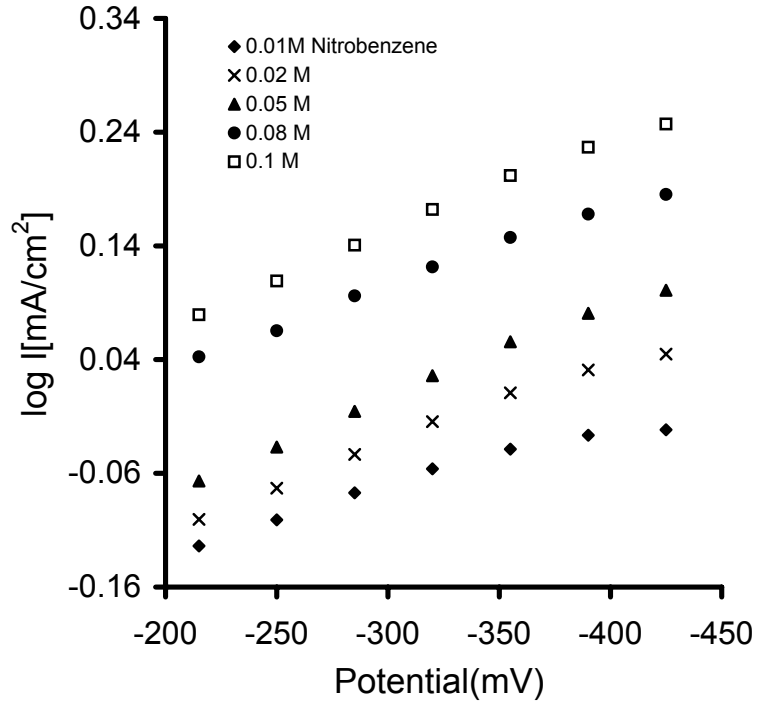

Figure..5.16: Graph of log I against potential for nitrobenzene reduction with $NiCl_2$ doped PPy electrodes

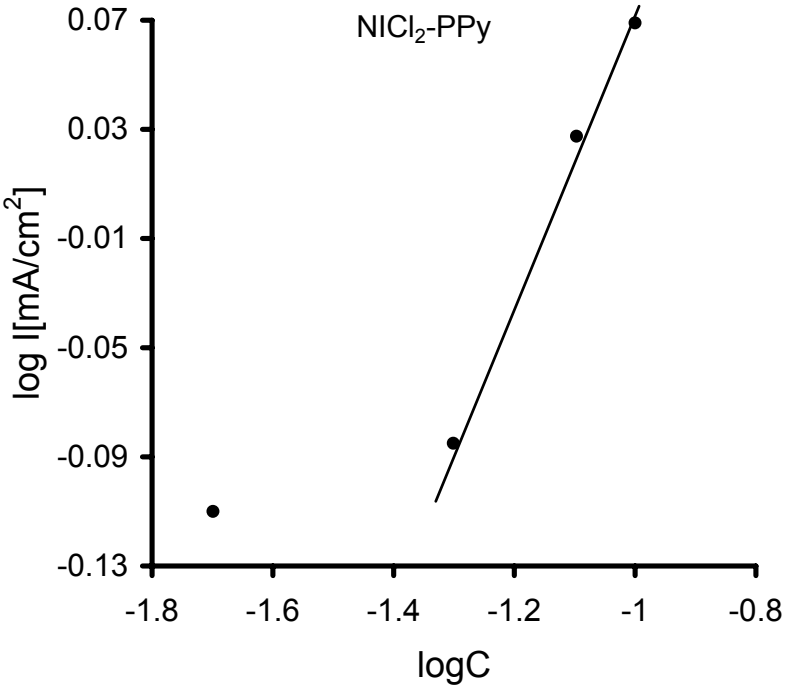

Figure 5.17: Graph of log I against log C for nitrobenzene reduction with $NiCl_2$ doped PPy electrodes

5.5. ELECTROCHEMICAL REDUCTIONS AT DIFFERENT ELECTRODES:

Electrochemical reductions of nitrobenzene were carried out at different electrodes to observe the nature of the cyclic voltammograms. For that purpose 10 continuous cycles were recorded from –1500mV to +1500mV. CV's for PPy modified by doping with $PdCl_2$, $ZrCl_4$ and $CuCl_2$ electrodes have been shown in the *figure 5.18 (A),(B) and (C)* respectively. From the figures it could be observed that the nature of the CV's are

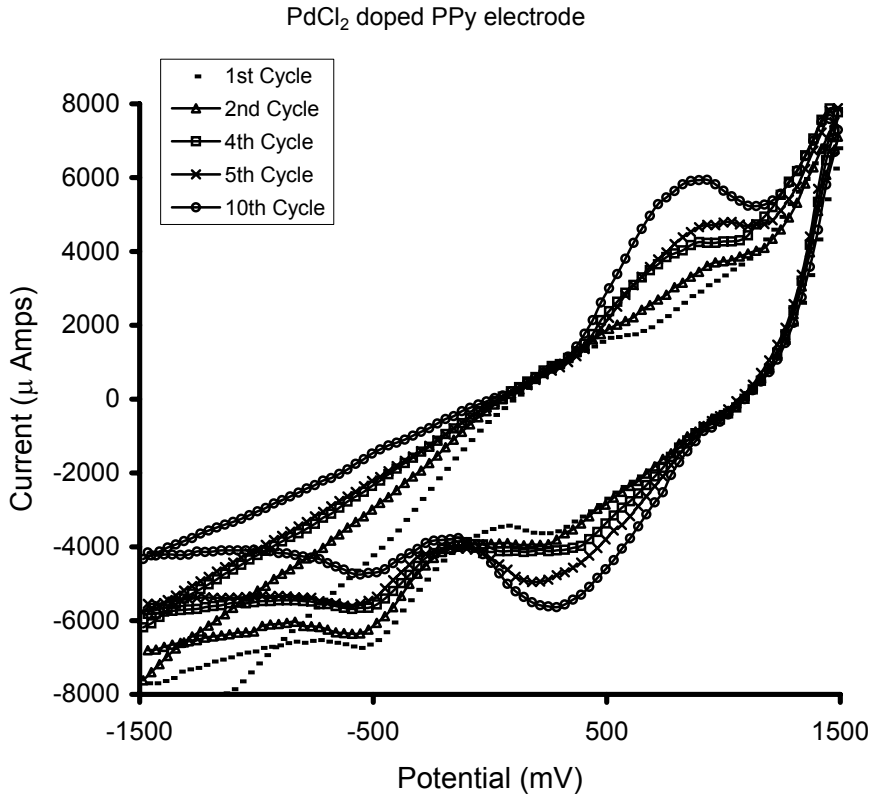

Figure .5.18.(A): CV's of continuous cycling for the electrochemical reduction of nitrobenzene using PPy modified with $PdCl_2$ electrode

different for different modified electrodes. In the figure (A) ie the CV's for PPy modified with $PdCl_2$ electrode, it could be observed that with the number of cycles peak current at –500mV decreases whereas the peak appearing at +300mV in the reduction cycle increases with cycle. The anodic peak in the +875mV region also increases with the cycle.

In case of $ZrCl_4$ doped PPy electrode, from the CV's [figure (B)] it could be seen that the cathodic peak at –500mV which is attributed to the reduction of nitrobenzene does not change with increase in number of cycles, i.e. the peak height remains constant throughout the cycling. But the anodic peak at +875mV and the peak appearing in the +450mV in the reduction cycle increase with increase in no of cycles.

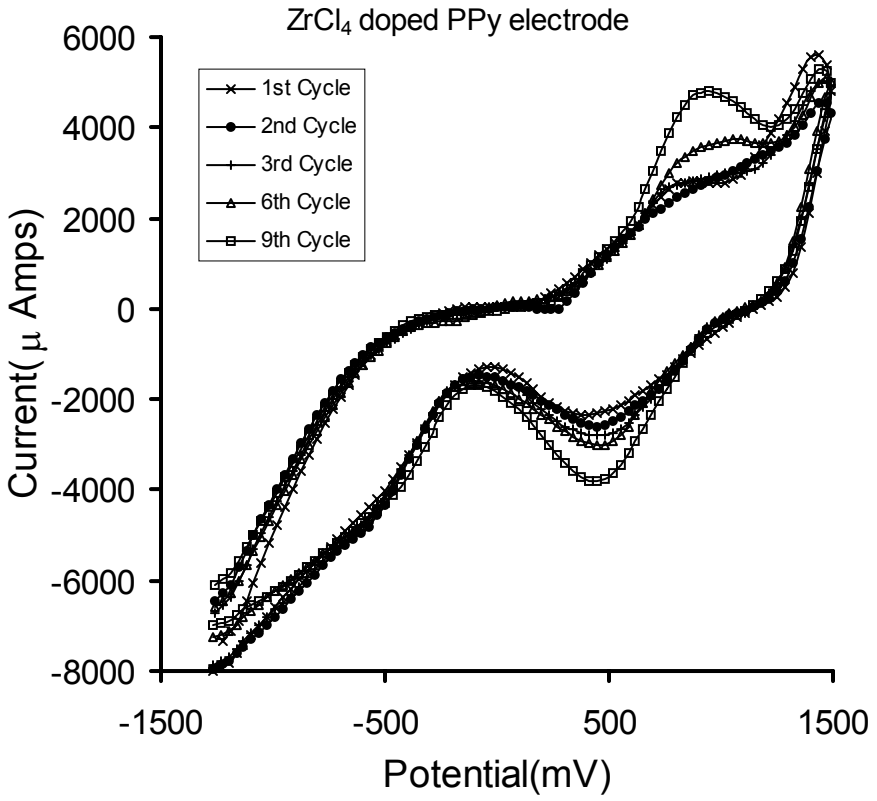

Figure 5.18.(B): CV's of continuous cycling for the electrochemical reduction of nitrobenzene using PPy modified with $ZrCl_4$ electrode

In case of $CuCl_2$ doped PPy electrode, CV's show that the cathodic peak at –500mV shifts towards more negative potential and peak height increases with cycling and at 10^{th} cycle the peak appears at –950mV. The anodic peak, which appears at +550mV, also shifts towards more positive potential and at 10^{th} cycle it appears at +1000mV. The peak, which appears at +150mV during reduction cycle, increases with cycle.

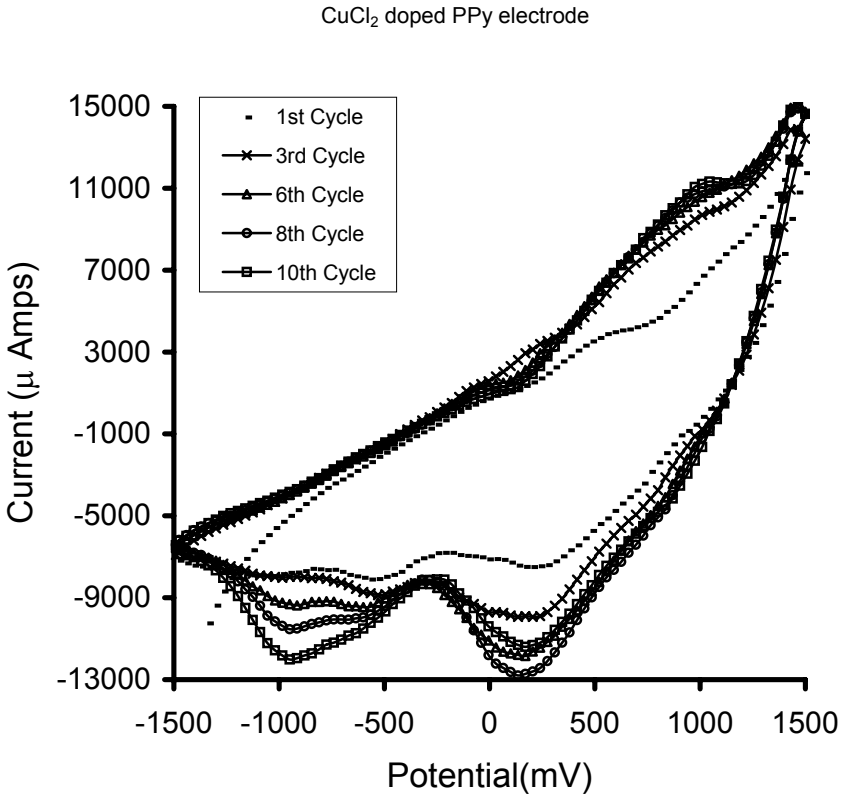

Figure .5.18.(C): CV's of continuous cycling for the electrochemical reduction of nitrobenzene using PPy modified with $CuCl_2$ electrode

From the above CV's it could be clearly seen that in the same electrolytic solution, different PPy modified electrodes behave in different manner. It can also possible that at different electrodes, different products will form. In case of $CuCl_2$ doped PPy electrode, shift in the cathodic peak (-500mV to –950mV) is observed, which might be due to the fact that product which got produced in the initial cycles might further reduced in the subsequent cycles. Therefore the initial peak at –500mV could not be seen as the reaction progressed.

5.6. ELECTROCHEMICAL REDUCTION OF NITROBENZENE AT DIFFERENT POTENTIALS

Electrochemical reduction of nitrobenzene was run at different electrode potential also to find out the effect of electrode potential on the electrochemical reaction. The reactions were run in the chronoamperometry mode instead of cyclic voltammetry mode. Reaction potential applied for the reactions were –500mV, -700mV, -850mV and –950mV for 5 hours at room temperature. The reaction product of these reactions were investigated by UV-Vis and FT-IR techniques.

UV-Vis studies

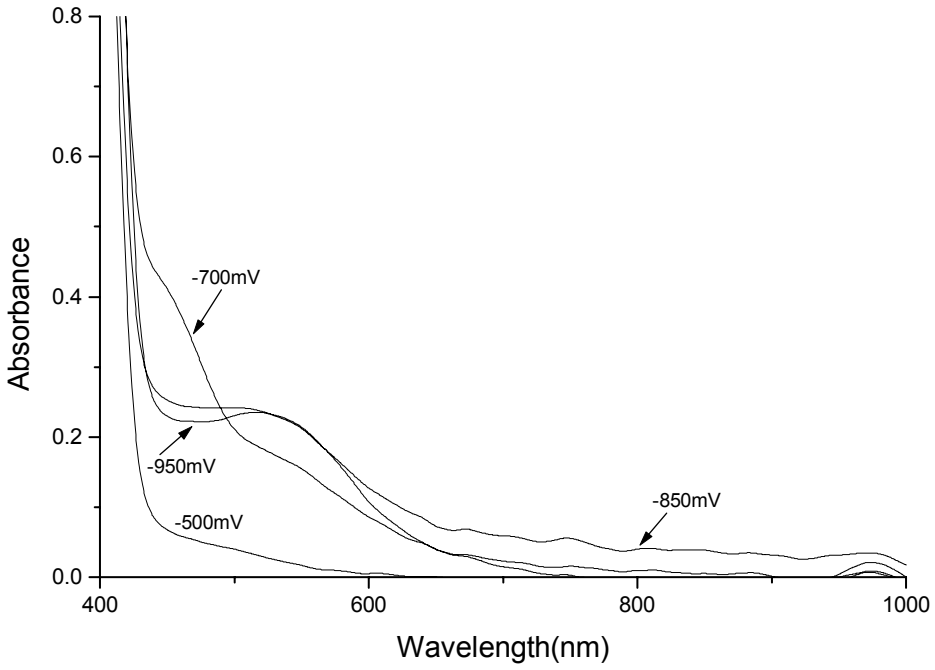

Figure 5.19: UV-Vis of the different electrochemical solutions

It was observed that the electrochemical solution after the reaction run at different potentials changes to different colors. The electrochemical solution, the reaction potential for which was -500mV was slightly yellow in color and the color of the electrochemical solution run at -7000mV was intense yellow. Whereas the reactions run at 850mV and 950mV was red in color with varying intensity. There is possibility of formation of azo derivatives also as one of the products of the side / coupling reactions which are known to show color. In the UV-Vis spectra *[Figure 5.19]* it was seen that nature of the spectra are

different for the solutions of different reactions run at various potential. It was observed that for the reaction run at –500mV, small peak at 450nm was seen, whereas for the reactions run at –700mV two peaks could be observed, one at 470nm and the other at 525nm. But in case of the reactions run at –850mV and –950mV only one peak was observed at 525nm region. From this result it can be said that at different electrode potentials different products are formed. From the UV-Vis spectra formation of azobenzene derivatives, e.g. 2,2 dihydroxyazobenzene etc can be predicted. The peaks appearing at 450nm and 525nm may be due to the azobenzene derivatives which is reported in various reports. [71-75]

FT-IR studies

The FT-IR spectra of these different electrochemical solutions were run which is shown in the *figure 5.20(A) and (B).* Figure (A) corresponds to the FT-IR of the solutions in the range 4000cm^{-1} to 2000cm^{-1} and figure (B) corresponds to 2000cm^{-1} to 500cm^{-1}.

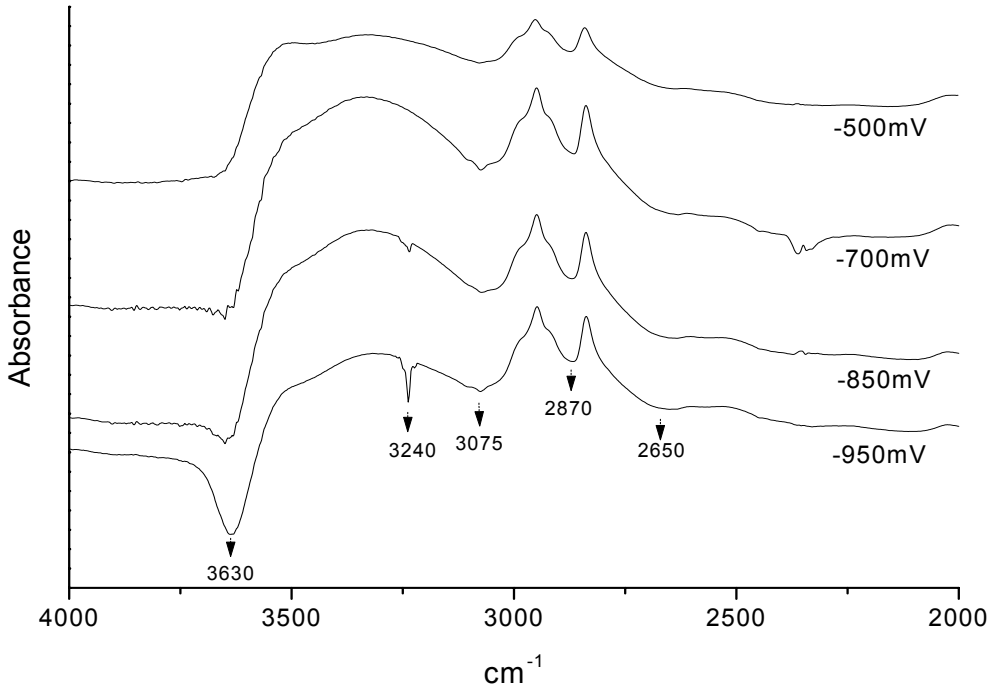

Figure 5.20(A): FT-IR spectra of different electrochemical solutions from 4000cm^{-1} to 2000cm^{-1}

Assignments of the peaks are given in the *table 5.2***.** It was seen in the IR that the reactions run at –950mV, peaks are prominent and sharp. In the figure (a) it was seen that the peak appearing at 3630cm^{-1} got stronger when the reaction was run at –950mV. A small peak also was seen at 3240cm^{-1} also. Both these peaks were attributed to the –NH stretching vibration.[76]

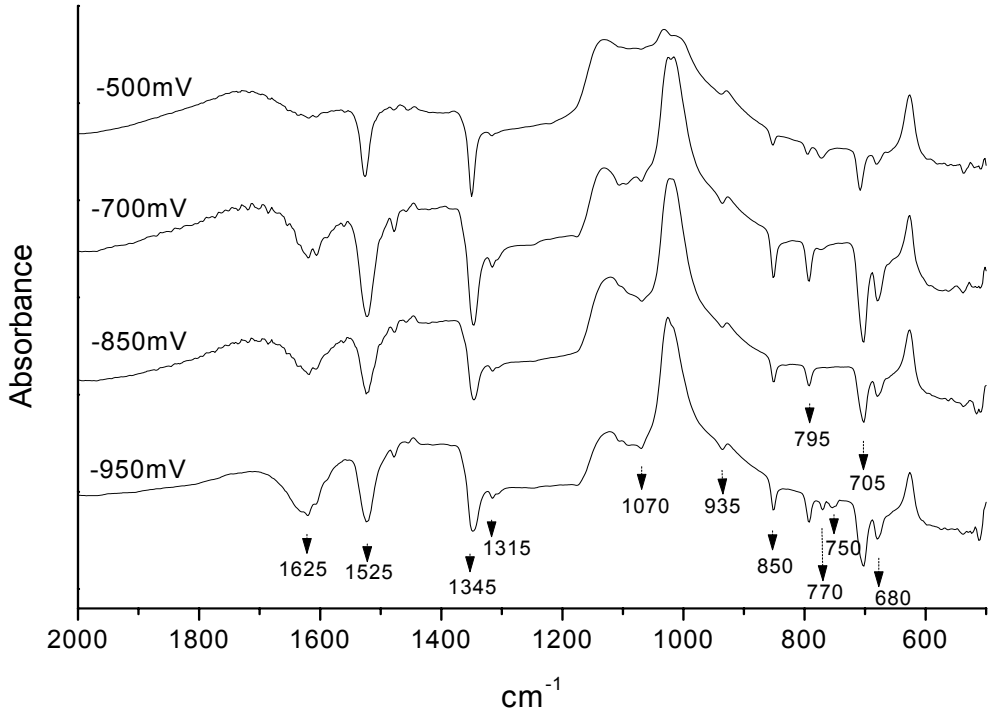

Figure 5.20.(B)FT-IR spectra of different electrochemical solutions from 2000cm^{-1} to 500cm^{-1}

In the figure (B) it was seen that the intensity of the peaks appearing at 1525cm^{-1} and 1345cm^{-1} almost same in all the cases but there is variation of intensity for other peaks. Both these peaks are assigned to the NO_2 and C-N vibration of R-NO_2 which indicates the presence of initial reactant nitrobenzene in the reaction mixture. The peak appearing at 1625cm^{-1} was due to primary -N-H bending and R-NH_2 scissor. The peak at 1625 cm^{-1} can also be attributed to the –N=N- vibration. The peaks at 1315cm^{-1}, 795cm^{-1} and 680cm^{-1} could be attributed to the phenyl amine. From all these studies it could be concluded that at –950mV aniline along with some azobenzene derivatives may form.

The reactions run at other potentials, possibility of formation of other intermediate products exist along with aniline and azobenzene derivative compounds.

Peak position (cm^{-1})	**-500mV**	**-700mV**	**-850mV**	**-950mV**	**Assignment**
3630	w	w	m	s	NH stretching vibration
3240	-	-	w	m	NH stretching vibration
3075	br	br	br	br	Aromatic C-H stretching
2870	w	s	s	s	
1625	w	m	m	s	N-H bending (primary), R-NH_2 scissor, -N=N-
1525	s	s	s	s	Aromatic R-NO_2
1345	s	s	s	s	C-N vibration of R-NO_2
1315	w	w	w	w	Aryl amine
1075	br	br	br	br	N-H inplane deformation
850					
795	vw	w	w	w	Aromatic NH_2
770	-	-	-	w	
680	vw	m	m	m	Phenyl –NH_2 / R-NH-R

Table 5.2 : Table of FT-IR assignment for the different reactions run at various potentials

5.7. REDUCTION OF REACTANTS OF DIFFERENT REDOX POTENTIAL:

It was observed that charge transfer process is the important player in the electrochemical reactions. Position of the energy levels of the electrodes and the redox potential of the

reactants are the important factors which determine the activity of the electrocatalyst, rate of the reaction etc. Hence to study the effect of different redox potential of reactant, electrocatalytic reduction of different reactants viz. nitrobenzene, benzaldehyde and acetophenone were carried out at $NiCl_2$ doped PPy electrode, CV's for which is shown in the *figure 5.21.* The redox potentials are -0.5V, -0.89V and –1.15V for nitrobenzene,

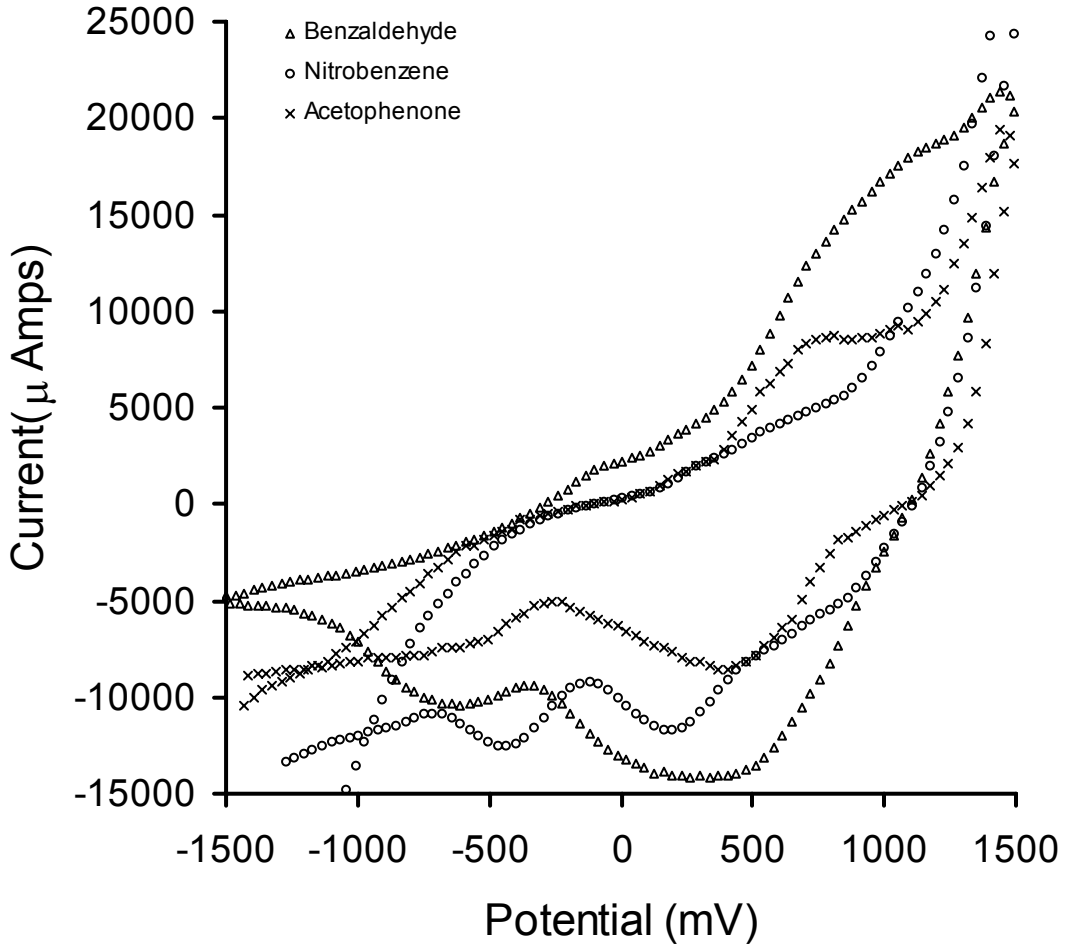

Figure 5.21: CV's for the electroreduction of different electrolyte at $NiCl_2$ doped PPy electrode

benzaldehyde and acetophenone respectively. All the potentials are mentioned here are with respect to SCE only. From the CV's it could be seen that at $NiCl_2$ doped PPy electrode the reduction peak current follows the trend for nitrobenzene > benzaldehyde >

acetophenone which is in accordance with the datas of the redox potentials, i.e. the substance with least negative or most positive potential reduces first among different reactants. From the CV's multiple peaks in case of nitrobenzene was observed which might be due to the formation of intermediates during the course of the reaction. To study the charge transfer process in these reduction process energy level representation was plotted with respect to $NiCl_2$ doped PPy electrode which is given in the *figure 5.22.*

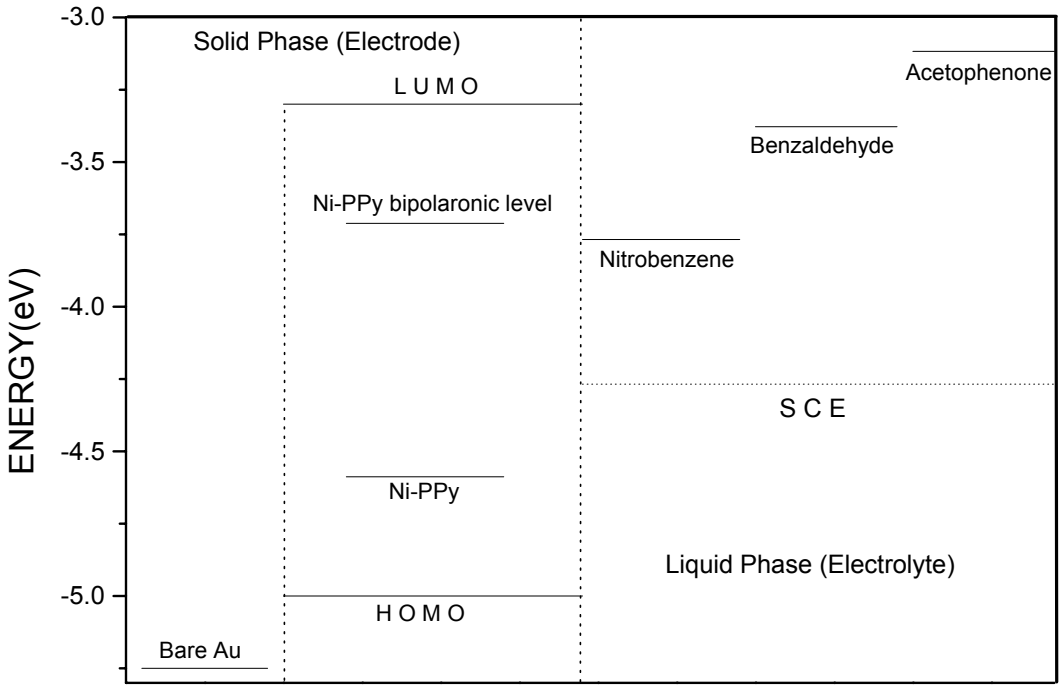

Figure 5.23: Energy level representation for the PPy-$NiCl_2$ electrode with different reactants

From the energy level representation it could be observed that in case of nitrobenzene reactant, it was easier for holes to be transferred from the $NiCl_2$ doped PPy electrode to the reactant rather than the other reactants viz. benzaldehyde and acetophenone. The hole transport from electrode to reactant leads to the reduction of nitrobenzene. The easier the hole transfer process from the electrode to the reactant, the more active is the species undergoing reduction process. In case of $NiCl_2$ doped PPy electrode nitrobenzene

undergoes reduction easily as compared to the benzaldehyde and acetophenone. Hence, proper modification of the conducting polymer electrode and selection of the reactant also will felicitate faster reaction. Activity and selectivity of the electrode as well as the reactant, nature or the direction of the reaction process i.e., reduction or oxidation also can be predicted from the energy level.

5.8. CONCLUSION

From all the above studies it could be predicted that modified PPy films are electro-catalytically active towards nitrobenzene reduction also. Dependence of height of the peak current with concentration in the cathodic region confirms the forward nature of the reaction. PPy alone also showed some catalytic activity but when it was modified by doping, catalytic activity got enhanced. Importance of electron/hole transfer process at the electrode interface as the controlling parameter for the electrocatalytic reaction can be understood from the energy level representation.

The enhancement in the electrocatalytic activity was more pronounced in case of PPy electrodes modified with higher electronegative dopants whereas when PPy films were modified with less electronegative dopants catalytic activity was less. With the help of energy level diagram for the different dopant ions with respect to PPy in contact with the reactant the mechanism of electron/hole transport process in the electrochemical reduction process is explained. It is seen that in the reduction processes, for PPy doped with $NiCl_2$ electrodes, it is easier for holes to be transferred from the electrode to the reactant than in other cases. The hole transport from electrode to the electrolyte or electron transport from reactant to the electrode leads to the reduction of nitrobenzene to the desired products.

In the present study it could also be seen that electrode material also plays an important role in the electrochemical reaction. When continuously several cycles were run with PPy electrodes modified with different dopants, nature and shape of the cyclic voltammograms varied with the incorporation of different dopants. From this, it can be said that for different electrodes different products may form or it can be said that activity and selectivity can be vary with different modified electrodes.

An interesting point could be observed from the present piece of work is that, when the reactions were run at different fixed potential [chronoamperometry] the electrochemical solutions turns to different colors. From this it can be concluded that potential of the reaction predicts the nature of the product or selectivity towards different products can be attained by selecting potential.

From the UV-Vis and FT-IR studies of the product analysis shows the formation of aniline along with azobenzene type coupling product. The FT-IR studies for different reactions run at different potentials show that when the reactions were run at higher potential the intensity of the peaks indicating aniline peaks got prominent as compared to the reactions run at lower potentials.

In another part of current experiment, electrochemical reduction of different reactants, viz. benzaldehyde, acetophenone and nitrobenzene were carried out with $NiCl_2$ doped PPy electrode. It was seen that peak current values were in the order of nitrobenzene > benzaldehyde > acetophenone. Here, among nitrobenzene (-0.5mV), benzaldehyde (-0.89mV) and acetophenone (-1.15mV), nitrobenzene having less negative potential is easier to reduce which can be seen in the energy level diagram of the different reactants plotted along with the $NiCl_2$ doped PPy electrode. It can e predicted from this studies that as the potential value of any reactant approaches towards vacuum level in the energy level representation the material will be difficult to reduce or it will be easier to oxidize.

Thus from all the above studies it can be predicted that the energy level is the most important factor which determines the rate of the reaction, path of the reaction and selectivity and activity of the electrode material

---

5.9. REFERENCES

1. D.H. Geske and A.H.Maki; J.Amer. Chem. Soc. *82(1960)2671*

2. D. E. Bartak, W. C. Danen, M. F. Marcus and M. D. Hawley, J. Org. Chem.*35 1206(1970)*
3. W. Kemula and T. M. Krygowski, Vol-XIII. Ch. 2. Encyclopedia of the Electrochemistry of the Elements; Ex. Ed. A. J. Bard, Asso. Ed. H. Lund, Marcel Dekker Inc., New York, *1973*
4. J. C. Smeltzer, P. S. Fedkiw.; J.Electrochem.Soc., *139(1992)1358*
5. J. C. Smeltzer, P. S. Fedkiw.; J.Electrochem.Soc., *139(1992)1366*
6. C. Yu, B.Liu and L. Ho; J.Org. Chem.*; 66(2001) 919*
7. W. H. Smith and A. J. Bard, J. Amer. Chem. Soc. *97(1975)5203*
8. A. Kalandyk and J. Stroka; J. Electroanal. Chem., *346(1993)323*
9. M.Inaba,Z.Ogumi and Z.Takehara; J.Electrochem.Soc. *140(1993)19*
10. C. Ravichandran, S. Chellammal and P. N. Anantharaman; J. Appl. Electrochem. *19 (1989) 465.*
11. G. Kokkinidis and K. Juttner Electrochim. Acta. *26(1981)971.*
12. L.-J.Fan, C.Wang, S.-C.Chang, Y.Yang; J.Electroanal.Chem.,*477(1999)111*
13. S. F. Dennis, .S. Powell and M. J. Astle; J. Amer. Chem.Soc, *71(1949)1484*
14. G. Seshadri and J. A. Kelbar; J.Electrochem. Soc.*146(10) (1999) 3762*
15. P.Zuman and Z.Fijalek J.Electroanal.Chem., *296(1990)583*
16. J-C. Gard, J. Lessard and Y. Mugnier; Electrochimica Acta; *5(1993)677*.
17. F. Markem, S. Kumbhat, G. H. W. Sanders, R. G. Compton; J. Electroanal. Chem., *414 (1996) 95*
18. G. Kokkinidis, A. Papoutsis and G. Papanastasiou; J. Electroanal. Chem. *359(1993) 253*
19. M. F. Bento, M. J. Medeiros and M. I. Montenegro, C. Beriot and D. Pletcher; J. Electroanal. Chem. *345(1993) 273*
20. P. Zuman and Z Fijalek; J. Electroanal. Chem*. 296(1990) 583.*
21. P. Zuman and Z Fijalek; J. Electroanal. Chem. *296(1990) 589.*
22. H. Shindo and C. Nishihara; J. Electroanal. Chem. *263 (1989) 415*
23. S. Sakaki, H. Koga, K. Tao, T. Yamashita, T. Iwashita and T. Hamada.; J. Chem. Soc., Dalton Trans., (*2000)1015.*

24. A. Cyr, P. Huot, J -F. Marcoux, G. Belot, E. Laviron and J. Lessard, Electrochim. Acta.*34(1989)439.*

25. Yu. B. Vassiliev, V. S. Bagotzky, O. A. Khazova, N. N. Krasnova, T. A. Sergeeva and V. B. Bogdanovich; Electrochim.Acta. *26(1981)546*

26. B. Kwiatek and M. K. Kalinowski; J. Electroanal.Chem. *226(1987)61.*

27. T. R. Nolen and P.S.Fedkiw; J.App.Electrochem. *20(1990)370*

28. J.-K.Chon and W.-K.Paik; J.Korean Chem.Soc. *21(1977)404.*

29. W. H. Smith and A. J. Bard, J. Amer. Chem. Soc. *97 (1975)5203*

30. P.Giannoccaro and E.Pannacciulli; Inorg.Chim.Acta;*117(1986)69.*

31. C. Nishihara and H. Shndo; J. Electroanal. Chem., *221(1987)245.*

32. G. Belot, S. Desjardins and J. Lessard; Tet.Lett. *25 (1984)5347*

33. J. K. Chon and W. K. Paik; J. Korean Chem. Soc.; *21(1977)404*

34. J. K. Chon and W. K. Paik; Bull. Korean Chem. Soc.; *2(1981)1*

35. S. Sternberg amd M.Ungureanu; Revue Roumaine de Chimie; *32(1987)1123*

36. Yu. B. Vassiliev, V. S. Bagotzky, O. A. Khazova, T. N. Yastrebova and T. A. Sergeeva; Electrochim. Acta. *26(1981)563*

37. L. Chuang, I. Fried and P. J. Elving, Anal. Chem., 36(1964)2426

38. P. J. Kulesza, L. R. Faulkner; Colloids and Surfaces *41(1989)123.*

39. P. N. Pintauro and J. R. Bontha; J. Appl. Electrochem;*21(1991)799*.

40. J. Marquez and D. Pletcher; Electrochim. Acta. *26(1981)1751.*

41. C. Nishihara and H Shndo; J.Electroanal.Chem., *202(1986)231*

42. S. C. Chang, C. Wang, L. J. Fan, Y. Tang, A. Hamelin; J. Electroanal. Chem., *415(1996)169.*

43. T. Komura, T. Kobayashi, T.Yamaguti K.Takahashi, J.Electroanal.Chem. *454(1998)145.*

44. J. Losada, I. del Peso, L. Beyer; J. Electroanal. Chem.; *447 (1998) 147.*

45. A. Malinauskas, R. Holze; J. Electroanal. Chem. *461 (1999) 184*

46. J. W. Sobczak, B. Lesiak, A. Jablonski, A. Kosinski and W. Palczewska; Polish. J. Chem. *69 (1995) 1732.*

47. M. Higuchi, I. Ikeda and T. Hirao; J. Org. Chem. *62 (1997) 1072*

48. B. Fabre, G. Bidan; Electrochim. Acta. *42 (1997) 2587*

49. E. K. W. Lai, P. D. Beattie, S. Holdcroft; Synth. Metal. *84 (1997) 87.*

50. A. Drelinkiewicz, M. Hasik, M. Kloc; Synth. Metal *102 (1999) 1307.*

51. W. H. Kao and T. Kuwana; J. Am. Chem. Soc. *106(1984)473.*

52. G. Tourillon and F. Garnier; J. Phys. Chem.. *88(1984)5281.*

53. F. T. Avork and E. Barendrecht; Electrochim. Acta. *35(1990)135.*

54. K. Ogura, N. Endo and M. Nakayama; J.Electrochem.Soc.*145(1998)3801*

55. M. T. Giacomini, E. A. Ticianelli, J. McBreen and M. Balasubramanian; J. Electrochem. Soc. *148 (2001)323*

56. M. C. Lefebvre, Z. Qi, P. G. Pickup; J.Electroanal.Chem.*146(1999)2054*

57. L. Doubova, G. Mengoli, M. M. Musiani and S. Valcher; Electrochim. Acta. *34 (1989)337.*

58. R. Aydin, F. Koleli; J. Electroanal. Chem. *535 (2002) 107*

59. F.V.Aguadro, S.G.Granados,S.S.Succar, C.B.Charreton and F.Bedioui; New J.Chem.*21(1997)1009*

60. D. E. Bartak, B. Kazee, K. Shimazu and T. Kuwana; Anal. Chem. 1986, 58, 2756.

61. A. Zouaoui, O. Stephan, M. Carrier and J -C. Moutet; J. Electroanal. Chem.*474(1999)113*

62. L Coche and J. Moutet; J. Am. Chem. Soc,*109(1987)6887*

63. S. W. Huang, K. G. Neoh, C. W. Shih, D. S. Lim, E. T. Kang, H. S. Han, K. L. Tan, Synth. Metal *96(1998)117*

64. T. Komura, T. Kobayashi, T. Yamaguti K. Takahashi, J. Electroanal. Chem. *454 (1998)145.*

65. E. T. Kang , K. Neo , K. L. Tan, Adv. Poly. Sci., *106(1993)136.*

66. K. L. Tan, B. T. G. Tan, E. T. Kang and K. G. Neoh; J. Chem. Phys. *94(8)(1991)5382,*

67. S. W. Huang, K. G. Neoh, E. T. Kang, H. S. Han and K. L. Tan; J. Mater. Chem., *8 (8) (1998)1743.*

68. M. Hasik, A. Bernasik, A. Adamczyk, G. Malata, K. Kowalski, J. Camra; Euro. Poly. Journal. *39(2003)1669.*

69. E. T. Kang, K. G. Neoh, Y. K. Ong, K. L. Tan, and B. T. G. Tan; Macromolecules *24 (1991)2822.*

70. M. Heyrovsky, S. Vavricka, J. Electroanal. Chem. *28(1970)409*

71. Y. Hirose, H. Yui and T. Sawada; J. Phys. Chem. A *106 (2002) 3067*

72. T. Buffeteau, F. L. Labarthet, M. Pezolet and C.Sourisseau; Macromolecules *34 (2001)7514*

73. C. Chun, M. -J. Kim, D. Vak and D. Y. Kim; J.Mater.Chem.,*13(2003)2904*

74. T. Srikhirin, A. Laschitsch, D. Neher and D. Johannsmann; Appl. Phys. Lett *77 (2000) 963*

75. W. Kemula, R. Sioda; Nature *197(1963)588.*

76. "Application of Absorption spectroscopy of organic compounds" by J.R.Dyer, Easter Economy Edition, New Delhi, 1991

Chapter VI
SUMMARY & CONCLUSION

SUMMARY AND CONCLUSION

The catalytic activity of conducting polymers in various types of reactions has been investigated in these present studies. Both oxidation and reduction processes have been looked into. The catalytic activity has been mainly investigated by monitoring electrochemical processes. In some cases, the chemical reactions under standard conventionally known conditions have been carried out using conducting polymer particles as catalysts. Amongst the various conducting polymers, polypyrrole and polyaniline doped / incorporated with active agents have been studied. The electrochemical studies show that considerable enhancement of electrocatalytic activity of conducting polymers in the doped/modified state as compared to the unmodified one.

In order to carry out these studies in systematic manner, the conducting polymers viz. polypyrrole and polyaniline were synthesized and then thoroughly characterized by various physico-chemical techniques. The synthesis of conducting polyaniline and polypyrrole was carried out by chemical as well as electrochemical route. Modification of these polymers was done by incorporating these with copper phthalocyanine or different transition metal dopants. From the various physico-chemical techniques applied for characterization, modification of these polymers could be confirmed. In the FT-IR and UV-Vis spectroscopic study of different modified polypyrrole powders, "doping induced bands" or the "bipolaronic bands" could be observed which suggests the modification due to doping. The different bands in the spectra of all the doped materials appeared to be sharp, broader or well defined whereas in case of undoped PPy peaks were weak and ill defined. The XRD studies of different PPy modified powders showed that these were mainly amorphous in nature having very little structure in the XRD pattern. Apart from very small peak at 2θ of about 26°, there was little structure in the XRD. However, changes in the position of the amorphous halo with the dopant ion were observed which led to the conclusions regarding the dopant induced changes in the average inter-chain distance (R).

The PPy modified with different dopants were thoroughly characterized by the XPS studies in order to obtain detailed information about the dopant oxidation state as well as the effect on the polymer. The presence of Cl2p core level spectra reveals the presence of the dopants in the polymer and /or the distribution of the dopant within the polymer moieties. In the C1s core level spectra, the curve appeared to be asymmetric in nature suggesting disorder effects due to cross-linking, chain termination or non α-α′′ bonded carbons, as well as due to carbon in partially saturated rings. After deconvolution three different components were seen in these spectra. In the case of N1s core level spectra also, the peaks were asymmetric on the higher BE value. Structural disorder is not believed to be the reason of the shoulder of N1s peak, since polymerization defects directly affect the carbon spectrum much more than the nitrogen spectrum. The three nitrogen components obtained after deconvolution were assigned to the three electrostatically inequivalent groups of N atoms. The dopant anions bears localized charge, and these anions are located in between polypyrrole chains, they produces electric fields at the nitrogen sites, making the atoms near to the anion more positive charged than the others. It could be seen that for doped samples, both C1s and N1s the contribution of charged species was more compared to the undoped powder while for undoped sample, the percentage of neutral component is maximum. Detailed analysis of the XPS spectra was carried out in all the cases and the total percentage of charged species (Q) was estimated from the same.

From the measurement of electrical properties of different doped PPy, the activation energy for conduction was estimated and it was observed that the activation energy of doped PPy powders was related to the electronegativity of the dopant ions, i.e. for PPy doped with higher electronegative transition metal salts, the activation energy was found to be higher. This led to the conclusions that each dopant gives rise to different levels (similar to impurity levels in semiconductors) in the conducting polymer which are specific to that dopant.

From the ESR studies, free carrier concentration, N(s) value, was determined and it was observed that N(s) value was dependent on the electro-negativity of the dopant. It decreased with the increase of electronegativity. The ESR studies indicated that the

dopant ion generates free/mobile carriers, the density of which was dependent on the additional impurity states created within the band gap of the conducting polymer.

The cyclic voltammetry study of undoped and doped Ppy films in the electrolyte containing distilled water and H_2SO_4 (no monomer or reactant) showed that the wave shape of undoped PPy was narrow whereas for doped ones it was broad indicating complex formation between the dopant and the PPy in case of doped films. The extent of complex formation was dependent on how the conducting polymer was incorporated with the dopant ; in the case of incorporation during polymerization the complex formation was the highest.

The electrocatalytic activity of modified PPy film electrodes towards oxidation of alcohols, alkenes and reduction of nitrobenzene, benzaldehyde and acetophenone were investigated by carrying out cyclic voltammetry, detailed analysis using Tafel plot, kinetics etc.

The electrochemical studies of oxidation of methanol and hexene and reduction of nitrobenzene showed that electronegativity of the dopants in the PPy plays an important role in determining the catalytic activity of the modified electrodes. It was observed that for the electrochemical oxidation reactions PPy doped with lower electronegative dopant like $ZrCl_4$ was catalytically more active as compared to the electrodes doped higher electronegative dopants. Whereas, in case of reduction processes, it was observed that the behavior of electrodes with respect to dopant ion electronegativity was found to be exactly opposite, i.e. PPy modified with higher electronegative dopants like $CuCl_2$, $NiCl_2$ were catalytically more active.

The studies of the electrochemical oxidation and reduction reactions with in situ doped PPy electrodes showed their higher catalytic activity as compared to the ex situ doped ones. Higher activity was explained on the basis of better complexation in case of insitu doped PPy electrodes, which were proved in the different characterization studies.

It was observed that the roughness and thickness of the films were also important factor in the electrochemical reactions. More the roughness the higher was the catalytic activity, which might be due to the more number of active catalytic sites possible in the rougher film. In case of study on the thickness variation of films, it was found that more the thickness more was the catalytic activity. This might be due to the fact that with thickness of films the rate of electron transport through the polymer matrix and the rate of diffusion of substrates through the polymer matrix increased. And in case of thicker films availability of higher surface area was also more as compared to the films of less thickness.

Studies of electrochemical oxidation of methanol using ion beam irradiated PPy electrodes showed tremendous enhancement in the catalytic activity. This catalytic activity further enhanced when these PPy films were doped with transition metal dopants prior to irradiation. Better catalytic activity in case of irradiated samples might be due to better complexation. XPS studies of irradiated samples showed that the PPy films chemically treated with dopants, here $PdCl_2$, did not form completely doped system but contained some amount of the dopant salt at the surface level. These ions were pushed deeper into the films and get fully mixed after ion beam irradiation, which resulted in bringing the nitrogen species to surface, which were otherwise shielded by the Pd ions. Substantial amount of complex formation also appeared to take place by co-ordination between Pd and nitrogen atom. Thus, ion beam irradiation of these films leads to essentially pushing the Pd ions deeper and mixing better with the polymer matrix leading to higher amount of complex formation. Such Pd complexes with nitrogen containing hetero-compounds are well known to be excellent catalysts for oxidation of organic compounds including Wackers process.

Electrochemical oxidation of alkenes with polyaniline modified with copper phthalocyanine was also carried out. It was found that these electrodes were quite effective towards oxidation reactions. Catalytic activity incase of CuPc-Pani films might be due to the better complex formation between Pani and copper phthalocyanine moiety, which was confirmed from the XPS, IR, UV-Vis, and XRD studies. Further, Wacker type oxidation process can be envisaged in conducting polymers in which these switch

from one oxidation state to another. This might be the case when electrochemical oxidation of decene was carried out using Pani doped with $PdCl_2$ electrodes in presence of $CuCl_2$ in the electrolytic solution, where $CuCl_2$ helped in regenerating the catalyst.

All the above work showed enhancement of electrocatalytic activity of conducting polymers in the doped/modified state as compared to the unmodified one. It was observed that these conducting polymer films were found to be catalytically more active in certain cases than the traditional noble metal catalyst like Pt. The kinetic studies for methanol oxidation indicated that the electrocatalytic activity of these polymers is similar to that reported for other electrodes (Pt, Pt/Rh etc.) but with an added advantage that the activation energy is lower and charge transfer efficiency is higher.

In the electrochemical reduction processes, importance of electrode potential, nature of the electrodes and the reduction potential of reactants on the reaction were investigated.
It could be observed from the above studies that electrode material also played an important role in the electrochemical reaction. When continuously several cycles were run with PPy electrodes modified with different dopants, nature and shape of the cyclic voltammograms varied with the incorporation of different dopants. From this, it could be said that for different electrodes different products might form or activity and selectivity can vary with different modified electrodes. When electrochemical reduction reactions of nitrobenzene were run at different potential, different colors were observed. Thus it could be concluded that the reaction potential of the electrode predicts the nature of the product i.e. the selectivity towards different products can be attained by selecting the potential as well as the dopant.

All these different observations lead to following conclusions regarding the catalytic activity of conducting polymers especially in electro-oxidation or electro-reduction processes for organic compounds. There are several factors influencing the catalytic efficiency of conducting polymers which can be grouped in to two major categories (I) structural and morphological factors and (II) internal chemical doping induced factors. In the first category one may consider the change in surface roughness, better complex

formation, internal and external doping effects, result of ion beam irradiation etc. On the other hand, in the second group the factors affecting the catalytic efficiency are not easily understood since these are specific to dopant and its nature. Broadly speaking, one can define a quality factor (Q/R) for a doped conducting polymer where Q is the percentage of charged species (determined from XPS) and R is the average inter chain distance (determined from XRD). This quality factor appears to correlate well the catalytic efficiency of the doped conducting polymer with the dopant. Higher the value of (Q/R) higher is the electro-catalytic activity.

The outstanding feature of the present research is the model which has been proposed with the help of energy level diagram for the different dopant ions with respect to PPy in contact with the reactant. This gives better understanding of these various observations in more definite terms of charge transfer process across the electrode / electrolyte (or reactant) interface. It is similar to the energy level representation for semiconductor electrodes used for photo-electrochemical reactions. With the help of energy level representation made on the basis of the energy bands (LUMO, HOMO, impurity levels, bipolaronic level etc.) for the conducting polymer and the oxidation/ reduction potentials for the reactant with respect to vacuum, the mechanism of electron/hole transport process in the electrochemical oxidation/reduction process could be explained. It is known that conducting polymers in the doped state are p-type semiconductors with the additional impurity states created within the band gap as estimated from the activation energy. It was seen that in the electrooxidation processes, for PPy doped with $ZrCl_4$ (lower electronegative dopant) electrode, it was easier for electrons to be transferred from the reactant (methanol /hexene) to the electrode leading to oxidation. On the other hand, in the reduction process, hole transfer was easier from the $NiCl_2$ (higher electronegative dopant) doped PPy to the nitrobenzene, which leads to the reduction of nitrobenzene. Thus, the rate controlling step appears to be mainly dominated by the charge transfer from or to the electrode which depends on the relative positions of the energy levels available in the electrode material.

The above hypothesis is confirmed even further when electrochemical reactions with different reactants are carried out at same conducting polymer electrode having one dopant ion (see Table 6.1). For example, it was observed that the compound with less potential difference (nitrobenzene) with respect to the upper most level in the conducting polymer was easier to reduce while the reactant having large difference (acetophenone) was difficult to reduce.

Modified PPy electrode		Reactant	Highest Current Under Optimum Conditions [Electrocatalytic Activity]
PPy-$ZrCl_4$	For oxidation	Methanol	7 mA/cm^2
PPy-$ZrCl_4$		Hexene	2.7 mA/cm^2
PPy-$ZrCl_4$		Decene	1.6 mA/cm^2
PPy-$NiCl_2$	For Reduction	Nitrobenzene	2.7 mA/cm^2
PPy-$NiCl_2$		Benzaldehyde	1.6 mA/cm^2
PPy-$NiCl_2$		Acetophenone	1.2 mA/cm^2

Table 6.1: Electro-catalytic activity of the same electrode for different reactants

This model not only gives deeper understanding of the electro-catalytic process but also brings out the importance of the charge transfer in the same. Further, it can be used very effectively to predict if certain reaction can be carried out with a given conducting polymer. For example, if the energy level of the reactant falls out side the window of the LUMO and HOMO states, one can safely predict least electrochemical activity. On the other hand, one can choose appropriate dopant for enhancing the electro-catalytic efficiency by matching the appropriate levels in the materials Thus, from all the above studies it can be predicted that the energy level is the most important factor which determines the rate of the reaction, path of the reaction and selectivity and activity of the electrode material.

Finally, these studies have given clear demonstration of the effective applications of conducting polymers as catalysts in electrochemical as well as regular conventional chemical reactions. It is interesting point out here that in the chemical oxidation of decene using polyaniline incorporated with CuPc electrode, the oxidation products such as decanol and decanoic acid were obtained (confirmed from the GC and FT-IR studies) which are not normally seen under typical reaction conditions for the conventional Wacker type oxidation using $PdCl_2$ / $CuCl_2$ catalyst. This opens up new possibilities of using these polymer based catalysts giving alternate products which are not easy to obtain. Hence, by proper modification of the conducting polymers it may be possible to obtain new and better catalysts which may even replace the conventional catalysts. Moreover these polymer based catalysts are very cost effective (1/10 to 1/30 of Pd or Pt based catalysts) and can be easily separated from the reaction mixture giving added advantages in the industrial processes. The field is far wide and open and possibilities are very promising.

Patents and Publications:

Patents:

1. A process for preparation of an electrode useful for electrocatalytic oxidation of alkenes.
   Radhakrishnan S and Adhikari Arindam, 152/DEL/2002
2. A process for the electrocatalytic oxidation of alkenes
   Radhakrishnan S and Adhikari Arindam, 181/DEL/2002
3. A process for the electrocatalytic reduction of nitro-aromatic compounds.
   Radhakrishnan S and Adhikari Arindam, 173/DEL/2002
4. A process for the preparation of conducting polymer electrodes useful for electrocatalytic oxidation of alcohols
   Radhakrishnan S and Adhikari Arindam, NF-263/2003

   (Indian and US patent filed)

Publication

Electrocatalytic Properties of the Ion Beam irradiated Conducting Polypyrrole

S. Radhakrishnan, Arindam Adhikari and D. K. Awasthi

Chemical Physics Letter 341(2001) 518